DISCLAIMER NOTICE

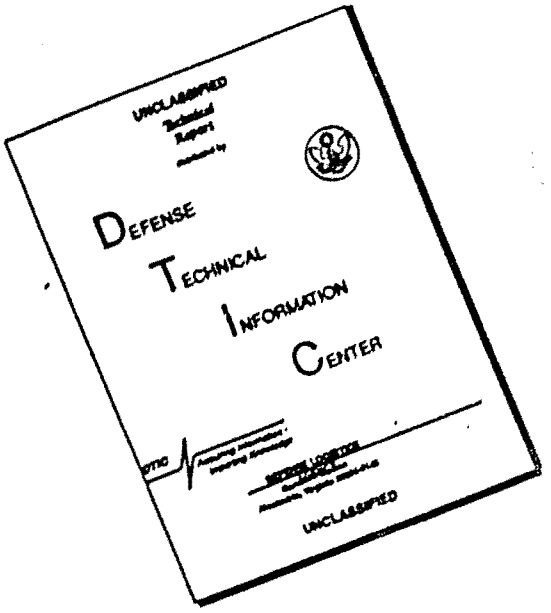

THIS DOCUMENT IS BEST QUALITY AVAILABLE. THE COPY FURNISHED TO DTIC CONTAINED A SIGNIFICANT NUMBER OF PAGES WHICH DO NOT REPRODUCE LEGIBLY.

U. S. ARMY
TRANSPORTATION RESEARCH COMMAND
FORT EUSTIS, VIRGINIA

TRECOM TECHNICAL REPORT 63-68

A STUDY OF ROUGH-TERRAIN-INDUCED STRUCTURAL LANDING LOADS

Task 1D121401A14602
(Formerly Task 9R38-01-019-02)
Contract DA 44-177-TC-735

December 1963

prepared by:

DOUGLAS AIRCRAFT COMPANY, INC.
Long Beach, California

5904-63

DISCLAIMER NOTICE

When Government drawings, specifications, or other data are used for any purpose other than in connection with a definitely related Government procurement operation, the United States Government thereby incurs no responsibility nor any obligation whatsoever; and the fact that the Government may have formulated, furnished, or in any way supplied the said drawings, specifications, or other data is not to be regarded by implication or otherwise as in any manner licensing the holder or any other person or corporation, or conveying any rights or permission, to manufacture, use, or sell any patented invention that may in any way be related thereto.

* * *

DDC AVAILABILITY NOTICE

Qualified requesters may obtain copies of this report from

Defense Documentation Center
Cameron Station
Alexandria, Virginia 22314

* * *

This report has been released to the Office of Technical Services, U. S. Department of Commerce, Washington 25, D.C., for sale to the general public.

* * *

The findings and recommendations contained in this report are those of the contractor and do not necessarily reflect the views of the U. S. Army Mobility Command, the U. S. Army Materiel Command, or the Department of the Army.

HEADQUARTERS
U S ARMY TRANSPORTATION RESEARCH COMMAND
FORT EUSTIS, VIRGINIA

This report has been reviewed by this command and is considered to be technically sound. The report is published for the exchange of information and the stimulation of ideas.

JOHN E. YEATES
Project Engineer

JAMES G. MC HUGH
Group Leader
Aeromechanics Group

APPROVED.

FOR THE COMMANDER:

LARRY M. HEWIN
Technical Director

Task 1D121401A14602
(Formerly Task 9R38-01-019-02)

Contract DA44-177-TC-735
TRECOM Technical Report 63-68

DECEMBER 1963

A STUDY OF ROUGH-TERRAIN-INDUCED STRUCTURAL LANDING LOADS

PHASES I AND II

Analytical Determination of the Effect of Rough Terrain on the Loads, Weight, and Performance of an Army Tactical Airplane

PREPARED BY

DOUGLAS AIRCRAFT COMPANY, INC.
AIRCRAFT DIVISION
LONG BEACH, CALIFORNIA

FOR

U.S. ARMY TRANSPORTATION RESEARCH COMMAND
FORT EUSTIS, VIRGINIA

FOREWORD

The work described in this report was accomplished by the Douglas Aircraft Company, Aircraft Division, Long Beach, California, for the U. S. Army Transportation Research Command, Fort Eustis, Virginia. This report represents the work conducted under Phases I and II of Contract DA44-177-TC-735, with Mr. J. E. Yeates, U. S. Army TRECOM, technical monitor.

The project was conducted by the Douglas Aircraft Company, with Mr. F. C. Allen, Supervisor of Structural Research, providing the technical direction and Messrs. D. M. Rehder and L. B. Mosby acting as chief technical investigators.

CONTENTS

	Page
FOREWORD	iii
LIST OF TABLES	vii
LIST OF ILLUSTRATIONS	ix
LIST OF SYMBOLS	xv
SUMMARY	1
INTRODUCTION	2
Objectives	2
The OV-1 Airplane and Gear	4
The VTOL Airplane	5
Rough-Terrain Categories	6
METHODS OF ANALYSIS	8
General	8
Basic Assumptions	9
Load Determination	11
Rough-Terrain Representation	12
Equations of Motion	14
The Check-out	15
Conditions Computed	15
Structural Weight Estimation	15
Airplane Performance	16
RESULTS	25
Loads	25
Weight Increases	31
The Effect on Performance of Increased Structural Weight	32
Comparison of OV-1 and VTOL Performance	33
CONCLUSIONS	39
RECOMMENDATIONS	41
APPENDIX I - EQUATIONS OF MOTION	43

CONTENTS

	Page
APPENDIX II - DESIGN CRITERIA FOR ROUGH TERRAIN LANDINGS	59
REFERENCES	64
TABLES	68
FIGURES	91
DISTRIBUTION	161

TABLES

Table		Page
1	OV-1 Airplane - General Data	68
2	VTOL Airplane Size Variation	68
3	VTOL Airplane Weight Summary	69
4	Terrain Designators for Matrix I	70
5	Terrain Designators for Matrix II	71
6	Terrain Designators for Matrix III	73
7	Terrain Designators for Matrix IV	74
8	Airplane Concentrated Masses and Their Locations	75
9	Computed Conditions	76
10	VTOL Airplane Performance Summary	80
11	Structural Component Weight Penalties	81
12	Terrain Roughness Requiring Structural Reinforcement of OV-1 Airplane	86
13	Terrain for Equal VTOL/OV-1 Performance	88

ILLUSTRATIONS

Figure		Page
1	OV-1 Mohawk Airplane General Configuration.	91
2	OV-1 Main Gear.	92
3	OV-1 Nose Gear.	93
4	The VTOL Airplane.	94
5	The Terrain Designation System.	95
6	Airplane Mass Breakdown.	96
7	Types of Rough Terrain Considered.	97
8	Comparison of Analytical Results with Airplane Drop Tests. Main Gear.	98
9	Comparison of Analytical Results with Airplane Drop Tests. Nose Gear	99
10	OV-1 Total Take-Off Distance Versus Gross Weight and Take-Off Runway Parameter.	100
11	OV-1 Take-Off Speed Versus Gross Weight.	101
12	OV-1 Lift and X-Force During Take-Off at Taxi Attitude with Take-Off Thrust.	102
13	OV-1 Horizontal Distance from Lift-off to a 50-foot Obstacle Versus Gross Weight.	103
14	OV-1 Increase in Take-Off Distance Due to Rotation from Taxi Attitude to Fly Away Attitude Versus Gross Weight.	103
15	OV-1 Total Landing Distance Versus Gross Weight and Landing Runway Parameter.	104
16	OV-1 Approach Speed Versus Gross Weight.	105
17	OV-1 Forces and Pitching Moment During Landing Roll-Out at Taxi Attitude with Full Reverse Thrust.	106

ILLUSTRATIONS

Figure		Page
18	Mission Profile	107
19	Specific Range at Sea Level Versus Airspeed and Gross Weight for the OV-1 with Two 150-Gallon External Fuel Tanks.	107
20	OV-1 Radius Versus Fuel Aboard at Take-Off.	108
21	Main and Nose Gear Time Histories. Landing on Level, Smooth Terrain, Three-Point Attitude.	109
22	Wing Bending Moment and Torque Time Histories. Landing on Level, Smooth Terrain, Three-Point Attitude.	110
23	Acceleration Time Histories. Landing on Level, Smooth Terrain, Three-Point Attitude.	111
24	Variation of Maximum Loads with Ground Slope.	112
25	Main and Nose Gear Time Histories. Landing in Three-Point Attitude on Level Terrain with High Rolling Coefficient of Friction, $\mu_S = .4$ and $\mu_R = .7$.	113
26	Variation of Maximum Loads with Rolling Coefficient of Friction.	114
27	Vertical Load on Main Gear for Bumps in Different Locations Relative to Point of Touchdown.	115
28	Main Gear Load Versus Time for a Three-Inch Bump 137 Inches Long.	116
29	Main and Nose Gear Time Histories. Landing in Three-Point Attitude on Level Terrain, Gear Hits Single Bump at Most Critical Point. Bump Length = 27.4 Inches, Height = 3 Inches	117

ILLUSTRATIONS

Figure		Page
30	Wing Bending Time Histories. Landing on Level Terrain, Nose Gear Hits Bump at Most Critical Distance of Bump ℄ to Main Gear Touchdown, Three-Point Attitude. Bump Length = 27.4 Inches, Height = 3 Inches	119
31	Maximum Main Gear Vertical Load Versus Bump Height, Bump Length and Sinking Speed.	120
32	Effect of Cable Impact on A-4B Gear Loads.	121
33	Ground Loads for a 17 Ft/Sec Landing on Continuous Undulations, Length = 27.4 Inches, Height = 3 Inches.	122
34	Wing Bending Moments for a 17 Ft/Sec Landing on Continuous Short Undulations, Length = 27.4 Inches, Height = 3 Inches.	123
35	Main and Nose Gear Time Histories. Landing in Three-Point Attitude on Level Terrain Having Continuous Undulations 27.4 Inches Long and 3 Inches High.	124
36	Wing Bending Moment Time Histories. Landing in Three-Point Attitude on Level Terrain Having Continuous Undulations 27.4 Inches Long and 3 Inches High.	126
37	Fuselage Time Histories. Landing in Three-Point Attitude on Level Terrain Having Continuous Undulations 27.4 Inches Long and 3 Inches High.	127
38	Ground Loads for a 17 Ft/Sec Landing on Continuous Undulations, Length = 137 Inches, Height = 3 Inches.	128
39	Wing Bending Moments for a 17 Ft/Sec Landing on Continuous Long Undulations, Length = 137 Inches, Height = 3 Inches.	129

ILLUSTRATIONS

Figure		Page
40	Vertical Gear Load and Wing Bending Moment for a 17 Ft/Sec Landing on a Series of Two 3-Inch Bumps Spaced 242 Inches Apart.	130
41	Airplane Response for Roll-Out or Taxi. Wing Lift Equals Zero, Bump Spacing = 126 Inches, Height = 2 Inches, Length = 27.4 Inches, V_A = 84.5 Knots.	131
42	Airplane Fuselage Response for Roll-Out or Taxi. Wing Lift Equals Zero, Bump Spacing = 90.6 Inches, Height = 2 Inches, Length = 27.4 Inches, V_A = 84.5 Knots.	132
43	Airplane Engine Response for Roll-Out or Taxi. Wing Lift Equals Zero, Bump Spacing = 90.6, Height = 2 Inches, Length = 27.4 Inches, V_A = 84.5 Knots.	133
44	Comparison of Rigid and Flexible Aircraft Loads for a 17 Ft/Sec Landing on a 3-Inch Bump 27.4 Inches Long.	134
45	Comparison of Rigid and Flexible Aircraft Loads for a 17 Ft/Sec Landing on a 3-Inch Bump 242 Inches Long.	135
46	Structural Weight Penalty Versus Ground Slope.	136
47	Structural Weight Penalty Versus Undulation Height. Undulation Length = 13.7 Inches.	137
48	Structural Weight Penalty Versus Undulation Height. Continuous Undulations, Length = 27.4 Inches.	138
49	Airplane Weight Penalty Versus Undulation Height. Continuous Undulations, Length = 45.67 Inches.	139
50	Structural Weight Penalty Versus Undulation Height. Continuous Undulations, Length = 137 Inches.	140

ILLUSTRATIONS

Figure		Page
51	Structural Weight Penalty for 3-Inch Bump Versus Bump Location. Main Gear Hits Bump with Airplane in Three-Point Attitude.	141
52	Structural Weight Penalty Versus Bump Location. Nose Gear Hits Bump with Airplane in Three-Point Attitude.	142
53	Structural Weight Penalty Versus Location of Bump. Main Gear Hits Bump with Airplane in Tail Down Attitude.	143
54	Structural Weight Penalty Versus Bump Length. Constant Height Bump Located at Critical Distances from Main Gear Touchdown. Single Bump Contour, Height = 3 Inches, $\mu_s = .4$.	144
55	Structural Weight Penalty Versus Bump Height. Constant Height-to-Length Ratio Bumps Located at Critical Distances From Main Gear Touchdown. Length/Height = 9.12, $\mu_s = .4$.	145
56	Structural Weight Penalty Versus Coefficient of Rolling Friction. ($\mu_s = .4$)	146
57	Effect on OV-1 Performance of Structural Weight Penalty. Take-Off Weight Increases as Structural Weight is Added.	147
58	Effect on OV-1 Performance of Structural Weight Penalty. Take-Off Weight Held Constant by Decreasing the Fuel Weight as Structural Weight is Added.	148
59	Radius Versus Take-Off Weight for the VTOL Airplane and for the OV-1 Airplane with Varying Amounts of Added Structural Weight.	149
60	Take-Off Runway Parameter Versus OV-1 Structural Weight Penalty and Runway Length Required for Equal VTOL/OV-1 Performance.	150

ILLUSTRATIONS

Figure		Page
61	Take-Off Runway Parameter Versus Runway Slope and OV-1 Runway Length Required for Equal VTOL/OV-1 Performance.	151
62	Take-Off Runway Parameter Versus Undulation Height and Runway Length Required for Equal VTOL/OV-1 Performance. Undulation Length = 27.4 Inches.	152
63	Take-Off Runway Parameter Versus Undulation Height and OV-1 Runway Length Required for Equal VTOL/OV-1 Performance. Undulation Length = 45.67 Inches.	153
64	Take-Off Runway Parameter Versus Undulation Height and OV-1 Runway Length Required for Equal VTOL/OV-1 Performance. Undulation Length = 137 Inches.	154
65	Take-Off Runway Parameter Versus Bump Length and OV-1 Runway Length Required for Equal VTOL/OV-1 Performance. Bump Height = 3 Inches.	155
66	Take-Off Runway Parameter Versus Bump Height and OV-1 Runway Length Required for Equal VTOL/OV-1 Performance. Bump Length = 9.12 x Bump Height.	156
67	Take-Off Runway Parameter Versus Rolling Coefficient of Friction and Runway Length Required for Equal VTOL/OV-1 Performance.	157
68	Sign Conventions.	158

LIST OF SYMBOLS

Note: Symbols used in the Appendix are listed therein.

A	one-half amplitude of a terrain undulation with a 1-cos shape, inches
a_x	airplane acceleration parallel to the horizontal datum plane, feet per second^2
D	aerodynamic drag force, pounds
F_H	vertical force at attachment point of landing gear to wing, pounds
g	acceleration of gravity, feet per second^2
L	length of a bump or of a single cycle of continuous undulation, inches; also, lifting force, pounds
M	aerodynamic moment, inch-pounds
M_α	moment of all forces on the landing gear about point of attachment to the wing, inch-pounds
P_V	load on landing gear at ground contact point normal to the horizontal datum plane, pounds
P_D	load on landing gear at ground parallel to the horizontal datum plane, pounds
S	ground run distance during take-off or landing, feet; also, spacing of discreet bumps, inches
T	engine thrust, pounds
V_A	velocity of airplane parallel to the horizontal datum plane, knots
V_{APR}	landing approach speed, knots
V_L	landing speed, knots
V_v	velocity of airplane normal to the horizontal datum plane, feet per second

LIST OF SYMBOLS (Cont'd)

W	airplane weight, pounds
X	total force (thrust minus drag) on airplane parallel to the horizontal datum plane, pounds
x	distance of the tire point of contact from the point of touchdown, inches
$X_{\mathcal{C}_L}$	distance of bump center-line from point of landing gear touchdown, inches
Z	height at any point of a terrain irregularity from a horizontal datum plane, inches
Z_{MAX}	maximum height of terrain irregularity = 2A, inches
θ	slope of ground at point of contact or general slope of landing area, degrees
μ_B	braking coefficient of friction
μ_R	rolling coefficient of friction
μ_S	sliding coefficient of friction
ρ	runway parameter; the average resistance to horizontal motion of the airplane caused by terrain slope and rolling coefficient of friction, expressed as a fraction of airplane weight

SUMMARY

This report contains an analytical investigation of the effect of rough terrain on the loads, weights, and performance of the OV-1 airplane during landings. The load calculations, which were conducted on an IBM 7090 computer, considered the internal operating mechanism of the landing gear and the flexibilities of the gear and structure as a mutually interacting dynamic system. The equations of motion and certain details of the computer program are provided in Appendix I.

A determination was made of the terrain roughness at which modification to the airplane was considered necessary and the terrain roughness at which the reduced performance of the OV-1 airplane, due to increased weight, became equal to or inferior to a VTOL aircraft of equal weight.

This work was concerned with the determination of maximum loads and corresponding weight and performance penalties; however, observations were made regarding the importance of repeated loads during landing or taxiing on surfaces with multiple irregularities.

The primary results of the investigation appear in Tables 12 and 13, which show the terrain roughness at which structural reinforcement is considered necessary and the terrain roughness at which the performance of the airplane becomes equal to that of a VTOL aircraft of the same weight.

INTRODUCTION

OBJECTIVES

The general purpose of this investigation was to obtain information on the effect of rough terrain on structural loads of aircraft so that rough-terrain loads criteria may be developed. More specifically, the objectives were as follows:

1. To determine analytically the variation of loads on the OV-1 airplane with terrain roughness and the corresponding changes in weight and aircraft performance,

2. To determine the terrain roughness at which modification to the OV-1 aircraft is desirable or necessary, and

3. To determine the degree of terrain roughness at which the reduced performance of the OV-1 airplane, caused by increased weight, becomes equal or inferior to the performance of a VTOL aircraft of the same gross weight.

The need for the establishment of new structural design criteria for rough-terrain operations arises from the fact that current Army aircraft are designed to meet Air Force, Navy or Federal Aviation Agency requirements. These aircraft are not, in general, designed for loads that may be imposed by some of the Army's specialized missions, particularly rough-terrain operations.

The problem involved in establishing these design criteria is to specify the extent of the roughness to which the aircraft must be subjected upon landing. It is apparent that an aircraft which has a finite landing speed cannot be designed for all possible degrees of landing area roughness. It is assumed that the design roughness should be no greater than that which will impose weight penalties sufficient to make a VTOL aircraft more efficient. The reasons for the project objectives thus become clear: By examining the effect of rough-terrain landings on several aircraft configurations, it is hoped to obtain an approximate idea of a reasonable terrain roughness to be used in the design of future Army aircraft.

The problem of landing area roughness has been of concern for many years to both civil and military organizations. It has long been recognized that normal irregularities in commercial landing fields have contributed to the fatigue damage of transport aircraft, and the work described in References 1 to 3 was conducted to define the magnitude and frequency of undulations at some of the large airports of the world. The Navy has experienced numerous landing gear failures which were attributed to running over an arresting cable at the time of impact and is currently conducting an investigation for the development of a gear which will alleviate the loads experienced under those circumstances.

The terrain roughness encountered by Army aircraft at their forward bases is of greater magnitude and requires special consideration. Previous TRECOM-funded programs have involved experiments with large, high-flotation tires (Reference 4) and actual landing tests with several fixed-wing Army aircraft on rough terrain (Reference 5). The current investigation is the first Army-sponsored project which approaches the problem on a strictly analytical basis. It is hoped that the results will develop an understanding of the factors involved and will provide a base for the formulation of design criteria for rough-terrain operations.

THE OV-1 AIRPLANE AND GEAR

The OV-1 airplane, upon which this investigation is based, is shown in Figure 1. Pertinent general data are given in Table 1. The OV-1 is a two-place, twin turboprop airplane built by the Grumman Aircraft Engineering Corporation. It was designed to operate from small, unimproved fields and is primarily a tactical observation and photographic airplane.

The OV-1 is equipped with a retractable tricycle landing gear, having a full-swiveling non-steerable nose wheel. The internal mechanism of both main and nose gear incorporates a conventional hydropneumatic shock strut equipped with a metering pin-orifice arrangement characteristic of airplanes designed for high sink speeds. General arrangement sketches of the main and nose gear are shown in Figures 2 and 3.

The OV-1 configuration used for this ground loads study is the airplane equipped with empty 150-gallon wing tanks, 4 HVAR rockets on the wing racks, and 670 pounds of fuel in the fuselage tank. The corresponding gross weight is 11,771 pounds with the center of gravity at fuselage station 159.8 and 22.3 inches below the fuselage reference line. The basic take-off weight for performance calculations is 14,340 pounds, the configuration being identical to the landing configuration except for full fuel (i.e., fuselage and external wing tanks full) and less rockets.

References 5 through 30 give pertinent structural weight and aerodynamic data on the airplane. The following fundamental items of structural design criteria are summarized for the reader's convenience.

Maximum design limit load factors at design flight gross weight	5.0, -2.0
Design limit speed	390 knots (EAS)
Design limit sinking speed	17.0 fps
Design ultimate sinking speed at design landing gross weight of 10,715 pounds	20.8 fps

THE VTOL AIRPLANE

The VTOL aircraft chosen for comparison with the OV-1 is shown in Figure 4. This aircraft is a canard, tilt wing vehicle powered by two Lycoming LTC4B-8 shaft turbines driving four variable cambered propellers. The engines and propellers are interconnected to permit single engine operation in the event of an engine failure and for increased cruising economy. The aircraft is a modified version of the Douglas D-847 retrieval VTOL previously designed for a mission comparable to that considered for this study.

Fixed equipment installed in the VTOL aircraft has been selected to duplicate the OV-1 installation for the observation mission. The fuselage can accommodate all fuel internally and thus does not require the external fuel installation provided on the OV-1. The aircraft has a limit load factor of 4.0 at take-off weight to be compatible with the OV-1 at design take-off weight.

The VTOL aircraft size required to achieve mission capability equivalent to that of the OV-1 is determined by investigation of several sizes over a range of take-off gross weight from 10,000 to 16,000 pounds.

Fuselage and engine size, engine installation losses, and propeller efficiency are assumed to be the same for all weights. Propeller size is determined by the requirement for a static thrust-to-weight ratio of 1.05 for sea level hot day ($89.6^{\circ}F$) operation. Wings are sized by holding constant the clearance between the forward propellers and the fuselage, and by maintaining the same aspect ratio and span ratio between the forward and aft wings.

Dimensions of the VTOL aircraft at the four weights considered for this study are given in Table 2. The weight breakdown used to obtain fuel weight is contained in Table 3.

ROUGH-TERRAIN CATEGORIES

A requirement of this project was to relate the limiting landing conditions to terrain roughness described in accordance with a terrain designation system developed by the Planning Research Corporation, Los Angeles, California, presented in Reference 31. An example of a terrain designator is given in Figure 5. In that report terrains are classified by the use of four matrices. The first matrix defines operational area, length and width dimensions, and general slopes in width and length directions. The second matrix defines height, spacing and slope of terrain undulations. The third matrix defines height, spacing and type of obstacles. The fourth matrix defines the soil as to its California bearing ratio and soil classification. The variations of each parameter in each matrix with terrain roughness are shown in Tables 4 through 7.

Several simplifications of the terrain roughness spectrum were required by limitations of the project size and by limitations of the computing capabilities. These are listed and discussed below (paragraph numbers correspond with matrix numbers):

I. No side force calculations were included in the computing program. Therefore, width slope, parameter 2 in the first matrix, is zero in all conditions.

II. Obstacles as well as undulations were two-dimensional, that is to say cylindrical, with axes at right angles to the motion of the airplane. This simplification resulted from the first, since a skewed or non-uniform bump would induce side loads.

III. Obstacles were limited in shape to [illegible] bumps with the minimum radius approximately equal to that of the tire. This simplification was required for two reasons. First, the computing program as originally conceived was incapable of handling the case where there were two points of contact of the wheel with the ground, and secondly, no tire load-deflection data were available for the deformation of the tire by a loading surface of small radius. A program revision was made to allow a slightly smaller minimum bump radii than tire radius by using a step integration across the bump rather than a convergence procedure on tire radius. However, a bump radius restriction was still required.

IV. The soil characteristics were described in the calculations by the parameters of sliding and rolling coefficients of friction, and the results are so presented. A literature search was made in an attempt to correlate rolling and sliding coefficients of friction to the soil capacity and classification of matrix IV. Certain equations are available to determine wheel sinkage and rolling coefficient of friction from basic soil parameters for slow and steady vehicle movements (see References 33 to 35). This data, however, is not applicable to the impact and high velocity conditions encountered on landings. Therefore, the results are quoted in terms of rolling coefficient of friction.

METHODS OF ANALYSIS

GENERAL

The methods used to accomplish the objectives stated in the Introduction are described in general terms, after which a more detailed description of each phase is presented.

To determine analytically the variation in loads of the OV-1 airplane with terrain roughness, computations were made using an IBM program which simulated the operational characteristics of the gear and the elastic properties of the gear and airplane structure. The input to the computing program consisted of the initial velocities, both vertical and horizontal, the attitude of the airplane, and the contour and character of the ground. To assure that the computing program was representing the aircraft adquately, initial runs were made simulating drop tests which were made by the aircraft manufacturer on the aircraft itself, and the analytical results were compared with the test results.

The output of the computing program gave time histories of load or element acceleration. Critical values of load at any instant of time were then used to compute changes in weight.

Weight changes were obtained by theoretical stress analysis methods typical of those used in advanced design. Although the methods used for determining weight variation were not complex, the bookkeeping was extensive since there were many cases and numerous loads for each case which affected different portions of the structure. Weight changes were plotted as a function of terrain roughness parameter such as size of bump, spacing, or coefficient of friction. In order to analyze adequately the effect of terrain roughness on the performance of the OV-1 airplane, the performance characteristics of the aircraft were first derived for arbitrary variations in airplane weight. Therefore, take-off performance was computed as a function of take-off weight, landing performance was derived as a function of landing weight, and radius performance was obtained as a function of take-off weight and fuel quantity. The methods used to calculate these performance characteristics are described and are based on data supplied by the Grumman Aircraft Engineering Corporation (GAEC). Correlation with the results obtained by the GAEC was made. The performance characteristics of the VTOL aircraft selected for comparison were also determined.

Based on the methods and equations derived to describe the performance characteristics of the OV-1 as a function of weight, the effects of various terrain conditions were next developed. These characteristics were then compared with those of the VTOL airplane, in order to determine the terrain conditions for which a VTOL airplane of the same gross weight as the OV-1 had a radius equal to that of the OV-1.

BASIC ASSUMPTIONS

The basic assumptions used in this analysis and their effect on the results are discussed in the following paragraphs.

1. Weight increments for this analysis were based on ultimate sinking speeds of 17, 12 and 8 feet per second with respect to a horizontal datum plane. Since the OV-1 was designed and tested for an ultimate sinking speed of 20.8 feet per second, strength margins existed for 17.0 or less feet per second landings on smooth terrain. Positive weight increments were therefore obtained only after the terrain roughness became high enough to use up this strength margin. The terrain roughness at which "modification to the OV-1 aircraft is desirable or necessary"* was assumed to be those degrees of terrain roughness where the weight increment became positive.

   It is evident that these points are highly dependent on the basic sinking speed assumption, and that all weight increments are affected by it to a greater or lesser extent.

   Design sinking speeds should ideally be established after the examination of large quantities of statistical data on actual landings of aircraft. Since such data were not available for airplanes operating in and out of unimproved areas, three sinking speeds were chosen so that the effect of the basic sinking speed assumption can be easily determined.

2. The rigidity of the OV-1 airplane was assumed to remain constant as loads increased. In other words, as the weight increased because of rough-terrain loads, no corresponding changes in rigidity were

* See objective number 2, page 2

made. Obviously, then, the computed weight increases are only a first approximation. An iteration to improve accuracy was not considered practical principally because of the enormous labor involved. The effect of the assumption is to cause less accuracy at the higher weight increments.

3. All surface roughness was assumed to be of the 1-cosine shape. Various terrain slopes and rolling coefficients corresponding to various degrees of landing area softness were also investigated. The 1-cosine shape was used because it was a good approximation of typical natural undulations and because it provided a convenient mathematical treatment. By relating the results to the maximum height of bump, the maximum slope, or length, a means has been provided for obtaining approximate performance penalties for bumps of other shapes. Since maximum loads were always obtained before the crest of the bump, the shape of the approach side is of importance. The solutions are, therefore, considered applicable to asymmetric bumps where the shape of the approach side conforms to a 1-cosine curve and the shape of the down side is of little consequence.

4. Surface roughness was assumed to be cylindrical with axis in a horizontal plane normal to the motion of the airplane. This assumption was a corollary of the basic concept of the project that asymmetric initial conditions would not be included in the calculations.

5. In the investigation of the effect of continuous terrain slope, it was assumed that the airplane attitude was adjusted by the pilot to the slope of the landing area but that the sinking speed relative to the horizontal datum plane was unchanged. The landing area slope which was assumed upward in the direction of flight caused an effective increase in sinking speed equal approximately to the slope times the forward velocity. This assumption obviously gave higher weight increments and greater performance penalties than would be obtained if the pilot adjusted completely to the slope and landed at seventeen feet per second measured normal to the ground.

LOAD DETERMINATION

Loads were determined from a computing program based on Reference 36. Modifications to this work were introduced to include landing and taxiing on a non-uniform area and to provide print-out of accelerations and loads at discrete points throughout the airplane. Since the mathematical statement of rough terrain and the accompanying data required in the solution exceeded the total capacity of the former program, it was re-coded in Fortran language.

The computing program coded in Fortran language generates the ground contact loads and structural accelerations on an elastic airplane, accounting for the feed-back between the airplane and the main and nose landing gears during landing and taxiing. The non-linearities of the tire spring rates, air compression in the oleo, hydraulic damping, metering pin cross-sectional area, and drag forces dependent upon skidding and rolling ground coefficients of friction were considered. The flexibility of the gear and of the airplane is accounted for by the inclusion of several natural modes of vibration which were determined from the results of the manufacturer's ground vibration tests corrected to the configuration used in this report.

In the interest of simplification, certain limitations were imposed on this analysis, but these are inherent neither in the general method nor in the computing equipment available. For instance, the bumps were assumed to be of 1-cosine shape. They could have been made more complex. A constant forward velocity of 84.5 knots was assumed. The angle of the strut with the vertical was assumed constant for each case computed. A constant sliding coefficient of friction before spin-up and a constant rolling coefficient of friction after spin-up were used.

The tire load-deflection curve was represented by a series of straight lines of sufficient number to provide a satisfactory approximation of the exact curve. This procedure permitted the inclusion of a relatively sharp break in the curve at a point near full tire compression.

Four flexible modes of vibration were used in the analysis with frequencies of 7.06, 7.76, 9.04 and 13.6 cycles per second. This was sufficient to describe accurately the elastic characteristics. However, the number of degrees of freedom permissible in the program exceeds those needed in the current studies and allows for future adaptation of the

program to analytical studies of unsymmetrical landings. The airplane was divided into a number of discrete mass items for purpose of this analysis. The division is illustrated in Figure 6.

The airplane equations of motion were written to include aerodynamic forces and their variation with both rigid body and elastic motion. Thus, aerodynamic damping was included. Damping occurs through the instantaneous local plunging or flapping velocities of each area of the wing. The finite aspect ratio value of $dC_L/d\alpha$ was applied to the elastic wing through "strip theory". Aerodynamic damping was of importance in those investigations involving a sequence of bumps and was a factor in determining the degree of convergence or divergence of the loads. It was of less importance in the investigations involving single bumps combined with landing impact.

The analysis was so arranged that it could be started with any set of initial conditions. All displacements and velocities of the airplane and gear were input at the starting time. The assumption was made that the airplane touched down with a constant descent velocity. All accelerations immediately prior to touchdown were assumed to be zero.

ROUGH-TERRAIN REPRESENTATION

Landing surface irregularities were represented by the types of terrain shown in Figure 7. These consist of:

(a) Slopes in the direction of airplane motion

(b) Soft earth as indicated by various sliding and rolling coefficients of friction

(c) Single bumps

(d) Continuous identical undulations

(e) Series of discrete bumps.

The protuberances investigated under (c), (d) and (e) consisted of cylindrical, 1-cosine bumps of various heights and lengths oriented at right angles to the direction of airplane motion. The magnitudes of surface irregularities were progressively increased until the weight increments resulting therefrom brought the performance of the STOL airplane down to that of the VTOL airplane. The investigation was limited

to protuberances with concave radii equal to or greater than the radius of the tire. Computational difficulties arose when bumps outside this range were considered because of the fact that the tire then made contact with the ground at two locations.

The number of cycles of "continuous" undulations considered in each landing was a function of wave length. Thus, ten cycles were used when the length was 27.4 inches; five cycles were used with a 45-inch wave length and 3 cycles were used at 137-inch wave length. To a large extent, this limit was created by the computing machine time required to run each case; however, some justification for this procedure lies in the anticipated character of the terrain. The short undulations can be considered to be a plowed field, the furrows of which are both uniform and continuous. The long undulations might be considered natural irregularities. The probability of encountering more than three such protuberances of equal wave length is rather remote.

The frequency of the continuous undulations* started at 125 cycles per second (L = 25 inches) and extended down to 12.5 cycles per second (L = 137 inches), a value just below the highest of the structural frequencies used in the analysis. The series of discrete bumps were spaced further apart and were designed to excite the lower structural modes. Each of these series contained two identical bumps.

The 1-cosine function was written in terms of the start and finish distance of the irregularity from the point of touchdown or start of taxi, and in terms of the one-half amplitude "A". If "Z" designates the height of the roughness from the horizontal datum plane, and "x" the distance from the point of touchdown, then

$$Z = A \left[1 - \cos 2\pi \left(\frac{x - x_{Start}}{x_{Fin} - x_{Start}} \right) \right] \qquad (1)$$

* Frequency of the undulations is defined as $\frac{V}{L}$, where V is the landing speed in inches per second and L is the wave length in inches.

where x_{Start} = the distance from point of touchdown to start of bump

x_{Fin} = the distance from point of touchdown to the end of the bump.

The slope at any point is

$$\frac{dZ}{dx} = \frac{2\pi A}{x_{Fin}-x_{Start}} \text{ SIN } 2\pi \frac{x-x_{Start}}{x_{Fin}-x_{Start}} \quad . \qquad (2)$$

The maximum slope of this irregularity occurs when $x-x_{Start} = 1/4\ (x_{Fin}-x_{Start})$ or, in other words, at a point 1/4L from the beginning of the bump. Hence,

$$\left|\frac{dZ}{dx}\right|_{Max} = \frac{2\pi A}{L} = \frac{\pi Z_{Max}}{L} \quad . \qquad (3)$$

It has been noted that, in the consideration of bumps or undulations, the smallest curvature of the irregularity was always maintained approximately equal to the tire radius. If the radius of curvature is substantially less than the wheel radius, the mathematical solution is divergent. Refinements to the program could have been introduced to take into account radii smaller than the wheel; however, to do this adequately, an investigation into the tire load-deformation characteristics for each size obstacle would also have been necessary. This was clearly beyond the scope of the project. In any event, subsequent calculations showed that a 1-cosine bump of a size large enough to comply with the minimum radius requirement was, indeed, a small bump insofar as the induced load-time pulse was concerned. The load pulse resulting from the minimum length bump investigated was completed in the order of .01 second.

EQUATIONS OF MOTION

The equations of motion which have been used in the computing program are given in Appendix I. The items of structural load, velocities, displacements and accelerations which were obtained from the program are listed on page 57 (Appendix I).

THE CHECK-OUT

In order to have some proof that the computing program was duplicating the action of the actual airplane, calculations were made using the initial conditions which were approximately the same as those used for drop tests that were made on the airplane. The calculated loads were then compared to the measured loads. The results of this comparison are shown in Figures 8 and 9.

CONDITIONS COMPUTED

Table 9 shows the conditions computed. These conditions were divided into groups which were arranged to provide data on the effect of one or two major variables on the airplane loads. Thus, Category "A" provides data on the effect of terrain slope plus secondary information on the effect of sliding coefficient of friction; Category "B" provides information on the effects of bump size, Category "B-4" being a special investigation to determine the effect of a series of discrete bumps; Category "C" provides information on the effect of continuous undulations plus secondary information on the effect of sliding coefficient of friction; and Category "J" provides information on the effect of rolling coefficient of friction. Six conditions were also computed to investigate the effects of taxiing over evenly spaced bumps.

STRUCTURAL WEIGHT ESTIMATION

Weight increases were determined from load-time histories of critical loading conditions imposed on the various structural components. Allowable stresses were taken from the Grumman Aircraft Company stress analysis report for each structural area. Weight penalties were adjusted to reflect existing margins of safety of each structural item in question on the OV-1 airplane.

Fuselage bending weight penalties were calculated using the concept of equivalent thickness. The fuselage was divided into sections with the average combined skin-stiffener cross-sectional area reduced to an equivalent thickness. New required equivalent thicknesses were then calculated for each representative section for the loads imposed by each new loading condition. Total fuselage bending weight was obtained by integrating the sectional area requirements over the entire fuselage length. Fuselage shear requirements

were determined using the same representative fuselage sections as above for bending. The shear weight increase for the entire fuselage was determined by integrating the sectional requirements.

Wing weight requirements for wing shear, torsion, and bending were determined separately. Required bending areas were determined as described above for fuselage bending. Wing vertical shear was assumed to be resisted by the shear webs only and wing torsion by the total wing box, i.e., skins and shear webs. Representative weights for spanwise sections were determined and integrated as before for total weight values. Weight increments for the store stations, equipment racks and engine supports were calculated by determining the components of each which are affected by the various loading conditions, assuming a linear relationship between the weight of the component and the load. Equipment rack weights determined in this manner were added to the section fuselage weight in which they were located.

Weight penalties for the landing gears and their supporting structures were determined with the aid of the data and equations contained in Reference 37. Side loads on the landing gears were not calculated in this study. Side loads on the landing gears would affect the strength requirements of the landing gears and their support structure but would have a negligible effect on the strength requirements of the basic wing and fuselage structure. The weight penalties which were calculated for increased vertical and drag loads are considered to be conservative, and since the provision for increased vertical and drag loads will inherently provide increased strength for side loads, no increased weight penalty for side loads was considered necessary.

AIRPLANE PERFORMANCE

Performance Characteristics of the OV-1 Mohawk

In the following paragraphs, the methods of determining the take-off, landing and radius characteristics of the OV-1 Mohawk airplane are described. Included in this description are the definition and derivation of the landing and take-off runway parameter, ρ_{TO} and ρ_{L}.

The take-off, landing and radius characteristics of the OV-1 are derived from aerodynamic and engine data obtained from the Grumman Aircraft Engineering Corporation (GAEC).

The equations used to determine the take-off and landing performance, which are derived in the following paragraphs, allow determination of the take-off and landing performance for variations in gross weight, runway friction and runway slope for the entire range of variables considered in this study. The aerodynamic forces and engine characteristics used in these calculations are given in Reference 30. The aerodynamic forces are based on wind tunnel tests of a 1/7-scale model, and the engine characteristics are derived from engine and propeller manufacturers' estimates corrected for installation effects. The radius characteristics of the OV-1 are obtained for various airplane gross weights and fuel quantities based on the propulsion system data shown in Reference 30 and aerodynamic data derived by the GAEC from flight test results supplied informally to the Contractor.

Take-off Performance

Derivation of the take-off ground roll equation, climb distance over a 50-foot obstacle, and the take-off runway parameter, ρ_{TO}, are given in the following paragraphs. The total take-off distance over a 50-foot obstacle as a function of airplane weight and take-off runway parameter is shown in Figure 10. These distances are shown for a main flap deflection of 15 degrees. The take-off speeds shown in Figure 11 correspond to the minimum single engine control speed given in Reference 30. The total take-off distance is the sum of the ground roll distance required to accelerate to take-off speed plus the ground roll distance covered during rotation from taxiing attitude to flying attitude plus the horizontal distance required to clear a 50-foot obstacle. The take-off distance methods given below result in total take-off distances that agree with those given in Reference 30. Take-off distances given in Reference 30 show good agreement with flight test results.

Ground Run Distance

Take-off ground run distance is obtained from

$$S = \frac{1.69^2}{2} \int_0^{(V_{to})^2} \frac{d(V^2)}{a_x}$$

The acceleration, a_x, is obtained from the summation of the forces parallel to the ground:

$$a_x = \frac{g}{W} \left[X - \mu_R (W \cos \theta - L) - W \sin \theta \right] .$$

The X force (thrust minus drag) and the lifting force, L, are dependent on aircraft speed, angle of attack, and engine thrust. These forces are shown in Figure 12 versus speed at take-off thrust and at the taxi angle of attack of 6.8 degrees.

In order to define the effects of runway slope and overall coefficient of runway friction in a single parameter, a take-off runway parameter, ρ_{TO}, has been developed. Such a parameter makes it unnecessary to consider the separate effects of runway slope and coefficient of friction and thus simplifies the presentation of the terrain effects on take-off distances. The take-off runway parameter, ρ_{TO}, is defined as

$$\rho_{TO} = \sin \theta + \mu_R (\cos \theta - L/W) .$$

In order for this take-off runway parameter to account for the combined effects of runway slope and overall coefficient of runway friction, the integrated average of the lift-to-weight ratio (L/W) during take-off must be constant for all weights considered. An investigation of the lift-to-weight ratio for the range of take-off weights considered showed that the lift-to-weight ratio varied from .53 to .58 for practicable values of runway slope and coefficient of friction. An average value of the lift-to-weight ratio of .55 was used. For small values of runway slope, the cosine of the runway slope can be set equal to one, and therefore the runway take-off parameter may be expressed as

$$\rho_{TO} = \sin \theta + .45 \mu_R .$$

Expressing the X force shown in Figure 12 as a function of speed by

$$X = 6400 - .42\ V^2$$

and using the above-defined runway parameter, the acceleration may be written

$$a_x = \frac{g}{W}\left(6400 - .42\ V^2 - \rho_{TO}\ W\right) .$$

The integral for ground run distance is

$$S = \frac{1.69^2}{2}\ \frac{W}{g}\int_0^{(V_{TO})^2} \frac{d(V^2)}{6400 - \rho_{TO}\ W - .42V^2} .$$

With the weight and runway parameter constant, integration of this expression yields

$$S = -\frac{1.69^2}{2g}\ \frac{W}{.42}\ \ln\left[1 - \frac{.42}{6400 - \rho_{TO}\ W}\ V_{TO}^2\right] .$$

The above determination of the take-off ground run distance does not account for the effect on ground run distance due to rotating the airplane from the taxi attitude to the take-off attitude. As described in Reference 30, an additional ground run distance to account for the effects of rotation must be added to the distances derived above to obtain the total ground run distance. These distances are shown in Figure 14.

Distance Over 50 Feet

The horizontal distances covered from lift-off to a 50-foot obstacle are shown in Figure 13. These distances, which were taken from Reference 30, are based on a pull-up after take-off utilizing a load factor that results in a speed at the obstacle that is equal to the take-off speed.

The sum of the calculated ground roll distance, the incremental distances to account for rotation effects, and the distances covered in the climb to 50 feet, results in total take-off distances which agree well with those shown in Reference 30.

Landing Performance

Derivation of the landing distance equations and the landing runway parameter, ρ_L, are given in the following paragraphs. The total landing distances as a function of airplane weight and landing runway parameter are given in Figure 15. These distances are shown for a 45-degree main flap deflection. The landing speeds shown in Figure 16 are 10 percent higher than the stall speed given in Reference 30. The total landing distance is the sum of the horizontal distance from a 50-foot obstacle to touchdown and the ground distance required to stop.

Distances To Clear a 50-Foot Obstacle

The horizontal distance from a 50-foot obstacle to touchdown is based on holding a constant sink rate of 14 feet per second and constant approach speed to touchdown. No flare is included prior to touchdown. The distance is calculated by

$$S = 50 \left[\frac{1.69 \times V_{Apr}}{V_v} - 1 \right]$$

Ground Roll Distance

The ground roll distance has been determined in two segments. The first segment, which accounts for the time delay during application of reverse thrust, has been approximated by the distance required for a 2-second ground roll without changing speed. This approximation is necessary because the ground roll distance covered during this phase is dependent upon the pilot technique used to apply reverse thrust, and unknown variations in engine power and aerodynamic characteristics that occur during transition to full reverse thrust.

The second segment of the ground roll is the distance required to stop with full reverse thrust and maximum braking. Second segment distance is given by

$$S = -\frac{1.69^2}{2} \int_0^{(V^2_{Apr})} \frac{d(V^2)}{a_x}$$

The acceleration, a_x, is given by

$$a_x = \frac{1}{W/g} \quad (T - D - W \sin \theta - \mu_B P_{v_m})$$

The normal force on the main wheels, P_{v_m}, is obtained by summing moments about the airplane c.g. and forces normal to the ground.

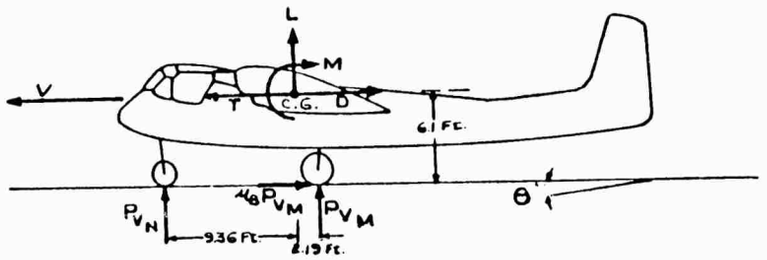

$$M + 9.36\ P_{v_n} - 6.1\ {}_B P_{v_m} - 2.19\ P_{v_m} = 0$$

$$W \cos \theta - L - P_{v_m} - P_{v_n} = 0$$

Combining the above and solving for the force on the main wheels, P_{v_m}, yields

$$P_{v_m} = \frac{9.36}{9.36 + 2.19 + 6.1\mu_B} \left(W \cos \theta - L + \frac{M}{9.36}\right)$$

Substituting for P_{V_m} in the equation for acceleration,

$$a_x = \frac{1}{W/g}\left\{T - D - W\left[\sin\theta + \frac{9.36\mu_B}{11.55 + 6.1\mu_B}\left(\cos\theta - \frac{L - \frac{M}{9.36}}{W}\right)\right]\right\} .$$

As in the case of the take-off distance calculations, a runway parameter has been developed in order to allow a single representation of the effects of the runway slope and rolling coefficients of friction. This parameter, ρ_L, is defined as

$$\rho_L = \sin\theta + \frac{9.36\mu_B}{11.55 + 6.1\mu_B}\left[\cos\theta - \frac{L - \frac{M}{9.36}}{W}\right] .$$

In order that this function, ρ_L, adequately combines the effects of runway slope and rolling coefficients of friction, the integrated average value of the expression $\frac{L - \frac{M}{9.36}}{W}$ must be constant for all landing weights considered.

For practical ranges of runway slopes and coefficients of friction, it was found that this parameter did allow correlation of these two variables into a single function.

For small values of runway slope, the cosine of the runway slope is set equal to one. Substituting the average, integrated value of $\frac{L - \frac{M}{9.36}}{W}$ into the above expression for ρ_L results in the following expression for the landing runway parameter:

$$\rho_L = \sin\theta + \frac{9.36\mu_B}{11.55 + 6.1\mu_B} .$$

The acceleration is then

$$a_x = \frac{1}{W/g}\quad (T - D - \rho_L W) .$$

Using the above expression for the acceleration, the equation for second segment distance is

$$S = -\frac{1.69^2}{2}\ \frac{W}{g}\ \int_0^{(V_{Apr})^2} \frac{d\,(V^2)}{T - D - \rho_L W} .$$

The thrust, T, and airplane drag, D, for the landing roll-out with full reverse thrust applied are shown versus speed in Figure 17. Because of the shape of the combined thrust minus drag forces versus speed, a good approximation of average thrust and drag may be obtained by evaluating these terms at .5 times the landing speed. Using these approximate average forces, the second segment stopping distance is obtained from

$$S = -\frac{1.69}{2}\frac{W}{g}\frac{V_{Apr}^2}{T_{.5V_{Apr}} - D_{.5V_{Apr}} - \rho_L W} \quad .$$

The total landing ground roll is the sum of the distances calculated for the two roll-out segments.

The sum of the two roll-out segments and the distance over a 50-foot obstacle results in total landing distances that are in good agreement with those shown in Reference 30.

Radius Determination

The radius characteristics of the OV-1 have been determined for a mission that includes a warmup and take-off allowance, cruise to the target at speed for maximum range at sea level, one minute over the target at maximum speed, and return at speed for maximum range at sea level with a reserve allowance consisting of 10 percent initial fuel. Fuel consumptions are based on the engine manufacturer's specification and are increased 5 percent. The mission profile is shown in Figure 18. These radii have been determined for the OV-1 configured with two 150-gallon external fuel tanks and without external armament. The fuel tanks are retained throughout the mission. The cruise characteristics of the OV-1 in this configuration are presented in Figure 19 as specific range (nautical miles per pound) versus weight and airspeed.

Figure 20 presents the radius as a function of fuel on board for two basic weights (take-off weight less fuel). These basic weights correspond to the unmodified OV-1 airplane (10,491 pounds) as derived from Reference 25, and for an arbitrary increase in basic weight of 2000 pounds. The internal fuel capacity of 1900 pounds is derived from Reference 30. No changes in the airplane external lines are considered for the modified airplane.

Performance of the VTOL Airplane

The radius capability of the VTOL airplane used for comparison with the OV-1 has been calculated based on estimated airplane drag and engine fuel consumption from engine manufacturer's specifications.

The drag characteristics of the VTOL are determined from analysis of parasite drag and induced drag. The method used to obtain parasite drag was developed from a study of flight test data on twenty-one airplanes of varying configurations. This method relates the parasite drag of the airplane components to their respective wetted areas, fineness ratio or thickness ratios, and an equivalent flat plate skin friction coefficient. The induced drag, which is determined by the effective airplane span, is estimated by use of wind tunnel data on a similar, canard VTOL configuration and theoretical analysis of interference effects between forward and aft wings. These methods are described in detail in Reference 38. The total parasite drag area, f, and effective span, b_e, are tabulated in Table 2.

Basic engine fuel consumption characteristics are obtained from Reference 39. The engine performance has been reduced by 6 percent to account for installation losses. An estimated propeller efficiency at cruise of .83 is used.

The mission specified for this study consists of a sea level cruise out on two engines, military power climb to 4000 feet, plus 1 minute military power combat, and cruise back at sea level. Five minutes at normal rated power is assumed for warmup, take-off, and landing, and a reserve of 10 percent of total fuel is provided.

The calculated values of combat radius and maximum speed for the VTOL configuration are summarized in Table 10 for the four airplane weights considered.

RESULTS

LOADS

Eighty items of information were obtained at .002-second intervals or less from the loads computing program for each of the landing conditions noted in Table 9. The items of load information consisted of time histories of ground reactions, gear loads, gear displacements, wing and fuselage accelerations, shears and bending moments, and accelerations of major mass items (see page 57, Appendix I). The presentation of this complete mass of data in the present report would not serve a useful purpose; however, typical load data are presented to show significant results. Curves of the data from typical landings on each of the most important types of terrain are presented. Loads and accelerations for a landing on smooth terrain are also presented (Figures 21 to 23) so that the effects of terrain variation may be visualized by comparison. Results will be categorized according to the surface irregularities shown in Figure 7.

1. Terrain Slope

In computing the loads for landings on runways which sloped upward in the direction of airplane motion, it was assumed that the pilot could adapt the airplane attitude to the local slope, but that the flight path and, hence, the horizontal and vertical velocities, established by reference to the horizon, were unchanged. Under these conditions, slopes created an effective increase in sinking speed equal to

$$\Delta V_V = 1.689 V_A \sin \theta \quad \text{(feet per second)}$$

where V_V is in feet per second and V_A is in knots. At the airplane landing speed, V_A, 84.5 knots, each degree of slope created in increment of vertical speed of 2.5 feet per second. The variation of maximum vertical and horizontal landing gear loads with slope is shown in Figure 24.

It is possible to consider a uniform slope as the limiting case of a long bump. Hence, the results are approximately applicable to long smooth bumps with maximum slopes as shown. A long bump can be defined for these purposes as one which the half-length

(distance from beginning to the apex) is longer than the distance traveled during the period of impact. For this aircraft, high gear loads exist for approximately 0.2 second, and a long bump has a half-length of roughly 30 feet.

2. Soft Earth Landings

The effect of landings on soft earth is illustrated in Figure 25, which shows the gear loads experienced when the rolling coefficients of friction is 0.7 and the sliding coefficient is .4.

Soft earth landings have been investigated by the simple process of varying the static and rolling coefficients of friction which are used in the computations. The problem of relating the coefficients to measurable characteristics of the soil is left to other investigators. In this regard, it would appear that considerable work remains to be done inasmuch as rolling coefficients of friction which have been obtained under slow moving conditions probably are not applicable to the relatively high aircraft landing speeds.

Intuitively, one realizes that the important load in this case is the drag load on the gear. Figure 26 shows the variation of maximum drag load with rolling coefficient for the three initial sinking speeds together with the corresponding vertical loads. From these curves it is apparent that main gear vertical loads are not significantly increased by increases in coefficient of friction but that the drag load is increased substantially. Nose gear vertical loads are increased because of the nose-down airplane pitching moment created by the higher drag forces.

3. Single Bumps

The magnitude of the vertical gear load increment obtained when the airplane landed upon a single bump was dependent not only on the height of the bump, the sharpness or wave length, and the initial sinking speed, but also on the position of the airplane's initial touchdown relative to the bump. The last consideration made it necessary to determine the critical point of touchdown for each landing before proceeding with the rest of the investigation. Figure 27 shows the variation of the main gear

vertical load with time for three landings. The variation of peak load with point of touchdown relative to the bump is shown, together with a comparison with the load experienced on a smooth runway. Less severe load increments were observed when the shock strut was fully compressed, since at that time the tire had recovered and it helped to absorb the bump.

Figure 28 shows the vertical gear load-time variation for a bump 137 inches long. It will be noted that the peak load was obtained as the wheel passed a point on the bump which was between the maximum slope and the summit of the bump. For the 1-cosine contour used here, this means that the peak load was obtained as the wheel passed a point between one-quarter and one-half of the length of the bump. The effect of sinking speed is shown in Figures 29 and 30 for landings on a terrain which includes a single bump 3 inches high and 27.4 inches long. Figure 31 shows the effect of wave length, sink speed, and bump height on the magnitude of the maximum vertical load. In these figures, all landings were made at the critical point of touchdown.

The large magnitude of the load increment caused by relatively small bumps, when the initial sinking speed is high, requires special comment. Examination of other portions of the computer program output shows that the tire bottoms (or becomes flat) during a normal 12-feet-per-second landing. If the wheel encounters a bump during the period when the tire is flat, a sharp, high-velocity pulse is imparted to the gear which is additive to that caused by the airplane's sinking speed. Since the metering pin-orifice dimensions are not designed for this condition, the oil flow is essentially blocked, and the gear becomes a rigid strut. This phenomenon has been noted with carrier aircraft where severe damage was incurred when the gear rolled over an arresting cable at the time of maximum tire deflection. Figure 32 shows the recorded load from such a landing. In this case, the bump consisted of a 1-3/8-inch, multi-strand arresting cable undoubtedly compressed somewhat under load.

Although the highest gear loads were experienced with short bumps, the wing loads were often maximum when the frequency of the bump approached that of the

structure. This is illustrated typically by the following comparison, which shows the relationship between maximum main gear vertical and maximum wing moment for two 3-inch bumps of different length:

3" Bump Length (V_v = 17 fps)	Max. Vertical Gear Load (Lb.)	Max. Wing Mom.-Sta. 40 (In.-Lb.)
27.4	111,500	1,862,000
137	62,620	2,007,000

This result is not surprising since an analogy can be drawn to the response of a single degree of freedom system in which the response to a pulse is a function of the ratio of frequency of the pulse to the frequency of the system.

4. Continuous Undulations

All landings on continuous undulations were made with the point of initial touchdown at the start of a wave -- in other words, at the bottom of a trough. It was also assumed, in effect, that the undulation preceding the point of touchdown did not exist inasmuch as contact with this protuberance was ignored. The first undulation did not produce as high a load as the maximum from a single bump of the same shape because initial touchdown was not in the most critical location.

Typical time histories of gear loads and wing bending moments are shown in Figures 33 through 39. Figures 33 and 34 are for continuous undulations 3 inches high and 27.4 inches long. The comparable loads for a smooth field landing with the same sinking speed are shown by the dashed line. Although the second and third undulations produce loads higher than the first, it can be seen that this occurs when the smooth field landing load is increasing and that it is not a diverging phenomenon. The loads experienced in passing over these undulations during landings at three sink speeds are illustrated in Figures 35 through 37.

Similar data for undulations 137 inches long are shown in Figures 38 and 39. This spacing corresponds approximately to the highest structural mode considered (second wing bending). The gear loads and wing moments are maximum at the first undulation. It will be noted that the maximum wing moment exceeds the maximum for the shorter undulation by approximately 20 percent. It is apparent again that maximum loads are obtained at a time when the energy of initial impact is being absorbed. No evidence of load reinforcement on the second and third undulations can be seen.

5. Series of Discrete Bumps

The point of touchdown for these landings was chosen so as to make the gear load from the first bump maximum as was done with the single bump. The second bump was spaced so as to supply load pulses at the natural frequencies of the structure.

Typical time histories of gear and wing loads are shown in Figure 40. It was found that in no case did the second bump gear load exceed that from the first, nor did a structural load from the second pulse exceed that from the first. Thus, maximum loads and weight penalties for the series of bumps were identical to those from the single discrete bumps.

6. General Comment on the Multiple Bump Cases

The lack of load reinforcement in both the continuous undulation and series of bump cases was quite unexpected. In retrospect, however, it now becomes obvious that the superposition of primary energy absorption with the bump effect must produce maximum loads in the early part of the load-time history. Undoubtedly substantial resonance would be introduced if the multiple bump cases were carried out over a longer distance; however, in the estimation of the author, this procedure would be rather unrealistic and unnecessarily conservative as a design criterion. It would appear prudent, nevertheless, to include a precautionary note to the effect that landings on terrain with many uniformly spaced bumps or undulations should be avoided.

7. Take-off and Taxi

Figures 41 to 43 show critical loads for taxiing over discrete bumps spaced to coincide with natural frequencies of the airplane. In this investigation it was assumed that the landing impact had taken place before the bump was encountered; hence, the shock strut and tire were in the static position and the wing lift was zero at the time the obstacles were encountered. Augmentation of the loads was noticed on the second and the third bumps, but it was not of great magnitude. The loads were small compared to the maximum loads caused by impact landings on the same sized bumps. Determination of the significance of these loads from the standpoint of fatigue would require a statistical knowledge of operations not currently available.

8. Effects of Airplane Flexibility

The effects of airplane flexibility were investigated for several cases by comparing the loads computed in the standard manner with those computed for a rigid airplane. The latter loads were obtained by removing the modal data from the computing program. A comparison of the flexible versus rigid loads for two discrete bump cases is shown in Figures 44 and 45. It will be noted that the gear loads are changed very little by airplane flexibility but that substantial dynamic effects are noted in the internal structural loads. When the bump is short, wing moments for the flexible airplane are less than those for the rigid airplane. When the bump is long, wing moments for the flexible airplane are substantially higher than those for the rigid airplane. Dynamic amplification up to 1.50 was measured on wing bending moments at the longer wave lengths.

WEIGHT INCREASES

Weight increases as a function of terrain roughness are presented in Figures 46 to 56. It is to be noted that all curves, except those which investigate bump location or spacing, present the weight increments for the worst landings on each type of terrain and for the worst combination of landings on a given terrain. Thus, for example, with the single bump landing, weights are given for landings in which the point of touchdown is most critical. Also, the weights include that produced by high nose-gear loads plus that caused by high main-gear loads even though the critical loads may be experienced by different landings on the same terrain.

The points at which these curves cross the abscissa are the terrain roughnesses at which modification to the OV-1 is necessary in order to prevent failure. Table 12 summarizes this information. The terrain designators of Reference 31 are included as well as the numerical value of the terrain irregularity. The fourth matrix has not been utilized for the reasons stated on page 7.

It will be noted that the terrain designators provided by Reference 31 are not ideally suited to the present application for the reason that in many cases the class designators cover too broad a range of terrain roughness. For example, it is not possible to distinguish between 0 and 3 degrees of slope or between 0 and 3 inches of undulation height although a large difference in aircraft loading occurs in these ranges. It would be more convenient in Matrix I if the class designators corresponded to the slopes in degrees, and in Matrices II and III if the undulation or obstacle height were designated in inches.

The question arises as to whether the principle of superposition can be used in the application of these curves. There are two types of superposition that might be desired. First is the case where the terrain itself is additive, as, for example, when a bump is superimposed on a slope. The second is where the airplane is required to operate from two different types of terrain at different times. In the latter case, it is obvious that the two weight increments should not be additive because part of the weight provided for one terrain might well serve to supply part of the strength required for the other. On the other hand, it is apparent that not all the weight supplied for one terrain would be useful in resisting loads encountered in the second. Hence, for record purposes and for future reference, Table 11 was prepared.

This table shows each airplane item affected by each type of terrain and the weight increment involved. By using this table in the manner described in the accompanying explanatory note, the proper total weight for two or more terrains can be derived.

When two terrains are actually superimposed as mentioned in the first case above, the addition of weights is more nearly correct. Non-linearities of the dynamic system which would normally make superposition impossible are reduced by the fact that under the critical conditions the hydraulic flow through the metering orifice is essentially blocked by high strut velocities. If two bumps are superimposed, the addition of weights is approximately correct only when the second bump is placed at the position on the first bump where maximum load occurs. It is evident by examination of Figure 27 that a small bump placed beyond the crest of a large bump will not produce an addition to the critical load. Additional work is needed to define more precisely the effects of superimposed terrains.

THE EFFECT ON PERFORMANCE OF INCREASED STRUCTURAL WEIGHT

Based on the performance methods described on pages 16 to 23, the effects of increased structural weight on radius, take-off and landing distance, and take-off and landing speeds are shown in Figures 57 and 58. These structural weight increases cover the range of weight increases considered in Figures 46 to 56. In order to describe completely the effects of the structural weight increases, two different conditions have necessarily been considered:

1. Increasing the airplane take-off weight by the increase in structural weight.

2. Holding the airplane take-off weight constant by decreasing the fuel weight in proportion to the structural weight.

The effects on performance due to Condition 1 above are shown in Figure 57. Reference to Figure 57 will show that there is only a slight decrease in radius due to the increased structural weight and that the take-off distance is increased as the structural weight increases.

Figure 58 summarizes the performance effects when the take-off weight is held constant by decreasing the fuel weight as structural weight is added. In this case a significant loss in radius results, primarily due to changes in fuel quantity as the structural weight changes. Since the take-off weight remains constant, there is no take-off distance penalty. It should also be noted in this latter case that, since the landing distance is always less than the take-off distance, the field length is established by the take-off characteristics of the aircraft.

COMPARISON OF OV-1 AND VTOL PERFORMANCE

In this study it has been assumed that the maximum structural weight penalty that should be considered for the OV-1 is that which would result in the radius of the OV-1 being equal to that of a VTOL aircraft having the same take-off weight as the OV-1. Two take-off conditions have been imposed on the OV-1 under this assumption:

1. The take-off weight is allowed to increase as the structural weight increases, resulting in an increase in take-off distance.

2. The take-off weight remains constant by decreasing the fuel weight as the structural weight is increased, resulting in a constant take-off distance.

Four terrain conditions have also been considered:

1. Varying field lengthwise slope.

2. Various length and height of continuous undulations.

3. Various sizes of discrete bumps.

4. Various degrees of field bearing capacity or softness, as expressed by the rolling coefficient of friction.

In this analysis the rolling coefficient and runway slope are described by the runway parameter, ρ_{TO} and ρ_{L}, described on page 16. It has been pointed out that it has not been possible to correlate these runway parameters with a specific type of soil description.

To compare the OV-1 and VTOL performance, Figure 59 has been prepared, which presents the radius of the OV-1 as a function of take-off weight and various structural weight penalties. The variation in take-off weight results from varying both the fuel weight and the structural weight penalties. The cross-hatched line in the upper right-hand corner represents the OV-1 with full fuel. Superimposed on Figure 59 is the variation in radius of the VTOL airplane with take-off weight.

If the take-off weight of the OV-1 is allowed to increase as the structural weight is increased, assuming, therefore, no field length limitation, the intersection of the VTOL radius-take-off weight curve with the OV-1 full fuel radius-take-off weight curve indicates the take-off weight and radius which are equal for the two types of aircraft. Furthermore, the maximum structural weight penalty that can be imposed on the OV-1 is indicated. This structural weight penalty amounts to approximately 1200 pounds. Thus, the OV-1 can operate from field for which the terrain roughness will require no more than 1200 pounds increase in structural weight before being inferior in performance to the VTOL airplane.

By definition, the take-off distance over a 50-foot obstacle establishes the runway length. If the runway length and, hence, the take-off weight remain constant, then the point of equal OV-1 and VTOL take-off weight and radius must be determined for less than full fuel weights of the OV-1. In order to determine the points of equal VTOL and OV-1 take-off weight and radius, Figure 60 has been prepared. The information in Figure 60 is obtained by:

1. Assuming a given runway length and runway parameter and from Figure 10 reading the take-off weight.

2. At this take-off weight from Figure 10, entering Figure 59 and, at the intersection of the VTOL radius take-off weight lines, reading the structural weight penalty of the OV-1.

For example, for a total runway length of 2000 feet and a runway parameter of 0.1, the take-off weight from Figure 10 is 14,700 pounds. For a take-off weight of 14,700 pounds in Figure 59, the intersection of the VTOL and OV-1 take-off weight-radius curves occurs at a structural weight

penalty of 800 pounds for the OV-1. As noted previously, the field length is established by the OV-1 take-off distance requirements since the take-off distances exceed the landing distances.

In order to correlate the structural weight penalties with the four terrain conditions considered, Figures 61 through 67 have been prepared. These figures are determined by associating the structural weight penalties shown in Figure 60 for the various runway lengths and runway parameters with the structural weight penalties required to operate from the various types of terrain considered in Figures 46 through 56. Thus, Figure 61 shows the landing runway slope for which equal VTOL-OV-1 take-off weight and radius are obtained for various runway lengths and take-off runway parameters.

Similarly, Figures 62 to 64 indicate the effects of undulation height and length. Figures 65 and 66 indicate the effects of bump length and bump height, and Figure 67 shows the effect of rolling friction.

To clarify the use and significance of Figures 61 through 67, illustrative examples are presented in the following paragraphs. Since the take-off runway parameter is a major variable in these curves, the definition and physical significance of this item will be reviewed first.

The take-off runway parameter, ρ_{TO}, is the average resistance to forward motion attributable to the runway during take-off, expressed as a fraction of airplane weight. It is composed of two components, one resulting from the horizontal component of the aircraft weight which exists on sloping terrain and the other from rolling friction. Mathematically,

$$\rho_{TO} = \sin\theta + .45\,\mu_R$$

where θ is the general slope of the take-off runway. The constant .45 accounts for the fact that during take-off part of the weight is supported by wing lift (see page 18). Values of ρ_{TO} from -0.1 to +0.3 are shown in the curves. A value of -0.1 could occur on a downhill take-off on a hard runway; a value of +0.3 could occur with many combinations of rolling coefficient of friction and/or upward slope of the take-off runway.

To illustrate the use of Figures 61 through 67, assume that one wishes to determine what landing area slope will require the addition of sufficient structural weight to the OV-1 airplane that its performance (range) will be reduced to that of a VTOL airplane of equal weight. The answer will depend on (a) the sinking speed which the airplane experiences during the landing and (b) the length, slope and hardness of the take-off runway. Assume the following as separate examples:

	(a)	(b)	(c)
Sinking Speed, fps	12	12	17
Take-off Runway Length, ft.	1500	1000	2000
ρ_{TO}	.1	.1	0

The answers are obtained from Figure 61 as shown below:

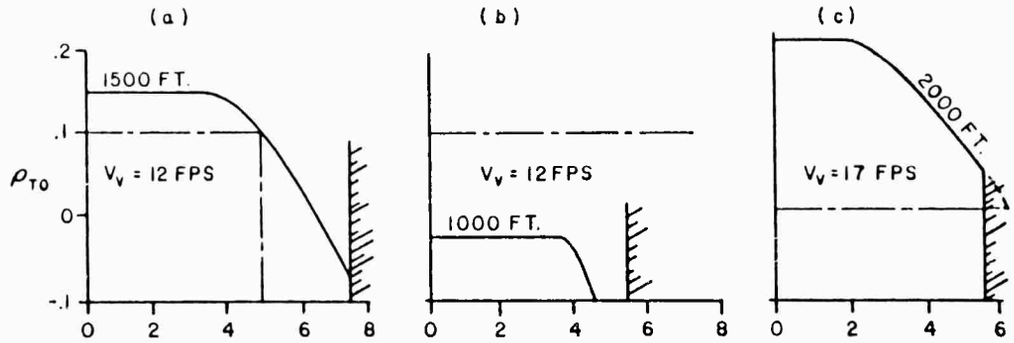

In example (a), the answer is 4.9°. In example (b) the answer is that with this short take-off runway, the OV-1 performance is inferior to the VTOL performance regardless of landing area slope. Under assumption (c), the answer is that the slope could be 6.2°, but because of OV-1 fuel capacity limitations, the range of the OV-1 and the VTOL aircraft is the same when the landing area slope is 5.5°.

The procedure for use of the other curves is identical to the above. Figure 65, however, requires special comment. The structural weight required to prevent failure when landing on a bump of a given height bears an inverse relationship to length of bump (i.e., the shorter the bump, the greater the weight increment). Hence, the intersection of the horizontal line corresponding to ρ_{TO} with the curve in Figure 65 gives the length of bump below which the OV-1 performance is inferior to the VTOL airplane performance. All other curves give values of terrain roughness above which the OV-1 performance becomes inferior to the VTOL airplane performance.

It should be noted that the effects of the take-off runway parameter shown in Figure 61 through 67 do not include structural weight penalties that may be associated with increased runway friction and slope during landing. The additional loads imposed on the aircraft during take-off due to increased runway slope and rolling coefficient of friction are negligible and thus require no increase in structural weight. However, for a field bearing capacity and slope described by the take-off runway parameters, significant structural weight penalties may be required to withstand loads imposed by high rolling friction during impact or by landing on a positive slope. Figures 61 and 67 show the values of runway slope and rolling coefficients, respectively, during landing which give equal OV-1 and VTOL performance. The slopes and rolling coefficients used to define these curves are independent of the values which are involved in the take-off parameter.

In order to reduce the volume of figures that can be obtained, the data in Figures 61 through 67 are shown for a sliding friction coefficient of 0.4 only, since the weight variation with sliding coefficient is relatively small. However, should data be desired for other values of the sliding coefficient of friction, similar curves may be determined in the manner described above.

Table 13 contains the terrain characteristics for equal OV-1/ VTOL performance for certain discrete points on the above curves. The corresponding terrain designators from Reference 31 are included.

load pulses which occur in landing on undulations or series of discrete bumps will create additional fatigue damage which should be considered in new designs.

RECOMMENDATIONS

The ultimate objectives of work in the area of rough-terrain loads are, first, to develop methods and obtain basic data which will permit the accurate prediction of aircraft loads by analytical means, second, to develop design criteria which may be used to establish initial conditions for the analytical computations and, third, to provide practical means for operating personnel to determine whether a particular field falls within the permissible limits of roughness for the aircraft they are using. With these objectives in mind and with the experience gained on the present project, the following recommendations are made:

1. In order to establish the accuracy of the dynamic analysis used herein, it is recommended that a test program be initiated in which the loads on a landing gear can be measured during simulated rough-terrain landings.

2. In order to permit the analytical study of landings on objects of small radius of curvature, it is recommended that load-deflection data be obtained for tires bearing on this type obstacle. In addition, it is recommended that the analytical methods be extended to permit the investigation of loads induced when a landing gear encounters an obstacle with radius smaller than the tire.

3. It is recommended that analytical studies be made of the side loads induced when a bump is traversed obliquely.

4. Statistical data on sinking speeds, approach speeds and airplane attitudes for airplanes operating in and out of unprepared fields should be obtained in order to provide fundamental information for the load criteria.

5. Additional work is needed to provide the means of converting fundamental soil characteristics to the rolling resistance of tires traveling at high speed on soft soil.

6. It is recommended that the terrain designation system be modified to make it more suitable for aircraft operation. Such modification would include the following:

APPENDIX I - EQUATIONS OF MOTION

NOTATION

Theory	Fortran	Definition	Units
$a, \dot{a}, \ddot{a}$	A	Motion at axle parallel with strut of unsprung mass of rolling assembly, positive down.	in.,sec.
$\bar{a}$		Distance from lower piston bearing to axle parallel to strut with strut fully extended.	in.
A_0		Gross orifice area w/o reduction for pin.	$in.^2$
A_1		Internal area of oleo piston	$in.^2$
A_2		Piston area based on i. d. of lower bearing	$in.^2$
A_p	AP	Metering pin area, function of strut stroke	$in.^2$
a_i		Slopes of line equation for pin diameter	-
$[A_{ij}]$		Aerodynamic damping coefficients	1/sec.
$\alpha \dot{\alpha} \ddot{\alpha}$	Alpha	Angular motion of rolling assembly	RAD.,Sec.
b_i		Intercepts of line equations for pin diameter	in.
$\bar{b}$		Distance from upper to lower piston bearing parallel to strut, strut fully extended	in.
$[B_{ij}]$		Coefficients of displacements in airplane equation of motion	$1/sec.^2$
C	C	Tire deflection	in.
$\bar{C}$		Damping coefficient perpendicular to strut	lb.-sec./in.

NOTATION (Cont'd)

Theory	Fortran	Definition	Units
C_D		Coefficient of discharge	-
C_C		Discharge coefficient for compression	-
C_E		Discharge coefficient for extension	-
C_N		Maximum allowable tire deflection	in.
$\lvert C_1 \rvert$		Coefficient of force from gear	$1/lb.sec.^2$
$\Delta, \dot{\Delta}, \ddot{\Delta}$	D	Motion at axle perpendicular to strut of unsprung mass of rolling assembly, positive aft	in.,sec.
$\bar{\Delta}, \dot{\bar{\Delta}}, \ddot{\bar{\Delta}}$	BD	Motion at axle in relative coordinates	in.,sec.
δ		Distance from axle to gear attach point with strut fully extended	in.
D_o	DO	Coefficient of oil damping force in oleo	$lb/sec.^2/ft.^2$
$\lvert D_1 \rvert$		Coefficient of moment from gear	$1/ft.lb.sec.^2$
$\bar{e}$		Distance from axle to strut $\mathbb{Q}$ normal to strut, positive for axle forward	in.
$\lvert E_1 \rvert$		Vector column of constants	$1/sec.^2$
ϕ		Angle of strut with vertical, positive for strut forward of gear attach point	
F_A	FA	Load on axle parallel to strut, positive down	lb.
$F_\perp$	FP	Load on axle $\perp$ to strut, positive aft	lb.

NOTATION (Cont'd)

Theory	Fortran	Definition	Units
F_H	FH	Load on airplane from gear, $\perp$ to reference plane, positive down	lb.
F_1	F1	Normal force on upper piston bearing, positive aft	lb.
F_2	F2	Normal force on lower piston bearing, positive aft	lb.
g		Gravitational constant	in./sec.^{2}
$\lvert G_i \rvert$		Coefficient of moment from gear	
$\lvert H_i \rvert$		Coefficient of force from gear	
I_R		Mass moment of inertia of rolling assembly	lb.in.sec.^{2}
K_1		Strut influence coefficient, deflection fwd. due to force acting down parallel to strut	in./lb.
K_{32}, K_{33}		$K_{32}+S\,K_{33}$ is deflection aft due to force acting aft perpendicular to strut	in./lb., 1/lb.
k_1, k_2		Coefficients of gear force for horizontal accelerations	-
λ		Instantaneous skidding velocity	ft./sec.
λ/V_L	SR	Slip ratio	-
ℓ_i		Intercepts in lines for tire load	lb.
m_i		Slopes in lines for tire load vs. deflection	lb./in.
n		Polytropic exponent for strut air load	-
o		Subscript to denote initial conditions	-

NOTATION (Cont'd)

Theory	Fortran	Definition	Units
P_A	PA	Strut air load	lb.
P_D	PD	Drag load in horizontal plane	lb.
P_E	PE	Airload in olec with strut extended	lb.
P_F	PF	Bearing friction force on strut	lb.
P_O	PO	Strut oil load	lb.
$P_\perp$	PP	Force at axle (relative coordinates) perpendicular to strut positive fwd.	lb.
P_T	PT	Tire load	lb.
P_V	PV	Vertical ground reaction load	lb.
$[P]$		Coefficients of generalized displacement	ft. or in.
$Q, \dot{Q}, \ddot{Q}$	A	Airplane motion, generalized coordinates	-, 1/sec., $1/sec.^2$
ρ_o		Mass density of hydraulic fluid	$lb.sec.^2/in.^4$
R_O		Radius of undeflected tire	in.
R	R	Instantaneous rolling radius of tire	in.
$[R]$		Coefficients of generalized acceleration	-
$S, \dot{S}, \ddot{S}$	S	Strut motion measured from full extension	in.,sec.
S_c		Maximum strut stroke	in.
S_i		Values of S associated with pin constants	in.

NOTATION (Cont'd)

Theory	Fortran	Definition	Units
$[S]$		Coefficients of $\ddot{Q}$ in equation for airplane loads	-
t		Time	sec.
Δt		Interval of numerical integration	sec.
t_F		End of integration	sec.
$\lvert T_{Hi} \rvert$		Generalized airplane coefficients of force at gear attaching point	in./lb.sec.^{2}
$\lvert T\alpha_i \rvert$		Generalized coefficients of moments at gear attaching point	1 lb/sec.^{2}
μ		Coefficients of friction identified (numerically) by its subscript	-
μ_1		Bearing coefficients friction before strut moves - static friction	-
μ_2		Bearing coefficients after strut moves	-
μ_s	GRMU	Ground coefficient sliding friction	-
μ_R	GRMU	Ground coefficient rolling friction	-
$\lvert u \rvert$		Arbitrary constants in equation for loads on airplane	-
V_E		Air volume in oleo strut extended	in.^{3}
V_L		Forward velocity of airplane	in./sec.
$[V]$		Coefficients of generalized velocities	in. or ft.

NOTATION (Cont'd)

Theory	Fortran	Definition	Units
W_U		Unsprung weight of gear	lb.
W_N		Airplane net weight supported by gear	lb.
X	X	Horizontal coordinate of ground contact point for rough terrain function	in.
X_i		Arguments in table of terrain roughness, $0 = i = 700$	in.
X_A	XA	Axle coordinate, horizontal displacement along terrain roughness	in.
X_1, X_2, X_3, X_4		Coordinates used to define terrain	in.
X_o		Initial (starting value) of X	in.
Y_B, $\dot{Y}_B$, $\ddot{Y}_B$	YB	Motion at top of strut	in.sec.
Z	Z	Vertical coordinate of ground contact point for rough terrain function	in.
Z_A	ZA	Axle displacement from touchdown, positive down	in.
Z_o		Initial (starting value) of Z	in.
θ		Ground slope	Rad.
TAN θ	TAN	Printed for instantaneous value of ground slope	-
A,B,C,D		Amplitudes of terrain roughness entered in X-table, positive down	in.
M_α	AM	Moment from gear, positive airplane nose up	ft.lb.

NOTATION (Cont'd)

Theory	Fortran	Definition	Units
p		Multiple of Δt at which printing of program output takes place	-
	VA	Vertical accelerations	
	PA	Pitching acceleration	
	SH	Shear	
	BM	Bending moment	
	TQ	Torque	
	AA	Airplane angle of attack	
	AV	Airplane pitching velocity	
	APA	Airplane pitching acceleration	
	VP	Airplane vertical position	
	VV	Airplane vertical velocity	
	AVA	Airplane vertical acceleration	
	HA	Airplane horizontal acceleration	

EQUATIONS OF MOTION

GEAR EQUATIONS

$$\ddot{\Delta} = \left[-P_V \sin\Phi + P_D \cos\Phi - P_\perp + W_U \sin\Phi\right] \div \frac{W_U}{g}$$

$$\ddot{a} = \left[- P_V \cos\Phi - P_D \sin\Phi + F_A + W_U \cos\Phi\right] \div \frac{W_U}{g}$$

$$= \left[T_{H_1}\right] \left| \ddot{Q}_1 \right| \cos\Phi \quad \text{Before the strut moves}$$

$$\ddot{\alpha} = \mu P_T \left(R_o - \frac{C}{2}\right) \div I_R$$

$$F_\perp = \left[-\bar{\Delta} - K_1 F_A\right] \div \left[K_{32} + S K_{33}\right]$$

$$P_\perp = - F_\perp + \bar{C} \dot{\Delta}$$

$$F_A = P_A + P_O + P_F$$

$$= \frac{W_U}{g} \ddot{a} + P_V \cos\Phi + \mu P_V \sin\Phi - W_U \cos\Phi$$

Before the strut moves

$$F_1 = \frac{P_\perp (\bar{a}-S) - F_A (\bar{e}-\bar{\Delta})}{\bar{b} + S}$$

$$F_2 = F_1 + P_\perp$$

$$P_F = \left|\mu_1 F_1\right| + \left|\mu_1 F_2\right|$$

$\dot{S} \geq 0$, P_F positive

$\dot{S} < 0$, P_F negative

$\mu_1 = \mu_1$ Before strut moves

$= \mu_2$ After strut moves

$$\ddot{Y}_B = \left[T_{H_1}\right] \left| \ddot{Q}_1 \right|$$

$$\ddot{\bar{\Delta}} = \ddot{\Delta} - \ddot{Y}_B \sin\Phi + (\delta - S) \left[T_{\alpha_1}\right] \left| \ddot{Q}_1 \right|$$

$$\ddot{S} = \left[T_{H_1}\right] \left| \ddot{Q}_1 \right| \cos\Phi - \ddot{a}$$

$$P_A = (P_E + 14.7A_2) \left[\frac{V_E}{V_E - SA_2}\right]^n - 14.7A_2$$

$$P_O = D_o \dot{S} \left|\dot{S}\right| \qquad D_o = \frac{\rho_o (A_1 - A_p)^3}{2\left[C_D (A_0 - A_p)\right]^2}$$

$$A_p = \frac{\pi}{4} (a_1 S + b_1)^2$$

$$C = R_o - R$$

$$P_T = \ell_1 + m_1 C$$

$$\lambda/_{V_L} = 1 - \frac{(R_o - \frac{C}{2})\dot{\alpha} + \dot{\Delta} \cos \phi}{V_L}$$

$\mu = \mu_S$ Before spinup

$= \mu_R$ After spinup

$$P_V = P_T \cos \theta + \mu P_T \sin \theta$$

$$P_D = - P_T \sin \theta + \mu P_T \cos \theta$$

Criterion for strut motion $F_A \geqslant P_E + P_F$

$$X_A = X_o + V_L t - \Delta \cos \phi + a \sin \phi$$

$$Z_A = Z_o + \Delta \sin \phi + a \cos \phi$$

$$X = X_A - R \sin \theta$$

$$Z = A \left[1 - \cos 2\pi \frac{X - X_1}{X_2 - X_1}\right] + C$$

$$\text{TAN } \theta = \frac{2\pi A}{X_2 - X_1} \sin 2\pi \frac{X - X_1}{X_2 - X_1} + C$$

$$R = \left[(X - X_A)^2 + (Z - Z_A)^2\right]^{1/2}$$

$$\sin \theta = \frac{\text{TAN } \theta}{(1 + \text{TAN}^2 \theta)^{1/2}}$$

$$\cos \theta = \frac{1}{(1 + \text{TAN}^2 \theta)^{1/2}}$$

AIRPLANE EQUATIONS

$$\left|\ddot{Q}_i\right| = \left[A_{ij}\right]\left|\dot{Q}_i\right| + \left[B_{ij}\right]\left|Q_i\right| + F_{H_1}\left|C_i\right|_1 + F_{H_2}\left|C_i\right|_2 + M_{\alpha_1}\left|D_i\right|_1 + M_{\alpha_2}\left|D_i\right|_2 + \left|E_i\right|$$

$$F_H = -F_A \cos\phi - F_\perp \sin\phi$$

$$M_\alpha = (\delta - S) F_\perp$$

$$\left[A_{ij}\right] = -\left[T^*MT + T^*A_1T\right]^{-1}\left[T^*A_2T\right]$$

$$\left[B_{ij}\right] = -\left[T^*MT + T^*A_1T\right]^{-1}\left[T^*KT + T^*CT + T^*A_3T\right]$$

$$\left|C_i\right| = \left[T^*MT + T^*A_1T\right]^{-1}\left|T^*_{H_i}\right|$$

$$\left|D_i\right| = \left[T^*MT + T^*A_1T\right]^{-1}\left|T_{\alpha_i}\right|$$

$$\left|E_i\right| = -\left[T^*MT + T^*A_1T\right]^{-1}\left\{W_{U_1}\left|T^*H_1\right| + W_{U_2}\left|T^*_{H_2}\right| - \delta_1 W_{U_1}\sin\phi_1\left|T^*\alpha_1\right| - \delta_2 W_{U_2}\sin\phi_2\left|T^*\alpha_2\right| - \left[T^*A_2T\right]\left|\dot{Q}_i\right|_{t=o}\right\} \quad \text{when} \quad \left|\ddot{Q}_i\right|_{t=o} = 0$$

INTEGRATION EQUATIONS

Prediction

$$\bar{X}_{N+1} = X_N + \Delta t\dot{X}_N + .5\,\Delta t^2\ddot{X}_N$$

$$\dot{\bar{X}}_{N+1} = \dot{X}_N + 1.5\,\Delta t\ddot{X}_N - .5\,\Delta t\ddot{X}_{N-1}$$

Correction

$$X_{N+1} = X_N + \Delta t\dot{X}_N + .5\,\Delta t^2\ddot{\bar{X}}_{N+1}$$

$$\dot{X}_{N+1} = \dot{X}_N + .5\,\Delta t\ddot{X}_{N+1} + .5\,\Delta t\ddot{X}_N$$

where $X = a, \Delta, \alpha, Q$

EQUATIONS FOR LOADS

Accelerations $= \left[R_{ij}\right] \left| \ddot{Q}_i \right|$

Shear, Bending Moment,

Torque $= \left[S_{ij}\right] \left| \ddot{Q}_i \right| + F_{H_1} \left|H_i\right|_1 + F_{H_2} \left|H_i\right|_2 + M_{\alpha_1} \left|G_i\right|_1 + M_{\alpha_2} \left|G_i\right|_2 + \left|u_i\right|$

Displacement $= \left[P_{ij}\right] \left| Q_i \right|$

Velocities $= \left[V_{ij}\right] \left| \dot{Q}_i \right|$

Horizontal Acceleration $= (k_1 P_{D_1} + k_2 P_{D_2}) \div W_N$

AERODYNAMIC LIFT AND MOMENT *

The following formulas for lift, "P", and moment, "M", take into account the change in aerodynamic forces during landing and taxi. It is assumed that the air stream velocity is constant, and that the contribution to lift of circulation lag is negligible.

$$P = -\rho b^2 \Delta X \left[v\pi\dot{\alpha} + \pi\ddot{h} - \pi ba\ddot{\alpha} \right] - 2\pi\rho\Delta X v^2 b\alpha$$
$$- 2\pi\rho\Delta X v b\dot{h} - 2\pi\rho\Delta X v b^2 (.5 - a)\dot{\alpha}$$
$$= -\pi\rho \left[b^2\Delta X\ddot{h} - b^3 a\Delta X\ddot{\alpha} \right] - \pi\rho v \left[b^2\Delta x\dot{\alpha} \right]$$
$$-\pi\rho v2 \left[b\Delta X\dot{h} + b^2 (.5 - a)\Delta X\dot{\alpha} \right] - \pi\rho v^2 2 \left[b\Delta X\alpha \right]$$

$$M = -\rho b^2 \Delta X \left[\pi (.5 - a) vb\dot{\alpha} + \pi b^2 (1/8 + a^2)\ddot{\alpha} - a\pi b\ddot{h} \right]$$
$$+ 2\rho\Delta X v b^2 \pi (a + .5) \left[v\alpha + \dot{h} + b (.5 - a)\dot{\alpha} \right]$$
$$= -\pi\rho \left[-ab^3\Delta x\ddot{h} + b^4 (.125 + a^2)\Delta Z\ddot{\alpha} \right]$$
$$-\pi\rho v \left[b^3 (.5 - a)\Delta X\dot{\alpha} \right]$$
$$-\pi\rho v2 \left[-b^2 (a + .5)\Delta X\dot{h} + b^3 (a^2 - .25)\Delta X\dot{\alpha} \right]$$
$$-\pi\rho v^2 2 \left[-b^2 (a + .5)\Delta X\alpha \right]$$

The aerodynamic coefficients occurring in the equations of motion are A_1, A_2, A_3. In the form given below, these coefficients are equivalent to those shown above.

Coefficient of $\ddot{h}$, $\ddot{\alpha}$

$$-\left[A_1 \right] = -\pi\rho \left[F_3 \right]$$

Coefficient of $\dot{h}$, $\dot{\alpha}$

$$-\left[A_2 \right] = -\pi\rho v \left[F_2 \right] - \pi\rho v d_1 \left[H_1 \right]$$

Coefficient of α

$$-\left[A_3 \right] = -\pi\rho v^2 d_1 \left[H_2 \right]$$

* Notation in this section is that of Theodorsen (Reference 42)

Where

$$\left[H_1\right] = \begin{bmatrix} \Delta Xb & \Delta Xb^2\ (.5 - a) \\ -\Delta Xb^2\ (.5 + a) & \Delta Xb^3\ (-.25 + a^2) \end{bmatrix}$$

$$\left[H_2\right] = \begin{bmatrix} 0 & \Delta Xb \\ 0 & \Delta Xb^2\ (.5 + a) \end{bmatrix}$$

$$\left[F_2\right] = \begin{bmatrix} 0 & \Delta Xb^2 \\ 0 & \Delta Xb^3\ (.5 - a) \end{bmatrix}$$

$$\left[F_3\right] = \begin{bmatrix} \Delta Xb^2 & -\Delta Xb^3 a \\ -\Delta Xb^3 a & \Delta Xb^4\ (.125 + a^2) \end{bmatrix}$$

d_1 is the slope of the lift curve over π. In Theodorsen's expressions $d_1 = 2\pi/\pi = 2$, which is infinte aspect ratio. For the general case in which $dC_L/d\alpha$ is experimentally determined, $d_1 = dC_L/d\alpha/\pi$. The generalized coefficients are $\left[T^*A_1T\right]$, $\left[T^*A_2T\right]$, $\left[T^*A_3T\right]$.

LOADS ON THE AIRPLANE STRUCTURE

The airplane may be fully represented in the generalized coordinate system. A maximum of eighteen generalized coordinates, Q, may be used. In the sectional coordinate system, X, the airplane is divided into as many mass bays as desired. Each bay may have six degrees of freedom: translation along or rotation about three axes. The transformation from generalized to sectional coordinates is given by $x = [T]Q$ where $[T]$ is a modal transform matrix. In the landing impact analysis the generalized vectors, Q, $\dot{Q}$, $\ddot{Q}$, are available at all times.

Through the use of the modal transform matrix, the sectional displacements, velocities, and accelerations at all points on the airplane structure are available for computing loads.

OUTPUT OF COMPUTER PROGRAM

The following were printed for each of two gears at time intervals of .002 sec. or less:

P_A	Strut air load	lb.
P_o	Strut oil load	lb.
P_F	Strut friction force	lb.
F_A	Axle load $\parallel$ strut	lb.
$F_\perp$ = FP	Axle load $\perp$ strut	lb.
$P_\perp$ = PP	Axle load $\perp$ strut in relative coordinates	lb.
F_1	Aft normal force on upper bearing	lb.
F_2	Forward normal force on lower bearing	lb.
P_T	Tire load	lb.
P_V	Vertical ground load	lb.
P_D	Horizontal drag load	lb.
F_H	Gear face on airplane	lb.
M_γ = AM	Gear pitching moment on airplane	ft.-lb.
A_P	Area of metering pin	$in.^2$
D_O	Oil force damping coefficient	$lb.sec.^2/in.^2$
λ/V_L=SR	Slip ratio	-
X_A, Z_A	Coordinates of axle	in.
X, Z	Coordinates of ground contact point	in.
TAN θ	Slope of terrain at ground contact point	-
C	Tire deflection	in.
R	Rolling radius of ground contact point	in.

OUTPUT OF COMPUTER PROGRAM (Cont'd)

$\mu_{R,S}$ =	GRMU ground coefficients of friction	-
$s, \dot{s}, \ddot{s}$	Strut motion in strut direction	in.,sec.
$a, \dot{a}, \ddot{a}$	Axle motion in strut direction	in.,sec.
$\Delta, \dot{\Delta}, \ddot{\Delta}$	Axle motion $\perp$ strut	in.,sec.
$\bar{\Delta}, \dot{\bar{\Delta}}, \ddot{\bar{\Delta}}$	Axle motion $\perp$ strut in relative coordinate	in.,sec.
$*Y_B, \dot{Y}_B, \ddot{Y}_B$	Motion at top of strut	in.,sec.
$\alpha, \dot{\alpha}, \ddot{\alpha}$	Angular motion of rolling assembly	Rad.,sec.
VA	Vertical acceleration at 10 stations	in./sec.^{2}
PA	Pitching acceleration at 4 stations	Rad./sec.^{2}
SH	Shear at 7 stations	lb.
BM	Bending moment at 7 stations	in.-lb.
TQ	Torque at 3 stations	in.-lb.
AA	Airplane pitch angle	Rad.
AV	Airplane pitching velocity	Rad./sec.
APA	Airplane Pitching acceleration	Rad./sec.^{2}
VP	Vertical position of airplane C.G.	in.
VV	Vertical velocity of airplane C.G.	in./sec.
AVA	Vertical acceleration of C.G.	in./sec.^{2}
HA	Horizontal acceleration of C.G.	g's

* These quantities are not computed before the strut moves. They are printed as zero.

OUTPUT OF COMPUTER PROGRAM (Cont'd)

The following data are general:

t	Time	sec.
$Q, \dot{Q}, \ddot{Q}$	Airplane response vectors	-

APPENDIX II

DESIGN CRITERIA FOR ROUGH TERRAIN LANDINGS

DISCUSSION

The requirements of Reference 40 represent an accumulation of experience with landing loads which has been developed over many years. Army aircraft, whose mission requires operation in and out of unprepared fields, should be designed for the requirements of Reference 40 and for the special conditions proposed herein.

Paragraph 3.2.1 of Reference 40 permits the use of analysis methods contained in Section 4 of the specification. These methods are simplifications or approximations of a dynamic analysis which are, perhaps, justified on the basis of long experience with and extensive analysis of airplanes which land on normal runways. Since the equivalent amount of background is not available for airplanes which are intended to land on rough terrain, and because the dynamic phenomena associated with such an operation are so complex, similar approximations in the determination of rough-terrain loads are not warranted. For these reasons, the proposed criteria require a complete dynamic analysis similar to that described in the body of this report. This recommendation is made with the full realization that initial calculations on a new airplane will still be a gross approximation because of the lack of accurate input data. However, the intent is that such initial calculations should be refined as the design progresses until a reasonably accurate solution is obtained. In this manner, an understanding of the dynamic phenomena will be evolved which will permit the development of approximate methods for preliminary designs on subsequent aircraft.

One of the primary parameters necessary for the design criteria is the airplane sinking speed. Ideally, the value chosen should be based on a statistical analysis of a large amount of flight test data from landings made on unprepared runways by typical Army aircraft. Since such data are lacking, the value chosen is based on the values provided in Table I of Reference 40 and corresponds to that of the USAF primary and basic trainers. The decision is somewhat arbitrary but is based on the assumption that a larger value than that of the typical Air Force airplane should be used because the unprepared fields may also be short fields. Short field landings will require unusual pilot techniques which include higher sinking speeds.

The factor of probability has always entered into design criteria and especially into landing loads criteria. A certain amount of attrition is expected and permissible on the basis that all airplanes should not be penalized by the weight necessary to provide strength for extreme conditions. The proposed criteria attempt to account for probability to the extent that engineering judgment is used to eliminate improbable combinations of loading conditions. Thus, sinking speeds higher than 13 feet per second may be expected on the basis of Navy experience with carrier landings. The proposed criteria combine the 13-feet-per-second sinking speed with slopes which effectively give the airplane strength for smooth field landings of 23 feet per second. However, strength is not required for extremely high sinking speeds combined with high slopes, nor for maximum slopes combined with maximum bumps. Also, the number of successive undulations is limited to two on the assumption that natural undulations will not normally be uniformly spaced.

The magnitude of the terrain roughness is based in general on the analysis provided in the present report and corresponds to those roughnesses which cause the performance of the STOL aircraft to become equal to that of the comparable VTOL aircraft. It is believed, however, that a gear designed especially for the alleviation of bump loads will provide strength for roughness with substantially less weight than computed herein. Hence, the bump height criterion has been increased approximately 50 percent. Inasmuch as the numerical values of terrain roughness have been established by a study of a specific airplane, the criteria should not be applied to vehicles of substantially different size or configuration without additional investigation.

The proposed criteria are written so that they may be introduced into MIL-8860 series of specifications in a manner similar to the special requirements for carrier-based aircraft (Reference 41).

PROPOSED CRITERIA

Airplane Strength and Rigidity

Additional Loads for Rough Terrain Landings

The paragraphs shall read the same as those in MIL-A-8862 except as follows:

1. Scope

1.1 This specification defines the strength and rigidity requirements for aircraft whose mission requires operation in and out of unprepared landing areas. The ground load requirements specified in MIL-A-8862 shall also apply.

3. Requirements

3.2.1 A dynamic landing loads analysis shall be performed which considers the operational characteristics of the gear and the elastic properties of the gear and airplane structure. The analysis shall provide ground loads and structural loads as a function of time for the initial conditions specified herein. The method and scope of the analysis shall be subject to approval of the Procuring Agency.

3.2.2 Not applicable.

3.2.7 Design Sinking Speed Requirements - A basic design sinking speed of 13 feet per second shall apply in conjunction with the landplane landing design gross weight.

3.2.8a Symmetrical Landings - The airplane shall land at the design sinking speed in the attitudes specified in Table II of MIL-A-8862 on terrain whose surfaces are defined by the following table:

TABLE I

Type of Terrain	Numerical Description	Remarks
Slopes in direction of aircraft motion	4° from horizontal datum plane	Lateral slope = 0
Soft earth	Coefficient of rolling friction = .2 to 1.0. Coefficient of sliding friction = .2 to .6.	
Bumps	Number = 2 (identical) Shape = 1-cosine Height = 3 inches Length = all critical Spacing = length	Oriented 90° with respect to aircraft motion. Point of touchdown relative to bump = most critical

Prior to ground contact, the airplane shall be in a steady state condition, i.e., all accelerations shall be equal to zero. Wing lift shall be equal to 1.0 W.

3.2.8b Unsymmetrical Landings - The airplane shall land on the terrain specified in paragraph 3.2.8a at the following combinations of initial sinking speed and roll angle:

V_v	Φ
fps	DEG.
11.5	5
6.5	7.5

The pitch attitudes shall be the highest and the lowest used in paragraph 3.2.8a. In the dynamic analysis, a three-gear analysis is preferred, but it shall be permissible to compute only loads for the first and second gears to contact the ground and to disregard the loads from the third gear.

3.2.9 Side Loads - Side loads shall be determined by a dynamic analysis in which the bumps described in Table I are oriented at 30, 45 and 60 degrees with the direction of airplane motion, or alternately, side loads in either direction equal to 0.4 times the maximum vertical load obtained from paragraph 3.2.8a shall be assumed to act at the rim of the wheel throughout the time of impact. In the latter method, the gear and structure loads from the side load at the ground shall be determined using rigid body assumptions.

3.3.4 Taxiing - The airplane shall traverse the terrain described in Table I at all speeds up to the landing speed. Prior to encountering this terrain, the airplane load factor shall be 1.0 and the tires and gear shall be in the static positions.

3.5.1 Rebound - The rebound load shall be either that specified in paragraph 3.5.1 of MIL-A-8862 or the load computed from the instantaneous release of the maximum gear load obtained from section 3.2.8a above, whichever is greater.

REFERENCES

1. Walls, James H., Houbolt, John C., and Press, Harry, "Some Measurements of Power Spectra of Runway Roughness", NACA TN 3305, November 1954.

2. Houbolt, John C., Walls, James H., and Smiley, Robert F., "On Spectral Analysis of Runway Roughness and Loads Developed During Taxiing", NACA TN 3484, July 1955.

3. Thompson, Wilbur E., "Measurements and Power Spectra of Runway Roughness at Airports in Countries of the North Atlantic Treaty Organization", NACA TN 4303, July 1958.

4. Schuck, George, "Rough Terrain Landing Gear Evaluation Program", Goodyear Aircraft Corp. Report GER 9244, 15 Mar. 1959 (ASTIA Document AD 206902).

5. Anon., "Report of Test. Project NR AVN 161. Service Test of the AO-1A Airplane", U. S. Army Aviation Board, Fort Rucker, Alabama, 9 June 1961.

6. Hesch, H. E., "Stress Analysis for the Grumman Model YAO-1 Main Landing Gear", Grumman Aircraft Engineering Corp. (GAEC) Report No. 1626, Apr. 27, 1959.

7. Pedigi, Howard, "Stress Analysis for the Grumman Model YAO-1 Nose Landing Gear", GAEC Report No. 1628, Apr. 15, 1959.

8. Taglarine, T. A., "Structural Description Report, Model AO-1AF", GAEC Report No. 3900.2.

9. Renkewitz, Fred E., and Alles, W., "Structural Weight and Balance, Moments of Inertia and Unit Inertia Loads, Model AO-1CF", GAEC Report No. 3901.

10. Sposito, J., and Besendorfer, W., "Ground Loads, Model AO-1CF", GAEC Report No. 3903.3.

11. Renkewitz, Fred E., and Terney, Norman, "Resultant Loads, Shears, Bending Moments and Torsions for Wing, Model AO-1CF", GAEC Report No. 3907.1.

12. Fleming, W. A., and Koczan, J., "Stress Analysis of Wing Center Section, Model AO-1CF", GAEC Report No. 3907.22.

13. Haliber, W. B., "Stress Analysis of External Store Supports, Model AO-1CF", GAEC Report No. 3907.29.

14. Krebs, N., "Fuselage Net Loads, Model AO-1CF", GAEC Report No. 3908.1.

15. Visconti, J., and Taglarine, T., "Elastic Analysis of Wing and Fuselage, Model AO-1CF", GAEC Report No. 3908.11.

16. Krebs, N., "Stress Analysis of Fuselage Nose Section, Model AO-1CF", GAEC Report No. 3908.211.

17. Johnston, J., Krebs, N., and Zarny, P., "Stress Analysis of Fuselage Mid-Section, Model AO-1CF", GAEC Report No. 3908.212.

18. Fleming, W., "Engine Attachment Loads, Model AO-1CF", GAEC Report No. 3909.1.

19. Fleming, W., "Stress Analysis of Engine Supports, Model AO-1CF", GAEC Report No. 3909.21.

20. Taglarine, T. A., "Strength Summary and Operating Restrictions, Model AO-1CF", GAEC Report No. 3920.

21. Griffiths, M. F., "Summary of Test Results, Model YAO-1", GAEC Report No. 3930.2.

22. Petralia, J. J., "Results of Main Landing Gear Static Tests, Model YAO-1", GAEC Report No. 3934.11.

23. Morrison, A., "Results of Main Gear Dynamic Tests, Model YAO-1", GAEC Report No. 3934.13.

24. Morrison, A., "Results of Nose Gear Dynamic Tests, Model YAO-1", GAEC Report No. 3934.23.

25. Aeder, R. G., "Actual Weight and Balance Report, 7th YAO-1 Airplane of Contract NOa(s) 57-841-C", GAEC Report No. 3951D.

26. Nordin, J. F., "Actual Weight and Balance Report, 1st AO-1AF Airplane of Contract NOw 60-0040", GAEC Report No. 3951J.

27. Zentgraf, John K., "Ground Vibration Survey of the YAO-1 Airplane", GAEC Report No. DA134-521.1.

28. Zentgraf, John K., "Ground Vibration Survey of the YAO-1 Airplane with External Stores", GAEC Report No. DA134-521.2.

29. Crafa, V. J., Sholinsky, A., and Ridley, A., "Justification of Aerodynamic Data for the Standard Aircraft Characteristics Chart of March, 1960, Model AO-1AF", GAEC Report No. X134-105-7.

30. Crafa, V. J., Sholinsky, A., and Ridley, A., "Substantiating Performance Data for the Standard Aircraft Characteristics Chart of March 1960", GAEC Report No. XA 134-105-8.

31. Bredahl, A. R., and Kiefer, E. P., "A Classification System for Unprepared Landing Areas", Planning Research Corporation, ARDC-TR-57-20, Jan. 1957 (ASTIA Document No. AD 115-606).

32. Bekker, M. G., "Evaluation of Vehicle Sinkage in Off-the-Road Locomotion", Land Locomotion Research Branch Report No. 3, June 1958, Dept. of the Army, Ordnance Corps, Ordnance Tank-Automotive Command, Center Line, Michigan.

33. Anon., Land Locomotion Research Laboratory Report No. 4, 1956, Dept. of the Army, Ordnance Corps, Ordnance Tank-Automotive Command, Center Line, Michigan.

34. Terzaghi, Karl, Theoretical Soil Mechanics, John Wiley and Sons, Inc., 1943.

35. Anon., "A Soil Value System for Landing Locomotion Mechanics", Landing Locomotion Research Branch Report No. 5, Dept. of the Army, Ordnance Corps, Ordnance Tank-Automotive Command, Center Line, Michigan.

36. Barndollar, E. J., "Dynamic Loads Analysis", Douglas Report SM 23895, Vol. V, Jan. 12, 1962.

37. Liebermann, Carl R., "Rolling Type Alighting Gear Weight Estimation", Society of Aeronautical Weight Engineers Technical Paper No. 210, May 1959.

38. Anon., "Tri-Service VTOL Transport Performance Data", Douglas Aircraft Co. Report No. ES 40206, Part II, Book 6, March 31, 1961.

39. Anon., "Lycoming Model LTC4B-8 Turboprop Engine", Lycoming Preliminary Model Specification No. 124.20, Jan. 16, 1961.

40. Anon., "Airplane Strength and Rigidity, Landplane Landing and Ground Handling Loads", Military Specification, MIL-A-8862(ASG), May 1960.

41. Anon., "Airplane Strength and Rigidity, Additional Loads for Carrier-Based Landplanes", Military Specification, MIL-A-8863(ASG), May 1960.

42. Theodorsen, T., and Garrick, I. E., "Nonstationary Flow About a Wing-Aileron-Tab Combination Including Aerodynamic Balance", NACA Report No. 736, 1942.

TABLE 1

OV-1 AIRPLANE - GENERAL DATA

Wing Span, ft.	42.0
Overall Length, ft.	41.0
Tail Height, ft.	12.7
Wing Area, sq. ft.	330
Airfoil	NACA 2412
Horizontal Surface Area, sq. ft.	85
Power Plant - 2 Lycoming T-53-L3 Turbo-Prop	

TABLE 2

VTOL AIRPLANE SIZE VARIATION

Take-Off Weight, lb.	10,000	12,000	14,000	16,000
Wing Span, ft.	5.4	7.1	9.0	11.0
Effective Span, ft.	24.0	26.5	29.2	32.1
Overall Length, ft.	43	43	43	43
Tail Height, ft.	19.0	19.0	19.0	19.0
Wing Area, sq. ft.	111	135	164	198
Propeller Diameter, ft.	5.4	7.1	9.0	11.0
Total f, sq. ft.	5.9	6.2	6.5	6.9
Airfoil				
Root	NASA 63-221			
Tip	NASA 63-218			
Power Plant	2 Lycoming LTC4B-8 Shaft Turbines			

TABLE 1

VTOL AIRPLANE WEIGHT SUMMARY

Gross Weight (lb)	10,000		12,000		14,000		16,000	
	Wt	Tot	Wt	Tot	Wt	Tot	Wt	Tot
Structure		2983		3292		3594		3991
Wing Group	291		446		611		875	
Tail Group	275		306		342		381	
Body Group	1278		1347		1395		1436	
Alighting Gear-Main	234		276		317		358	
-Nose	70		82		94		106	
Surface Controls	729		729		729		729	
Engine Section	106		106		106		106	
Propulsion		3187		3605		4035		4532
Engine	1140		1140		1140		1140	
Accessory Gear Boxes	983		983		983		983	
Air Induction System	40		40		40		40	
Exhaust System	60		60		60		60	
Lubricating System	20		20		20		20	
Fuel System	54		192		302		399	
Engine Controls	30		30		30		30	
Starting System	100		100		100		100	
Propeller Installation	760		1040		1360		1760	
Equipment		1931		1931		1931		1931
Instruments	145		145		145		145	
Hydraulics	130		130		130		130	
Electrical	551		551		551		551	
Electronics	395		395		395		395	
Armament	197		197		197		197	
Furnishings-Personnel	73		73		73		73	
-Misc Equip	66		66		66		66	
-Cockpit & Cabin	120		120		120		120	
-Emergency	68		68		68		68	
Air Conditioning	40		40		40		40	
Anti-Icing	50		50		50		50	
Photographic	89		89		89		89	
Auxiliary Gear-Handling	7		7		7		7	
Weight Empty		8101		8828		9560		10,454
Useful Load		1899		3172		4440		5546
Crew	400		400		400		400	
Fuel	947		2205		3460		4555	
Oil	28		28		28		28	
Trapped Fuel & Oil	23		38		51		62	
Armament	324		324		324		324	
Misc Equipment	177		177		177		177	

TABLE 4

TERRAIN DESIGNATORS FOR MATRIX I

MATRIX I – THE LANDING AREA

AREA LENGTH (1st and 2nd Digits – Matrix I)		WIDTH SLOPE (3rd Digit – Matrix I)		LENGTH SLOPE (4th Digit – Matrix I)	
Class Designator	Actual Length Available (feet)	Class Designator	Width Slope (Degrees)	Class Designator	Length Slope (Degrees)
00	> – 10000	0	0 – 2	0	0 – 2
01	8000 – 10000	1	2 – 4	1	2 – 4
02	6500 – 8000	2	4 – 5	2	4 – 5
03	5000 – 6500	3	5 – 9	3	5 – 9
04	4000 – 5000	4	9 – 12	4	9 – 12
05	3000 – 4000	5	12 – 15	5	12 – 15
06	2500 – 3000	6	15 – 20	6	15 – 20
07	2000 – 2500	7	20 – 30	7	20 – 30
08	1500 – 2000	8	30 – 45	8	30 – 45
09	1000 – 1500	9	> – 45	9	> – 45
10	900 – 1000				
11	800 – 900				
12	700 – 800				
13	600 – 700				
14	500 – 600				
15	400 – 500*				
16	300 – 400*				
17	200 – 300*				
18	100 – 200*				
19	50 – 100*				

Note – The Parameter Categories are read:
From and including the shorter length and up to but not including the longer length or greater slope.

* These dimensions may be considered as area diameters unless a width limitation is indicated.

TABLE 5

TERRAIN DESIGNATORS FOR MATRIX II

MATRIX II – THE SURFACE CONFIGURATION

UNDULATION HEIGHT (1st Digit – Matrix II)		UNDULATION SLOPE (2nd Digit – Matrix II)		UNDULATION SPACING (3rd Digit – Matrix II)
Class Designator	Height (Inches or feet as indicated)	Class Designator	Slope (Degrees)	Center-to-Center Distance*
0	< 3"	0	0 – 2	*See Table 8 for center-to-center distance values and class designator
1	3" – 6"	1	2 – 4	
2	6" – 12"	2	4 – 8	
3	12" – 18"	3	8 – 10	
4	18" – 24"	4	10 – 15	
5	2' – 5'	5	15 – 20	
6	5' – 10'	6	20 – 30	
7	10' – 25'	7	30 – 45	
8	25' – 50'	8	45 – 60	
9	50' – 100'	9	60 – 90	

Note – The parameter categories are read: From and including the lesser, and up to, but not including the greater, height or slope.

Descriptive Subscript Legend

C – Small Stream or Creek
D – Ditch or Embankment (cultural rather than natural formations)
E – Erosion Gullies (natural rather than cultural formations)
H – Holes (irrespective of how formed)
M – Mounds
P – Plowed, tilled or cultivated furrows
R – Roads
S – Sand Dunes or Sand Ripples
W – Undulations parallel to width
L – Undulations parallel to length

TABLE 5 (Cont'd)

MATRIX II CENTER-TO-CENTER SPACING AND CLASS DESIGNATORS FOR UNDULATION HEIGHT CATEGORIES

UNDULATION SPACING FOR HEIGHT CLASS (0) (less than 3 inches height)		UNDULATION SPACING FOR HEIGHT CLASS (1) (3 – 6 inches height)		UNDULATION SPACING FOR HEIGHT CLASS (2) (6 – 12 inches height)		UNDULATION SPACING FOR HEIGHT CLASS (3) (12 – 18 inches height)		UNDULATION SPACING FOR HEIGHT CLASS (4) (18 – 24 inches height)	
Class Designator	C-to-C Distance (feet)	Class Designator	C-to-C Distance (feet)	Class Designator	C-to-C Distance (feet)	Class Designator	C-to-C Distance (feet)	Class Designator	C-to-C Distance (feet)
0	> – 10	0	> 250	0	> 500	0	> 750	0	> 1000
1	8 – 10	1	100 – 250	1	250 – 500	1	500 – 750	1	750 – 1000
2	6 – 8	2	50 – 100	2	100 – 250	2	250 – 500	2	500 – 750
3	5 – 6	3	25 – 50	3	50 – 100	3	100 – 250	3	250 – 500
4	4 – 5	4	10 – 25	4	25 – 50	4	50 – 100	4	100 – 250
5	3 – 4	5	5 – 10	5	10 – 25	5	25 – 50	5	50 – 100
6	2 – 3	6	3 – 5	6	5 – 10	6	10 – 25	6	25 – 50
7	1 – 2	7	2 – 3	7	2 – 5	7	5 – 10	7	10 – 25
8	0.5 – 1	8	1 – 2	8	1 – 2	8	2 – 5	8	3 – 10
9	< 0.5	9	< 1	9	< 1	9	< 2	9	< 3

UNDULATION SPACING FOR HEIGHT CLASS (5) (2 – 5 feet height)		UNDULATION SPACING FOR HEIGHT CLASS (6) (5 – 10 feet height)		UNDULATION SPACING FOR HEIGHT CLASS (7) (10 – 25 feet height)		UNDULATION SPACING FOR HEIGHT CLASS (8) (25 – 50 feet height)		UNDULATION SPACING FOR HEIGHT CLASS (9) (50 – 100 feet height)	
Class Designator	C-to-C Distance (feet)	Class Designator	C-to-C Distance (feet)	Class Designator	C-to-C Distance (feet)	Class Designator	C-to-C Distance (feet)	Class Designator	C-to-C Distance (feet)
0	> 2500	0	> 2500	0	> 2500	0	> 2500	0	> 2500
1	1000 – 2500	1	1500 – 2500	1	2000 – 2500	1	2000 – 2500	1	2000 – 2500
2	500 – 1000	2	1000 – 1500	2	1500 – 2000	2	1500 – 2000	2	1750 – 2000
3	250 – 500	3	500 – 1000	3	1000 – 1500	3	1250 – 1500	3	1500 – 1750
4	100 – 250	4	250 – 500	4	750 – 1000	4	1000 – 1250	4	1250 – 1500
5	50 – 100	5	100 – 250	5	500 – 750	5	750 – 1000	5	1000 – 1250
6	25 – 50	6	50 – 100	6	250 – 500	6	500 – 750	6	750 – 1000
7	10 – 25	7	25 – 50	7	100 – 250	7	250 – 500	7	500 – 750
8	6 – 10	8	12 – 25	8	50 – 100	8	100 – 250	8	200 – 500
9	< 6	9	< 12	9	< 50	9	< 100	9	< 200

TABLE 6

TERRAIN DESIGNATORS FOR MATRIX III

MATRIX III – THE SURFACE ROUGHNESS (OBSTACLES)

Obstacle Height (1st Digit – Matrix III)		Obstacle Spacing (2nd Digit – Matrix III)	
Class Designator	Height (Inches or Feet as Indicated)	Class Designator	Edge to Edge Distance (Inches or Feet as Indicated)
0	< 3"	0	> 1000'
1	3" – 5"	1	500' – 1000'
2	5" – 7"	2	100' – 500'
3	7" – 9"	3	50' – 100'
4	9" – 12"	4	25' – 50'
5	12" – 18"	5	10' – 25'
6	18" – 36"	6	3' – 10'
7	3' – 6'	7	1' – 3'
8	6' – 10'	8	6" – 12"
9	> 10'	9	< 6" (Very dense)

Note – The Parameter categories are read: From and including the first number, to but not including the second number (heights and spacings).

Descriptive Subscript Legend

B – Bushes
C – Cultivated Crops
D – Tree Stumps
F – Fence
G – Grasses
M – Transient man-made obstructions (Haystacks, etc.)
P – Permanent man-made obstructions (Building, Power Lines, etc.)
R – Rocks (Imbedded as opposed to loose)
S – Stones (Loose surface rocks)
T – Trees
H – Hedges

TABLE 7

TERRAIN DESIGNATORS FOR MATRIX IV

MATRIX IV – SOIL DESCRIPTION AND BEARING CAPACITY

SOIL BEARING CAPACITY (1st and 2nd Digits – Matrix IV)		SOIL CLASSIFICATION (3rd and 4th Digits – Matrix IV)	
Class Designator	California Bearing Ratio	Class Designator	Soil Description and Group Symbol (Unified Soil Classification)
00	> 20	00	(GW) Group – Gravel – Sand Mixtures – Well Graded
01	15 – 20	01	(GP) Group – Gravel – Sand Mixtures – Poorly Graded
02	12 – 15	02	(GM) Group – Silt, Sand, Gravel Mixtures
03	10 – 12	03	(GC) Group – Clayey Gravels
04	9 – 10	04	(SW) Group – Well Graded Sands
05	8 – 9	05	(SP) Group – Poorly Graded Sands
06	6.5 – 8	06	(SM) Group – Silty Sands
07	5.5 – 6.5	07	(SC) Group – Clayey Sands
08	4.5 – 5.5	08	(ML) Group – Inorganic Silts
09	3.5 – 4.5	09	(CL) Group – Inorganic Clays
10	2.0 – 3.5	10	(OL) Group – Organic Silts
11	1.5 – 2.0	11	(MH) Group – Inorganic Elastic Silts
12	1.0 – 1.5	12	(CH) Group – Inorganic Clays – High Plasticity
13	0.5 – 1.0	13	(OH) Group – Organic Clay and Silt – High Plasticity
14	< 0.5	14	(Pt) Group – Peat and Highly Organic Soils

TABLE 8

AIRPLANE CONCENTRATED MASSES AND THEIR LOCATIONS

MASS NUMBER	STRUCTURAL ELEMENT	MASS Lb.Sec^2/In.	LOCATION	
			FUSELAGE STATION	WING STATION
1	Wing	.262	171	237
2	Wing	.625	172	185
3	Wing	.162	175	136
5	Wing	.575	169	107
6	Wing	.435	176	70
8	Wing	.303	177	40
4	Engine and Prop	2.860	128	109
7	Main Landing Gear	.416	185	55
9	Nose Landing Gear	.090	45	0
10	Fuselage	2.363	56	0
11	Fuselage	.805	114	0
13	Fuselage	2.063	173	0
14	Fuselage	.613	228	0
15	Fuselage	.384	285	0
16	Fuselage	.181	332	0
17	Fuselage	.056	374	0
18	Fuselage	.601	446	0
12	Fuselage Fuel	.868	163	0
20	Rocket	.385	159	213
21	Rocket	.385	159	237
19	Wing Tanks	.442	173	185

Notes: Mass given for one-half of airplane.
Unsprung mass of landing gears not included.

TABLE 9 COMPUTED CONDITIONS

* Denotes Nose Down Landing
Δ Denotes Tail Down Landing
All Dimensions in Inches

1. Category A - Varying Slope, θ

Slope θ	V_v = 17 Ft/Sec			V_v = 12 Ft/Sec			V_v = 8 Ft/Sec		
	Sliding Coefficient of Friction μ_s								
	.2	.4	.55	.2	.4	.55	.2	.4	.55
0	*	*	*Δ						
2	*Δ	*	*Δ						
4	*Δ	*	*Δ	*Δ	*Δ	*Δ			
6	*Δ	*	*Δ	*Δ	*Δ	*Δ	*Δ	*Δ	*Δ
8				*Δ	*Δ	*Δ	*Δ	*Δ	*Δ
10							*Δ	*Δ	*Δ

2. Category J - Variable Rolling Coefficient of Friction

μ_R	V_v = 17 Ft/Sec	V_v = 12 Ft/Sec	V_v = 8 Ft/Sec
.03	*Δ		
.1	*Δ		
.2	*Δ		
.4	*Δ		
.5		*Δ	*Δ
.7	*Δ	*Δ	*Δ
.9	*Δ	*Δ	*Δ
1.1		*Δ	*Δ
1.3		*Δ	*Δ

Note: For a discussion of the various categories refer to Page 15.

TABLE 9 (Cont'd) COMPUTED CONDITIONS

3. Category C - Continuous Undulations

Height Z_{MAX}	Undulation Length, L											
	13.7			27.4			45.67			137		
	Sliding Coefficient of Friction											
V_V = 17	.2	.4	.55	.2	.4	.55	.2	.4	.55	.2	.4	.55
.5	*Δ	*Δ										
1.0	*Δ	*Δ		*Δ	*Δ	*Δ						
1.5	*Δ	*Δ	*Δ									
2				*Δ	*Δ	*Δ						
3				*Δ	*Δ	*Δ	*Δ	*Δ	*Δ			
4				*Δ	*Δ	*Δ				*Δ	*Δ	*Δ
4.5							*Δ	*Δ	*Δ			
6							*Δ	*Δ	*Δ			*Δ
8										*Δ	*Δ	*Δ
V_V = 12												
3				*Δ	*Δ							
4				*Δ	*Δ							
4.5							*Δ	*Δ				
5				*Δ	*Δ							
6							*Δ	*Δ		*Δ	*Δ	*Δ
7							*Δ	*Δ				
9										*Δ	*Δ	*Δ
V_V = 8												
3				*Δ	*Δ							
4				*Δ	*Δ							
4.5							*Δ	*Δ				
4.6				*Δ	*Δ							
5				*Δ	*Δ							
5.5				*Δ	*Δ							
6							*Δ	*Δ		*Δ	*Δ	
7							*Δ	*Δ				
9										*Δ	*Δ	

TABLE 9 (Cont'd) COMPUTED CONDITIONS

4. Category B - Single Bumps

Bump Length, L	Bump Height, Z_{MAX}				
	1.5	3.0	3.75	5.0	7.5
13.7	*Δ				
27.4		*Δ			
34.25		*Δ	*Δ		
45.7		*Δ		*Δ	
68.5		*Δ		*	*Δ
137		*Δ		*	*
220		*Δ			
360		*Δ			

TABLE 9 (Cont'd) COMPUTED CONDITIONS

5. Category B-4, Series of Discrete Bumps

$\mu_S = 0.4, \mu_R = .03, Z_{MAX} = 2", L = 27.4"$

Nose Down Attitude

Spacing	68.5	90.6	126	189.5	220.7	242.6

6. Take-off and Taxi Conditions

Bumps Spaced to Excite Structural Modes

$\mu_R = .03$, Nose Down (3 Pt) Attitude

Bump Height = 2 Bump Length = 27.4

Velocity V_A = 84.5 Knots = 1710 In. Per Sec.

Spacing	Load Frequency Per Second	Total No. of Bumps
68.5	25	5
90.6	18.9	5
126	13.6	3
189.5	9.02	4
220.7	7.75	4
242.6	7.05	3

TABLE 10

VTOL AIRPLANE PERFORMANCE SUMMARY

Take-off Weight	(lb)	10,000	12,000	14,000	16,000
Total Fuel	(lb)	945	2205	3460	4555
Take-off Distance	(ft)	VTO	VTO	VTO	VTO
Radius at Sea Level	(n.mi.)				
2-Engines, 250 kts		52	165	270	350
Maximum Speed at Sea Level	(kts)				
Normal Power		420	410	400	390
Military Power		455	440	430	415

TABLE 11. STRUCTURAL COMPONENT WEIGHT PENALTIES

SINK SPEED = 17 FPS	VARIABLE GROUND SLOPE												VARIATION IN ROLLING COEFFICIENT					
COEFFICIENT OF FRICTION	θ = 0			θ = 2°			θ = 4°			θ = 6°			μ_s = .4					
μ_s (EXCEPT AS NOTED)	V_v = 17 FPS			V_v = 21.94 FPS			V_v = 26.85 FPS			V_v = 31.73 FPS			ROLLING COEFFICIENT OF FRICTION					
	.2	.4	.55	.2	.4	.55	.2	.4	.55	.2	.4	.55	.03	.1	.2	.4	.7	.9
MAIN GEAR WHEEL AND TIRE	0	0	0	6.75	7.3	7.86	33.7	35.6	37.5	80.5	82.1	83.8	0	0	0	0	0	4.0
MAIN GEAR AND SUPT STR	0	0	0	16.6	30.3	43.9	269.0	284.0	299.0	543.0	556.0	569.0	0	0	0	0	19.6	113.4
NOSE GEAR WHEEL AND TIRE	0	0	0	.88	1.44	2.0	8.14	8.87	9.61	16.8	16.2	17.7	0	0	0	0	6.6	13.0
NOSE GEAR AND SUPT STR	0	0	0	5.98	7.59	9.2	55.31	55.6	55.97	108.8	108.5	108.2	0	0	0	15.0	84.1	147.2
WING STATION 0 TO 55	0	0	0	0	0	0	55.1	51.8	48.4	204.0	202.0	200.0	0	0	0	0	23.05	0
WING STATION 55 TO 103	0	0	0	0	0	0	37.7	38.0	38.3	142.0	143.0	144.0	0	0	0	0	0	0
WING STATION 103 TO 203	0	0	0	0	0	0	3.5	3.5	3.5	27.0	27.0	27.0	0	0	0	0	0	0
ENG MT SUPT STR	0	0	0	3.0	4.0	7.0	31.0	32.0	33.0	66.0	66.5	67.0	0	0	0	0	0	0
EXT STORE RACK AND SUPT	0	0	0	0	0	0	0	0	0	12.0	12.0	12.0	0	0	0	0	0	0
FUS STA 66 TO 146	0	0	0	0	0	0	8.0	10.1	12.3	45.9	47.5	50.1	0	0	0	0	3.5	22.0
FUS STA 146 TO 230	0	0	0	1.75	3.0	5.0	21.5	45.8	35.7	70.46	75.3	83.9	0	0	0	0	2.0	15.0
FUS STA 230 TO 328	0	0	0	1.75	2.0	3.0	22.0	35.6	24.9	70.0	72.1	79.2	0	0	0	0	4.2	67.6
FUS STA 330 TO 415	0	0	0	0	0	0	0	0	0	7.0	8.0	8.9	0	0	0	0	0	12.1
TOTAL WEIGHT PENALTY*				36.8	55.7	78.5	571.0	630.0	629.0	1561	1587	1631	0	0	0	15.0	144.9	497.0

SINK SPEED = 12 FPS	θ = 4°			θ = 6°			θ = 8°			ROLLING COEFFICIENT OF FRICTION					
	V_v = 21.85 FPS			V_v = 26.8 FPS			V_v = 31.68 FPS			.5	.7	.9	1.1	1.3	
MAIN GEAR WHEEL AND TIRE	13.1	14.2	14.2	38.8	42.3	42.7	86.3	89.3	89.1	0	0	0	0	0	
MAIN GEAR AND SUPT STR	33.8	60.9	60.5	251.9	277.2	280.7	527.0	546.9	548.7	0	0	11.6	28.9	47.8	
NOSE GEAR WHEEL AND TIRE	1.0	1.8	2.2	9.0	9.6	10.0	17.5	18.1	18.4	0	0	.6	4.9	10.1	
NOSE GEAR AND SUPT STR	5.7	9.1	11.7	57.5	58.3	58.7	109.5	110.4	110.5	9.1	26.8	54.8	126.6	196.9	
WING STATION 0 TO 55	0	0	0	55.2	55.0	50.5	207.5	206.3	201.4	0	0	0	20.4	43.9	
WING STATION 55 TO 103	0	0	0	40.6	42.5	42.8	153.2	154.9	154.9	0	0	0	1.2	2.6	
WING STATION 103 TO 203	0	0	0	3.8	3.9	4.0	28.7	29.0	29.1	0	0	0	0	0	
ENG MT SUPT STR	6.2	8.1	8.3	31.5	33.0	33.4	66.6	67.6	67.9	0	0	0	0	0	
EXT STORE RACK AND SUPT	0	0	0	0	0	0	12.4	12.4	12.4	0	0	0	0	0	
FUS STA 66 TO 146	0	0	0	9.7	8.3	6.3	46.0	49.8	50.9	0	0	0	1.5	17.8	
FUS STA 146 TO 230	2.7	6.6	6.5	28.5	31.5	32.1	69.9	77.2	78.6	0	0	0	0	2.2	
FUS STA 230 TO 328	1.8	2.8	2.6	18.4	18.2	19.0	69.0	74.1	74.0	0	0	0	0	9.0	
FUS STA 330 TO 415	0	0	0	0	0	0	6.7	8.5	8.4	0	0	0	0	0	
TOTAL WEIGHT PENALTY*	64.6	104.4	107.1	570.0	608.2	608.8	1567	1622	1622	9.1	26.	67.4	176.0	339.7	

SINK SPEED = 8 FPS	θ = 6°			θ = 8°			θ = 10°			ROLLING COEFFICIENT OF FRICTION					
	V_v = 22.86 fps			V_v = 27.76 fps			V_v = 32.63 fps			.5	.7	.9	1.1	1.3	
MAIN GEAR WHEEL AND TIRE	20.1	21.4	21.4	57.7	60.0	60.1	99.9	103.0	103.2	0	0	0	0	0	
MAIN GEAR AND SUPT STR	75.9	103.8	105.8	346.1	360.9	362.5	579.2	599.4	601.2	0	0	0	.1	11.3	
NOSE GEAR WHEEL AND TIRE	2.7	3.4	3.9	10.7	11.4	11.7	19.4	20.0	20.3	0	0	0	0	0	
NOSE GEAR AND SUPT STR	16.3	18.6	21.0	67.9	68.7	68.8	120.7	121.6	121.5	0	0	12.8	34.5	56.9	
WING STATION 0 TO 55	0	0	0	100.4	99.2	93.8	237.8	236.8	232.3	0	0	0	0	0	
WING STATION 55 TO 103	0	0	0	69.4	72.0	72.5	179.0	180.7	180.5	0	0	0	0	0	
WING STATION 103 TO 203	0	0	0	9.2	9.4	9.5	37.0	37.3	37.3	0	0	0	0	0	
ENG MT SUPT STR	11.0	12.9	13.1	41.1	42.6	43.1	74.2	75.2	75.4	0	0	0	0	0	
EXT STORE RACK AND SUPT	0	0	0	.7	.8	.8	16.0	16.1	16.0	0	0	0	0	0	
FUS STA 66 TO 146	0	0	0	20.0	22.3	23.5	49.8	49.7	48.8	0	0	0	0	0	
FUS STA 146 TO 230	6.6	10.0	10.3	42.6	44.9	45.3	72.2	80.4	82.2	0	0	0	0	0	
FUS STA 230 TO 328	3.4	3.8	3.9	31.7	32.8	32.7	68.3	75.0	75.7	0	0	0	0	0	
FUS STA 330 TO 415	0	0	0	.1	.7	.7	6.3	7.8	8.1	0	0	0	0	0	
TOTAL WEIGHT PENALTY*		176.5	182.2	852.2	883.6	882.9	1766	1821	1821	0	0	12.8	34.6	68.6	

*See Note Page 86.

TABLE 11 (CONT'D). STRUCTURAL COMPONENT WEIGHT PENALTIES

SINK SPEED = 17 FPS	CONTINUOUS UNDULATIONS UNDULATION LENGTH = 13.7 INCHES							CONTINUOUS UNDULATIONS UNDULATION LENGTH = 27.4 INCHES												
	UNDULATION HEIGHT							UNDULATION HEIGHT												
COEFFICIENT OF FRICTION (EXCEPT AS NOTED)	1 INCH		1.5 INCHES			.5 INCH		1 INCH			2 INCHES			3 INCHES			4 INCHES		
	.2	.4	.2	.4	.55	.2	.4	.2	.4	.55	.2	.4	.55	.2	.4	.55	.2	.4	.55
MAIN GEAR WHEEL AND TIRE	0	0	0					0	0		1.6	1.7	4.2	4.4	8.4	8.7	8.7	16.4	15.4
MAIN GEAR AND SUPT STR	0	0	0					0	0		0	0	16.4	12.3	45.6	47.8	47.4	68.4	66.0
NOSE GEAR WHEEL AND TIRE	4.2	5.8	6.1	8.6	8.8	.6	.9	5.37	7.49	7.42	13.7	13.9	13.7	19.6	22.0	23.8	28.9	29.9	30.3
NOSE GEAR AND SUPT STR	7.1	10.1	14.4	16.4	16.2	1.6	1.15	12.2	15.8	15.8	34.5	34.9	33.1	58.5	63.2	61.5	78.9	74.7	76.4
WING STATION 0 TO 55	0	0	0					0			0	0	0	0	2.6	3.1	2.9	13.5	11.8
WING STATION 55 TO 103	0	0	0					0			0	0	0	0	.2	.2	.2	.8	.7
WING STATION 103 TO 203	0	0	0					0			0	0	0	0	0	0	0	0	0
ENG MT SUPT STR	0	0	0					0			0	0	0	0	0	.8	.8	1.2	1.7
EXT STORE RACK AND SUPT	0	0	0					0			0	0	0	0	0	0	0	0	0
FUS STA 66 TO 146	0	0	0					0			6.5	7.1	7.7	16.8	17.6	22.9	19.4	26.5	27.3
FUS STA 146 TO 230	0	0	0					0			1.7	1.3	5.2	3.5	16.4	17.0	16.6	24.5	23.4
FUS STA 230 TO 328	0	0	0					0			1.7	1.3	4.2	3.5	16.4	17.4	17.1	27.0	25.8
FUS STA 330 TO 415	0	0	0					0			0	0	0	0	0	0	0	0	0
TOTAL WEIGHT PENALTY *	11.3	15.9	20.5	25.0	25.0	2.2	2.05	17.57	23.29	23.22	60.0	60.5	85.1	119.7	195.4	205.8	225.1	289.7	285.3

SINK SPEED = 12 FPS	3 INCHES		4 INCHES		5 INCHES	
	.2	.4	.2	.4	.2	.4
MAIN GEAR WHEEL AND TIRE	0	0	0	0	0	0
MAIN GEAR AND SUPT STR	0	0	0	0	0	0
NOSE GEAR WHEEL AND TIRE	4.1	5.1	12.1	16.0	17.5	17.5
NOSE GEAR AND SUPT STR	17.0	23.5	63.9	88 0	105.7	111.1
WING STATION 0 TO 55	0	0	0	0	0	0
WING STATION 55 TO 103	0	0	0	0	0	0
WING STATION 103 TO 203	0	0	0	0	0	0
ENG MT SUPT STR	0	0	0	0	0	0
EXT STORE RACK AND SUPT	0	0	0	0	0	0
FUS STA 66 TO 146	0	0	0	8.3	6.9	8.0
FUS STA 146 TO 230	0	0	0	0	0	0
FUS STA 230 TO 328	0	0	0	0	0	0
FUS STA 330 TO 415	0	0	0	0	0	0
TOTAL WEIGHT PENALTY *	21.1	28.7	76.4	113.4	131.5	138.5

SINK SPEED = 8 FPS.	3 INCHES		4 INCHES		4.6 INCHES		5 INCHES		5.5 INCHES	
	.2	.4	.2	.4	.2	.4	.2	.4	.2	.4
MAIN GEAR WHEEL AND TIRE	0	0	0	0	0	0	0	0	0	0
MAIN GEAR AND SUPT STR	0	0	0	0	0	0	0	0	0	0
NOSE GEAR WHEEL AND TIRE	0	0	0	0	2.0	3.9	9.8	10.1	18.2	18.2
NOSE GEAR AND SUPT STR	0	0	0	0	2.7	17.0	55.7	58.7	109.2	115.8
WING STATION 0 TO 55	0	0	0	0	0	0	0	0	0	0
WING STATION 55 TO 103	0	0	0	0	0	0	0	0	0	0
WING STATION 103 TO 203	0	0	0	0	0	0	0	0	0	0
ENG MT SUPT STR	0	0	0	0	0	0	0	0	0	0
EXT STORE RACK AND SUPT	0	0	0	0	0	0	0	0	0	0
FUS STA 66 TO 146	0	0	0	0	0	0	0	0	8.2	8.6
FUS STA 146 TO 230	0	0	0	0	0	0	0	0	0	0
FUS STA 230 TO 328	0	0	0	0	0	0	0	0	0	0
FUS STA 330 TO 415	0	0	0	0	0	0	0	0	0	0
TOTAL WEIGHT PENALTY *	0	0	0	0	4.7	21.0	65.9	69.2	137.4	144.4

*See Note Page 86.

TABLE 11 (CONT'D). STRUCTURAL COMPONENT WEIGHT PENALTIES

SINK SPEED = 17 FPS COEFF. OF FRICTION,	CONTINUOUS UNDULATIONS UNDULATION LENGTH = 45.667 INCHES UNDULATION HEIGHT									CONTINUOUS UNDULATIONS UNDULATION LENGTH = 137 INCHES UNDULATION HEIGHT					
	3 INCHES			4.5 INCHES			6 INCHES			4 INCHES			6 INCHES		
	.2	.4	.55	.2	.4	.55	.2	.4	.55	.2	.4	.55	.2	.4	.55
MAIN GEAR WHEEL AND TIRE	5.3	6.52	8.9	28.2	36.3		49.4	66.4		12.2	12.9	13.6	88.0	87.0	86.0
MAIN GEAR AND SUPT STR	22.3	34.5	50.8	86.4	120.7		153.0	195.6		61.0	68.2	75.4	252.0	254.0	256.0
NOSE GEAR WHEEL AND TIRE	20.3	20.3	20.3	26.6	27.2		33.9	32.8		8.96	9.9	10.8	28.2	28.2	28.2
NOSE GEAR AND SUPT STR	59.2	56.4	56.7	93.6	97.5		150.7	150.3		39.3	39.7	40.0	121.0	121.0	121.0
WING STATION 0 TO 55	0	0	6.2	29.3	38.3		80.2	123.7		30.4	36.0	33.8	338.0	347.0	338.0
WING STATION 55 TO 103	0	0	0	1.8	2.3		26.7	28.3		11.8	15.8	17.5	166.0	174.0	172.0
WING STATION 103 TO 203	0	0	0	0	0		2.2	1.9		1.13	2.25	2.25	51.2	53.5	53.5
ENG MT SUPT STR	0	0	0	8.5	8.3		23.8	24.2		17.0	20.5	21.0	70.0	73.7	73.0
EXT STORE RACK AND SUPT	0	0	0	0	0		0	0		0	0	0	17.7	20.3	18.0
FUS STA 66 TO 146	20.8	22.5	22.7	50.9	57.2		89.2	96.0		0	0	0	43.0	40.9	40.9
FUS STA 146 TO 230	5.75	13.0	20.6	32.2	44.5		58.2	74.1		17.5	16.3	14.9	83.3	83.6	81.3
FUS STA 230 TO 328	6.95	10.8	18.1	33.1	63.3		99.4	142.8		21.5	23.0	21.0	161.0	164.0	160.0
FUS STA 330 TO 415	0	0	0	2.0	6.5		20.7	38.0		0	0	0	37.4	47.7	37.4
TOTAL WEIGHT PENALTY*	142.0	166.0	207.5	95.6	523.4		840.0	1055		225.0	250.0	255.5	1635	1687	1650

SINK SPEED = 12 FPS	4.5 INCHES			6 INCHES		7 INCHES		6 INCHES			9 INCHES		
	.2	.4		.2	.4	.2	.4	.2	.4	.55	.2	.4	.55
MAIN GEAR WHEEL AND TIRE	0	0		7.5	14.4	49.2	60.2	11.9	15.5	14.9	74.6	75.4	73.9
MAIN GEAR AND SUPT STR	0	0		112.0	181.2	388.5	418.7	156.0	174.0	179.4	527.1	538.2	531.9
NOSE GEAR WHEEL AND TIRE	13.9	14.8		27.3	26.2	34.2	32.8	9.1	9.7	10.7	20.3	20.8	20.7
NOSE GEAR AND SUPT STR	88.7	95.6		191.2	188.1	244.7	239.1	74.6	76.9	81.4	166.4	168.6	168.0
WING STATION 0 TO 55	0	0		13.6	17.0	85.0	100.6	26.7	34.3	33.4	253.8	260.9	259.9
WING STATION 55 TO 103	0	0		.8	1.0	9.3	11.5	5.7	8.8	10.1	114.6	121.8	123.8
WING STATION 103 TO 203	0	0		0	0	0	.1	0	0	0	24.3	26.1	26.8
ENG MT SUPT STR	0	0		0	0	8.1	9.9	12.1	15.3	16.6	48.9	51.7	52.7
EXT STORE RACK AND SUPT	0	0		0	0	0	0	0	0	0	9.9	10.8	11.1
FUS STA 66 TO 146	19.2	22.6		40.5	42.2	66.1	67.7	0	0	0	27.5	26.1	24.9
FUS STA 146 TO 230	0	0		13.8	23.5	55.2	59.0	19.5	19.3	18.2	72.3	72.6	71.3
FUS STA 230 TO 328	0	0		19.8	32.0	98.8	113.7	25.0	27.9	26.9	140.1	144.6	141.6
FUS STA 330 TO 415	0	0		0	2.1	21.4	27.5	0	1.0	.6	38.0	39.9	38.3
TOTAL WEIGHT PENALTY*	123.0	134.4		442.0	551.3	1156	1252	350.5	395.1	405.2	1714	1764	1748

SINK SPEED = 8 FPS	4.5 INCHES			6 INCHES		7 INCHES		6 INCHES			9 INCHES		
	.2	.4		.2	.4	.2	.4	.2	.4		.2	.4	
MAIN GEAR WHEEL AND TIRE	0	0		0	0	20.4	30.4	0	0		44.9	47.5	
MAIN GEAR AND SUPT STR	0	0		0	0	214.1	249.5	0	0		344.7	367.1	
NOSE GEAR WHEEL AND TIRE	1.5	1.8		20.9	19.9	28.6	27.2	3.4	3.7		12.9	12.6	
NOSE GEAR AND SUPT STR	6.4	10.7		141.3	139.4	205.7	200.5	30.1	32.0		107.5	107.2	
WING STATION 0 TO 55	0	0		0	0	27.5	30.1	0	0		125.4	135.5	
WING STATION 55 TO 103	0	0		0	0	1.6	1.8	0	0		35.3	40.0	
WING STATION 103 TO 203	0	0		0	0	0	0	0	0		6.9	7.9	
ENG MT SUPT STR	0	0		0	0	0	0	0	0		24.0	26.7	
EXT STORE RACK AND SUPT	0	0		0	0	0	0	0	0		0	0	
FUS STA 66 TO 146	0	0		9.4	7.8	19.6	18.0	0	0		7.2	7.0	
FUS STA 146 TO 230	0	0		0	3.0	28.7	33.1	0	.7		45.9	47.6	
FUS STA 230 TO 328	0	0		0	3.0	37.9	54.1	0	.7		80.1	89.0	
FUS STA 330 TO 415	0	0		0	0	3.3	5.6	0	0		14.3	18.0	
TOTAL WEIGHT PENALTY*	8.0	12.5		174.1	175.7	616.7	686.2	33.6	37.4		910.3	975.9	

*See Note Page 86.

TABLE 11 (CONT'D). STRUCTURAL COMPONENT WEIGHT PENALTIES

SINK SPEED = 17 FPS	VARIATION IN SINGLE BUMP LENGTH OR SLOPE BUMP HEIGHT = 3 INCHES BUMP LOCATED AT MOST CRITICAL DISTANCE OF BUMP ℄ TO MAIN GEAR TOUCHDOWN										LINEAR INCREASE IN BUMP HEIGHT AND LENGTH BUMP LOCATED AT MOST CRITICAL DISTANCE OF BUMP ℄ TO MAIN GEAR TOUCHDOWN					
	MAIN GEAR HITS BUMP					NOSE GEAR HITS BUMP					MAIN GEAR			NOSE GEAR		
	UNDULATION LENGTH										UNDULATION HEIGHT					
	27.4	45.67	137	220	360	27.4	45.67	137	220	360	1.5	3.0	5.0	1.5	3.0	5.0
MAIN GEAR WHEEL AND TIRE	85.4	64.8	8.05	.7	0	0	0	0	0	0	27.0	85.4	150.9	0	0	0
MAIN GEAR AND SUPT STR	251.8	175.5	38.9	0	0	0	0	0	0	0	94.5	251.8	439.7	0	0	0
NOSE GEAR WHEEL AND TIRE	0	0	0	0	0	47.7	37.7	13.7	15.5	1.6	0	0	0	34.3	47.7	53.5
NOSE GEAR AND SUPT STR	0	0	0	0	0	218.3	160.8	53.5	46.4	2.6	0	0	0	102.0	218.3	252.9
WING STATION 0 TO 55	121.2	74.97	0	0	0	35.4	31.5	0	0	0	24.9	121.2	260.7	0	35.4	86.4
WING STATION 55 TO 103	7.3	0	0	0	0	30.1	26.6	0	0	0	1.5	7.3	63.8	0	30.1	84.0
WING STATION 103 TO 203	0	0	0	0	0	8.1	6.4	0	0	0	0	0	6.8	0	8.1	17.4
ENG MT SUPT STR	7.4	4.28	0	0	0	19.4	20.4	7.3	7.5	0	0	7.4	26.2	0	19.4	39.5
EXT STORE RACK AND SUPT	0	0	0	0	0	0	0	0	0	0	0	0	0	0	0	6.9
FUS STA 66 TO 146	48.1	29.01	0	0	0	103.6	79.8	6.7	7.5	0	3.9	48.1	100.6	68.6	103.6	143.6
FUS STA 146 TO 230	97.1	74.8	13.6	0	0	16.4	0	0	0	0	34.6	97.1	201.9	0	16.4	19.4
FUS STA 230 TO 328	168.0	118.3	15.2	0	0	8.5	0	0	0	0	38.8	168.0	311.0	0	8.5	6.8
FUS STA 330 TO 415	47.8	26.25	0	0	0	3.5	0	0	0	0	3.1	47.3	104.6	0	3.5	2.8
TOTAL WEIGHT PENALTY *	893.0	596.0	77.3	.7	0	511.6	374.4	70.6	77.4	4.2	232.7	893.0	1902	208.4	511.6	756.2
SINK SPEED = 12 FPS	UNDULATION LENGTH										UNDULATION HEIGHT					
	27.4	34.25	45.67	68.5	137	27.4	34.25	45.67	68.5	137	1.5	3.75	7.5	1.5	3.75	7.5
MAIN GEAR WHEEL AND TIRE	3.2	2.3	.2	0	0	0	0	0	0	0	0	20.0	118.2	0	0	0
MAIN GEAR AND SUPT STR	11.2	12.5	0	0	0	0	0	0	0	0	0	215.3	840.5	0	0	0
NOSE GEAR WHEEL AND TIRE	0	0	0	0	0	39.8	35.9	30.0	21.1	6.4	0	0	0	19.4	42.2	71.5
NOSE GEAR AND SUPT STR	0	0	0	0	0	286.2	259.9	218.3	152.6	43.4	0	0	0	114.3	312.4	488.3
WING STATION 0 TO 55	0	0	0	0	0	0	0	0	0	0	0	18.6	222.9	0	13.4	136.5
WING STATION 55 TO 103	0	0	0	0	0	0	0	0	0	0	0	1.1	35.8	0	8.0	121.5
WING STATION 103 TO 203	0	0	0	0	0	0	0	0	0	0	0	0	.1	0	.4	29.0
ENG MT SUPT STR	0	0	0	0	0	2.3	3.4	2.2	0	0	0	0	14.7	0	11.4	52.5
EXT STORE RACK AND SUPT	0	0	0	0	0	0	0	0	0	0	0	0	0	0	0	12.8
FUS STA 66 TO 146	0	0	0	0	0	72.8	62.9	46.2	19.2	0	0	0	69.9	24.0	80.6	170.9
FUS STA 146 TO 230	3.1	3.2	1.3	0	0	0	0	0	0	0	0	28.5	146.1	0	0	73.9
FUS STA 230 TO 328	3.1	3.2	1.3	0	0	13.2	7.3	1.7	0	0	0	34.1	251.7	0	14.2	71.7
FUS STA 330 TO 415	0	0	0	0	0	4.0	1.9	0	0	0	0	2.3	81.8	0	4.2	32.6
TOTAL WEIGHT PENALTY *	20.6	21.4	2.8	0	0	433.2	383.1	306.0	196.1	50.0	0	328.6	2051	160.3	507.0	1396
SINK SPEED = 8 FPS	UNDULATION LENGTH										UNDULATION HEIGHT					
						27.4	34.25	45.67	68.5	137	3.75	5.0	7.5	3.75	5.0	7.5
MAIN GEAR WHEEL AND TIRE						0	0	0	0	0	0	9.0	65.9	0	0	0
MAIN GEAR AND SUPT STR						0	0	0	0	0	0	127.0	466.2	0	0	0
NOSE GEAR WHEEL AND TIRE						11.4	8.5	4.4	0	0	0	0	0	19.1	25.2	28.8
NOSE GEAR AND SUPT STR						61.9	45.8	23.6	0	0	0	0	0	124.2	188.0	240.3
WING STATION 0 TO 55						0	0	0	0	0	0	2.1	110.0	0	0	14.6
WING STATION 55 TO 103						0	0	0	0	0	0	.1	6.6	0	0	8.4
WING STATION 103 TO 203						0	0	0	0	0	0	0	0	0	0	.5
ENG MT SUPT STR						0	0	0	0	0	0	0	0	0	0	12.8
EXT STORE RACK AND SUPT						0	0	0	0	0	0	0	0	0	0	0
FUS STA 66 TO 146						4.8	0	0	0	0	0	0	24.5	20.1	30.6	63.6
FUS STA 146 TO 230						0	0	0	0	0	0	15.9	70.0	0	0	0
FUS STA 230 TO 328						0	0	0	0	0	0	25.3	144.7	0	0	0
FUS STA 330 TO 415						0	0	0	0	0	0	0	39.8	0	0	0
TOTAL WEIGHT PENALTY *						78.7	54.6	28.1	0	0	0	182.1	1001	165.6	249.0	380.6

*See Note Page 86.

TABLE 11 (CONT'D). STRUCTURAL COMPONENT WEIGHT PENALTIES

SINK SPEED = 17 FPS	SINGLE BUMP HEIGHT 3 INCHES SINGLE BUMP LENGTH 27.4 INCHES																
	MAIN GEAR HITS SINGLE BUMP - TAIL DOWN ATTITUDE						MAIN GEAR HITS SINGLE BUMP - NOSE DOWN ATTITUDE							NOSE GEAR HITS SINGLE BUMP - NOSE DOWN ATTITUDE				
	DISTANCE OF BUMP ℄ FROM MAIN GEAR TOUCHDOWN																
	73.7	83.7	133.7	163.1	173.7	280	73.7	83.7	95.2	133.7	213.7	280	283.7	200.5	240	288.1	300	385
MAIN GEAR WHEEL AND TIRE	46.0	46.0	70.2	85.4	80.2	64.0	57.6	57.9	52.2	34.0	8.0	0	0	0	0	0	0	0
MAIN GEAR AND SUPT STR	140.1	137.1	203.5	251.8	238.5	178.4	157.8	161.2	147.9	118.4	42.5	0	0	0	0	0	0	0
NOSE GEAR WHEEL AND TIRE	0	0	0	0	0	0	0	0	0	0	0	0	0	36.0	39.1	47.7	45.0	27.0
NOSE GEAR AND SUPT STR	0	0	0	0	0	0	0	0	0	0	0	0	0	152.6	184.4	219.3	207.7	107.0
WING STATION 0 TO 55	42.8	42.2	83.4	113.0	102.0	71.0	89.0	84.8	62.7	41.8	0	0	0	9.0	36.0	35.4	30.6	0
WING STATION 55 TO 103	0	0	0	6.8	0	0	0	0	0	0	0	0	0	9.56	34.3	30.1	26.1	0
WING STATION 103 TO 203	0	0	0	0	0	0	0	0	0	0	0	0	0	1.13	9.4	8.1	7.6	0
ENG MT SUPT STR	0	0	0	1.8	3.0	0	0	6.2	9.5	.5	0	0	0	14.5	24.0	19.4	17.0	0
EXT STORE RACK AND SUPT	0	0	0	0	0	0	0	0	0	0	0	0	0	0	0	0	0	0
FUS STA 66 TO 146	11.0	14.5	40.0	48.1	44.7	28.5	0	.5	0	0	0	0	0	51.0	73.7	103.6	92.0	0
FUS STA 146 TO 230	48.9	49.5	79.8	97.1	87.4	66.7	54.0	55.5	49.7	35.3	13.8	0	0	0	0	16.4	5.7	0
FUS STA 230 TO 328	77.1	71.0	142.9	168.0	147.4	107.0	99.5	98.0	77.4	46.5	15.8	0	0	0	4.0	8.5	5.0	0
FUS STA 330 TO 415	11.0	8.8	27.5	47.8	39.9	23.8	19.7	20.0	10.5	3.2	0	0	0	0	4.0	3.5	2.0	0
TOTAL WEIGHT PENALTY *	388.9	381.4	683.0	876.9	790.0	564.1	497.0	504.0	424.2	286.4	80.6	0	0	280.2	422.1	511.6	455.1	235.5
SINK SPEED = 12 FPS	DISTANCE OF BUMP ℄ FROM MAINGEAR TOUCHDOWN																	
		68.7	95.7	105.7	163.7	220.7			68.7	95.7	105.7	148.7	220.7	205.7	242.7	285.7	357.7	380.7
MAIN GEAR WHEEL AND TIRE		1.1	0	0	3.2	0			1.2	3.2	1.5	0	0	0	0	0	0	0
MAIN GEAR AND SUPT STR		0	0	0	26.6	0			0	11.2	0	0	0	0	0	0	0	0
NOSE GEAR WHEEL AND TIRE		0	0	0	0	0			0	0	0	0	0	24.8	28.7	34.1	39.8	38.3
NOSE GEAR AND SUPT STR		0	0	0	0	0			0	0	0	0	0	159.8	200.9	243.9	286.2	274.8
WING STATION 0 TO 55		0	0	0	0	0			0	0	0	0	0	0	0	0	0	0
WING STATION 55 TO 103		0	0	0	0	0			0	0	0	0	0	0	0	0	0	0
WING STATION 103 TO 203		0	0	0	0	0			0	0	0	0	0	.0	0	0	0	0
ENG MT SUPT STR		0	0	0	0	0			0	0	0	0	0	0	0	0	2.3	0
EXT STORE RACK AND SUPT		0	0	0	0	0			0	0	0	0	0	0	0	0	0	0
FUS STA 66 TO 146		0	0	0	0	0			0	0	0	0	0	26.3	40.0	58.0	72.8	68.5
FUS STA 146 TO 230		1.1	0	0	4.0	0			3.9	3.1	.5	0	0	0	0	0	0	0
FUS STA 230 TO 328		1.1	0	0	4.5	0			5.1	3.1	.5	0	0	0	0	3.3	13.2	9.3
FUS STA 330 TO 415		0	0	0	0	0			0	0	0	0	0	0	0	.3	4.0	3.0
TOTAL WEIGHT PENALTY *		3.3	0	0	38.4	0			10.2	20.6	2.6	0	0	214.7	275.8	349.4	433.2	407.1

*Note: Total Weight Penalty for each category is the sum of the weights of the applicable column (ΔW_1) times a growth factor equal to $\frac{11772 + \Delta W_1}{11772}$

TABLE 12

TERRAIN ROUGHNESS REQUIRING STRUCTURAL REINFORCEMENT OF OV-1 AIRPLANE

CATEGORY (PG. 15)	SINKING SPEED = 17 FT/SEC										
	WIDTH SLOPE (DEGREES)	LENGTH SLOPE (DEGREES)	UNDULATION HEIGHT (INCHES)	UNDULATION SLOPE (DEGREES)	UNDULATION SPACING (FEET)	BUMP HEIGHT (INCHES)	BUMP SPACING (FEET)	BUMP SLOPE (DEGREES)	μ_S	μ_R	TERRAIN DESIGNATION
A SLOPES	0	1.82	0	0	0	0	-	0	.2	.03	XX00-000-00X-XXXX
	0	1.69	0	0	0	0	-	0	.4	.03	XX00-000-00X-XXXX
	0	1.56	0	0	0	0	-	0	.55	.03	XX00-000-00X-XXXX
J SOFT SOIL	0	0	0	0	0	0	-	0	.4	.33	XX00-000-00X-XXXX
C CONTINUOUS UNDULATION	0	0	.37	4.85	1.14	0	-	0	.2	.03	XX00-027-00X-XXXX
	0	0	.40	5.25	1.14	0	-	0	.4	.03	XX00-027-00X-XXXX
	0	0	1.3	8.52	2.28	0	-	0	.2	.03	XX00-036-00X-XXXX
	0	0	1.0	6.55	2.28	0	-	0	.4	.03	XX00-036-00X-XXXX
	0	0	1.0	6.55	2.28	0	-	0	.55	.03	XX00-036-00X-XXXX
	0	0	.53	2.13	3.81	0	-	0	.2	.03	XX00-045-00X-XXXX
	0	0	.53	2.13	3.81	0	-	0	.4	.03	XX00-045-00X-XXXX
	0	0	3.20	4.2	11.42	0	-	0	.2	.03	XX00-124-00X-XXXX
	0	0	3.10	4.07	11.42	0	-	0	.4	.03	XX00-124-00X-XXXX
	0	0	3.00	3.93	11.42	0	-	0	.55	.03	XX00-114-00X-XXXX
B SINGLE BUMPS	0	0	0	0	0	3.00	-	1.5	.4	.03	XX00-000-1XX-XXXX
	0	0	0	0	0	.32	-	19.8	.4	.03	XX00-000-0XX-XXXX

TABLE 12 (Cont'd)

TERRAIN ROUGHNESS REQUIRING STRUCTURAL REINFORCEMENT OF OV-1 AIRPLANE

CATEGORY (PG. 15)	WIDTH SLOPE (DEGREES)	LENGTH SLOPE (DEGREES)	UNDULATION HEIGHT (INCHES)	UNDULATION SLOPE (DEGREES)	UNDULATION SPACING (FEET)	BUMP HEIGHT (INCHES)	BUMP SPACING (FEET)	BUMP SLOPE (DEGREES)	μ_S	μ_R	TERRAIN DESIGNATION
	SINKING SPEED = 12 FT/SEC										
A	0	3.67	0	0	0	0	-	0	.2	.03	XX01-000-00X-XXXX
	0	3.26	0	0	0	0	-	0	.4	.03	XX01-000-00X-XXXX
	0	3.23	0	0	0	0	-	0	.55	.03	XX01-000-00X-XXXX
J	0	0	0	0	0	0	-	0	.4	.40	XX00-000-00X-XXXX
C	0	0	2.65	17.3	2.28	0	-	0	.2	.03	XX00-056-00X-XXXX
	0	0	2.55	16.7	2.28	0	-	0	.4	.03	XX00-056-00X-XXXX
	0	0	2.57	10.1	3.81	0	-	0	.2	.03	XX00-045-00X-XXXX
	0	0	2.57	10.1	3.81	0	-	0	.4	.03	XX00-045-00X-XXXX
	0	0	4.5	5.9	11.42	0	-	0	.2	.03	XX00-124-00X-XXXX
	0	0	4.35	5.7	11.42	0	-	0	.4	.03	XX00-124-00X-XXXX
	0	0	0	0	0	3.00	-	3.0	.4	.03	XX00-000-1XX-XXXX
	0	0	0	0	0	.80	-	19.7	.4	.03	XX00-000-0XX-XXXX
	SINKING SPEED = 8 FT/SEC										
A	0	5.47	0	0	0	0	-	0	.2	.03	XX02-000-00X-XXXX
	0	5.37	0	0	0	0	-	0	.4	.03	XX02-000-00X-XXXX
	0	5.27	0	0	0	0	-	0	.55	.03	XX02-000-00X-XXXX
J	0	0	0	0	0	0	-	0	.4	.77	XX00-000-00X-XXXX
C	0	0	4.55	29.9	2.28	0	-	0	.2	.03	XX00-167-00X-XXXX
	0	0	4.35	28.6	2.28	0	-	0	.4	.03	XX00-167-00X-XXXX
	0	0	4.4	17.3	3.81	0	-	0	.2	.03	XX00-156-00X-XXXX
	0	0	4.4	17.3	3.81	0	-	0	.4	.03	XX00-156-00X-XXXX
	0	0	5.8	7.62	11.42	0	-	0	.2	.03	XX00-134-00X-XXXX
	0	0	5.8	7.62	11.42	0	-	0	.4	.03	XX00-134-00X-XXXX
B	0	0	0	0	0	3.00	-	12.5	.4	.03	XX00-000-1XX-XXXX
	0	0	0	0	0	2.0	-	19.7	.4	.03	XX00-000-0XX-XXXX

TABLE 13

TERRAIN FOR EQUAL VTOL/OV-1 PERFORMANCE

CATEGORY (PG. 15)	SINKING SPEED = 17 FT/SEC										
	RUNWAY LENGTH (FEET)	TAKE-OFF RUNWAY PARAMETER	LENGTH SLOPE (DEGREES)	UNDULATION HEIGHT (INCHES)	UNDULATION SLOPE (DEGREES)	UNDULATION SPACING (FEET)	BUMP HEIGHT (INCHES)	BUMP LENGTH (INCHES)	BUMP SLOPE (DEGREES)	μ_R	TERRAIN DESIGNATION
A SLOPES	2000	.2	2.5	0	0	0	0	0	0	.03	0701-000-00X-XXXX
	2000	.1	4.8	0	0	0	0	0	0	.03	0702-000-00X-XXXX
	1500	.1	3.00	0	0	0	0	0	0	.03	0801-000-00X-XXXX
	1500	0	4.75	0	0	0	0	0	0	.03	0802-000-00X-XXXX
	1000	-.1	2.85	0	0	0	0	0	0	.03	0901-000-00X-XXXX
J SOFT SOIL	2000	.2	0	0	0	0	0	0	0	.67	0700-000-00X-XXXX
	1500	.1	0	0	0	0	0	0	0	.82	0800-000-00X-XXXX
	1000	-.1	0	0	0	0	0	0	0	.740	0900-000-00X-XXXX
C CONTINUOUS UNDULATION	2000	.2	0	2.5	16.4	2.28	0	0	0	.03	0700-056-00X-XXXX
	1500	.1	0	3.5	23.0	2.28	0	0	0	.03	0800-167-00X-XXXX
	1000	-.1	0	2.8	18.4	2.28	0	0	0	.03	0900-056-00X-XXXX
	2000	.2	0	2.65	10.4	3.81	0	0	0	.03	0700-045-00X-XXXX
	2000	.1	0	5.5	21.6	3.81	0	0	0	.03	0700-166-00X-XXXX
	1500	.1	0	3.35	13.2	3.81	0	0	0	.03	0800-146-00X-XXXX
	1500	0	0	5.4	21.2	3.81	0	0	0	.03	0800-166-00X-XXXX
	1000	-.1	0	2.85	11.2	3.81	0	0	0	.03	0900-146-00X-XXXX
	2000	.2	0	3.6	4.73	11.42	0	0	0	.03	0700-124-00X-XXXX
	2000	.1	0	6.0	7.90	11.42	0	0	0	.03	0700-235-00X-XXXX
	1500	.1	0	4.2	5.52	11.42	0	0	0	.03	0800-124-00X-XXXX
	1500	0	0	5.9	7.75	11.42	0	0	0	.03	0800-134-00X-XXXX
	1000	-.1	0	3.9	5.12	11.42	0	0	0	.03	0900-124-00X-XXXX
B SINGLE BUMPS	2000	.2	0	0	0	0	3	155	3.48	.03	0700-000-1XX-XXXX
	2000	.1	0	0	0	0	3	70	7.71	.03	0700-000-1XX-XXXX
	1500	.1	0	0	0	0	3	125	4.32	.03	0800-000-1XX-XXXX
	1500	0	0	0	0	0	3	75	7.2	.03	0800-000-1XX-XXXX
	1000	-.1	0	0	0	0	3	140	3.86	.03	0900-000-1XX-XXXX
	2000	.2	0	0	0	0	.6	5.47	19.7	.03	0700-000-0XX-XXXX
	2000	.1	0	0	0	0	2.1	19.2	19.7	.03	0700-000-0XX-XXXX
	1500	.1	0	0	0	0	.9	8.2	19.7	.03	0800-000-0XX-XXXX
	1500	0	0	0	0	0	2.0	18.3	19.7	.03	0800-000-0XX-XXXX
	1000	-.1	0	0	0	0	.7	6.38	19.7	.03	0900-000-0XX-XXXX

TABLE 13 (Cont'd)

TERRAIN FOR EQUAL VTOL/OV-1 PERFORMANCE

CATEGORY (PG. 15)	SINKING SPEED = 12 FT/SEC										
	RUNWAY LENGTH (FEET)	TAKE-OFF RUNWAY PARAMETER	LENGTH SLOPE (DEGREES)	UNDULATION HEIGHT (INCHES)	UNDULATION SLOPE (DEGREES)	UNDULATION SPACING (FEET)	BUMP HEIGHT (INCHES)	BUMP LENGTH (INCHES)	BUMP SLOPE (DEGREES)	μ_R	TERRAIN DESIGNATION
A	2000	.2	4.5	0	0	0	0	0	0	.03	0702-000-00X-XXXX
	2000	.1	6.55	0	0	0	0	0	0	.03	0703-000-00X-XXXX
	1500	.1	5.0	0	0	0	0	0	0	.03	0802-000-00X-XXXX
	1500	0	6.5	0	0	0	0	0	0	.03	0803-000-00X-XXXX
	1000	-.1	4.7	0	0	0	0	0	0	.03	0902-000-00X-XXXX
J	2000	.2	0	0	0	0	0	0	0	1.02	0700-000-00X-XXXX
	1500	.1	0	0	0	0	0	0	0	1.26	0800-000-00X-XXXX
	1000	-.1	0	0	0	0	0	0	0	1.13	0900-000-00X-XXXX
C	2000	.2	0	5.0	32.8	2.28	0	0	0	.03	0700-177-00X-XXXX
	1500	.12	0	5.0	32.8	2.28	0	0	0	.03	0800-177-00X-XXXX
	1000	-.08	0	5.0	32.8	2.28	0	0	0	.03	0900-177-00X-XXXX
	2000	.2	0	4.75	18.7	3.81	0	0	0	.03	0700-156-00X-XXXX
	2000	.1	0	6.7	26.3	3.81	0	0	0	.03	0700-267-00X-XXXX
	1500	.1	0	5.5	21.6	3.81	0	0	0	.03	0800-166-00X-XXXX
	1500	0	0	6.6	26.0	3.81	0	0	0	.03	0800-267-00X-XXXX
	1000	-.1	0	5.0	19.7	3.81	0	0	0	.03	0900-156-00X-XXXX
	2000	.2	0	5.1	6.7	11.42	0	0	0	.03	0700-134-00X-XXXX
	2000	.1	0	6.4	8.4	11.42	0	0	0	.03	0700-235-00X-XXXX
	1500	.1	0	5.8	7.6	11.42	0	0	0	.03	0800-134-00X-XXXX
	1500	0	0	7.2	9.45	11.42	0	0	0	.03	0800-235-00X-XXXX
	1000	-.1	0	5.4	7.1	11.42	0	0	0	.03	0900-134-00X-XXXX
B	2000	.2	0	0	0	0	3	85	6.35	.03	0700-000-1XX-XXXX
	1500	.1	0	0	0	0	3	50	10.8	.03	0800-000-1XX-XXXX
	1000	-.1	0	0	0	0	3	70	7.72	.03	0900-000-1XX-XXXX
	2000	.2	0	0	0	0	1.5	13.7	19.7	.03	0700-000-0XX-XXXX
	2000	.1	0	0	0	0	3.8	34.6	19.7	.03	0700-000-1XX-XXXX
	1500	.1	0	0	0	0	2.0	18.3	19.7	.03	0800-000-0XX-XXXX
	1500	0	0	0	0	0	3.7	33.8	19.7	.03	0800-000-1XX-XXXX
	1000	-.1	0	0	0	0	1.6	14.6	19.7	.03	0900-000-0XX-XXXX

TABLE 13 (Cont'd)

TERRAIN FOR EQUAL VTOL/OV-1 PERFORMANCE

CATEGORY (PG. 15)	SINKING SPEED = 8 FT/SEC										
	RUNWAY LENGTH (FEET)	TAKE-OFF RUNWAY PARAMETER	LENGTH SLOPE (DEGREES)	UNDULATION HEIGHT (INCHES)	UNDULATION SLOPE (DEGREES)	UNDULATION SPACING (FEET)	BUMP HEIGHT (INCHES)	BUMP LENGTH (INCHES)	BUMP SLOPE (DEGREES)	μ_R	TERRAIN DESIGNATION
A	2000	.2	6.0	0	0	0	0	0	0	.03	0703-000-00X-XXXX
	2000	.1	7.9	0	0	0	0	0	0	.03	0703-000-00X-XXXX
	1500	.1	6.4	0	0	0	0	0	0	.03	0803-000-00X-XXXX
	1500	0	7.85	0	0	0	0	0	0	.03	0803-000-00X-XXXX
	1000	-.1	6.2	0	0	0	0	0	0	.03	0903-000-00X-XXXX
J	2000	.21	0	0	0	0	0	0	0	1.2	0700-000-00X-XXXX
	1500	.14	0	0	0	0	0	0	0	1.2	0800-000-00X-XXXX
	1000	-.05	0	0	0	0	0	0	0	1.2	0900-000-00X-XXXX
C	2000	.2	0	5.5	36.1	2.28	0	0	0	.03	0700-177-00X-XXXX
	1500	.1	0	6.2	40.7	2.28	0	0	0	.03	0800-277-00X-XXXX
	1000	-.1	0	5.85	38.4	2.28	0	0	0	.03	0900-177-00X-XXXX
	2000	.2	0	6.0	23.6	3.81	0	0	0	.03	0700-267-00X-XXXX
	2000	.1	0	7.4	29.1	3.81	0	0	0	.03	0700-267-00X-XXXX
	1500	.1	0	6.5	25.6	3.81	0	0	0	.03	0800-267-00X-XXXX
	1500	0	0	7.4	29.1	3.81	0	0	0	.03	0800-267-00X-XXXX
	1000	-.1	0	6.1	24.0	3.81	0	0	0	.03	0900-267-00X-XXXX
	2000	.2	0	6.8	8.95	11.42	0	0	0	.03	0700-235-00X-XXXX
	2000	.1	0	8.9	11.7	11.42	0	0	0	.03	0700-245-00X-XXXX
	1500	.1	0	7.4	9.72	11.42	0	0	0	.03	0800-235-00X-XXXX
	1500	0	0	8.8	11.6	11.42	0	0	0	.03	0800-245-00X-XXXX
	1000	-.1	0	6.9	9.05	11.42	0	0	0	.03	0900-235-00X-XXXX
B	2000	.21	0	0	0	0	3	25	21.6	.03	0700-000-1XX-XXXX
	1500	.13	0	0	0	0	3	25	21.6	.03	0800-000-1XX-XXXX
	1000	-.06	0	0	0	0	3	25	21.6	.03	0900-000-1XX-XXXX
	2000	.2	0	0	0	0	3.3	30.1	19.7	.03	0700-000-1XX-XXXX
	2000	.1	0	0	0	0	6.1	55.6	19.7	.03	0700-000-2XX-XXXX
	1500	.1	0	0	0	0	4.3	39.2	19.7	.03	0800-000-1XX-XXXX
	1500	0	0	0	0	0	6.1	55.6	19.7	.03	0800-000-2XX-XXXX
	1000	-.1	0	0	0	0	3.9	35.6	19.7	.03	0900-000-1XX-XXXX

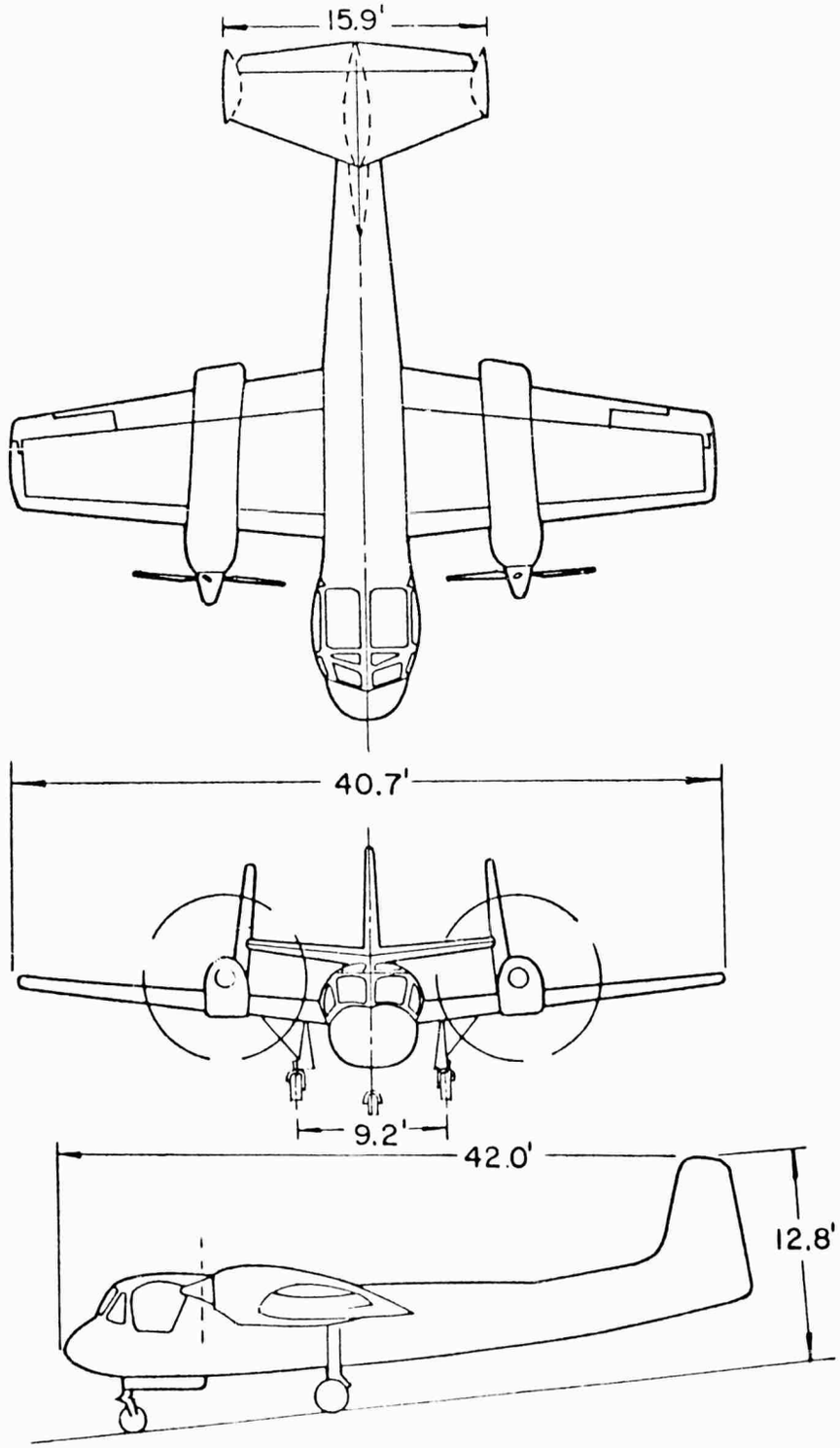

Figure 1. OV-1 Mohawk Airplane General Configuration.

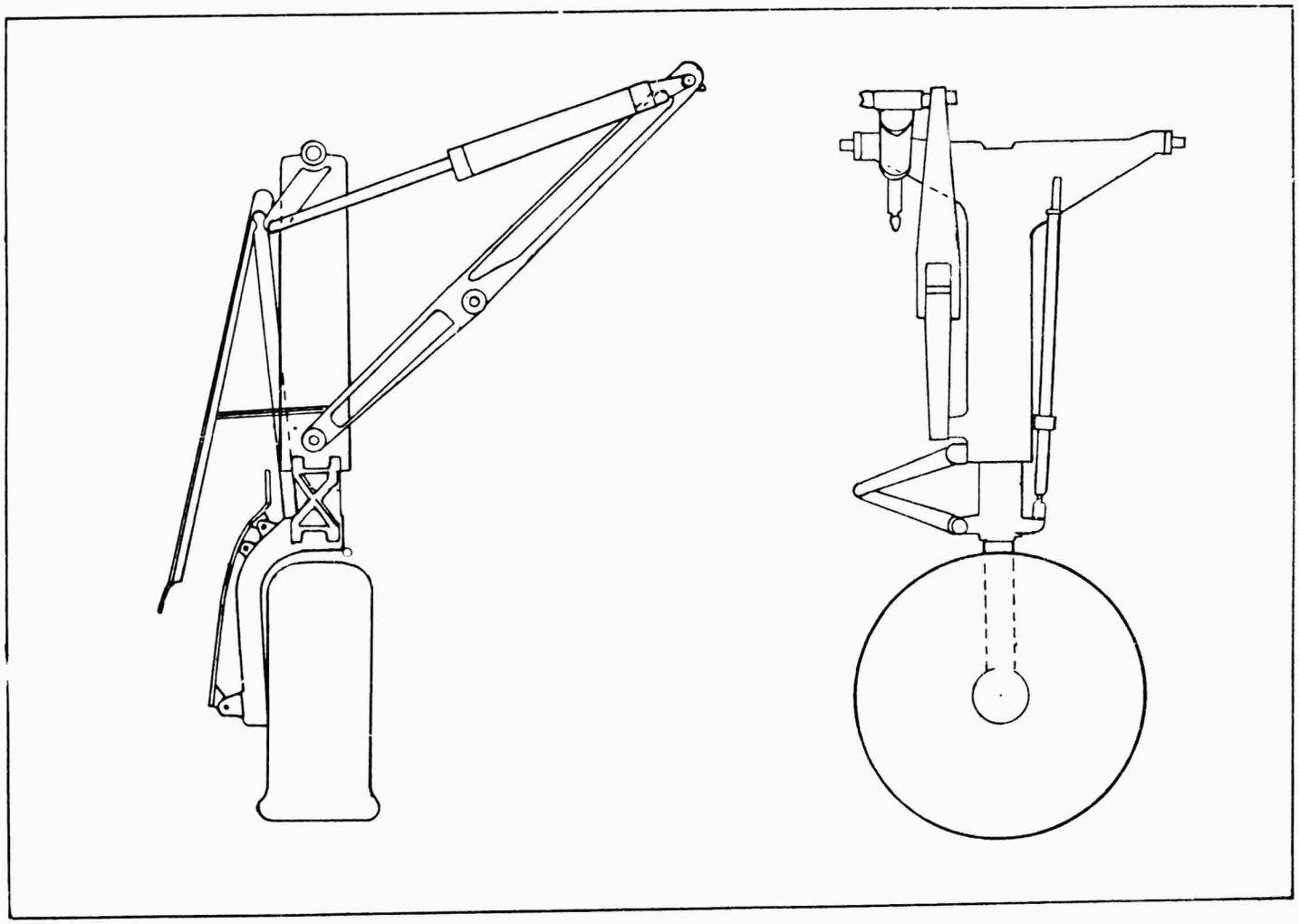

Figure 2. OV-1 Main Gear.

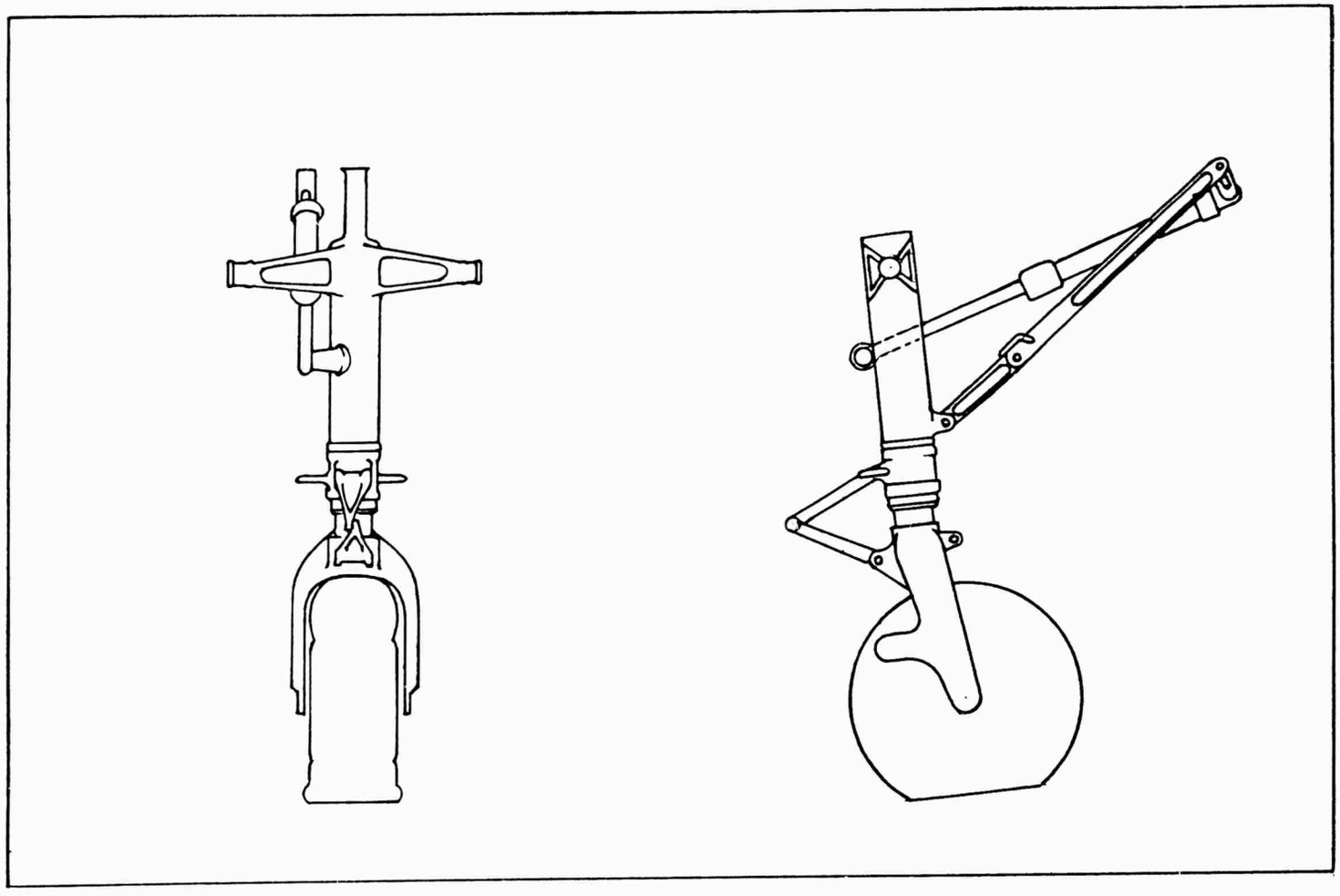

Figure 3. OV-1 Nose Gear.

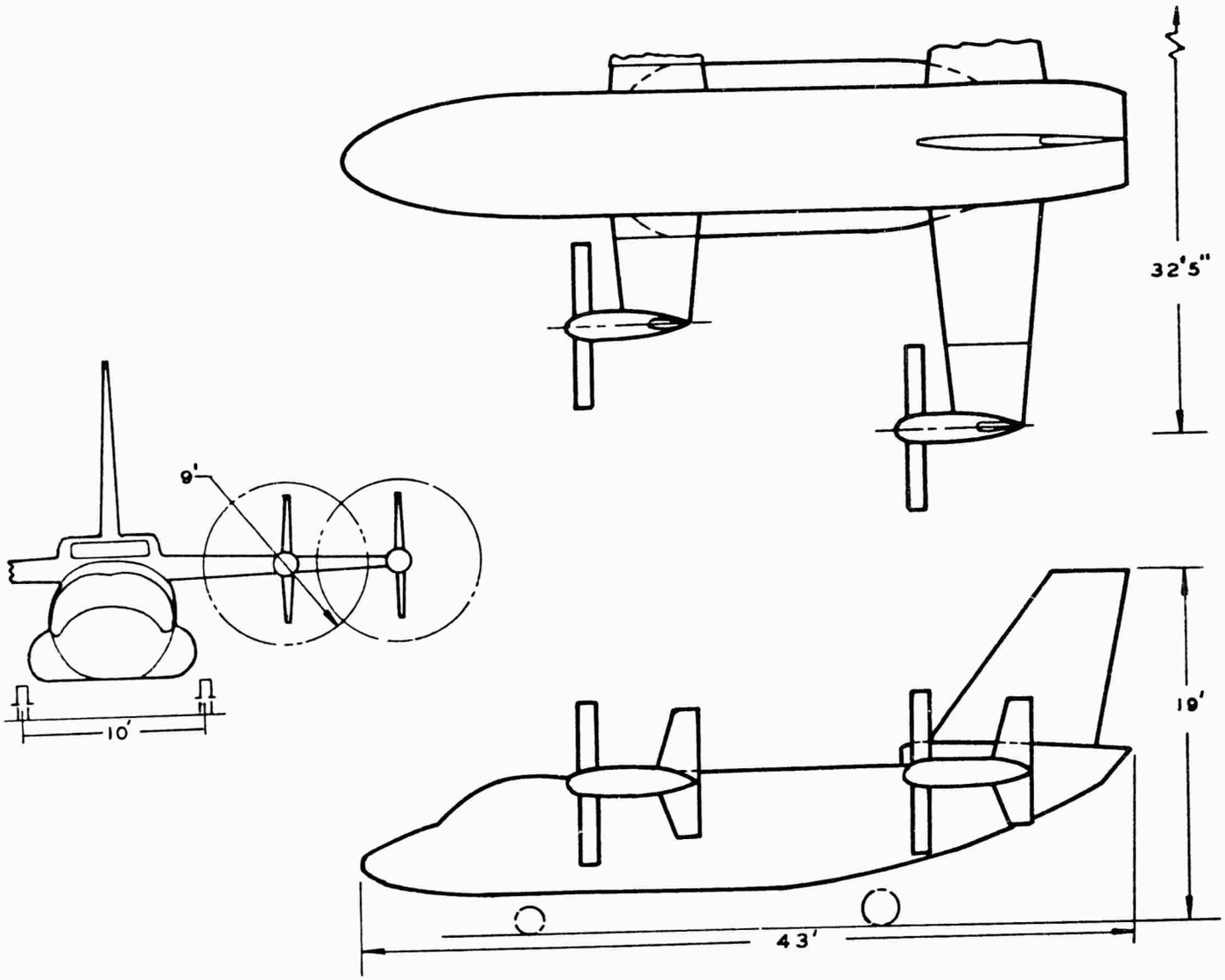

Figure 4. The VTOL Airplane.

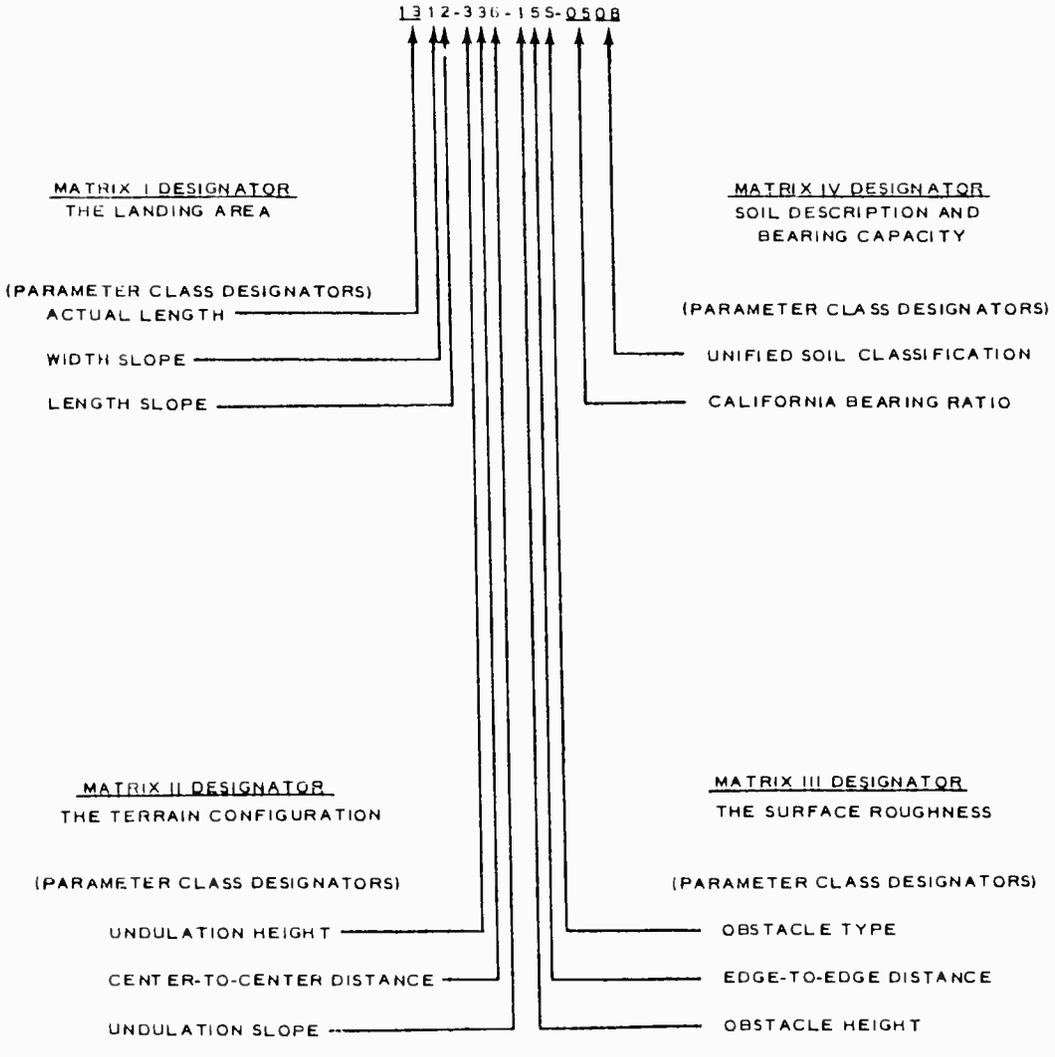

Reference Tables 4 through 7.

Figure 5. The Terrain Designation System.

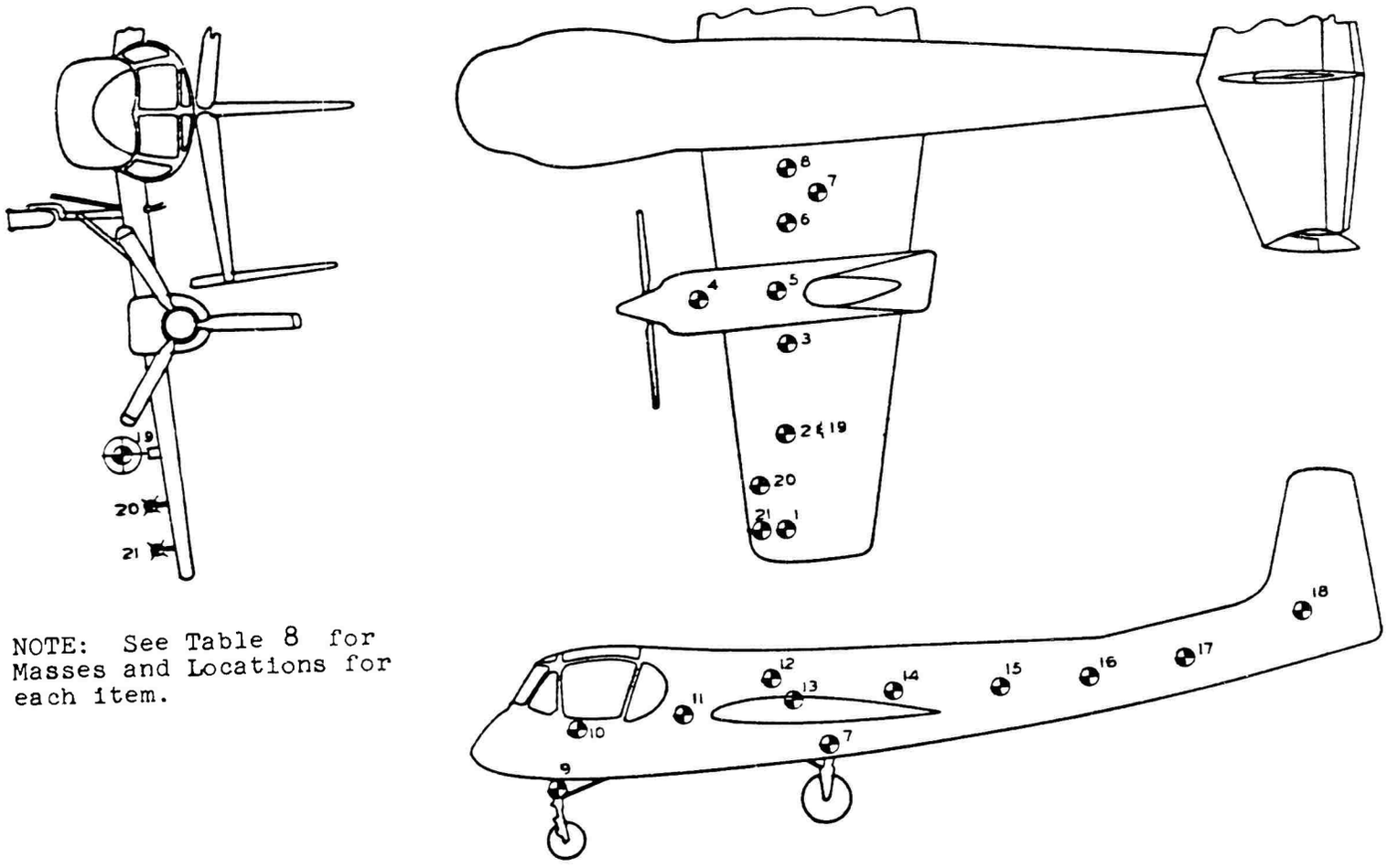

NOTE: See Table 8 for Masses and Locations for each item.

Figure 6. Airplane Mass Breakdown.

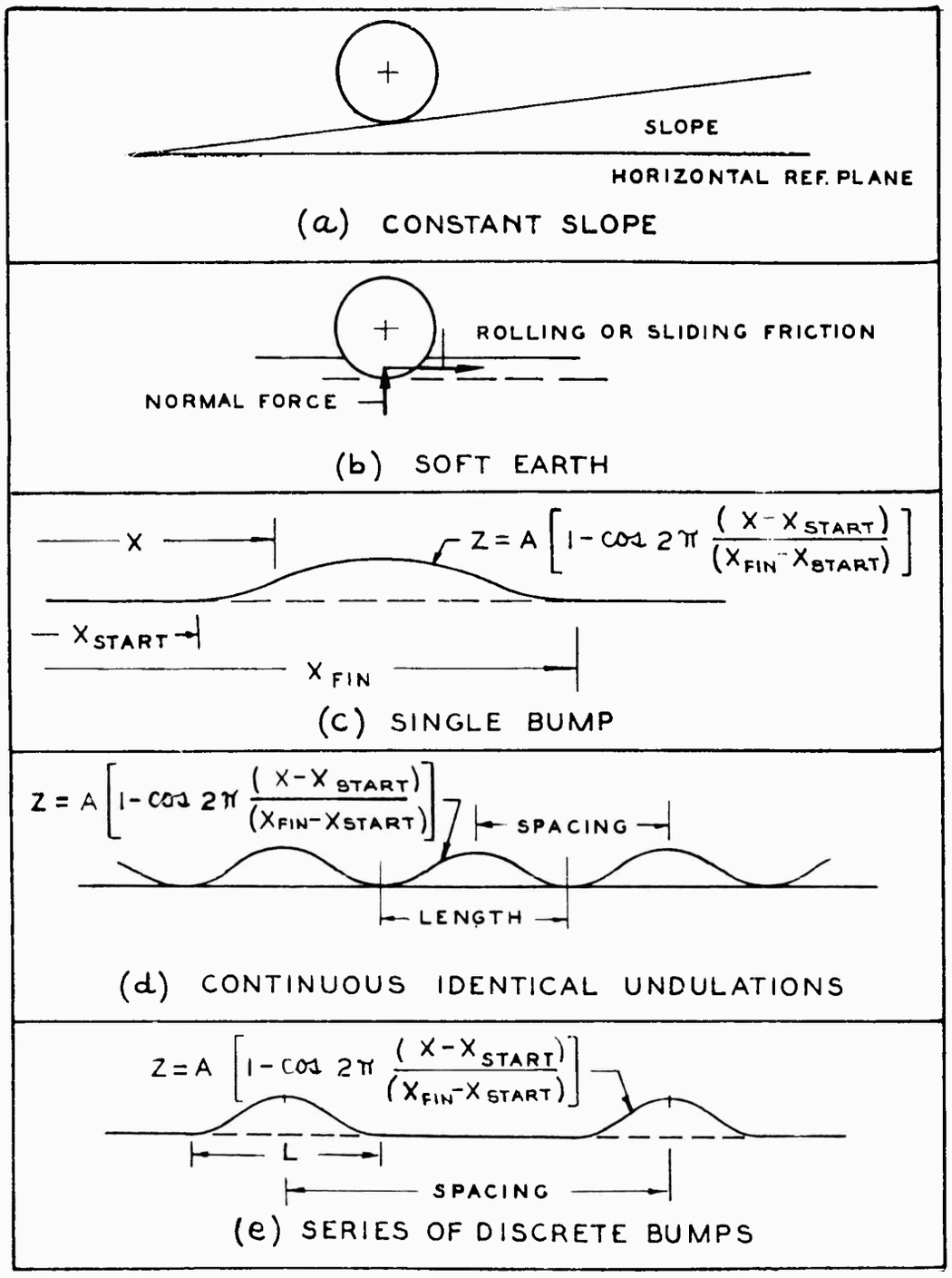

Figure 7. Types of Rough Terrain Considered.

	CALCULATED	TEST
ATTITUDE (FUSELAGE)	4° 12′	4° 15′
WEIGHT, LB.	11,771	10,715
V_V, F.P.S.	17	18
V_A, KNOTS	84.5	80.6
STRUT PRESSURE, P.S.I.	98	100
TIRE PRESSURE, P.S.I.	90	90

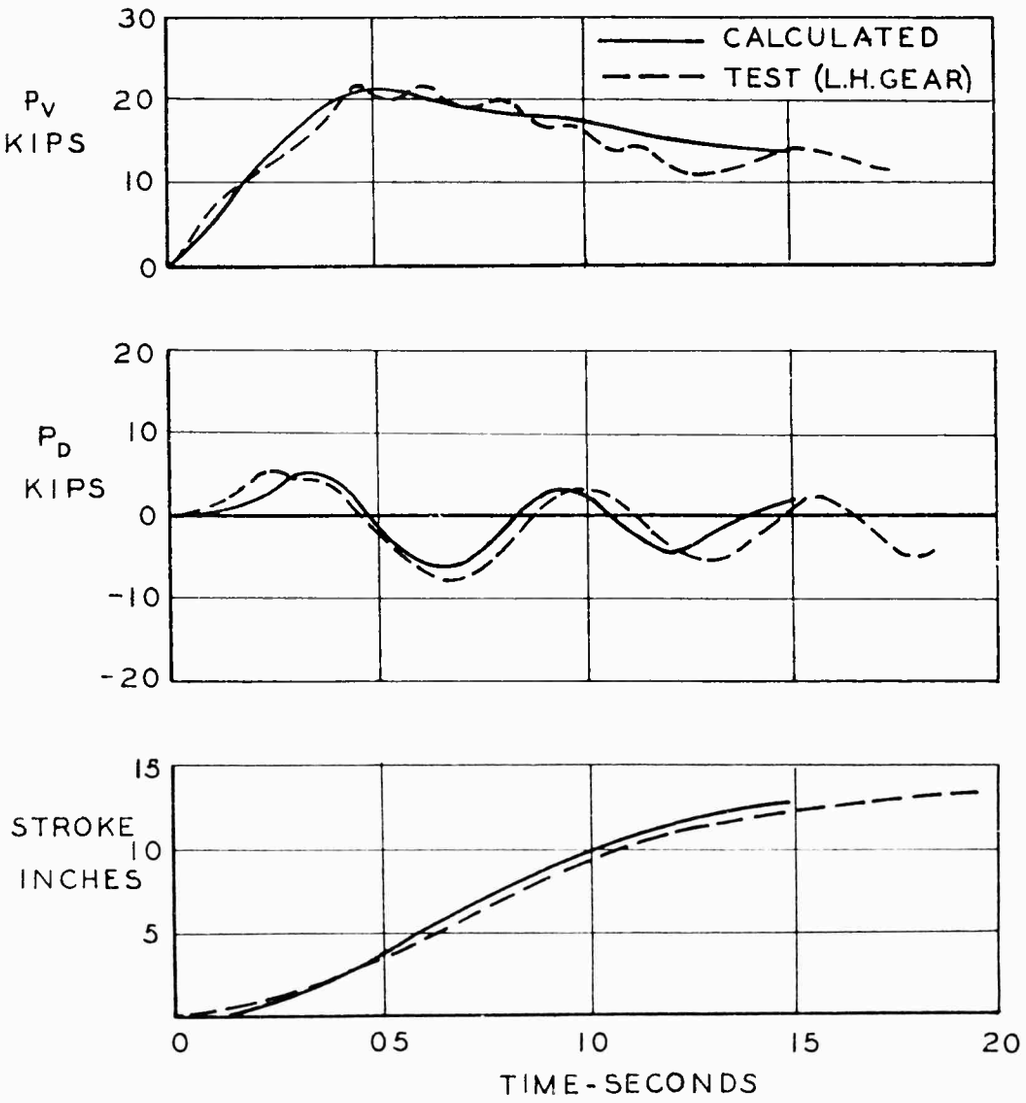

Figure 8. Comparison of Analytical Results with Airplane Drop Tests. Main Gear.

	CALCULATED	TEST
ATTITUDE (FUSELAGE)	4° 12′	4° 15′
WEIGHT, LB.	11,771	10,715
V_V, f.p.s.	17	18
V_A, KNOTS	84.5	80.6
STRUT PRESSURE, p.s.i.	47	45
TIRE PRESSURE, p.s.i.	47	65

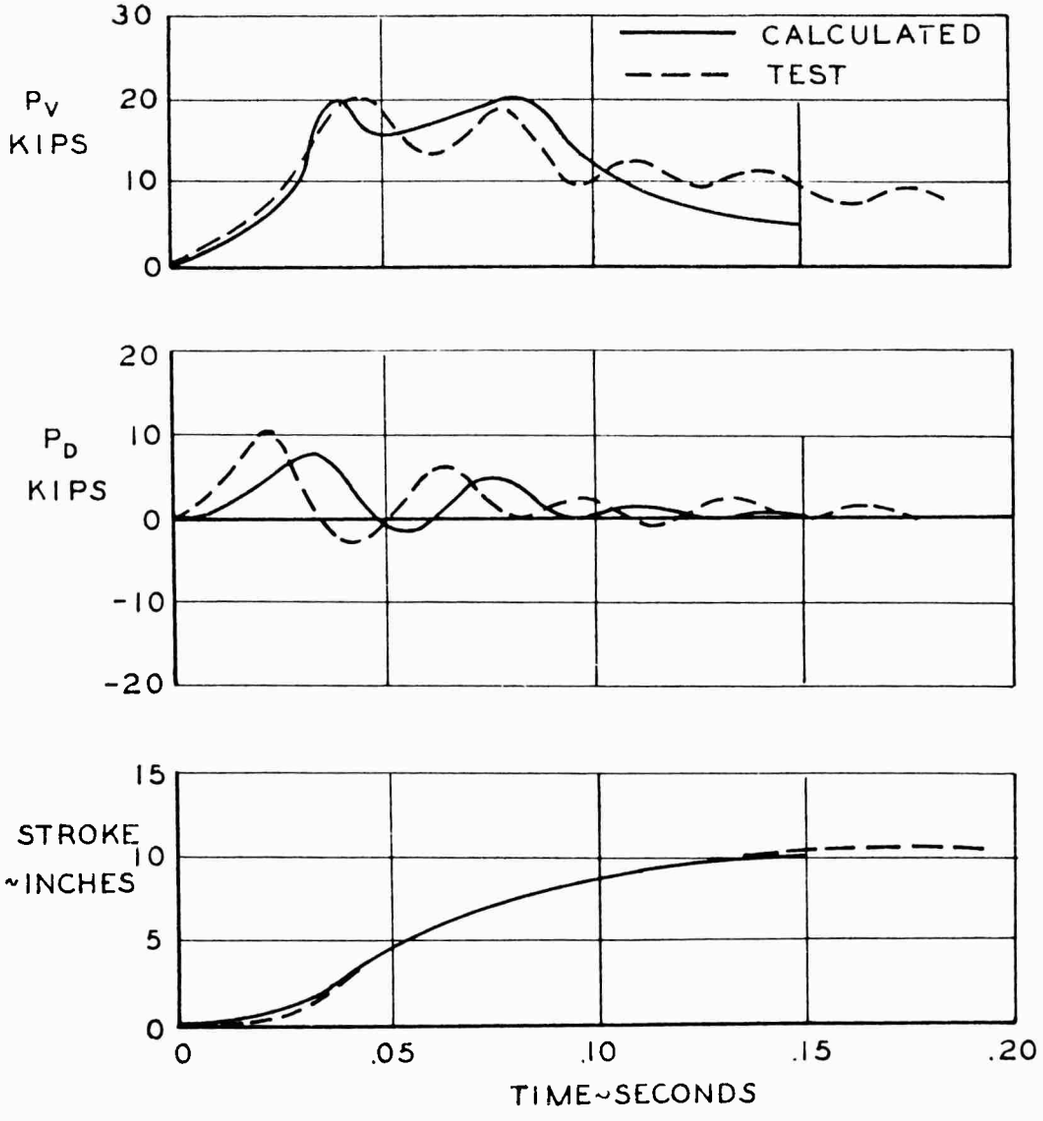

Figure 9. Comparison of Analytical Results with Airplane Drop Tests. Nose Gear.

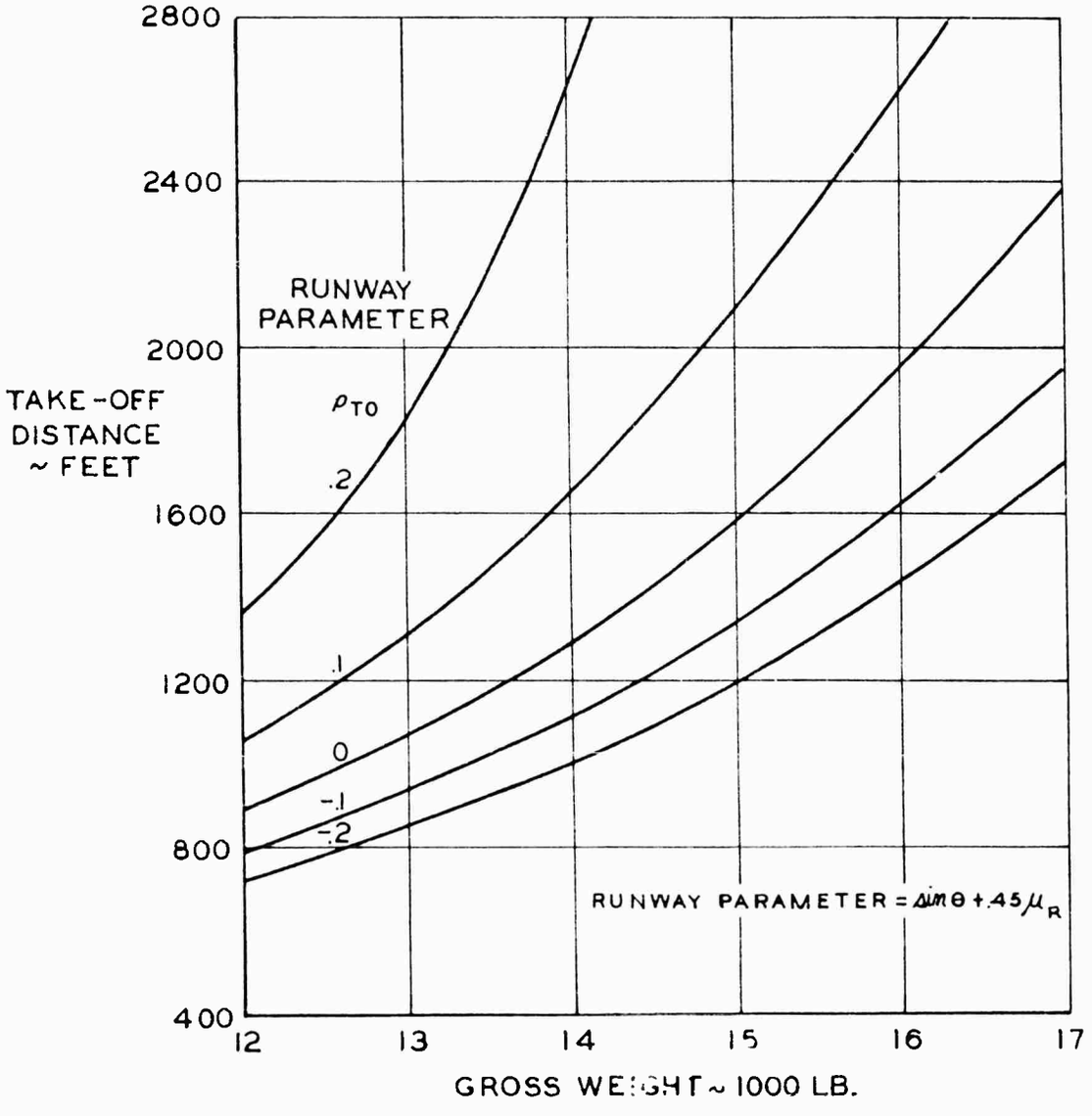

Figure 10. OV-1 Total Take-Off Distance Versus Gross Weight and Take-Off Runway Parameter.

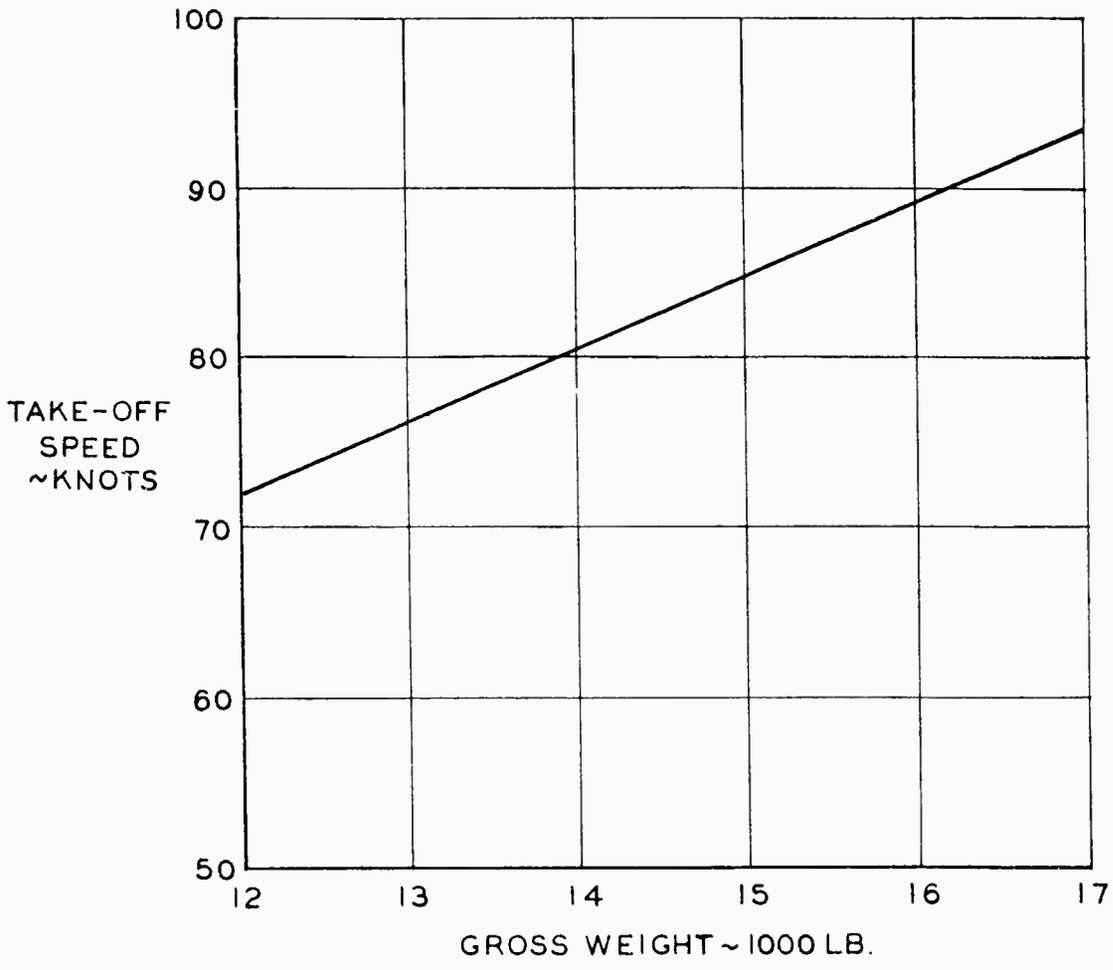

Figure 11. OV-1 Take-Off Speed Vs. Gross Weight.

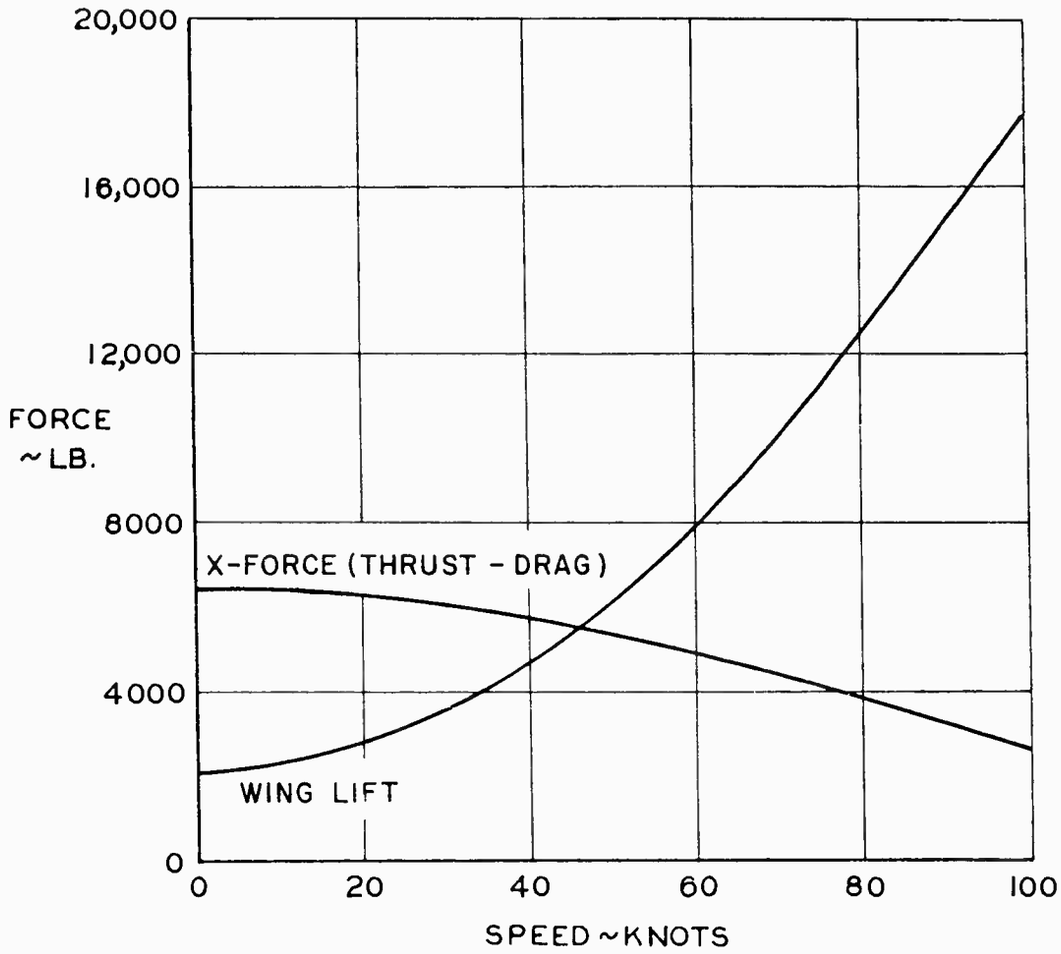

Figure 12. OV-1 Lift and X-Force During Take-Off at Taxi Attitude with Take-Off Thrust.

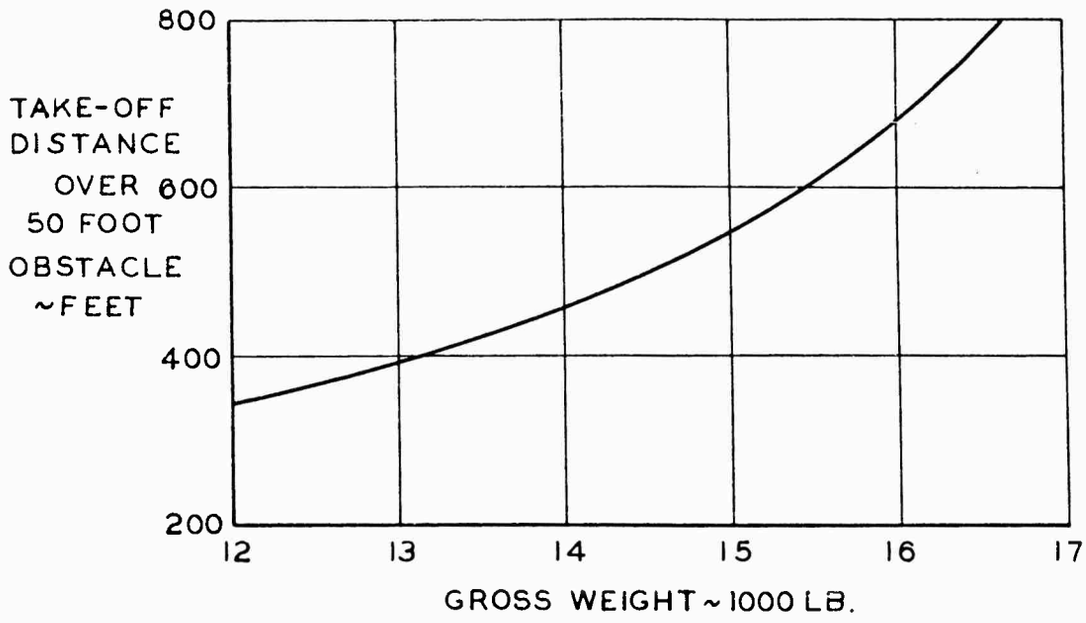

Figure 13. OV-1 Horizontal Distance from Lift-Off to a 50-Foot Obstacle Versus Gross Weight.

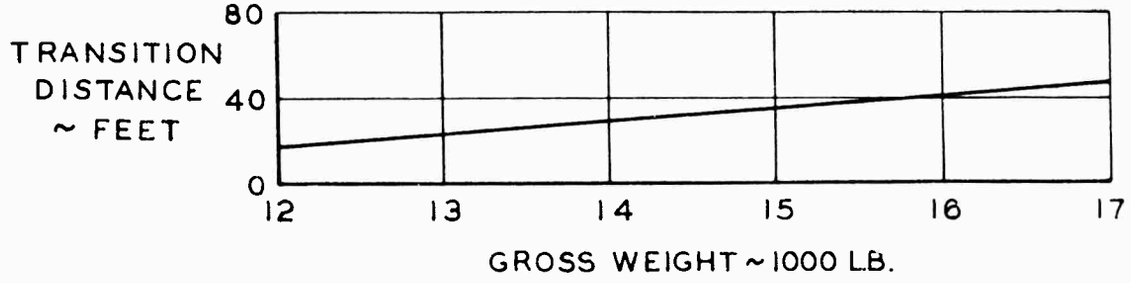

Figure 14. OV-1 Increase in Take-Off Distance Due to Rotatior from Taxi Attitude to Fly Away Attitude Versus Gross Weight.

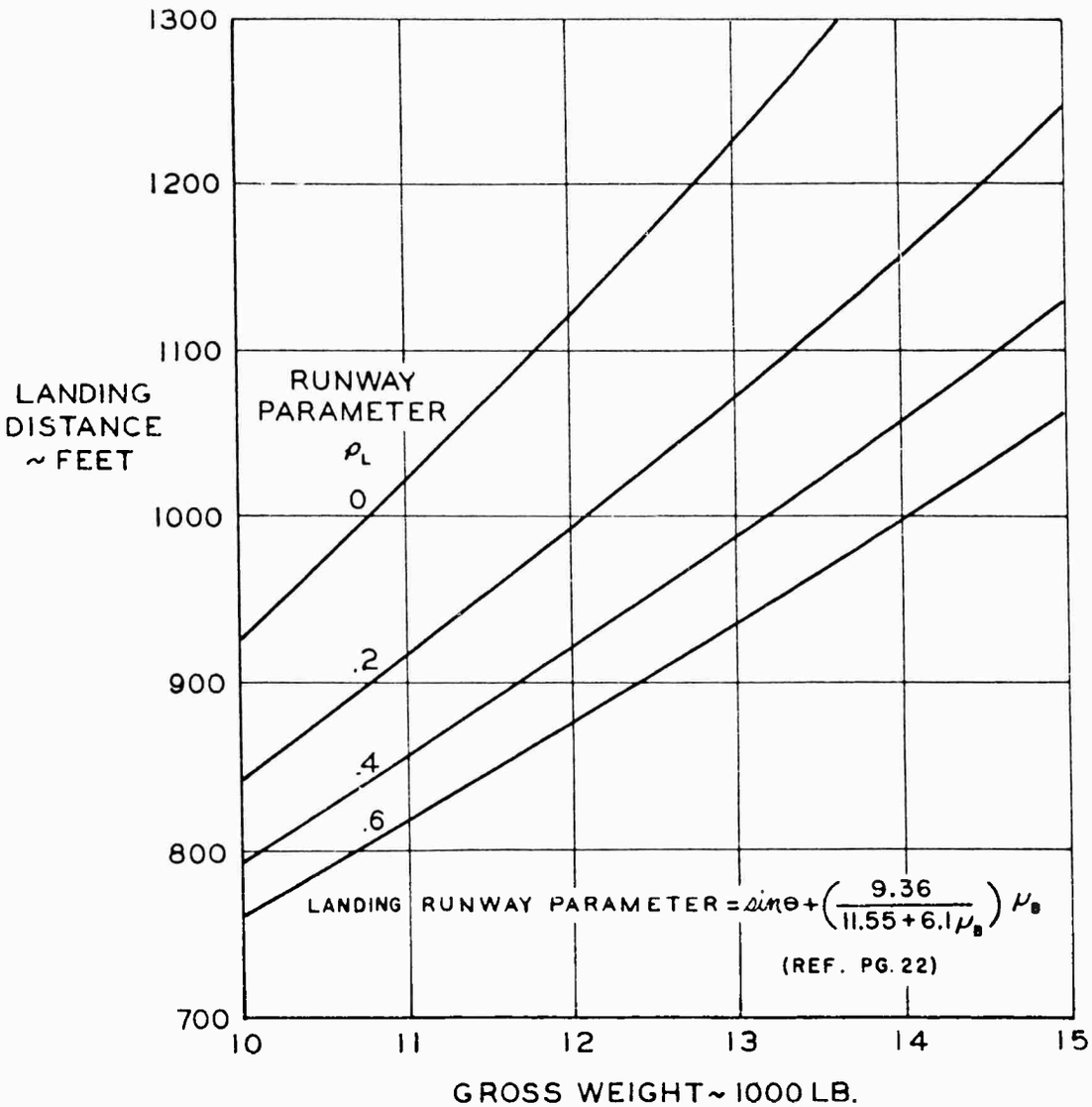

Figure 15. OV-1 Total Landing Distance Versus Gross Weight and Landing Runway Parameter.

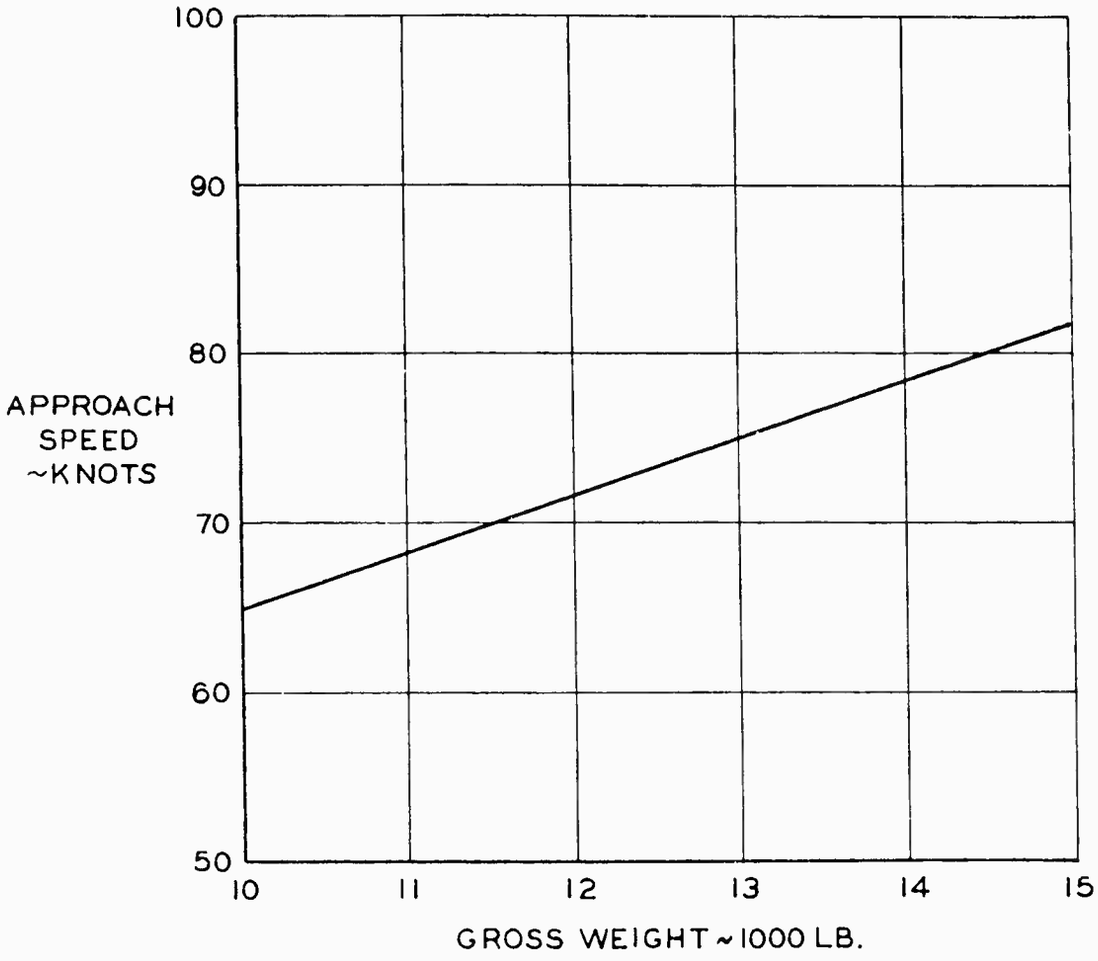

Figure 16. OV-1 Approach Speed Vs. Gross Weight.

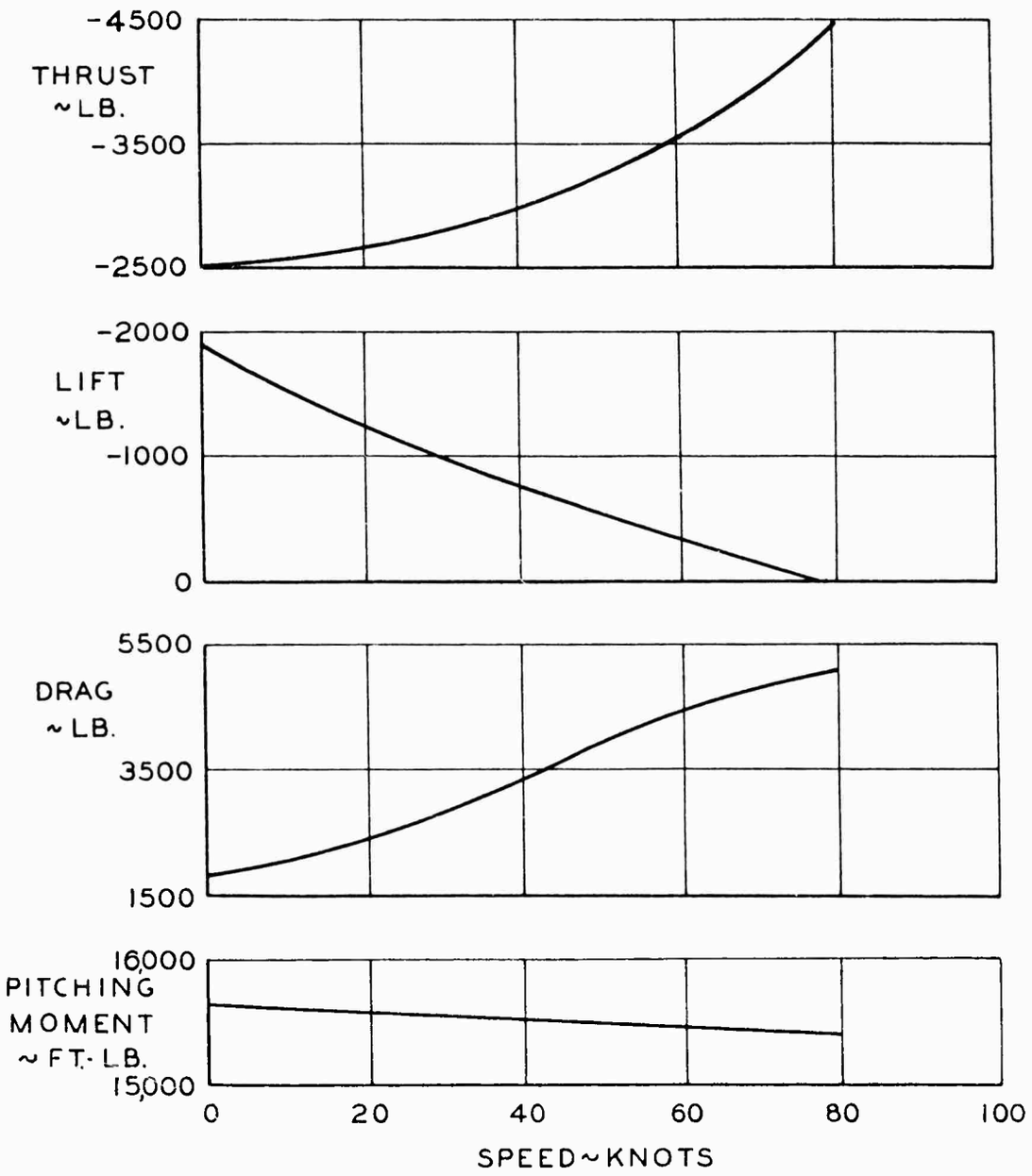

Figure 17. OV-1 Forces and Pitching Moment During Landing Roll-Out at Taxi Attitude with Full Reverse Thrust.

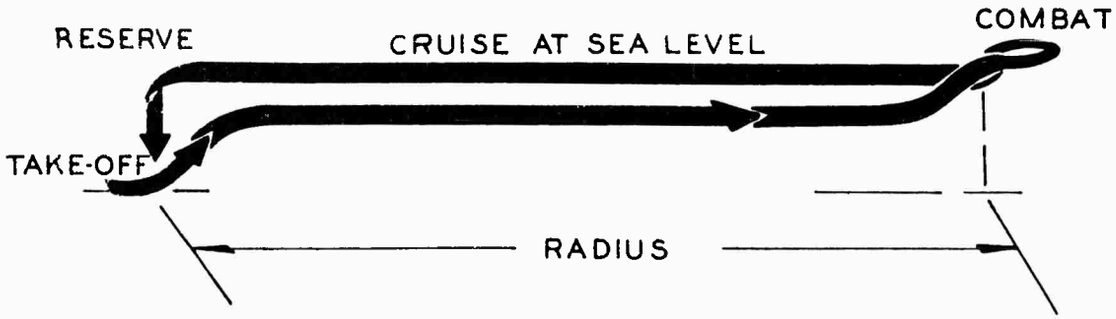

FUEL ALLOWANCE:

TAKE-OFF - 5 MINUTES @ S.L. NORMAL STATIC THRUST
COMBAT - 1 MINUTE @ 4000 FT. AT MAXIMUM SPEED
RESERVE - 10% OF FUEL AT TAKE-OFF

Figure 18. Mission Profile.

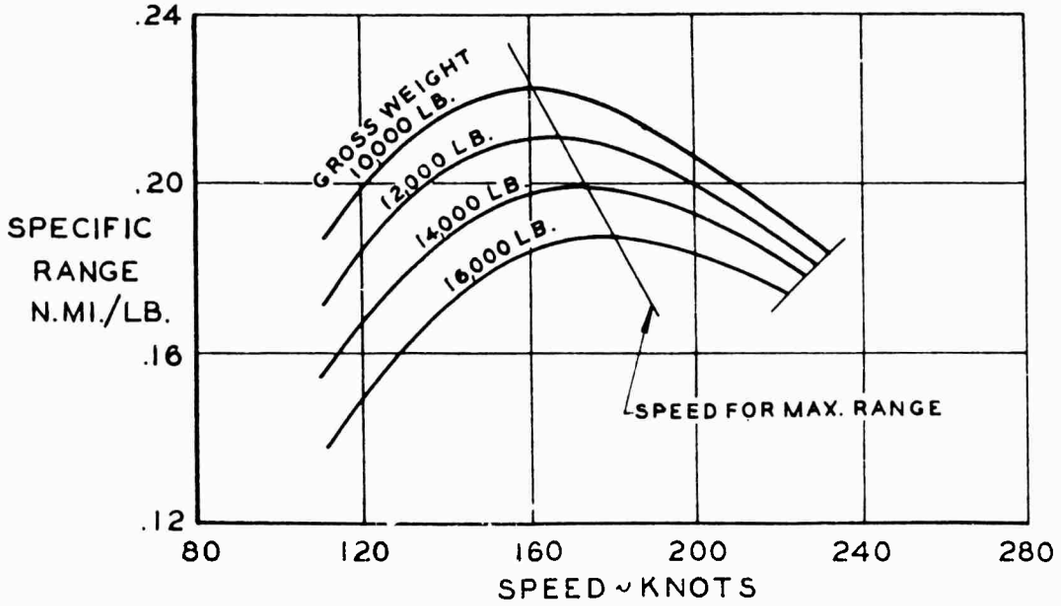

Figure 19. Specific Range at Sea Level Versus Airspeed and Gross Weight for the OV-1 with Two 150-Gallon External Fuel Tanks.

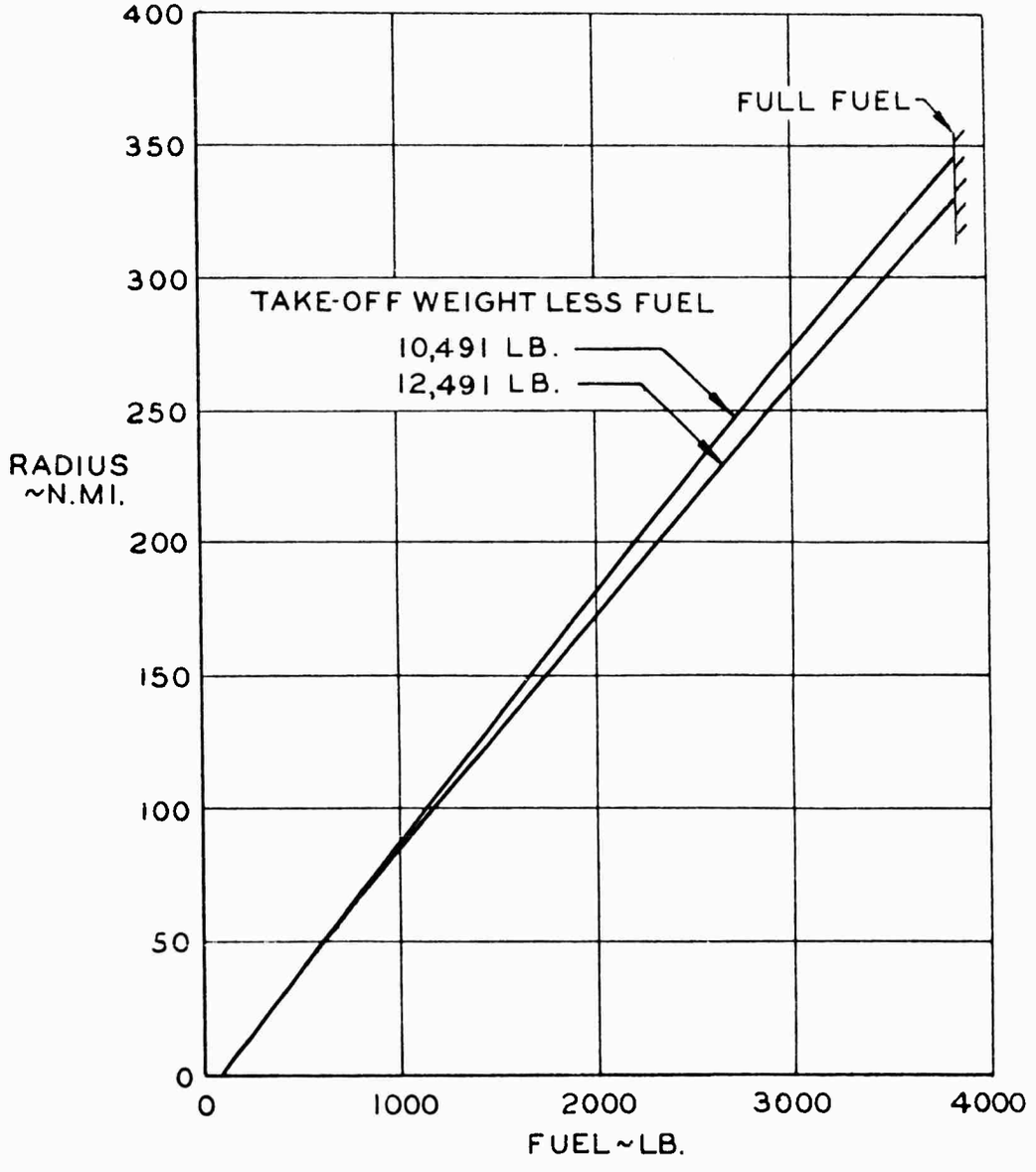

Figure 20. OV-1 Radius Versus Fuel Aboard at Take-Off.

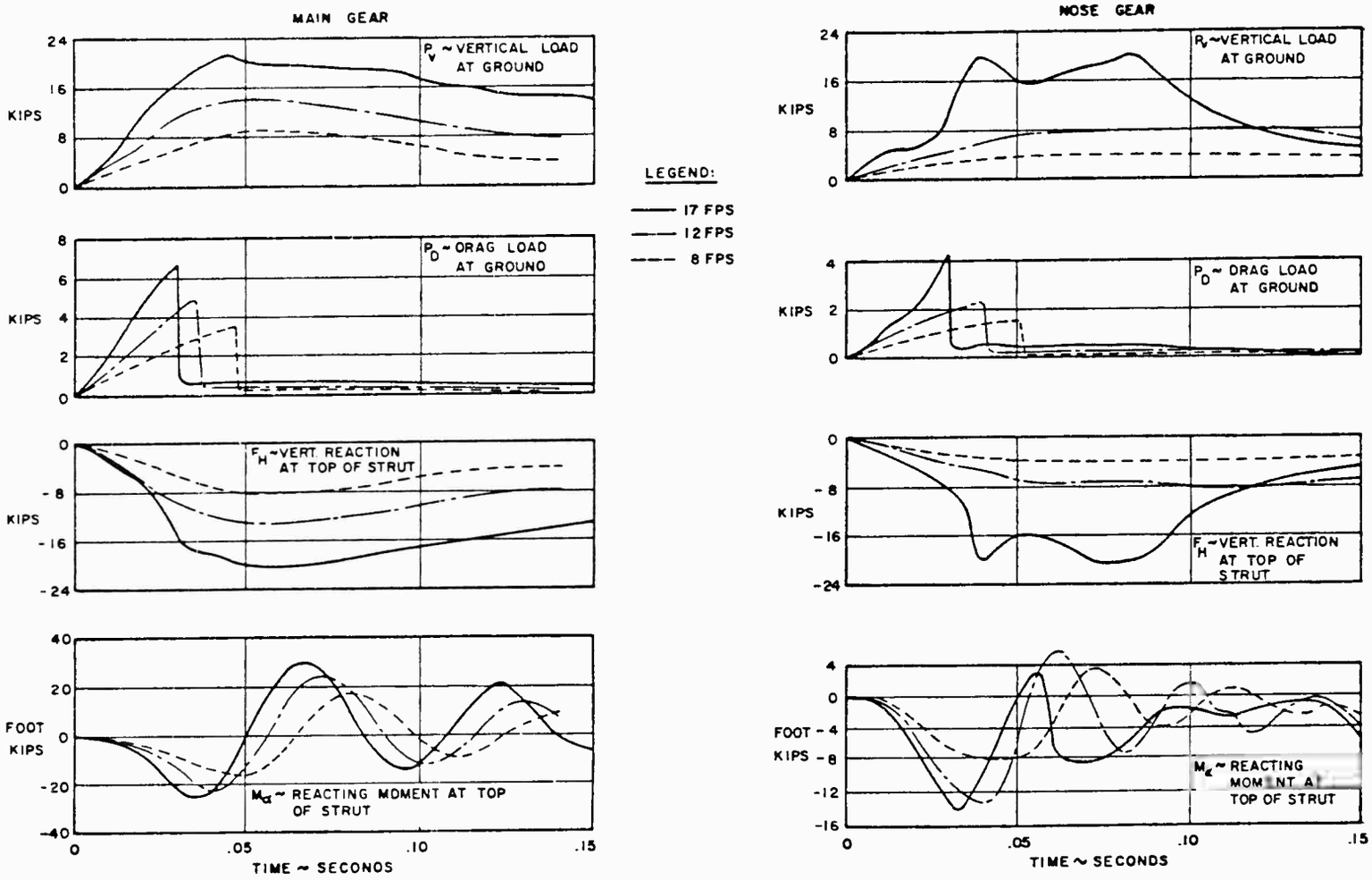

Figure 21. Main and Nose Gear Time Histories. Landing on Level, Smcoth Terrain, Three-Point Attitude.

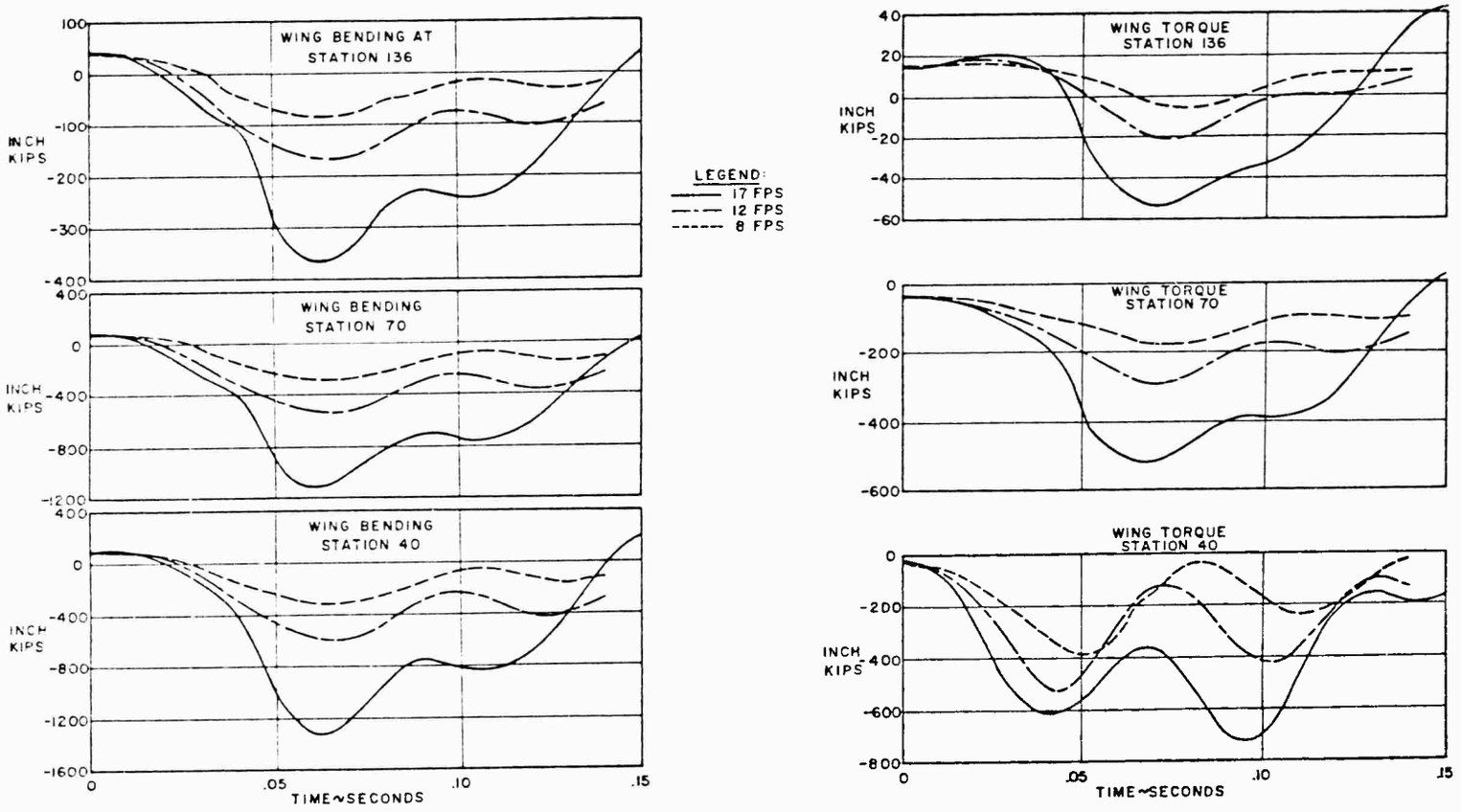

Figure 22. Wing Bending Moment and Torque Time Histories. Landing on Level, Smooth Terrain, Three-Point Attitude.

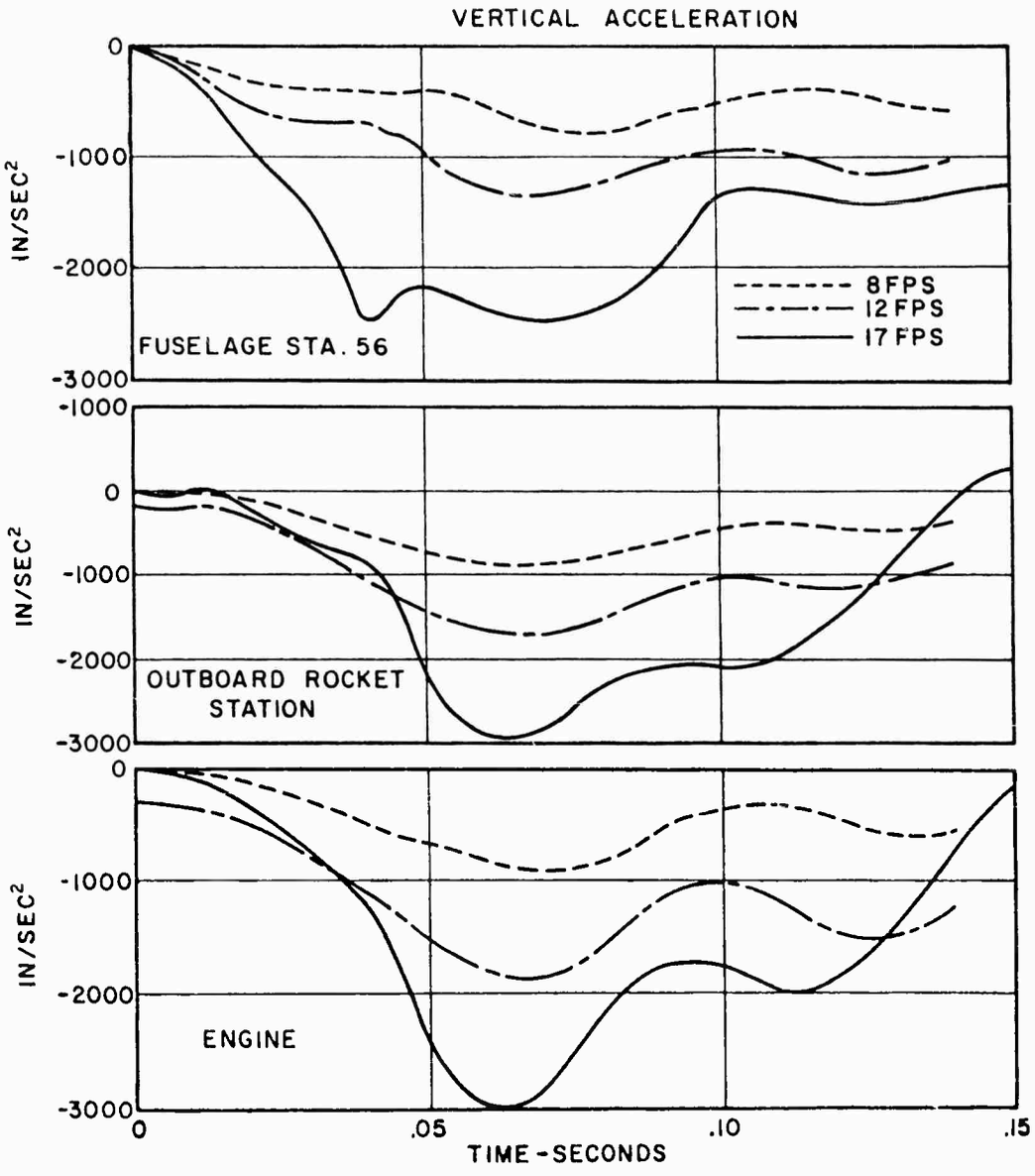

Figure 23. Acceleration Time Histories. Landing on Level, Smooth Terrain, Three-Point Attitude.

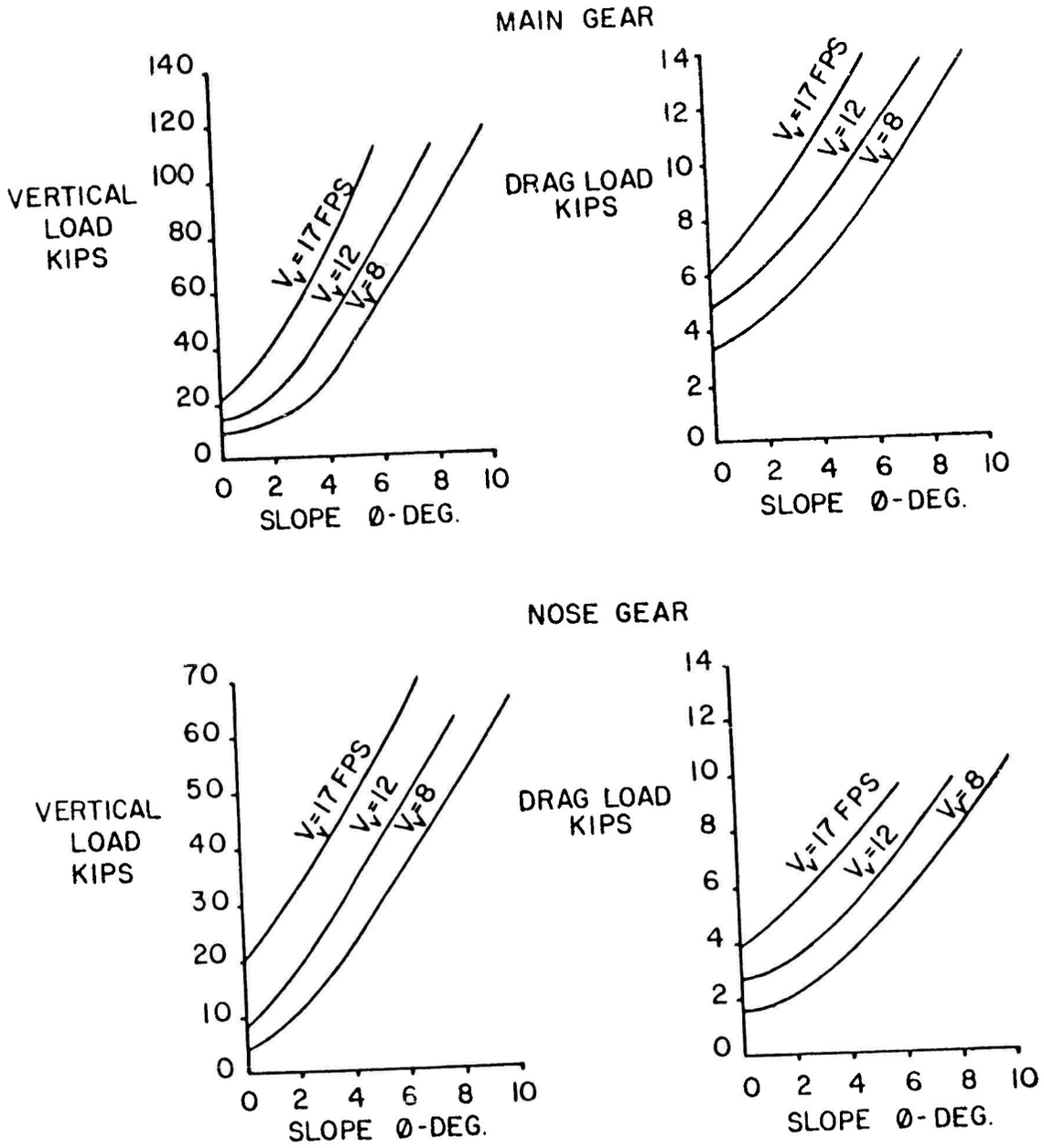

Figure 24. Variation of Maximum Loads with Ground Slope.

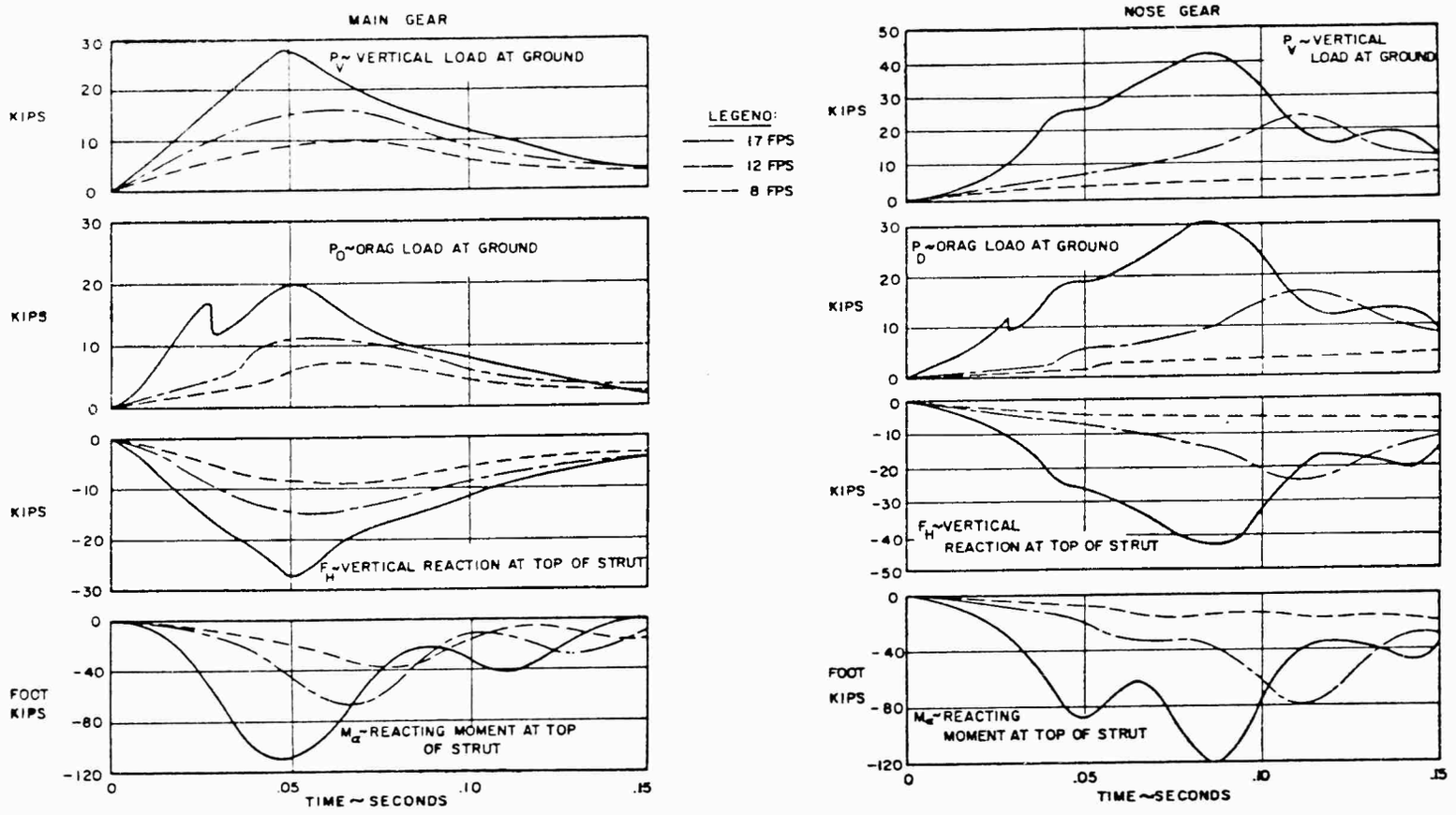

Figure 25. Main and Nose Gear Time Histories. Landing in Three-Point Attitude on Level Terrain with High Rolling Coefficient of Friction, μ_S = .4 and μ_R = .7.

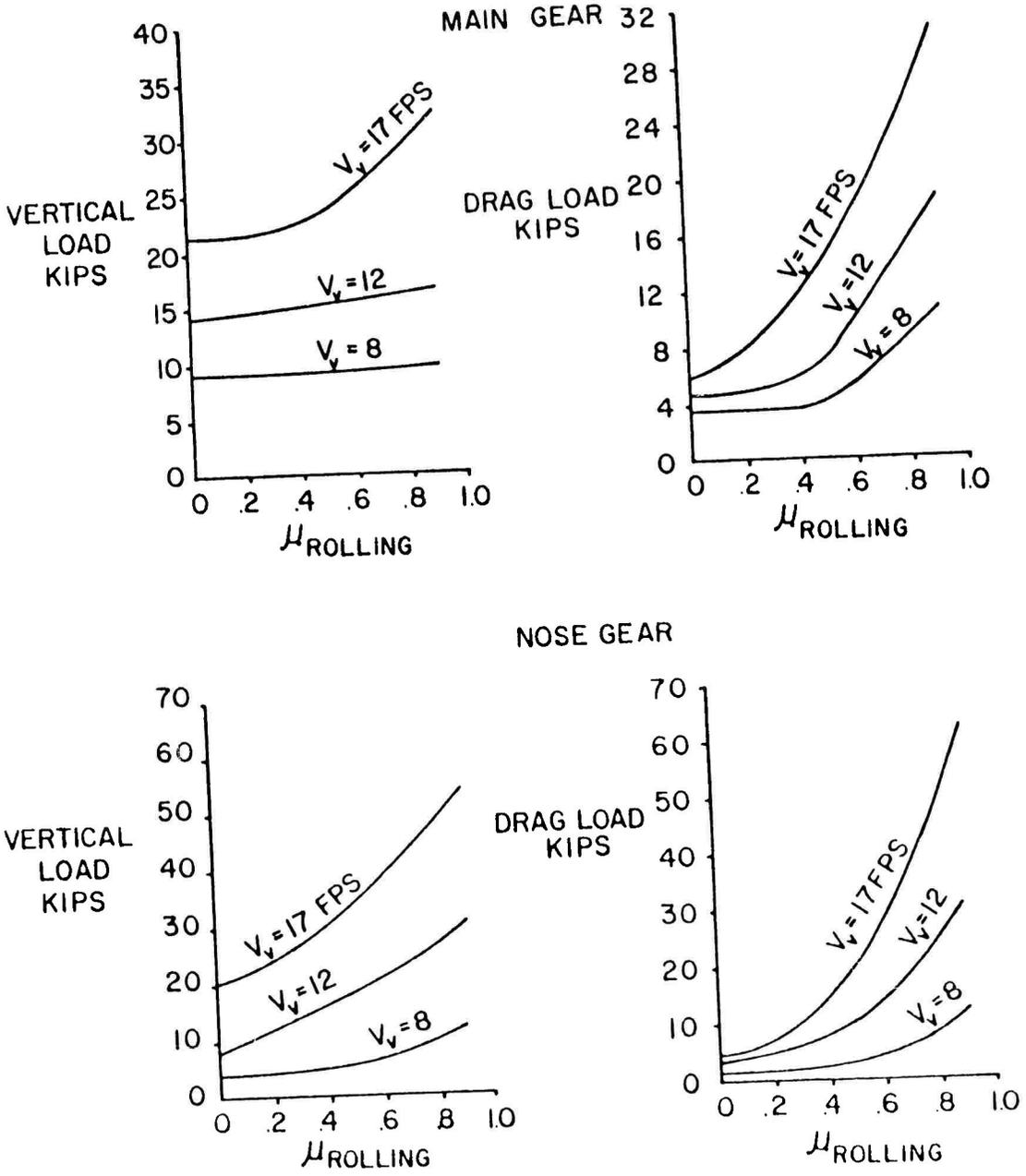

Figure 26. Variation of Maximum Loads with Rolling Coefficient of Friction.

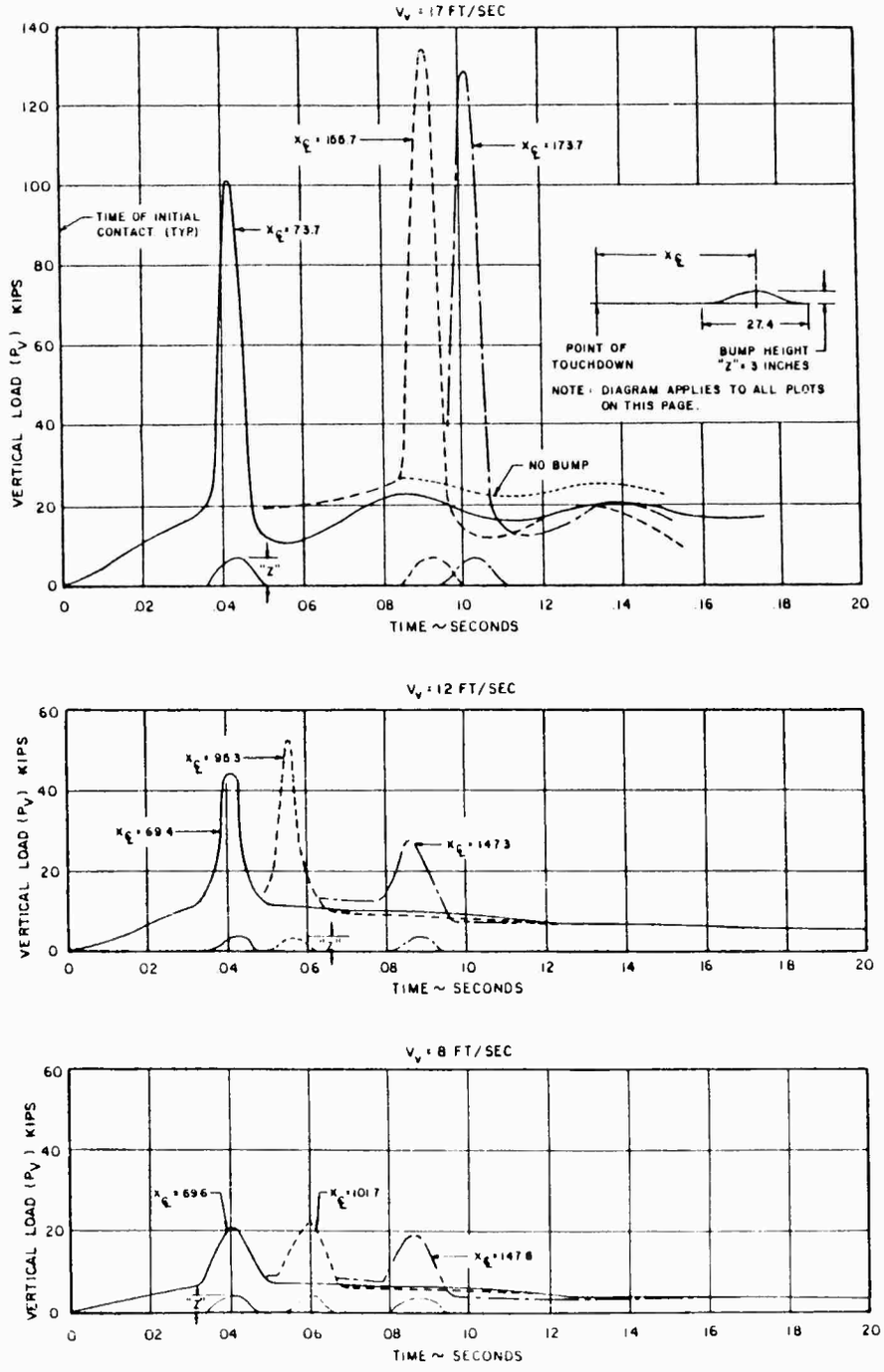

Figure 27. Vertical Load on Main Gear for Bumps in Different Locations Relative to Point of Touchdown.

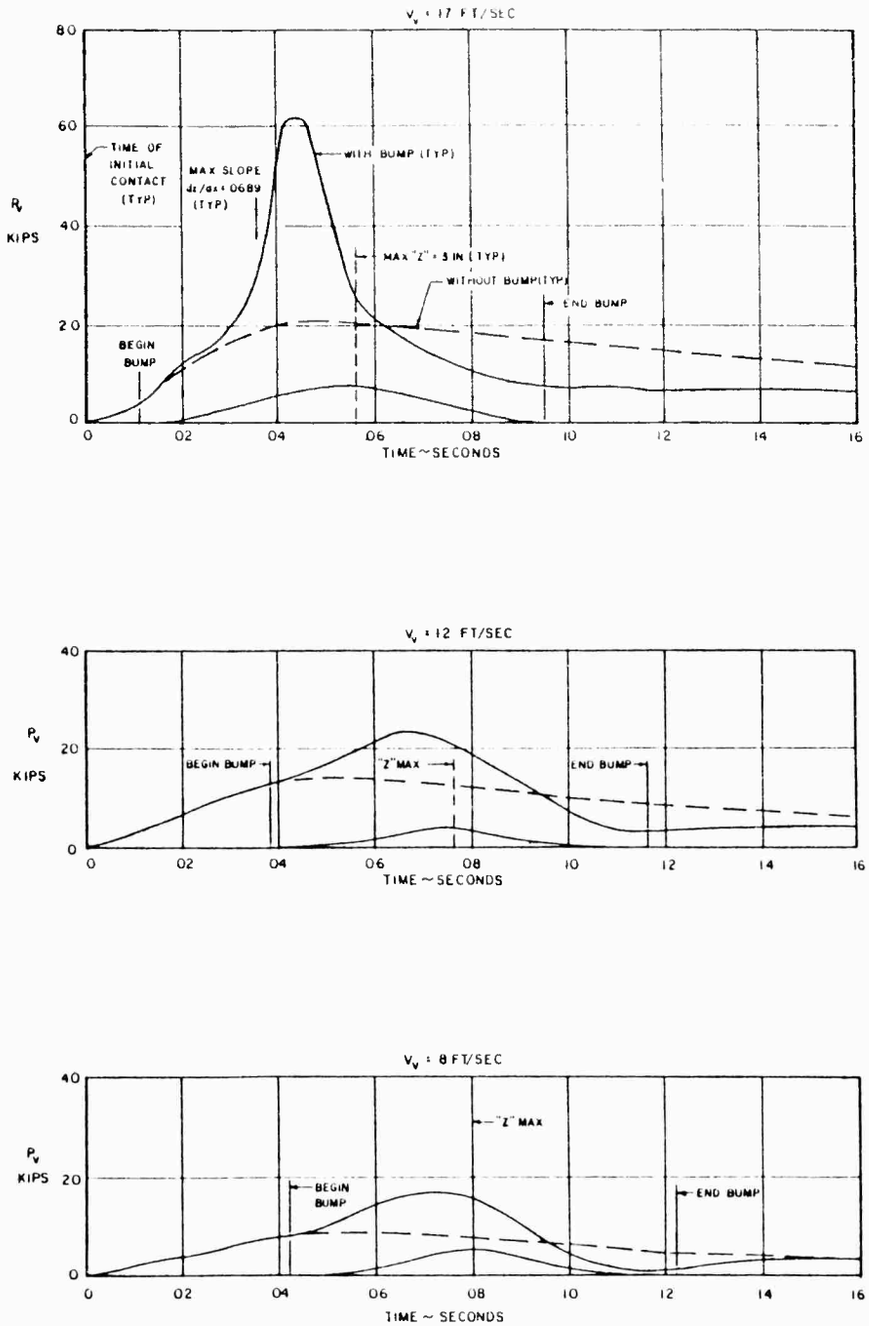

Figure 28. Main Gear Load Versus Time for a Three-Inch Bump 137 Inches Long.

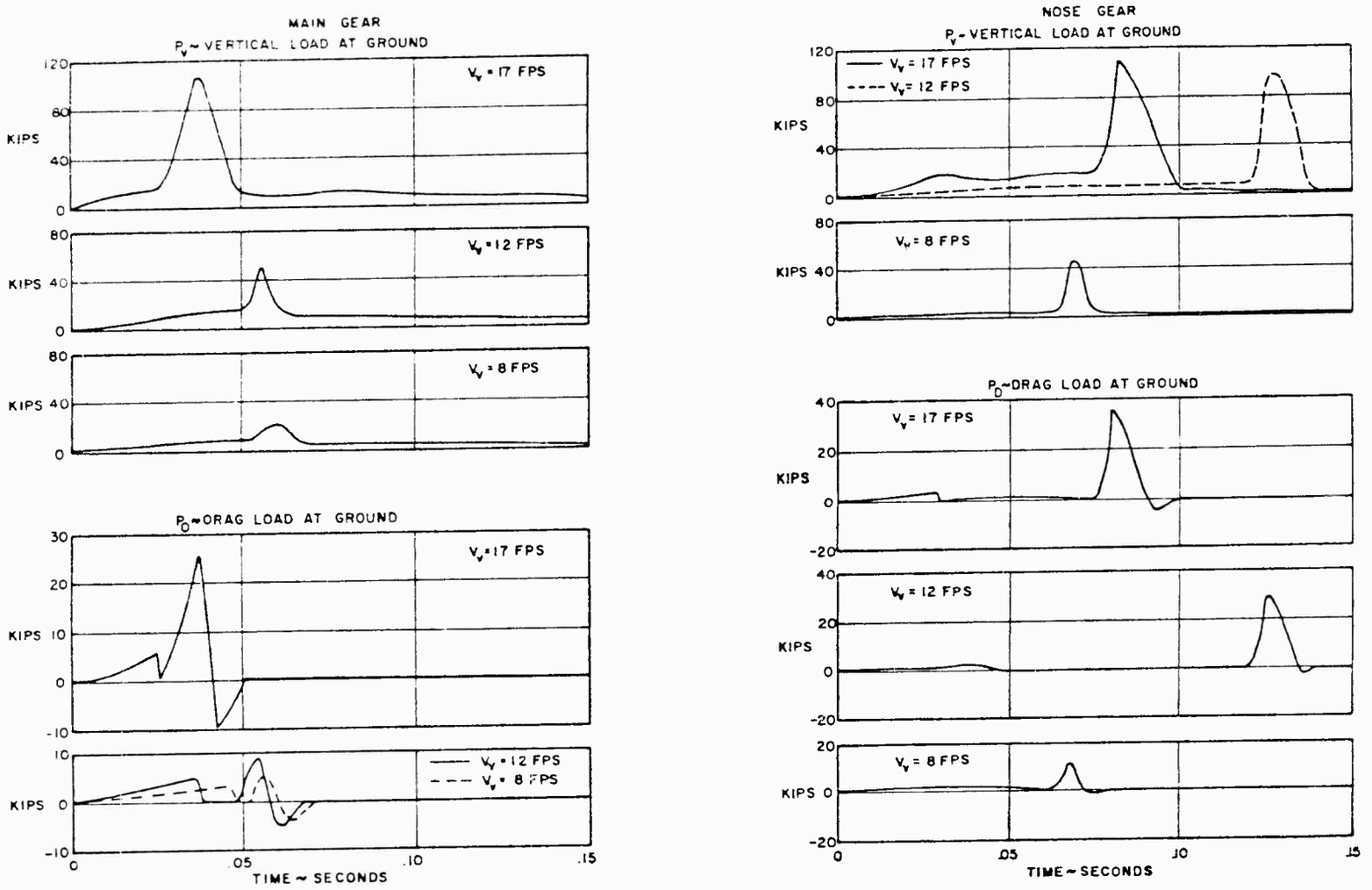

Figure 29. Main and Nose Gear Time Histories. Landing in Three-Point Attitude on Level Terrain, Gear Hits Single Bump at Most Critical Point. Bump Length = 27.4 Inches, Height = 3 Inches.

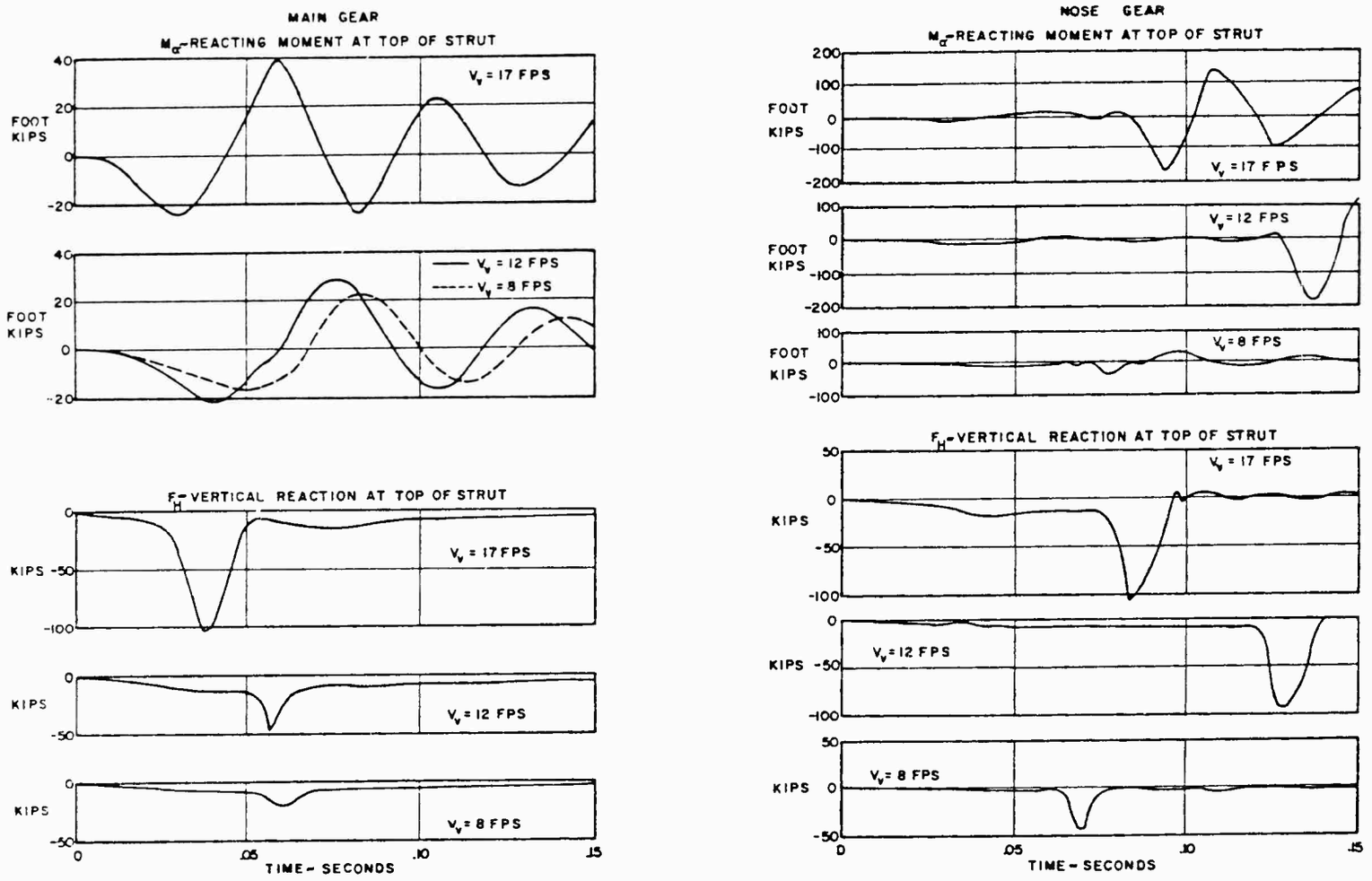

Figure 29 (Cont'd). Main and Nose Gear Time Histories. Landing in Three-Point Attitude on Level Terrain, Gear Hits Single Bump at Most Critical Point. Bump Length = 27.4, Height = 3 Inches.

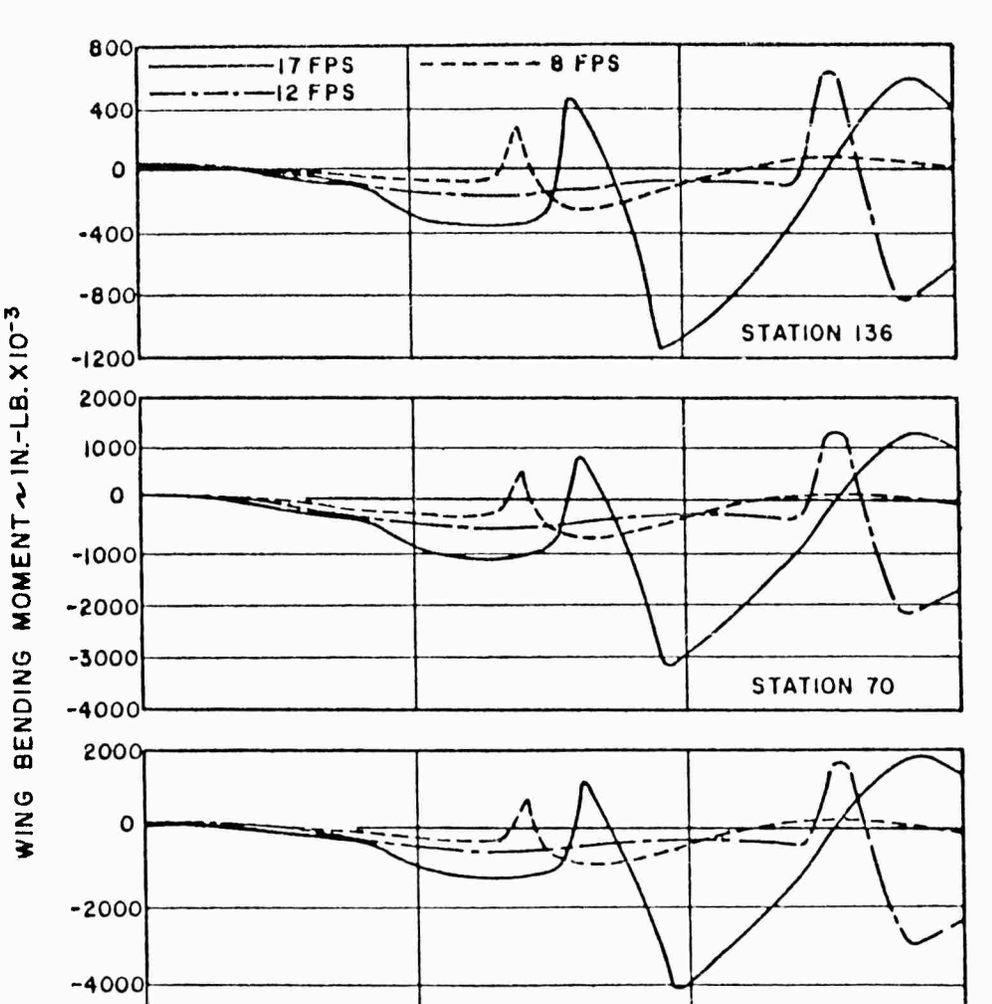

Figure 30. Wing Bending Time Histories. Landing on Level Terrain, Nose Gear Hits Bump at Most Critical Distance of Bump $\mathbb{Q}$ to Main Gear Touchdown, Three Point Attitude. Bump Length = 27.4 Inches, Height = 3 Inches.

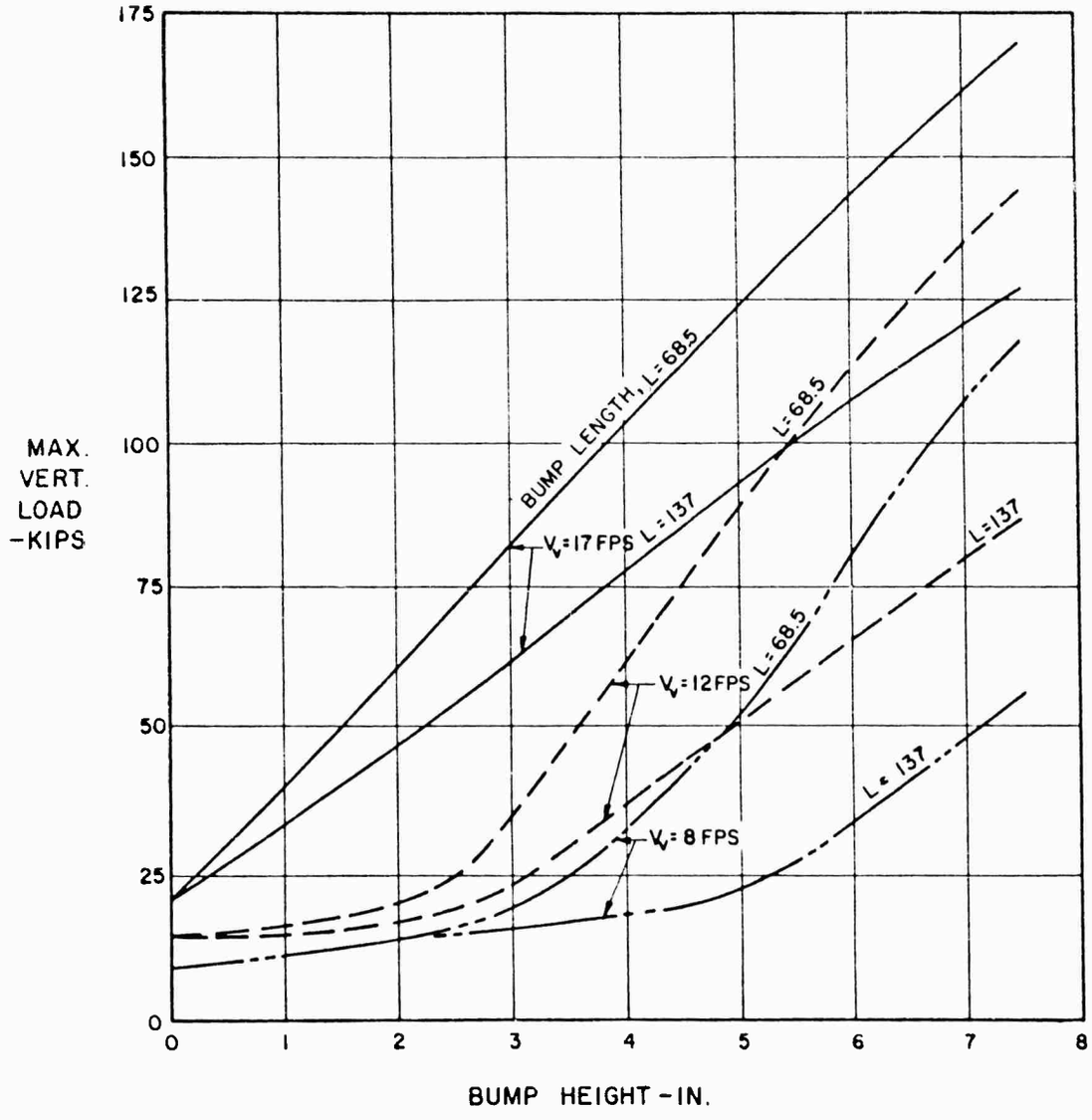

Figure 31. Maximum Main Gear Vertical Load Versus Bump Height, Bump Length and Sinking Speed.

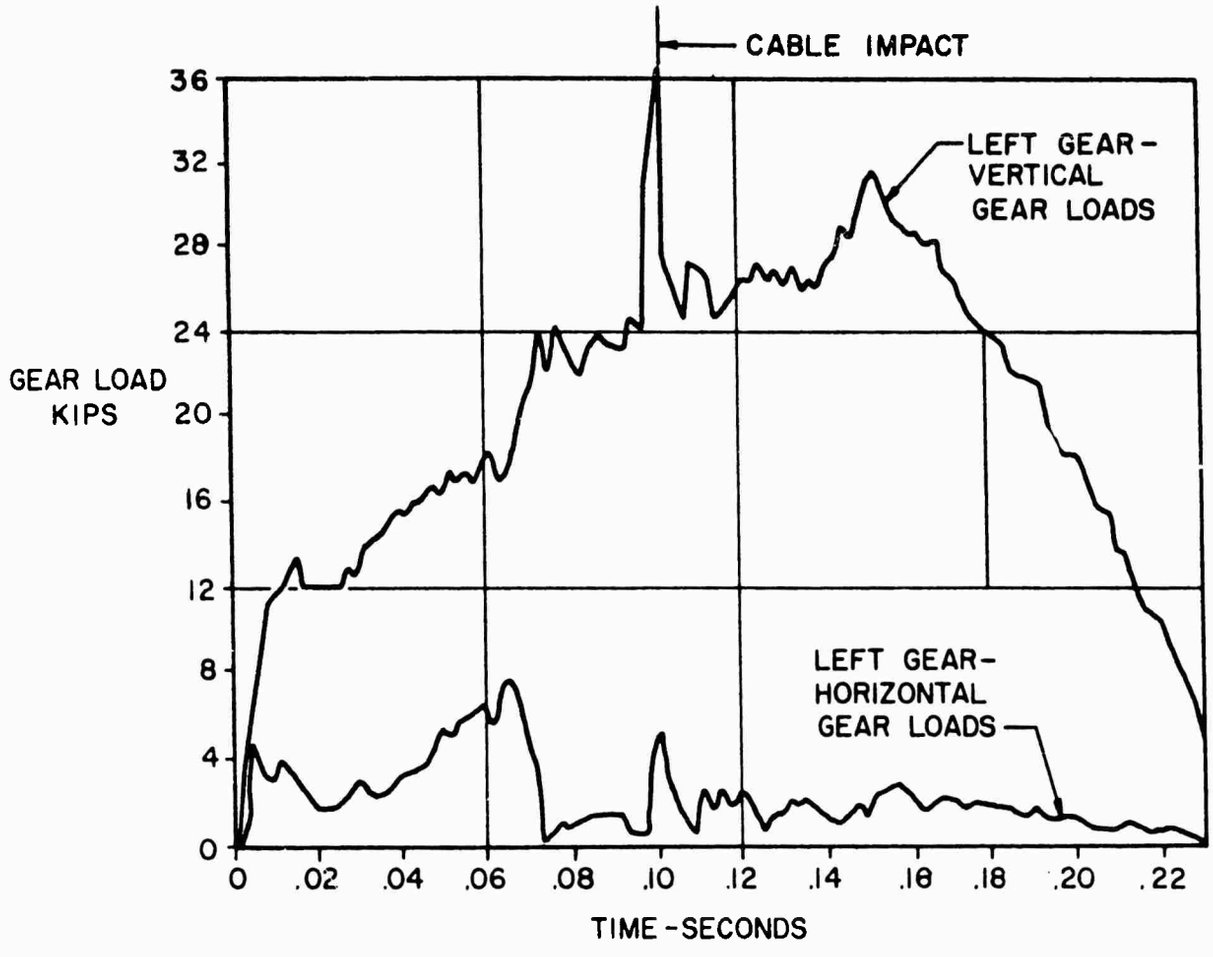

Figure 32. Effect of Cable Impact on A-4B Gear Loads.

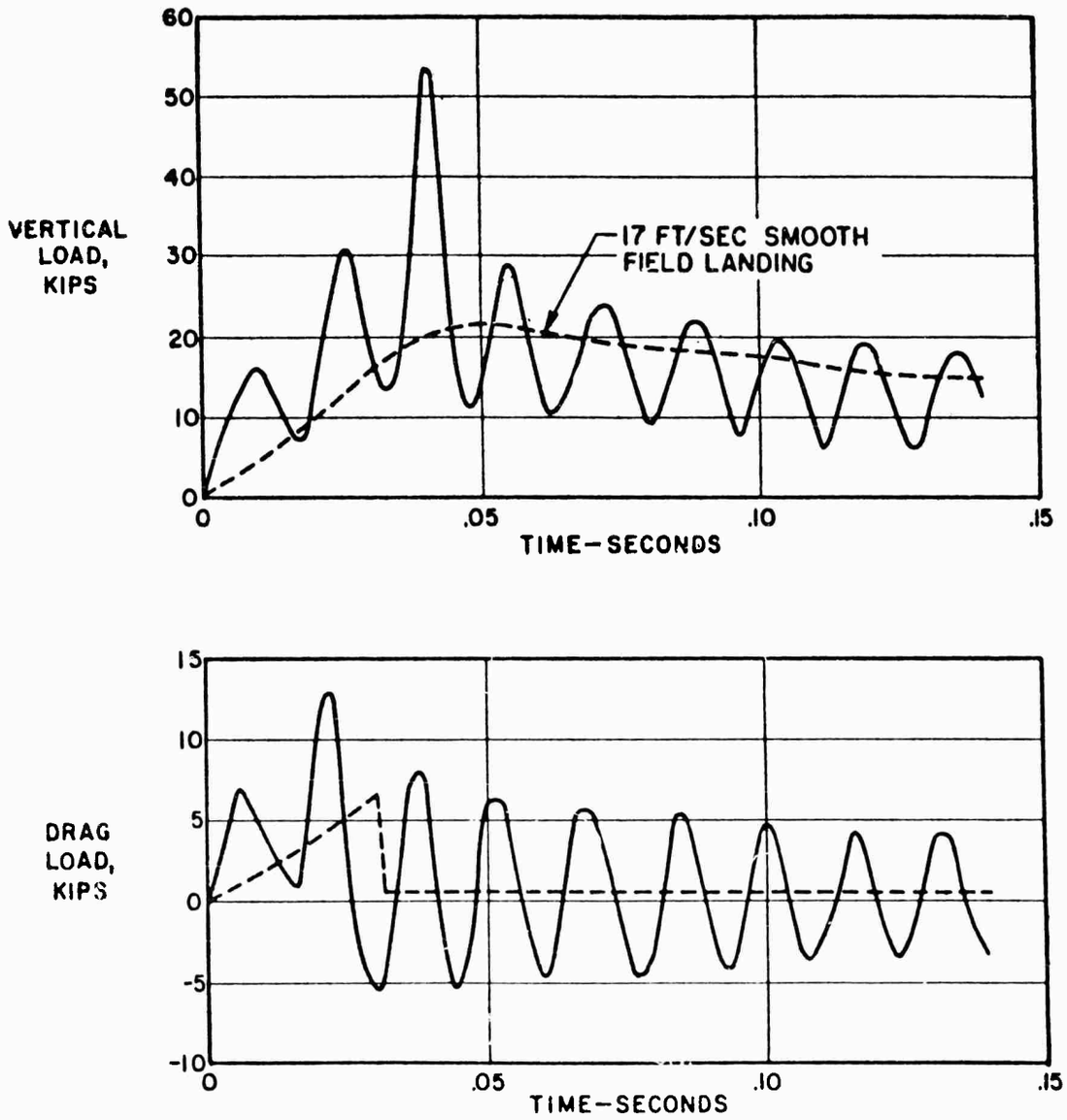

Figure 33. Ground Loads for a 17 Ft/Sec Landing on Continuous Undulations, Length = 27.4 Inches, Height = 3 Inches.

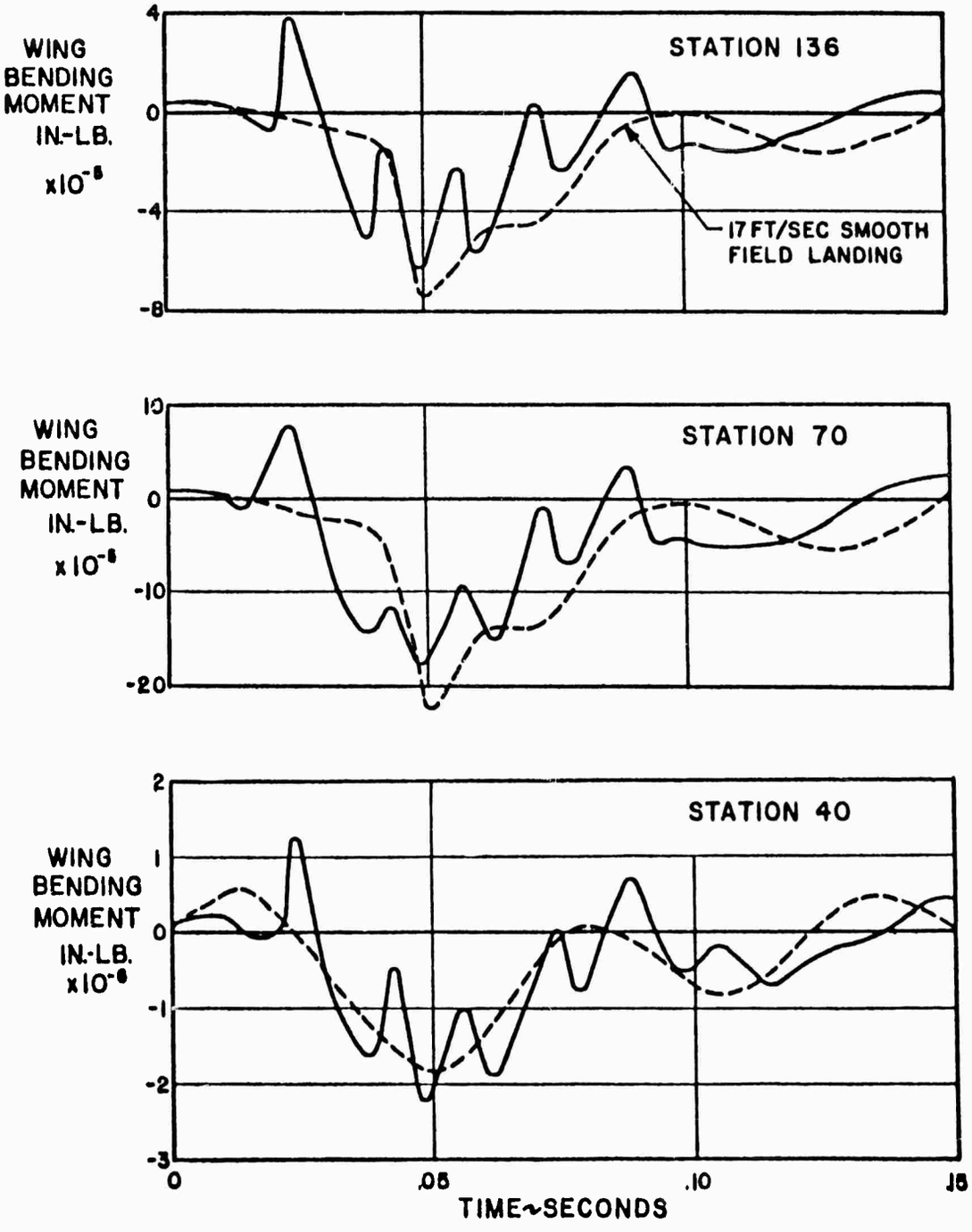

Figure 34. Wing Bending Moments for a 17 Ft/Sec Landing on Continuous Undulations, Length = 27.4 Inches, Height = 3 Inches.

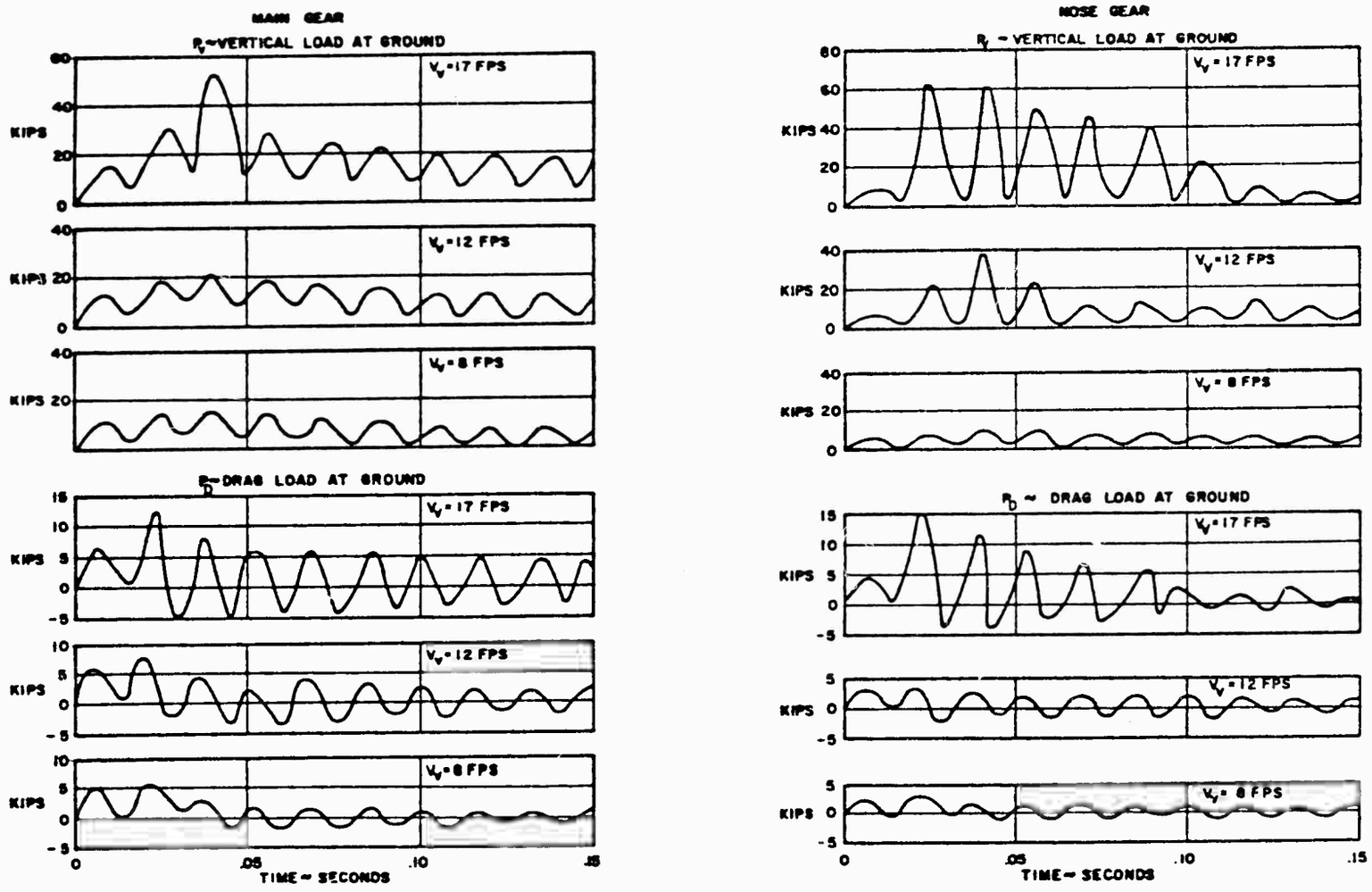

Figure 35. Main and Nose Gear Time Histories. Landing in Three-Point Attitude on Level Terrain Having Continuous Undulations 27.4 Inches Long and 3 Inches High.

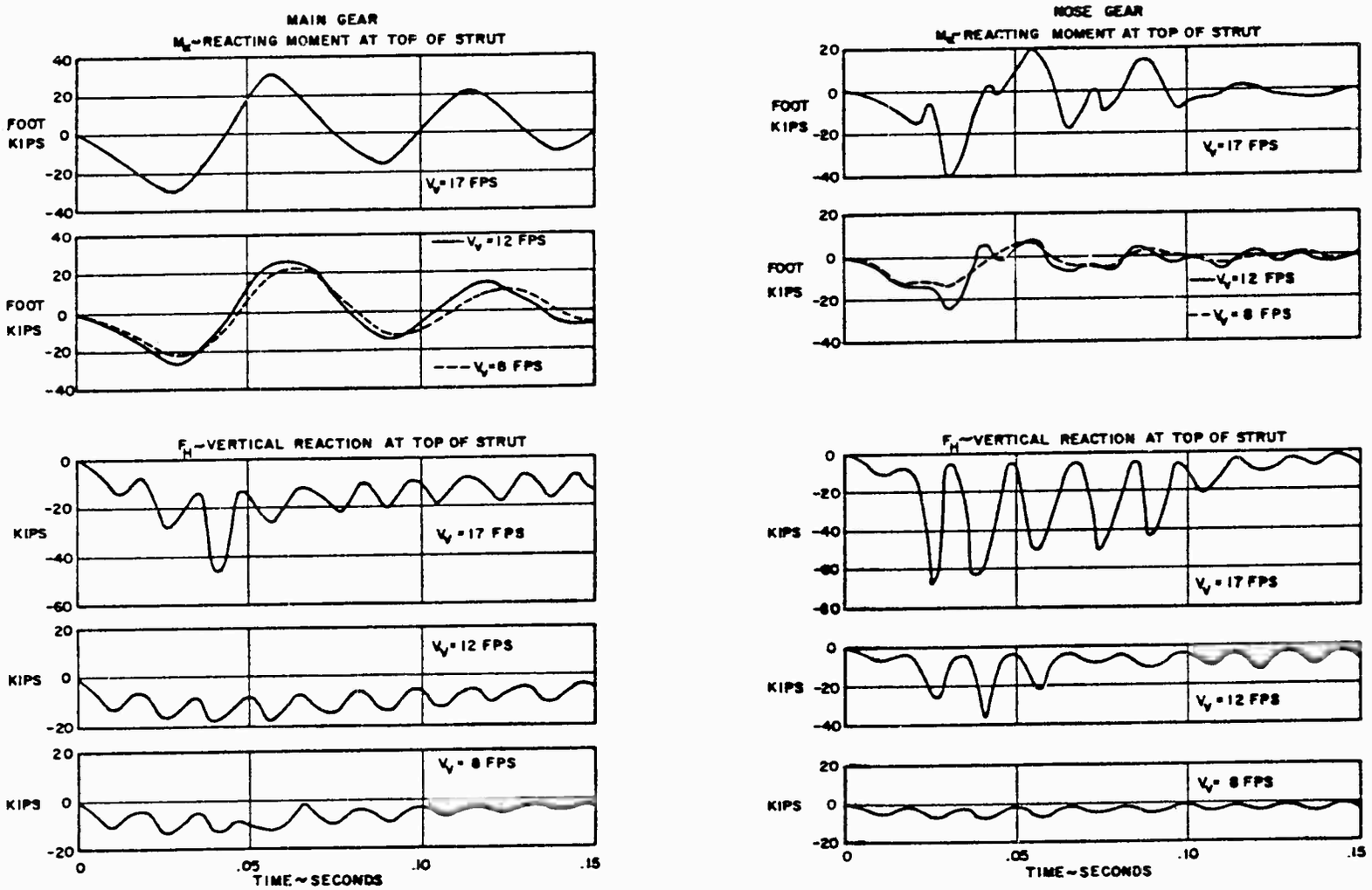

Figure 35 (Cont'd). Main and Nose Gear Time Histories. Landing in Three-Point Attitude on Level Terrain Having Continuous Undulations 27.4 Inches Long and 3 Inches High.

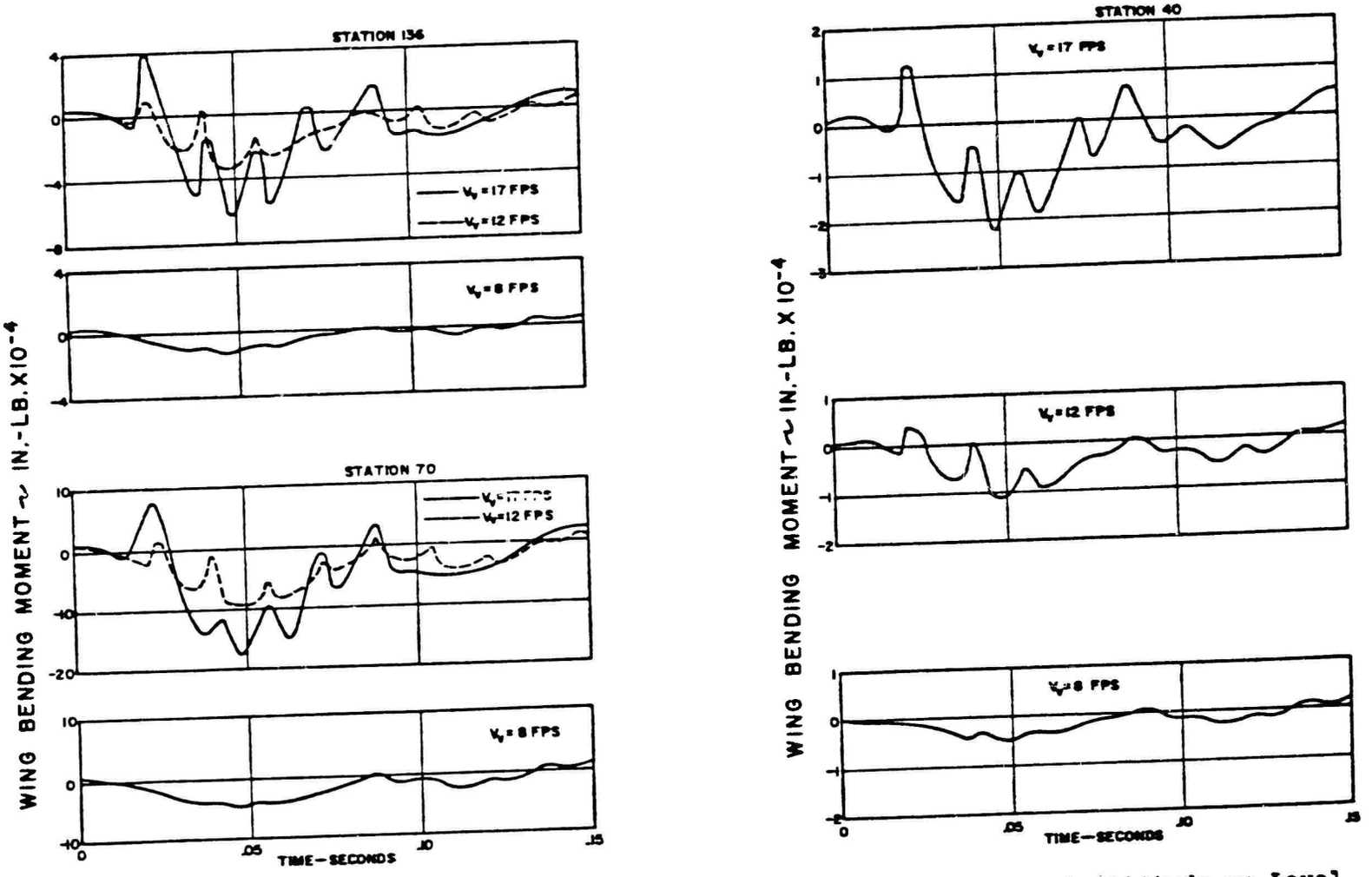

Figure 36. Wing Bending Moment Time Histories. Landing in Three-Point Attitude on Level Terrain Having Continuous Undulations 27.4 Inches Long and 3 Inches High.

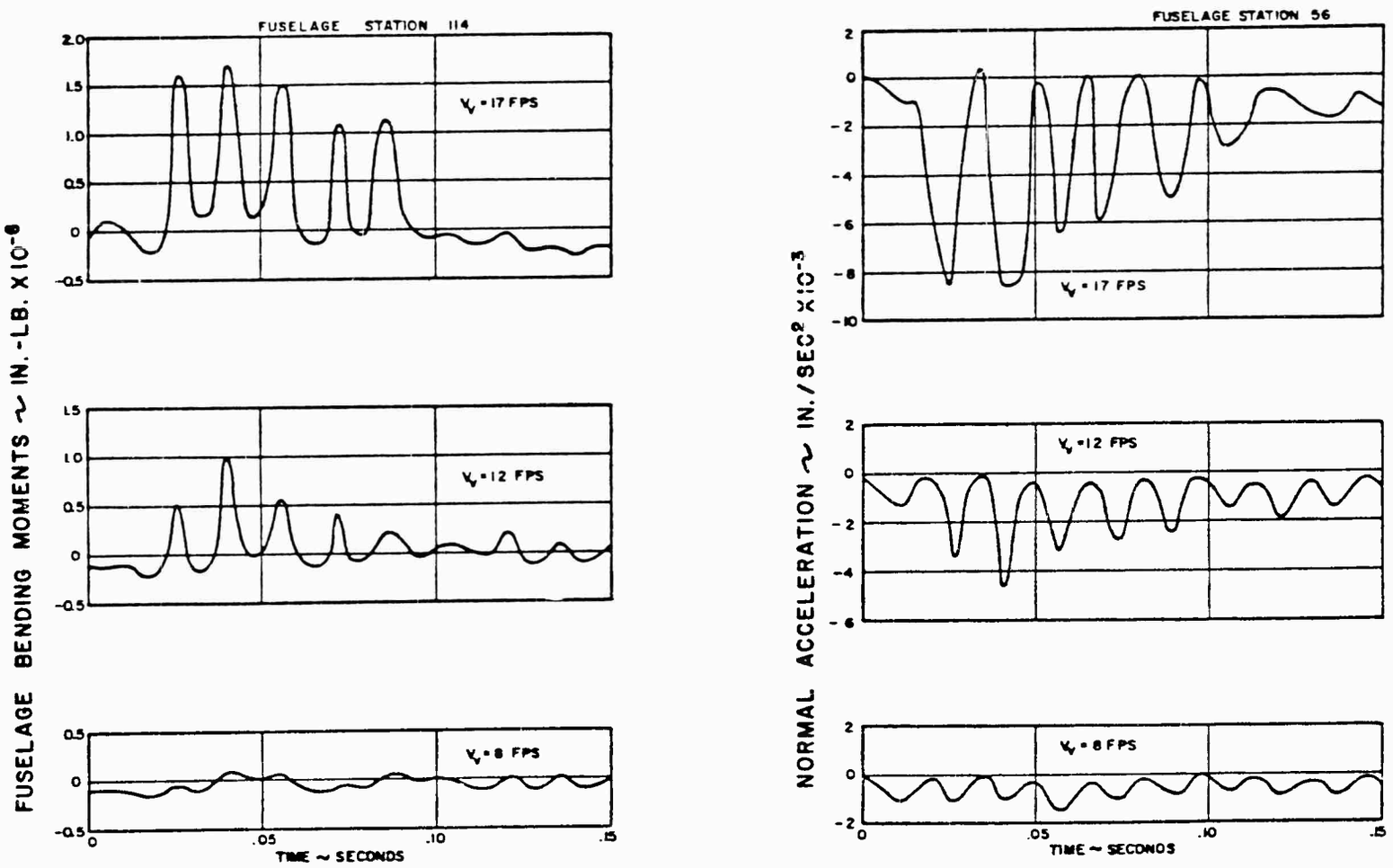

Figure 37. Fuselage Time Histories. Landing in Three-Point Attitude on Level Terrain Having Continuous Undulations 27.4 Inches Long and 3 Inches High.

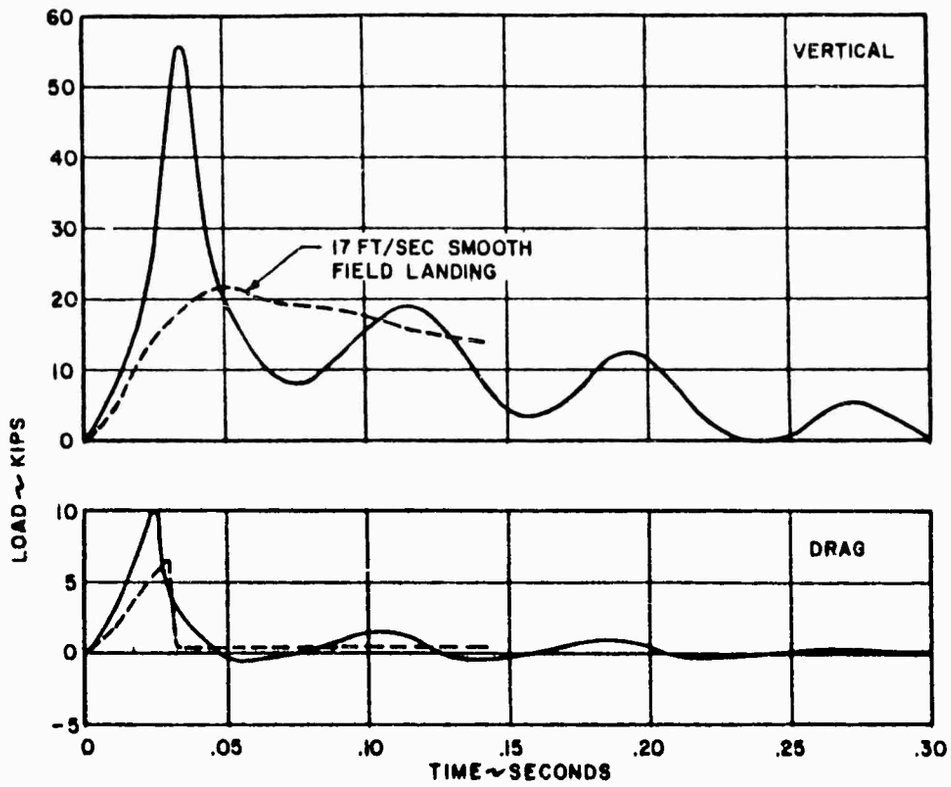

Figure 38. Ground Loads for a 17 Ft/Sec Landing on Continuous Undulations, Length = 137 Inches, Height = 3 Inches.

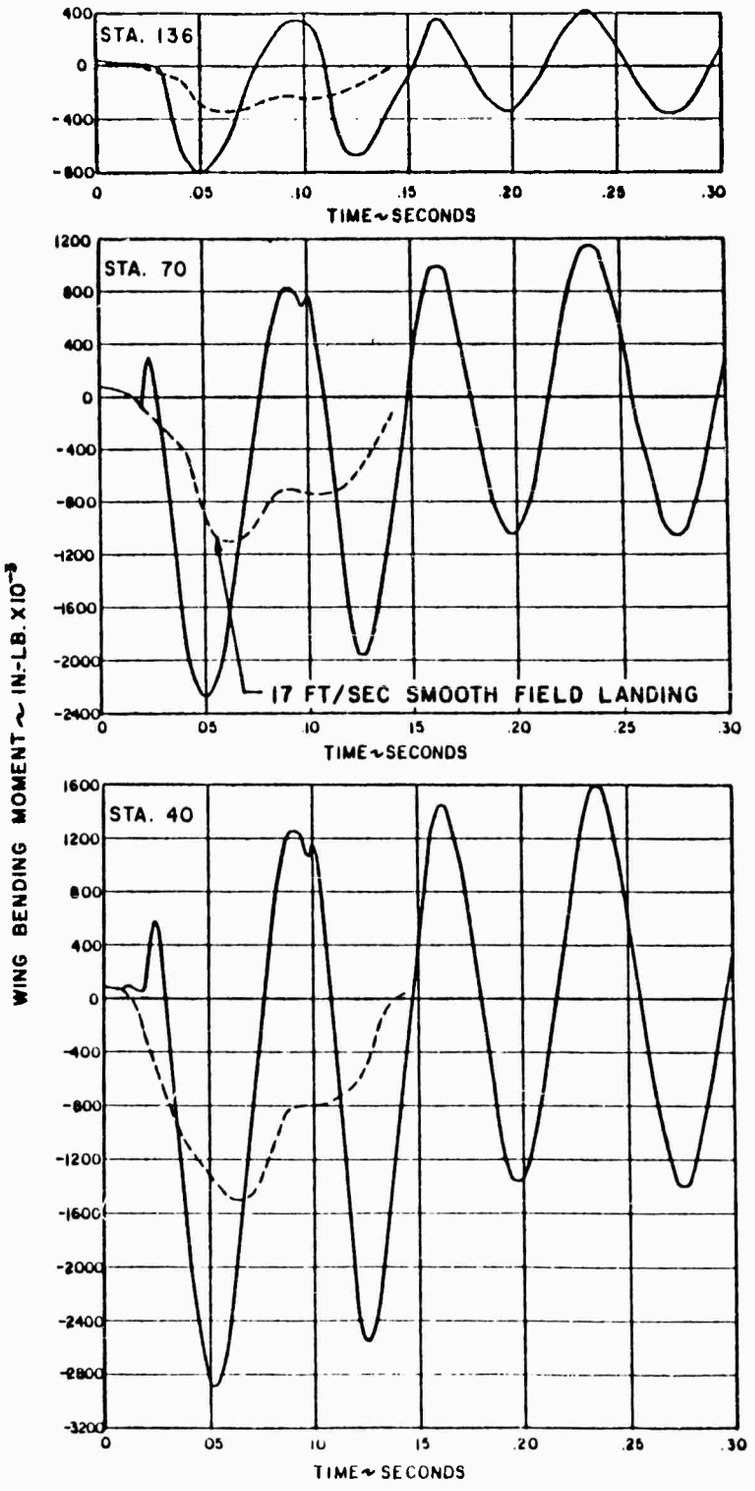

Figure 39. Wing Bending Moments for a 17 Ft/Sec Landing on Continuous Undulations, Length = 137 Inches, Height = 3 Inches.

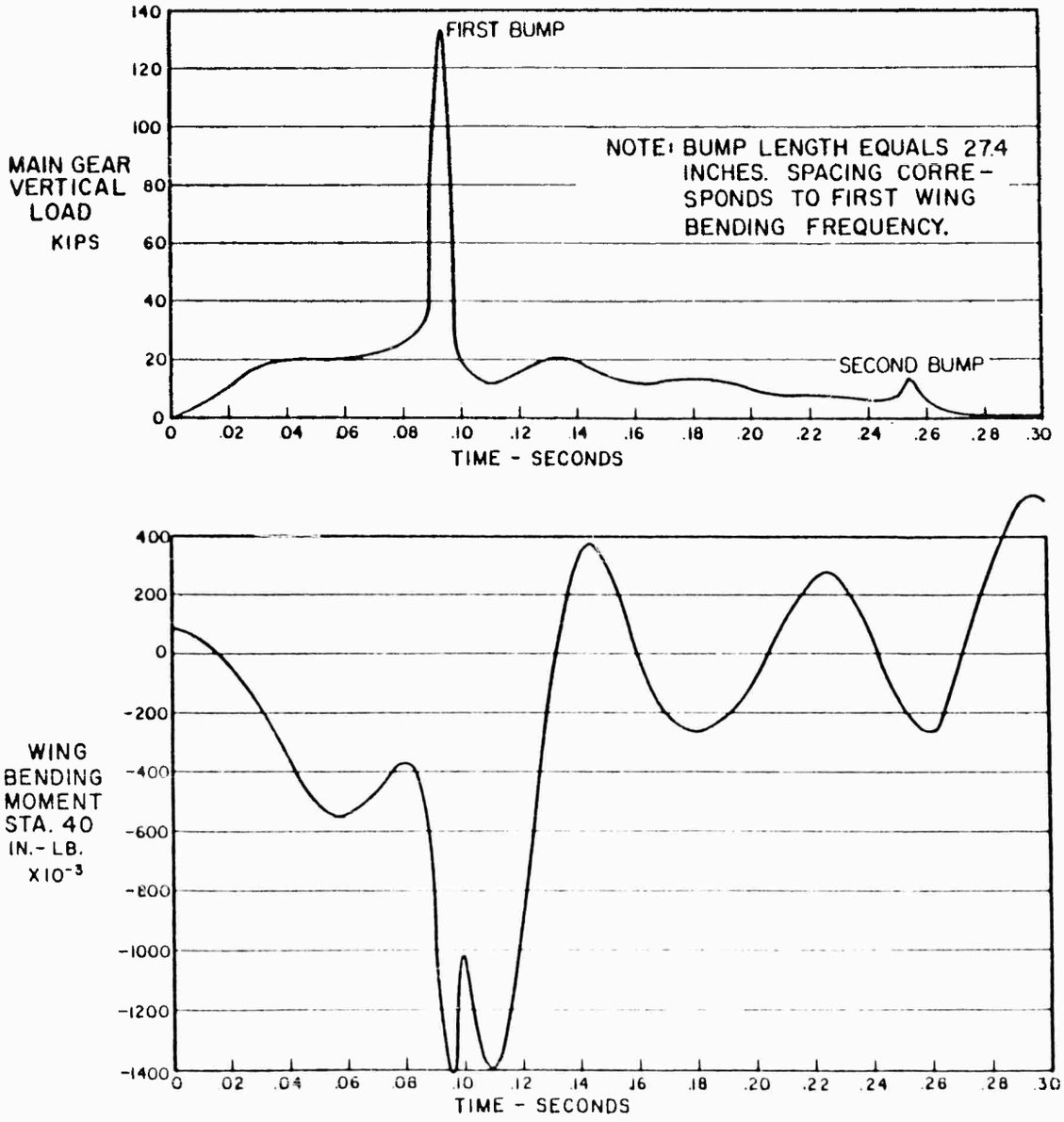

Figure 40. Vertical Gear Load and Wing Bending Moment for a 17 Ft/Sec Landing on a Series of Two 3-Inch Bumps Spaced 242 Inches Apart.

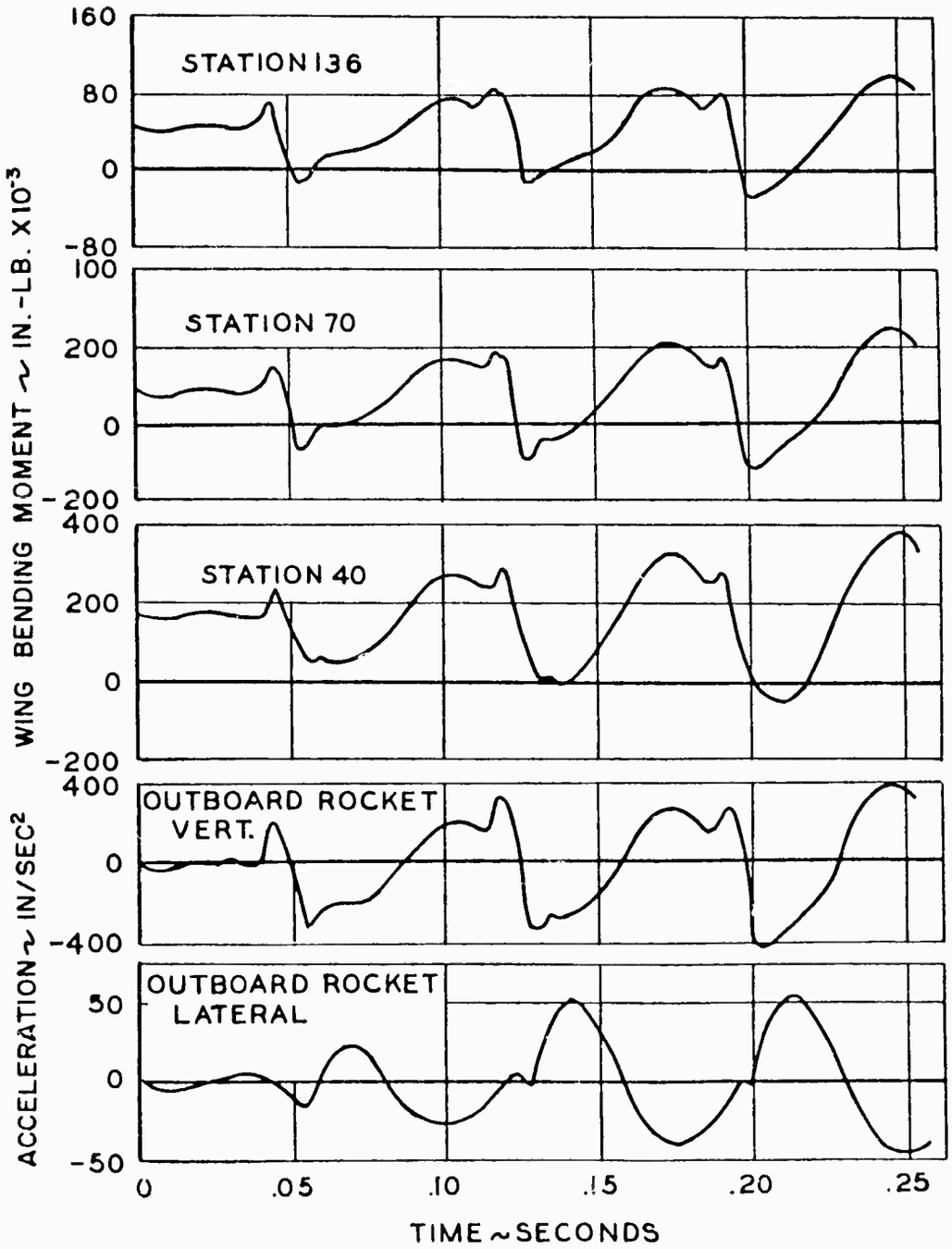

Figure 41. Airplane Response for Roll-Out or Taxi. Wing Lift Equals Zero, Bump Spacing = 126 Inches, Height = 2 Inches, Length = 27.4 Inches, V_A = 84.5 Knots.

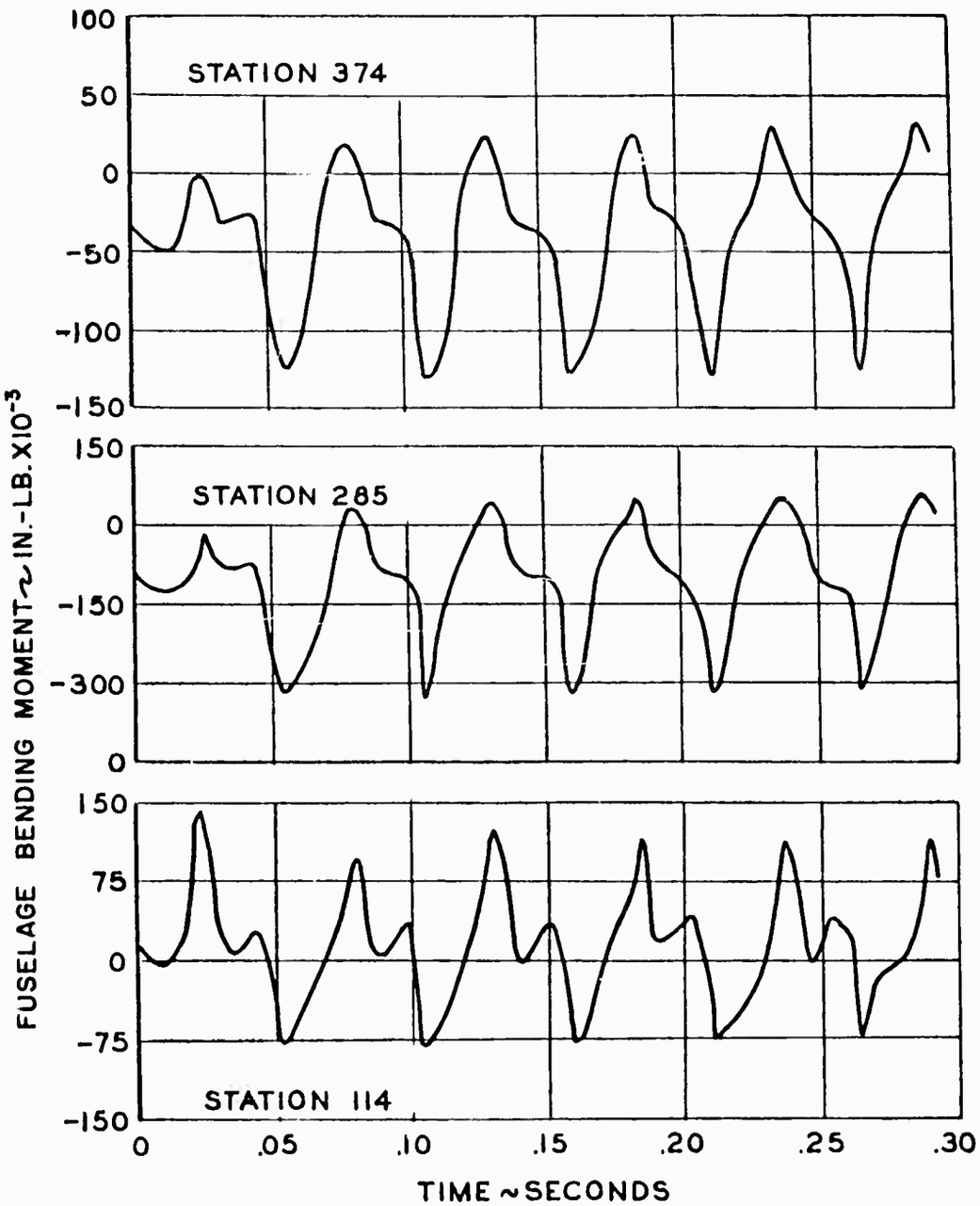

Figure 42. Airplane Fuselage Response for Roll-Out or Taxi. Wing Lift Equals Zero, Bump Spacing = 90.6 Inches, Height = 2 Inches, Length = 27.4 Inches, V_A = 84.5 Knots.

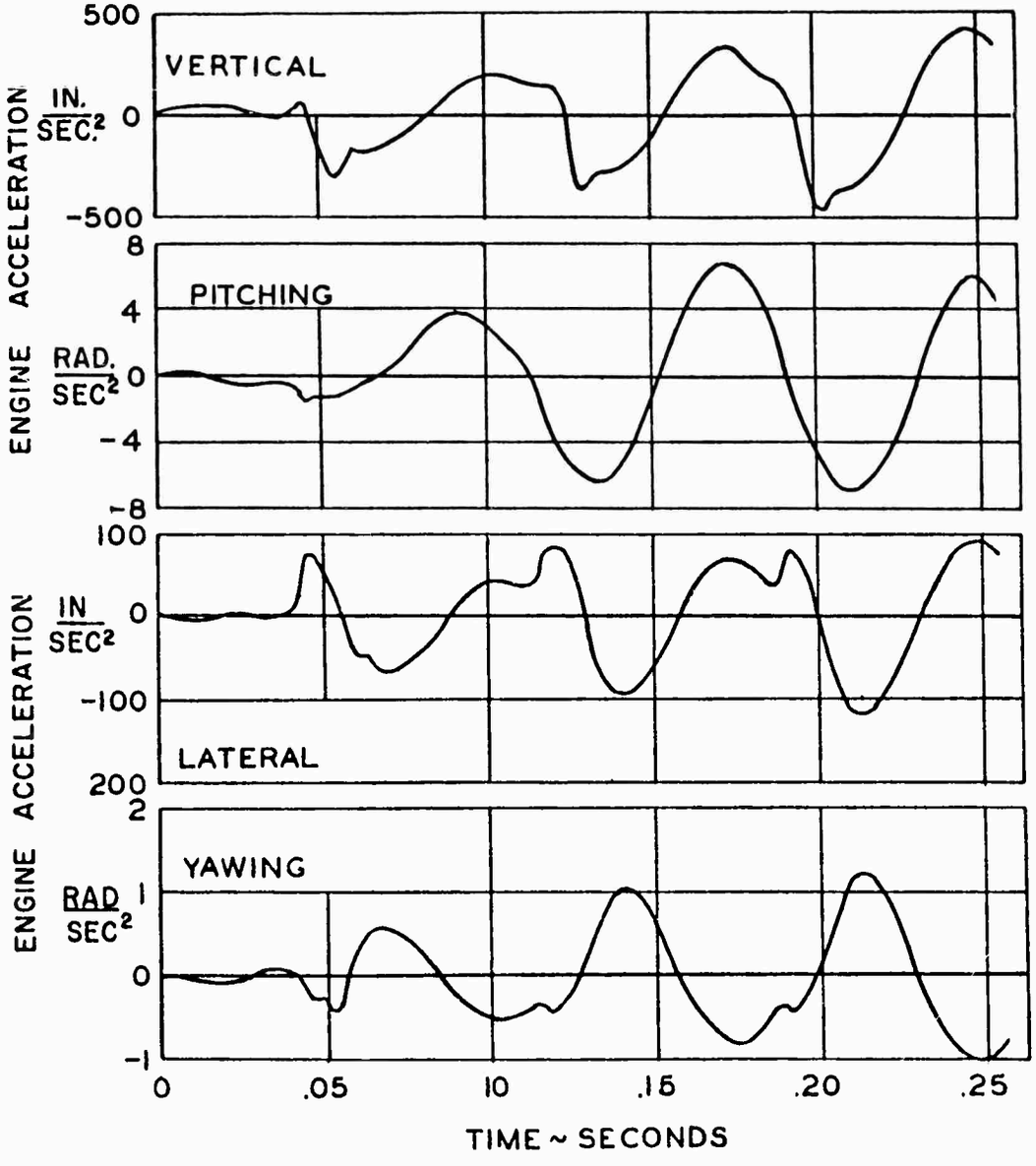

Figure 43. Airplane Engine Response for Roll-Out or Taxi. Wing Lift Equals Zero, Bump Spacing = 90.6, Height = 2 Inches, Length = 27.4 Inches, V_A = 84.5 Knots.

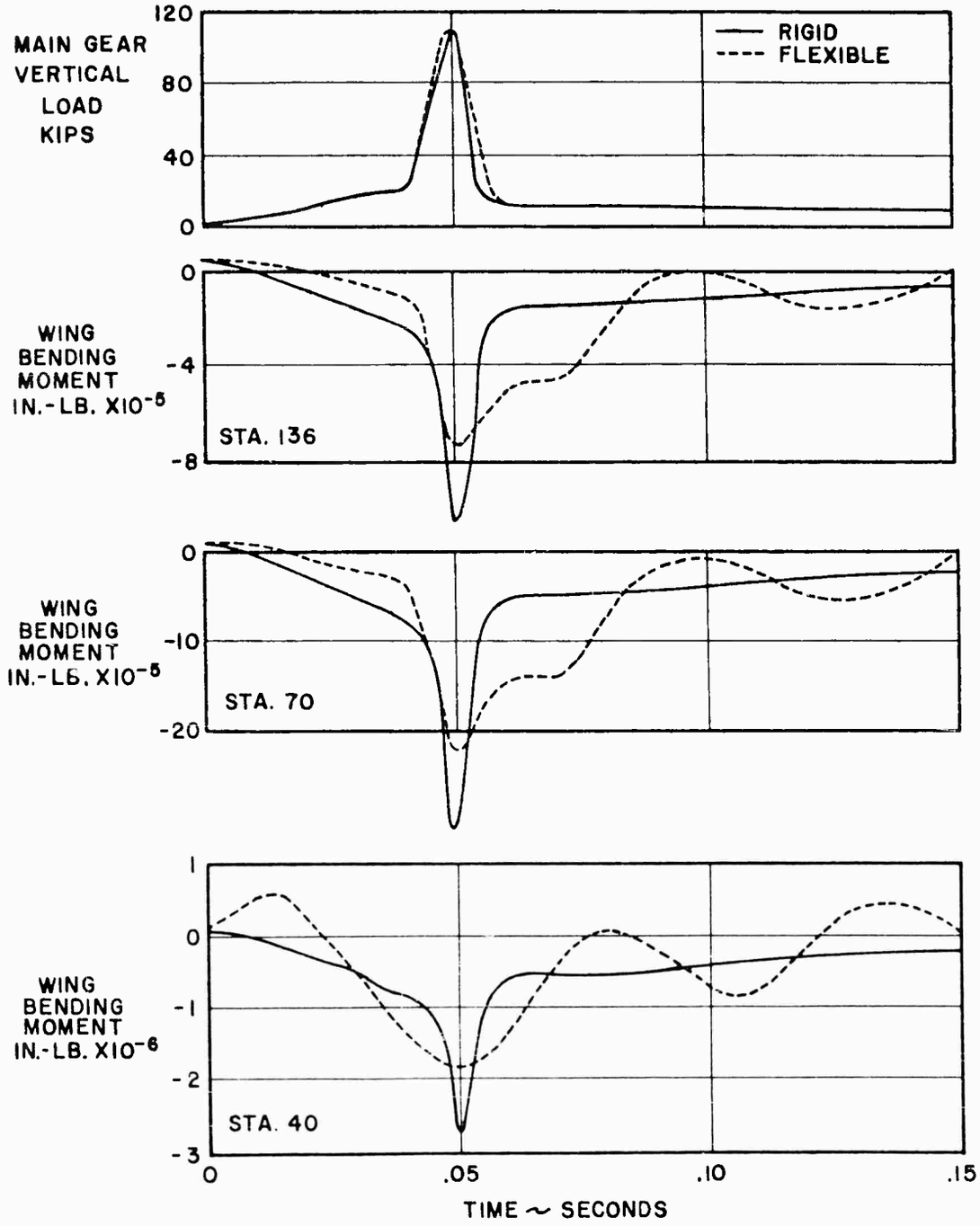

Figure 44. Comparison of Rigid and Flexible Aircraft Loads for a 17 Ft/Sec Landing on a 3-Inch Bump 27.4 Inches Long.

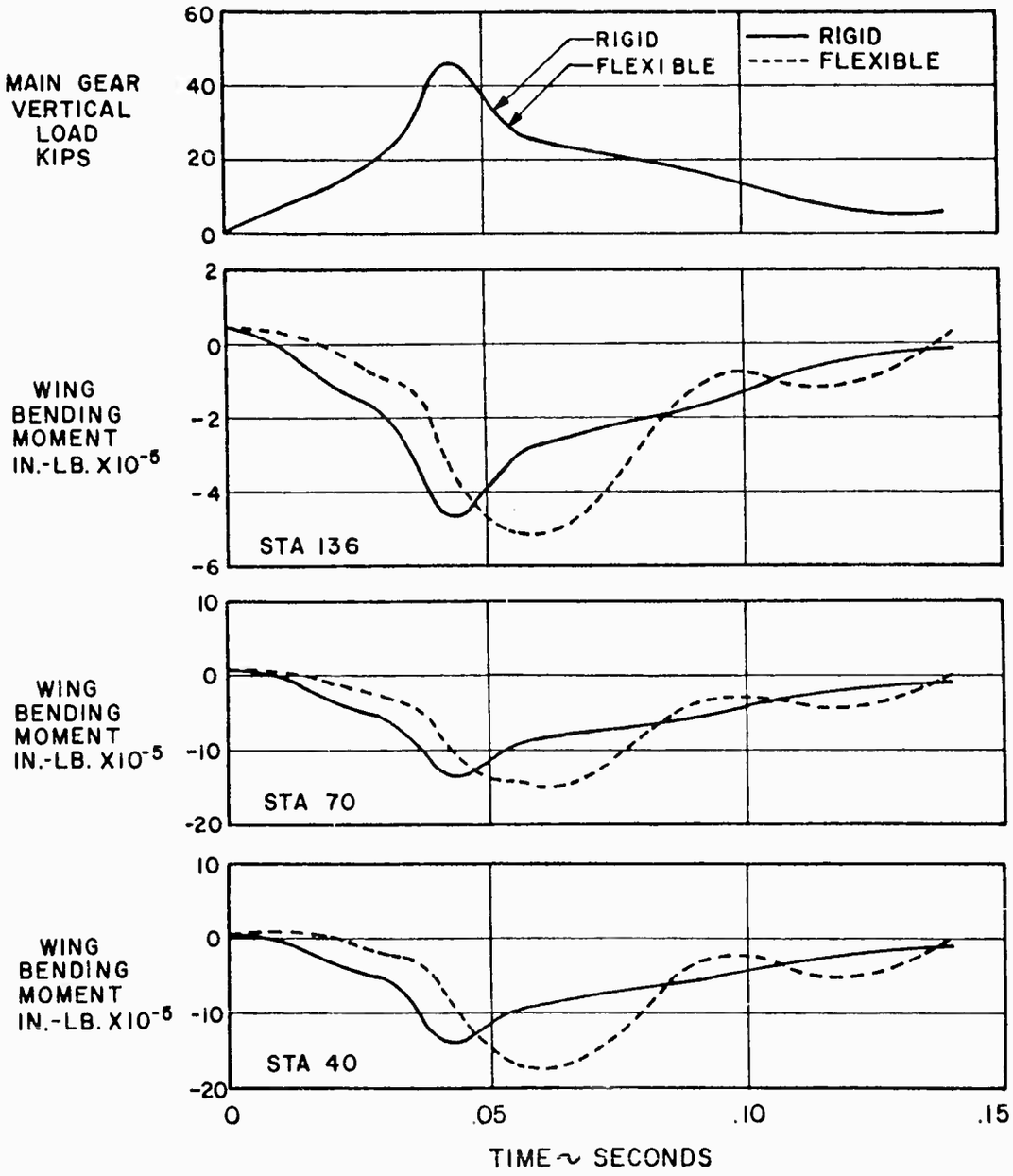

Figure 45. Comparison of Rigid and Flexible Aircraft Loads for a 17 Ft/Sec Landing on a 3 Inch Bump 242 Inches Long.

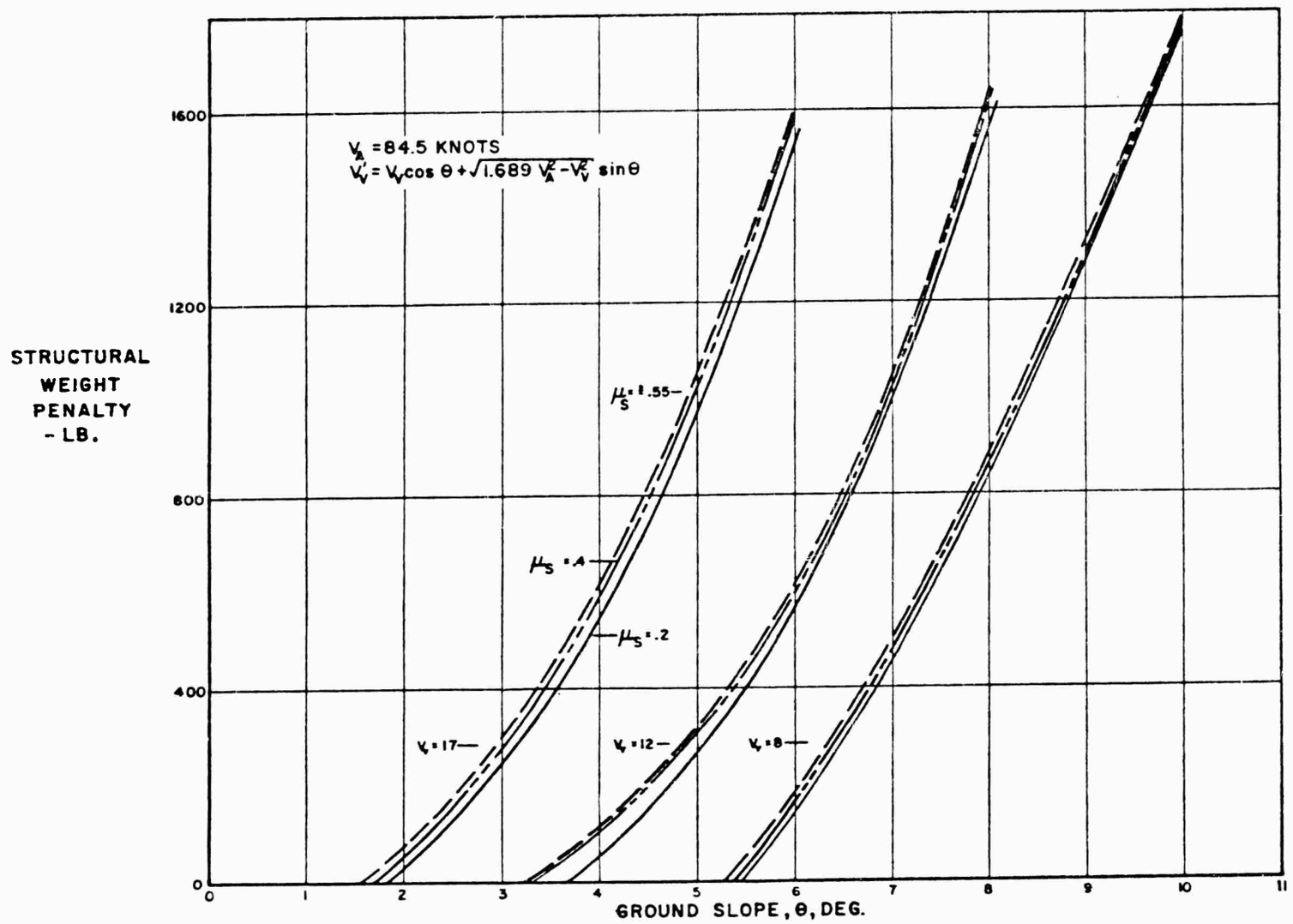

Figure 46. Structural Weight Penalty Versus Ground Slope.

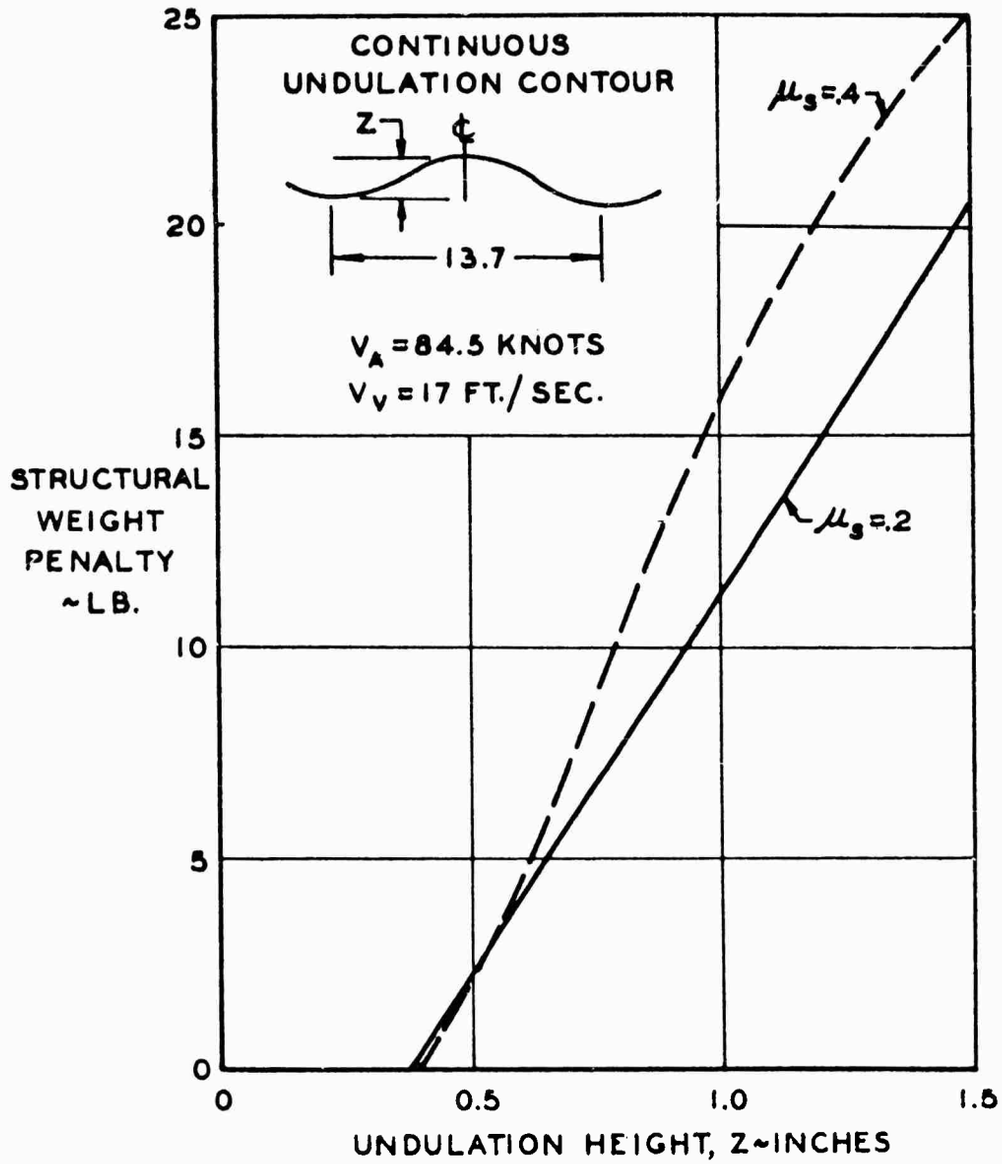

Figure 47. Structural Weight Penalty Versus Undulation Height. Undulation Length = 13.7 Inches.

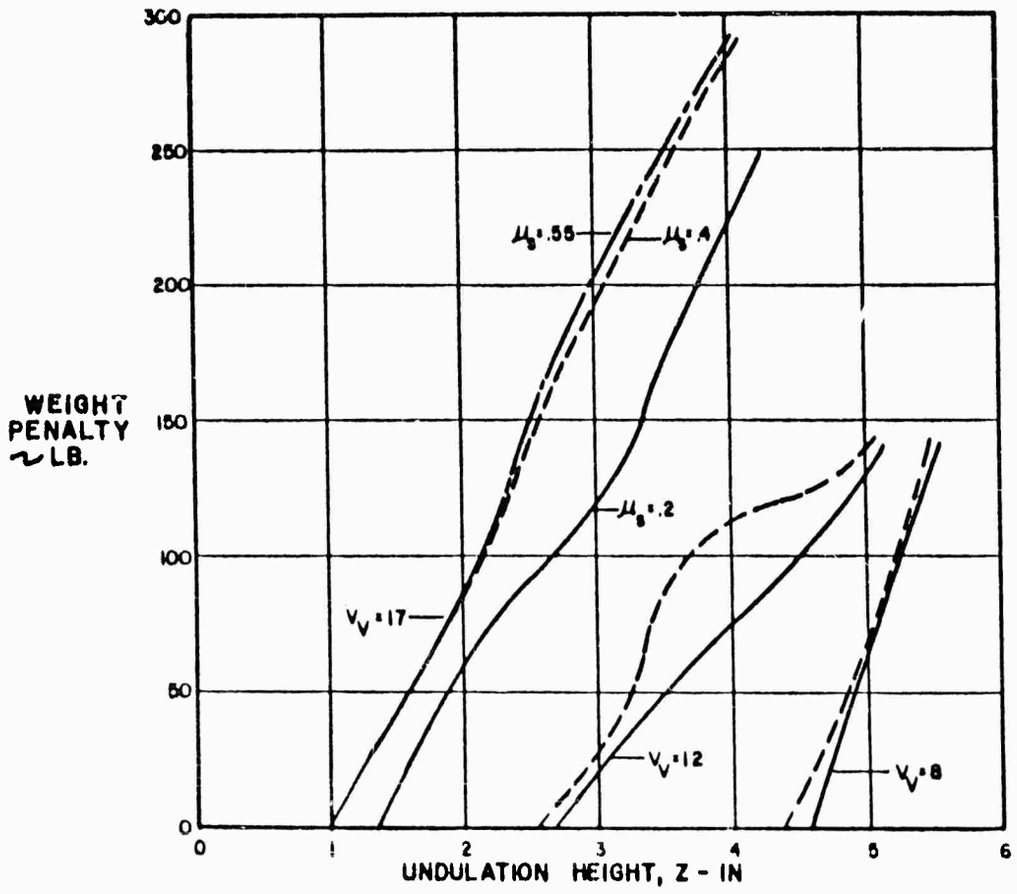

Figure 48. Structural Weight Penalty Versus Undulation Height. Continuous Undulations, Length = 27.4 Inches.

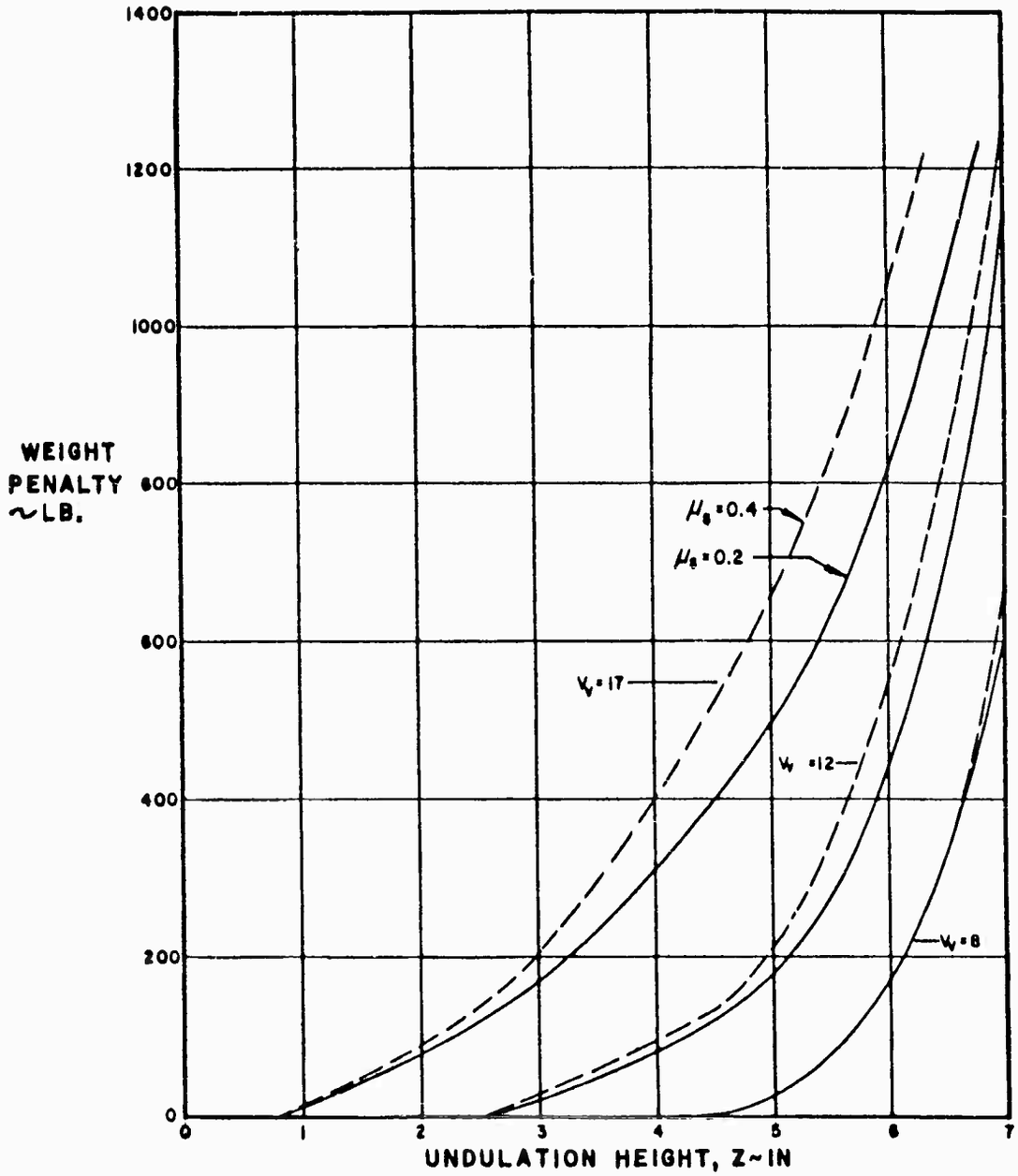

Figure 49. Airplane Weight Penalty Versus Undulation Height. Continuous Undulations, Length = 45.67 Inches.

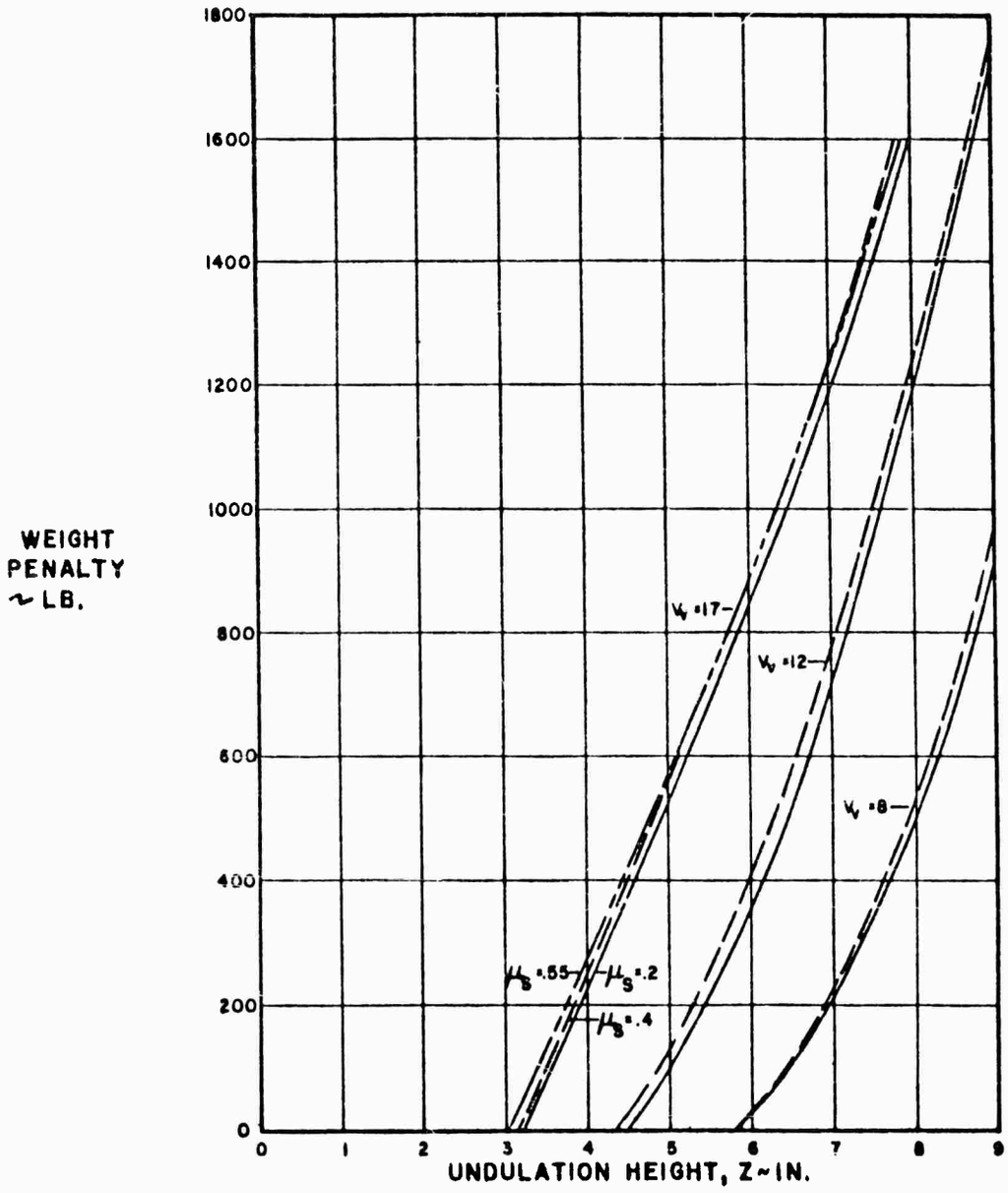

Figure 50. Structural Weight Penalty Versus Undulation Height. Continuous Undulations, Length = 137 Inches.

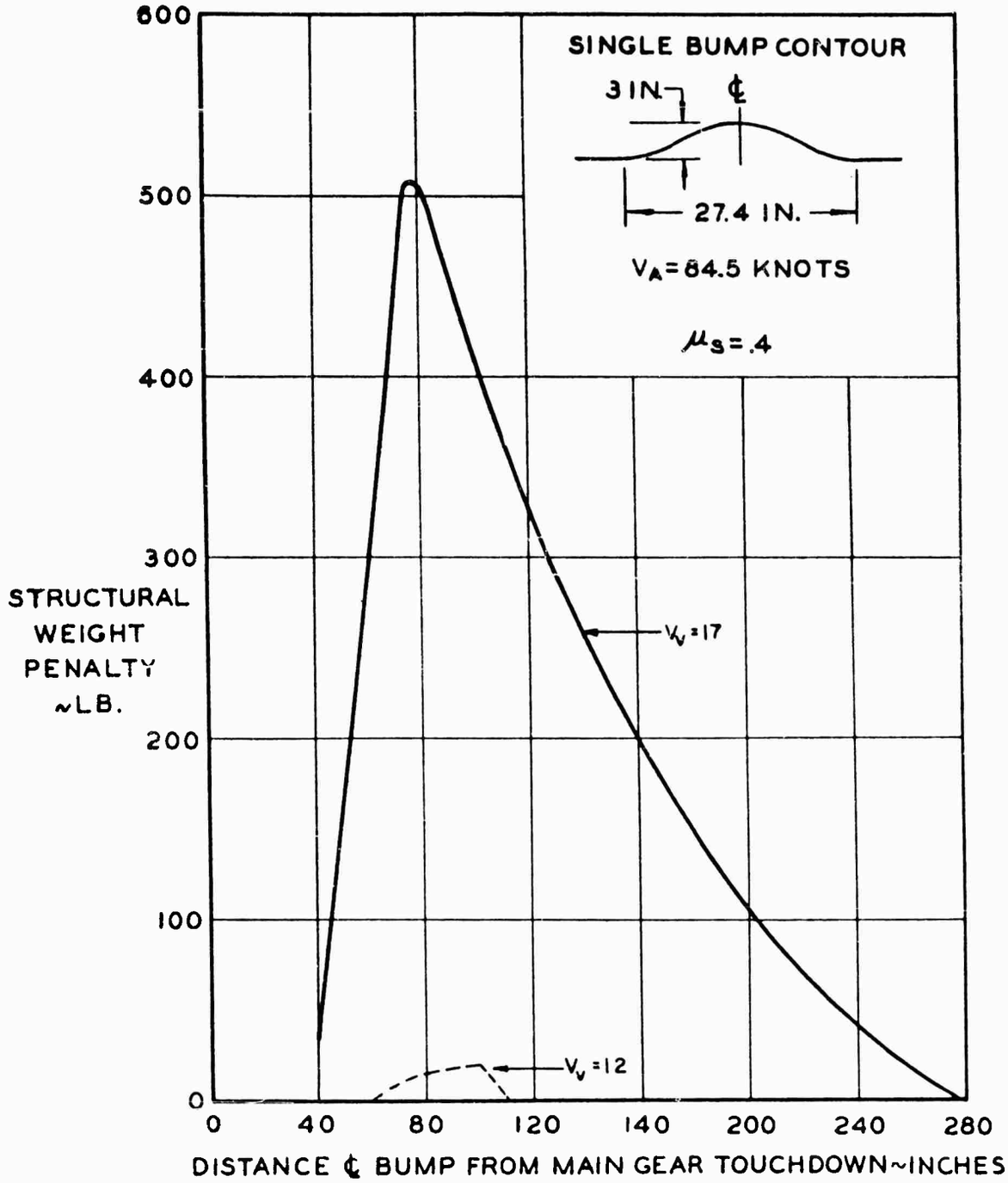

Figure 51. Structural Weight Penalty for 3 Inch Bump Versus Bump Location. Main Gear Hits Bump with Airplane in Three-Point Attitude.

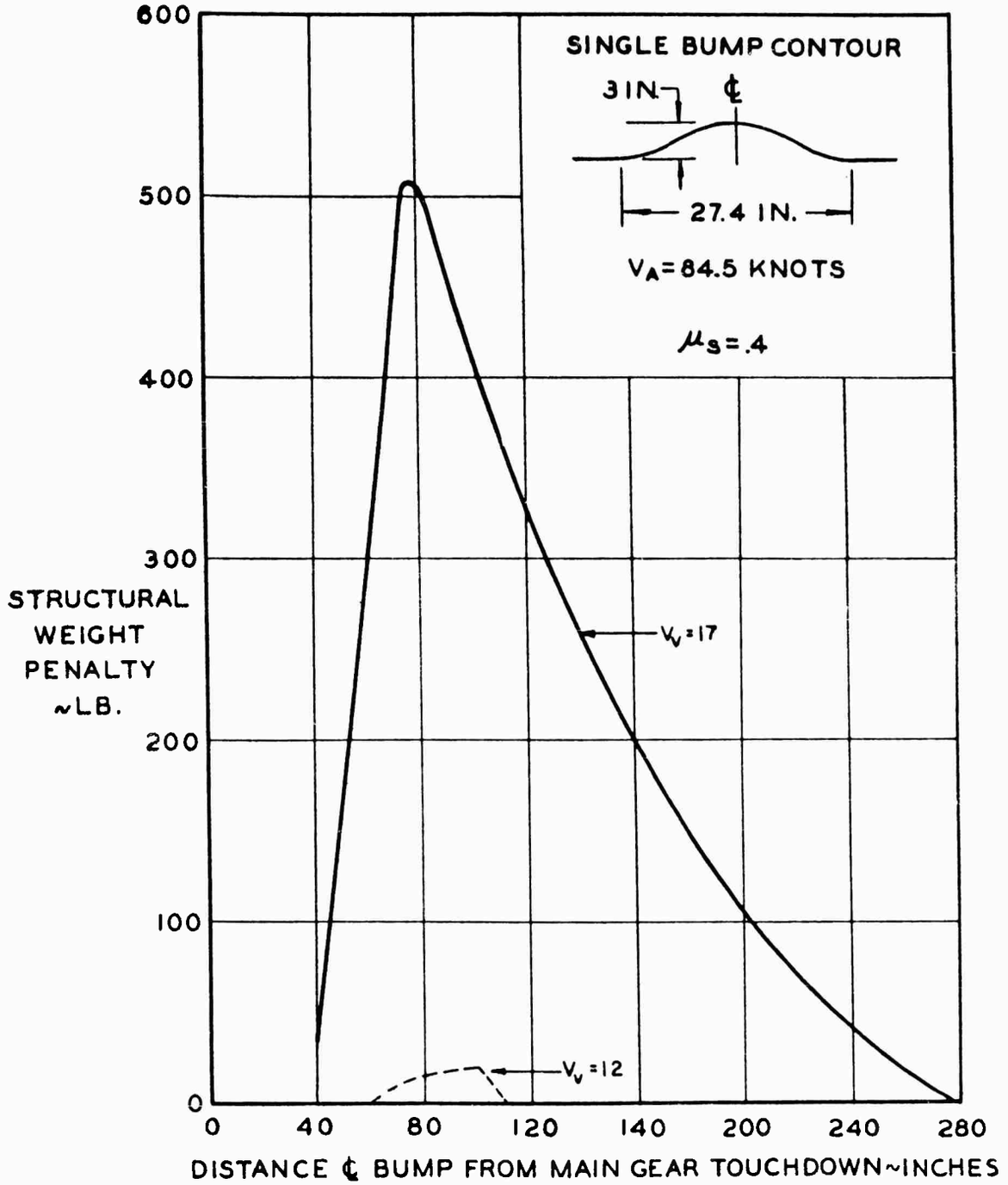

Figure 51. Structural Weight Penalty for 3 Inch Bump Versus Bump Location. Main Gear Hits Bump with Airplane in Three-Point Attitude.

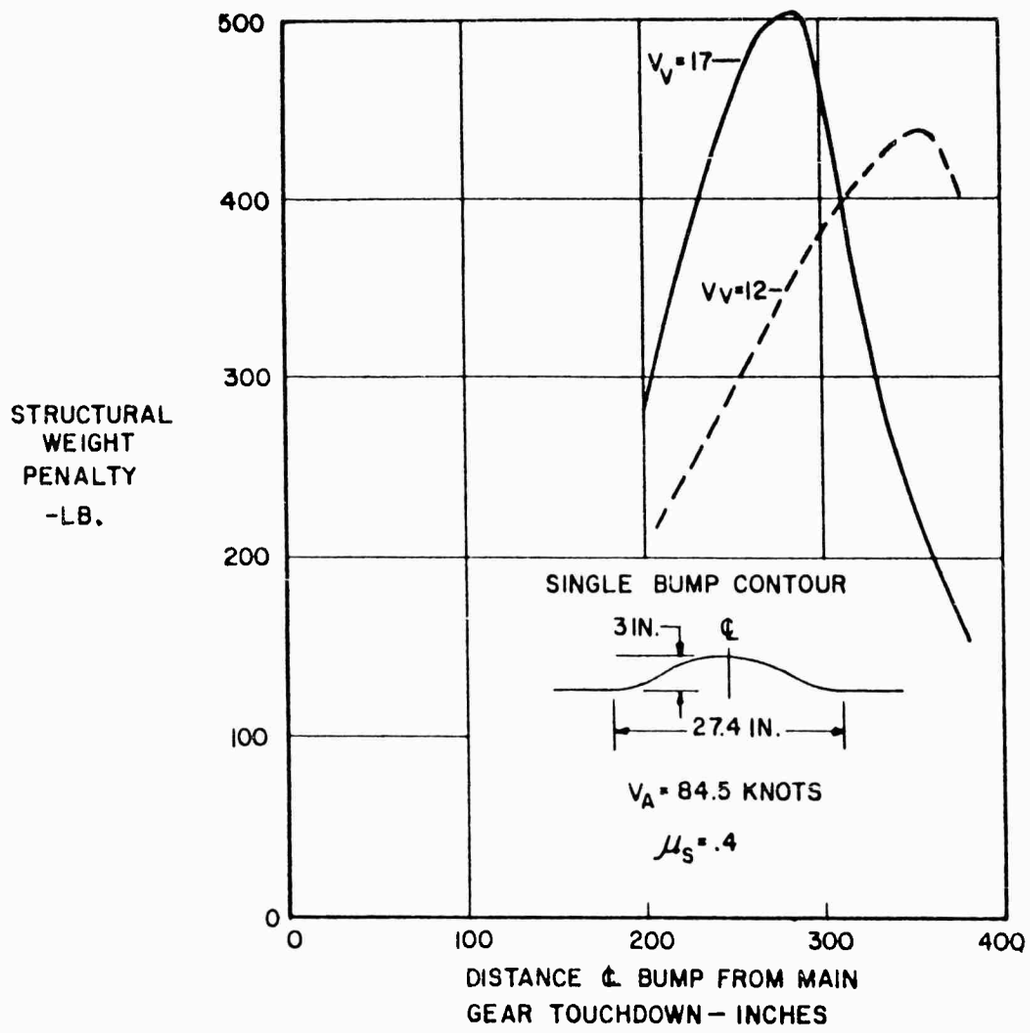

Figure 52. Structural Weight Penalty Versus Bump Location. Nose Gear Hits Bump with Airplane in Three-Point Attitude.

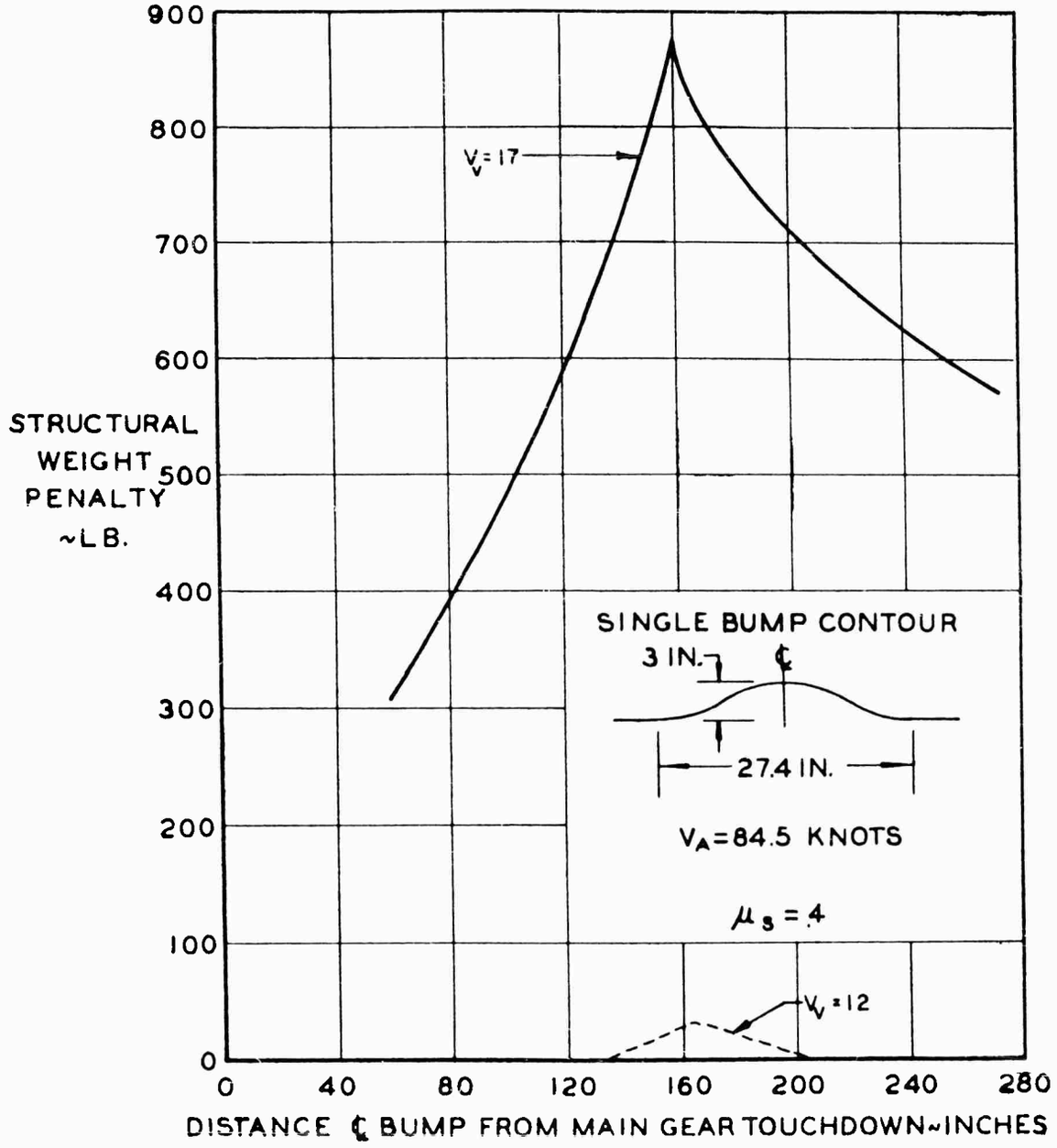

Figure 53. Structural Weight Penalty Versus Location of Bump. Main Gear Hits Bump with Airplane in Tail Down Attitude.

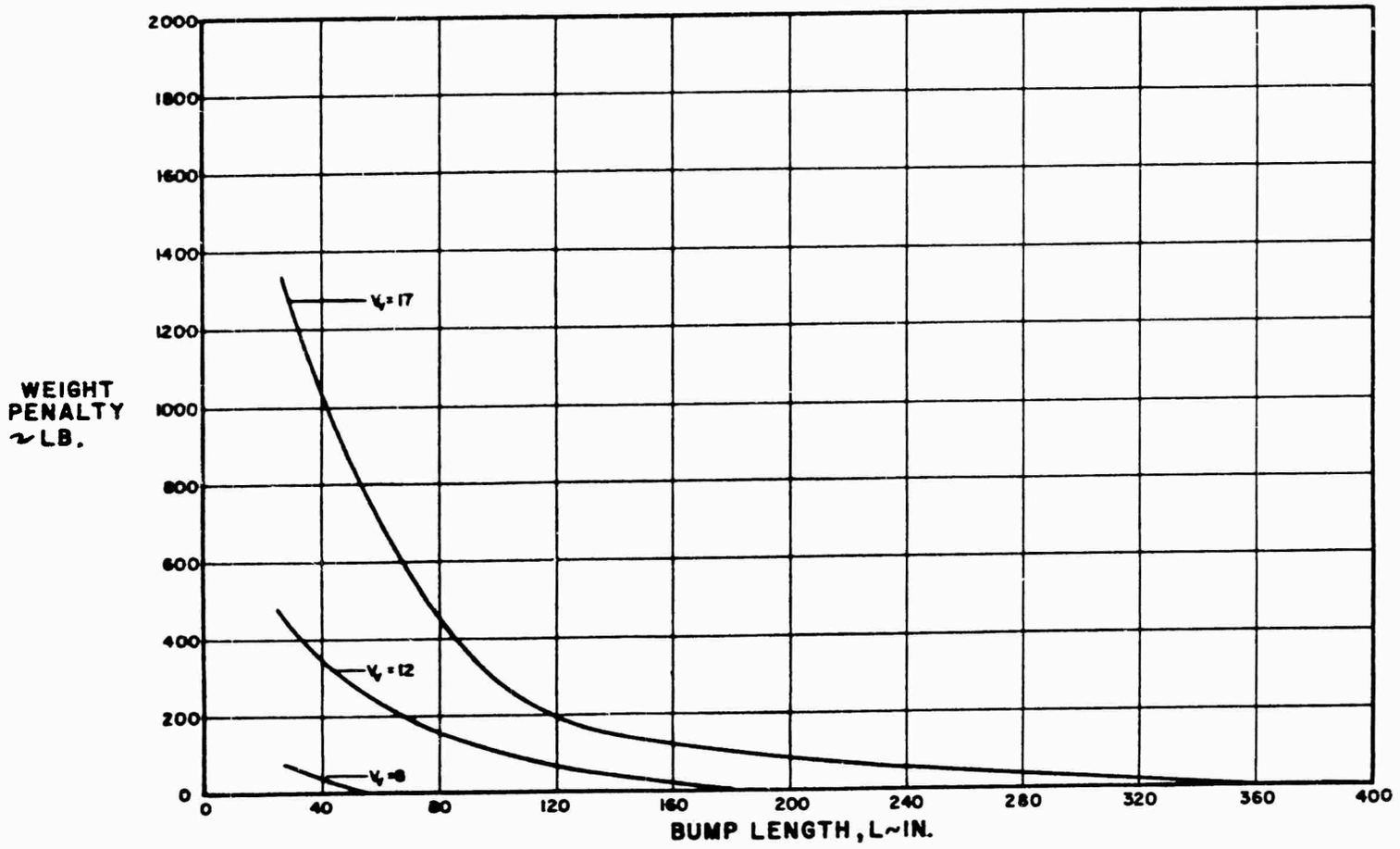

Figure 54. Structural Weight Penalty Versus Bump Length. Constant Height Bump Located at Critical Distances from Main Gear Touchdown. Single Bump Contour, Height = 3 Inches, μ_s = .4.

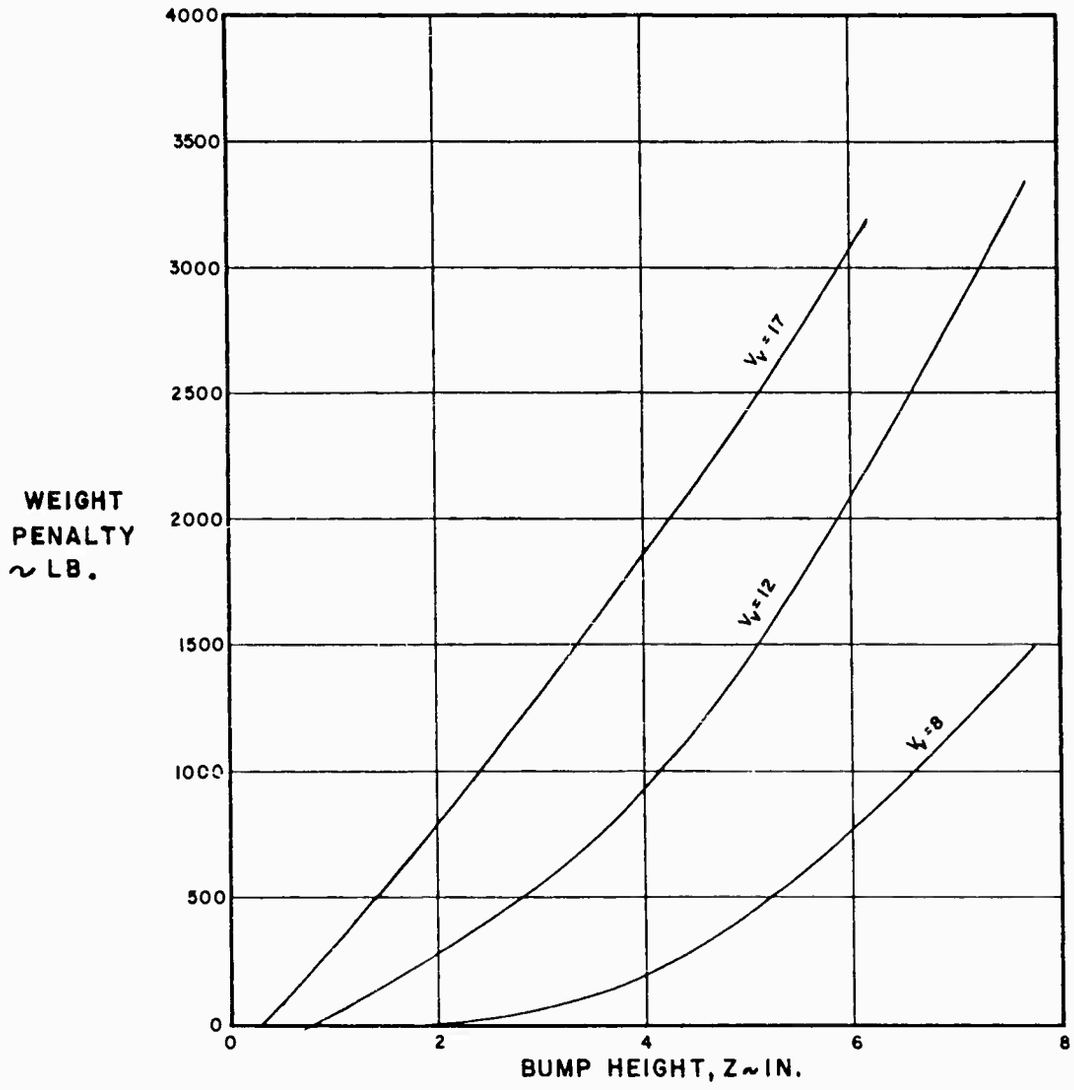

Figure 55. Structural Weight Penalty Versus Bump Height. Constant Height-to-Length Ratio Bumps Located at Critical Distances from Main Gear Touchdown. Length/Height = 9.12, μ_s = .4.

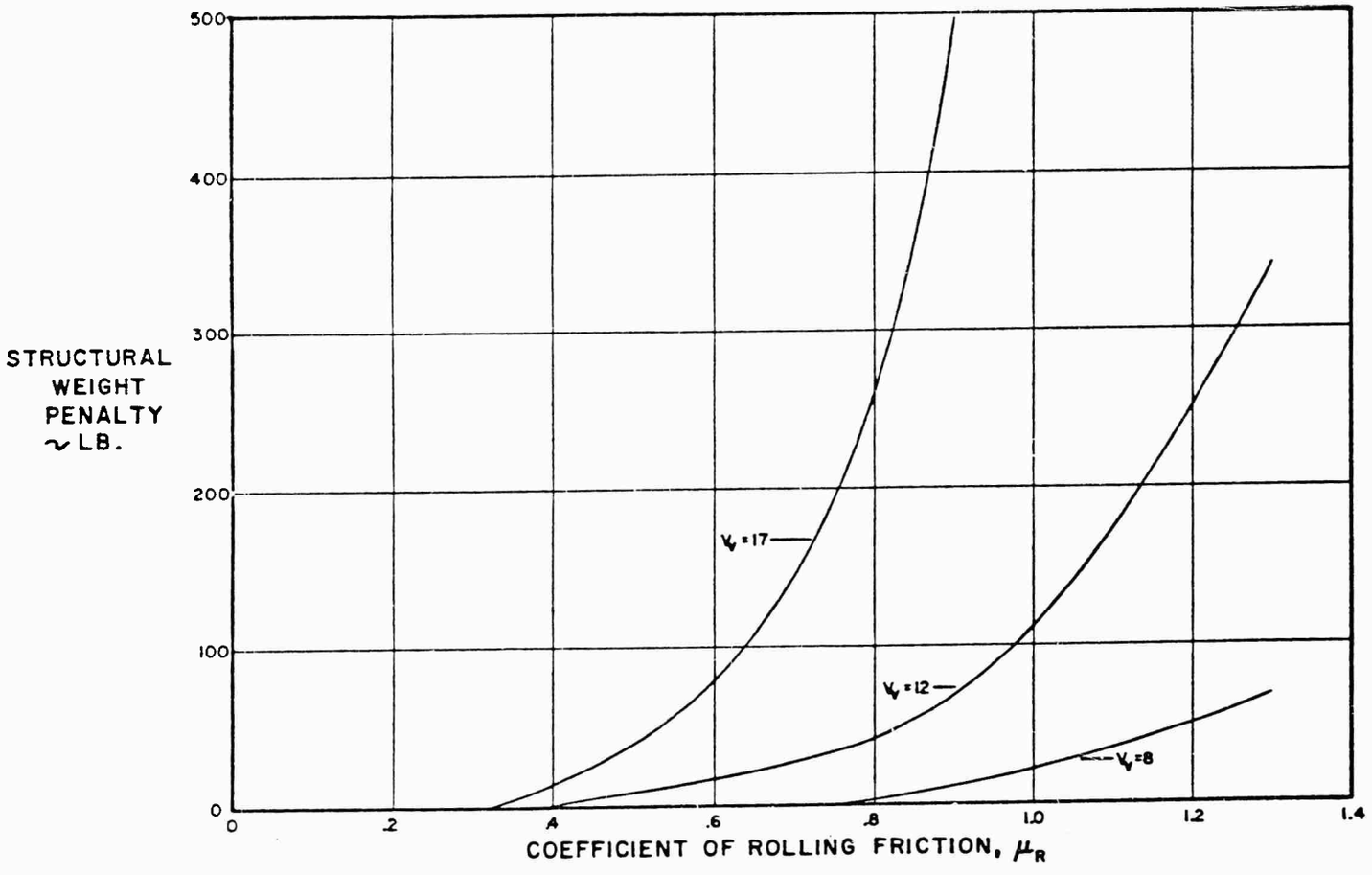

Figure 56. Structural Weight Penalty Versus Coefficient of Rolling Friction. (μ_s = .4)

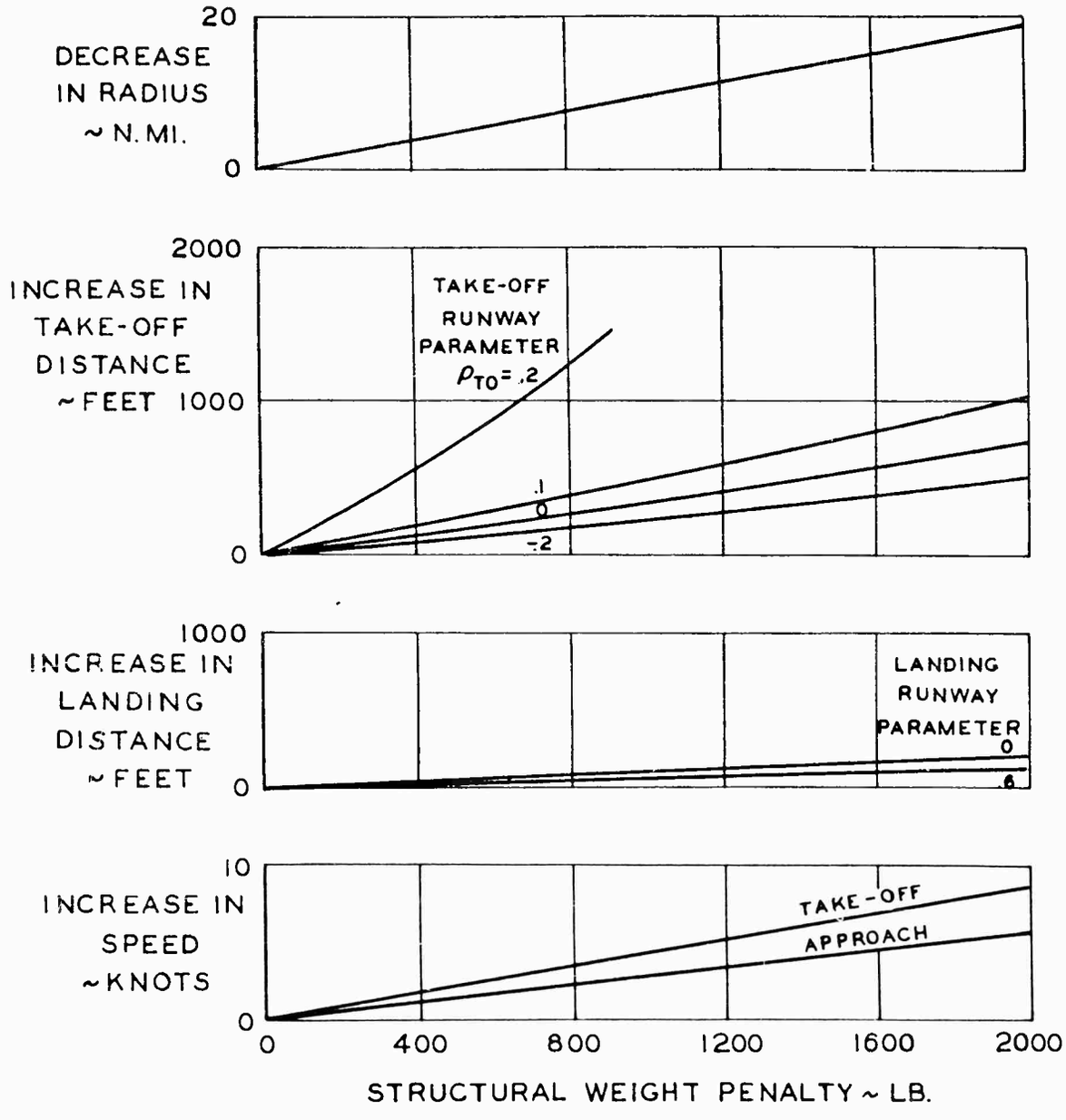

Figure 57. Effect on OV-1 Performance of Structural Weight Penalty. Take-Off Weight Increases as Structural Weight is Added.

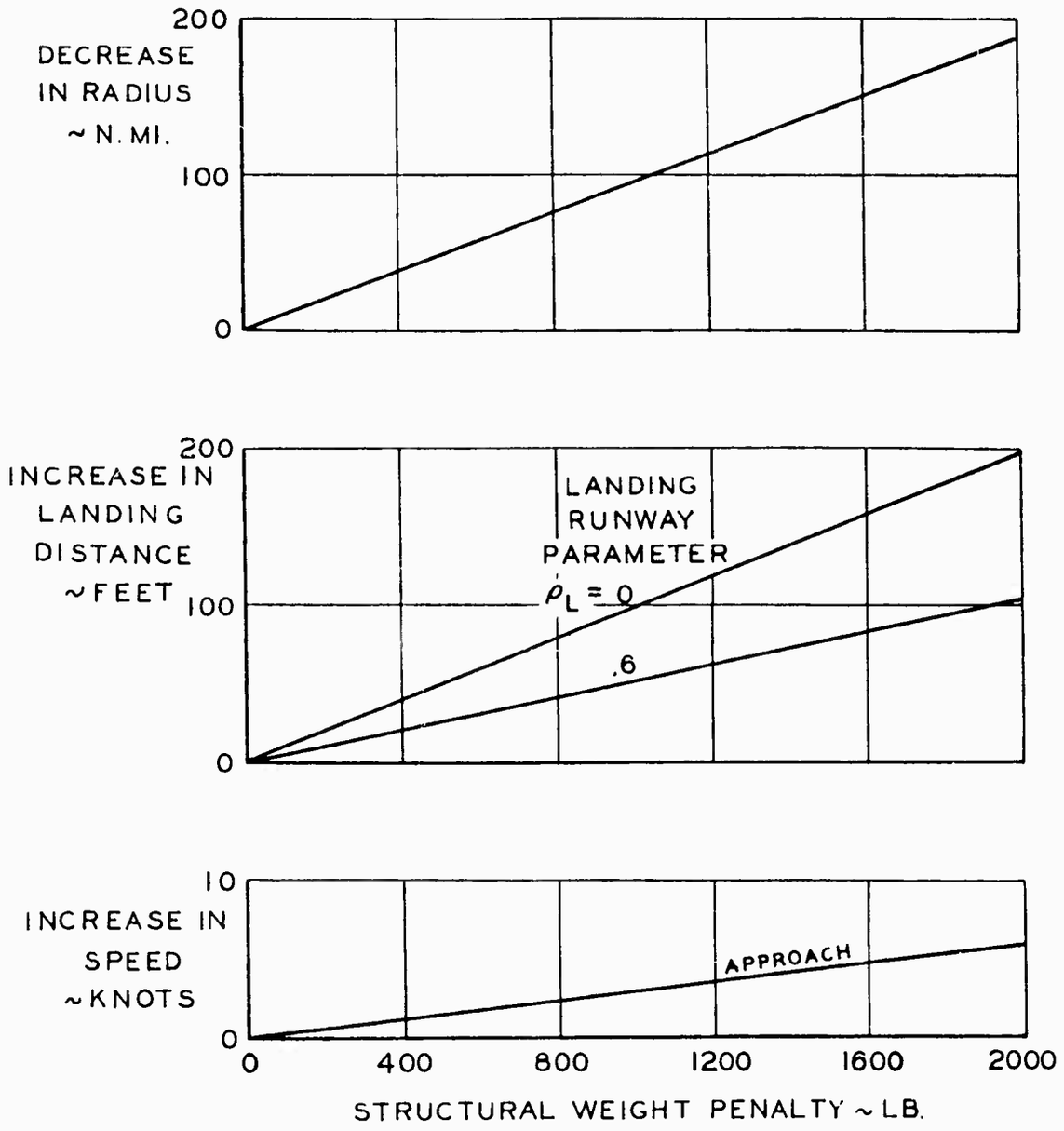

Figure 58. Effect on OV-1 Performance of Structural Weight Penalty. Take-Off Weight Held Constant by Decreasing the Fuel Weight as Structural Weight is Added.

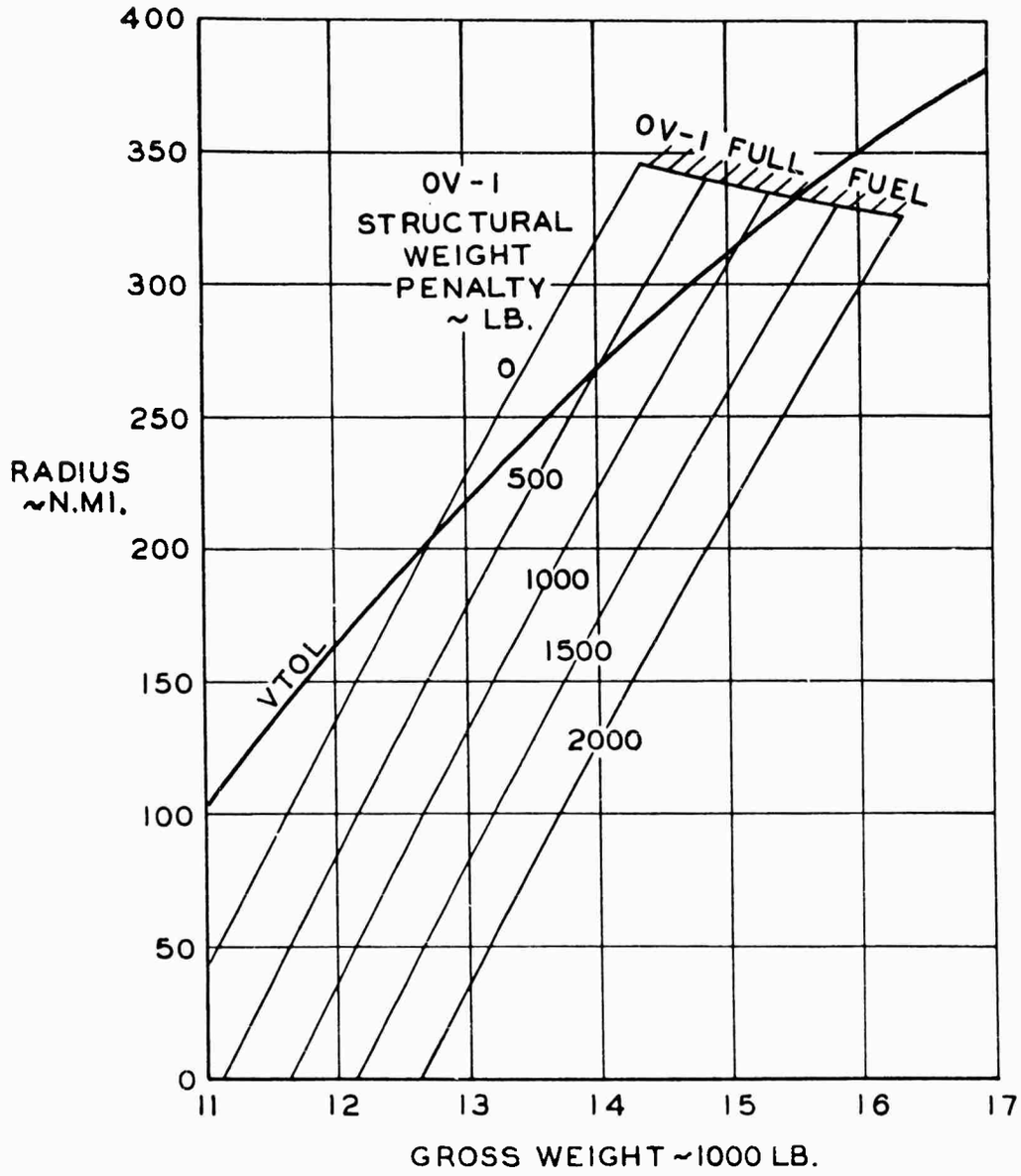

Figure 59. Radius Versus Take-Off Weight for the VTOL Airplane and for the OV-1 Airplane with Varying Amounts of Added Structural Weight.

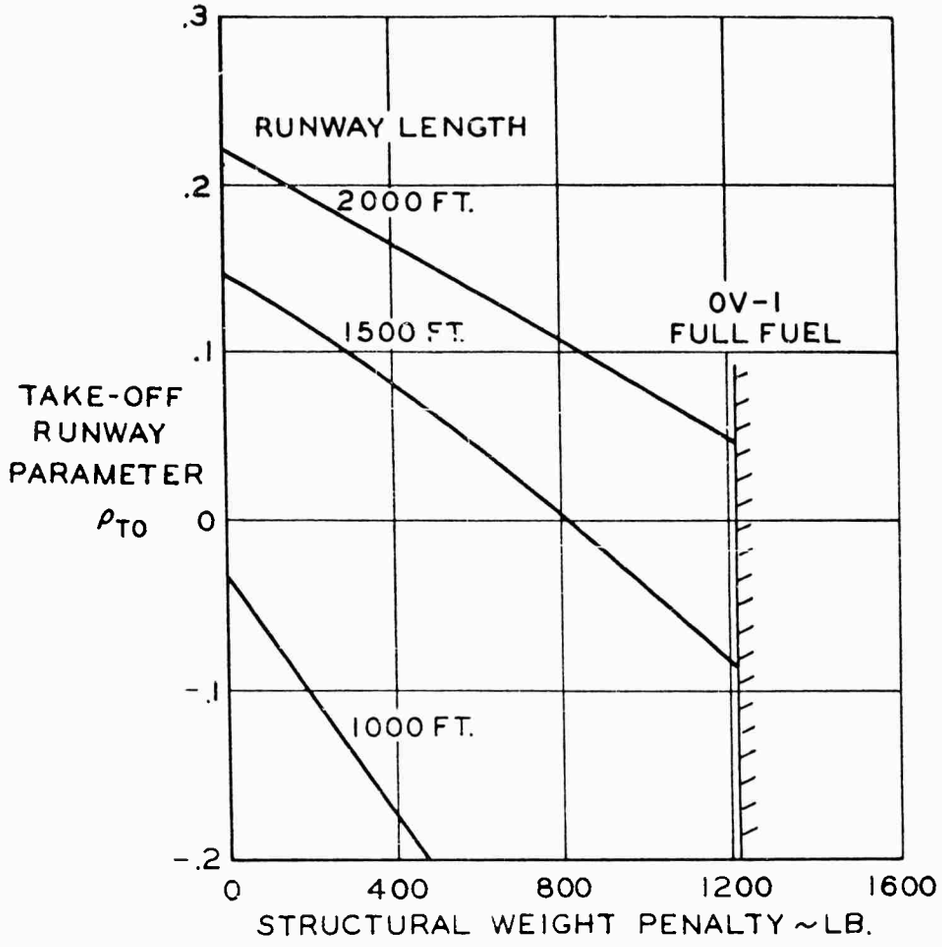

Figure 60. Take-Off Runway Parameter Versus OV-1 Structural Weight Penalty and Runway Length Required for Equal VTOL/OV-1 Performance.

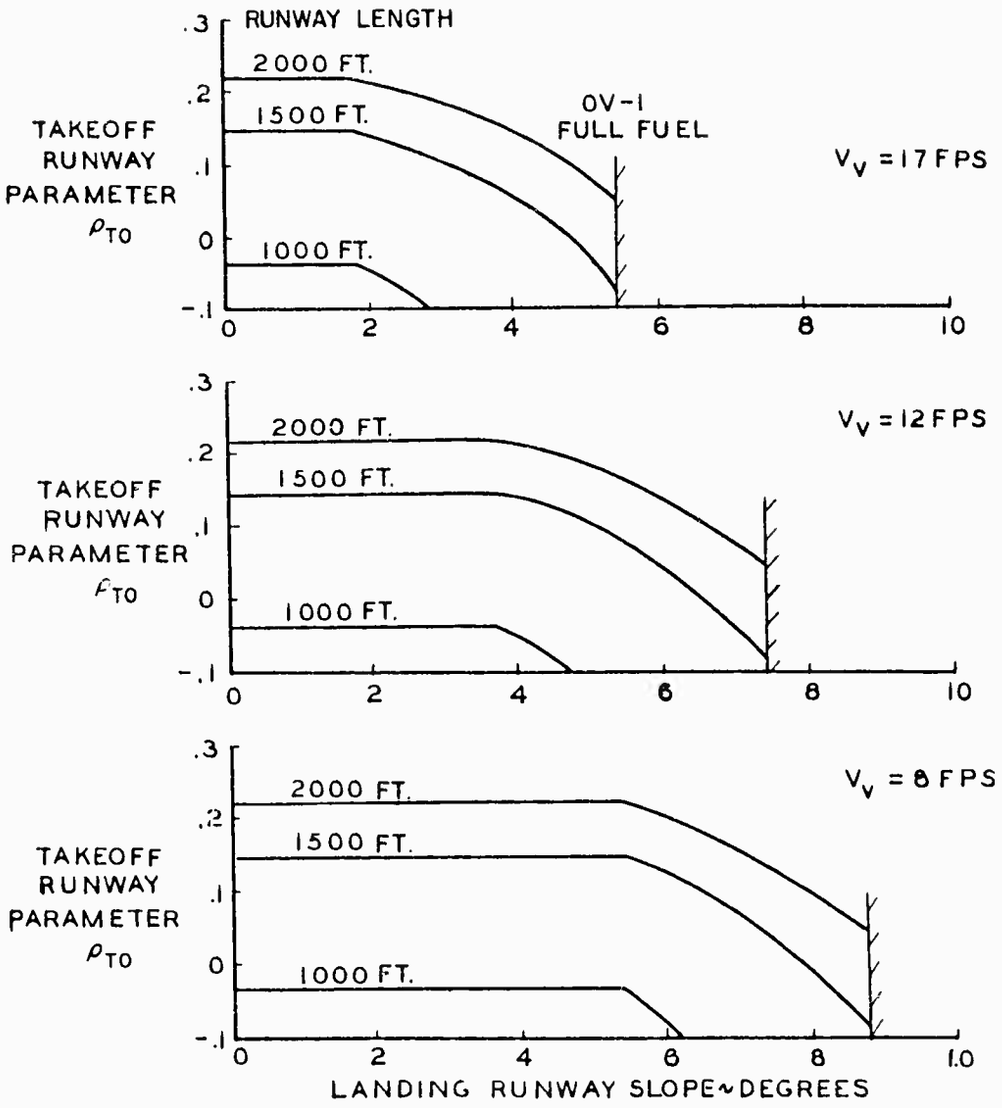

Figure 61. Take-Off Runway Parameter Versus Runway Slope and OV-1 Runway Length Required for Equal VTOL/OV-1 Performance.

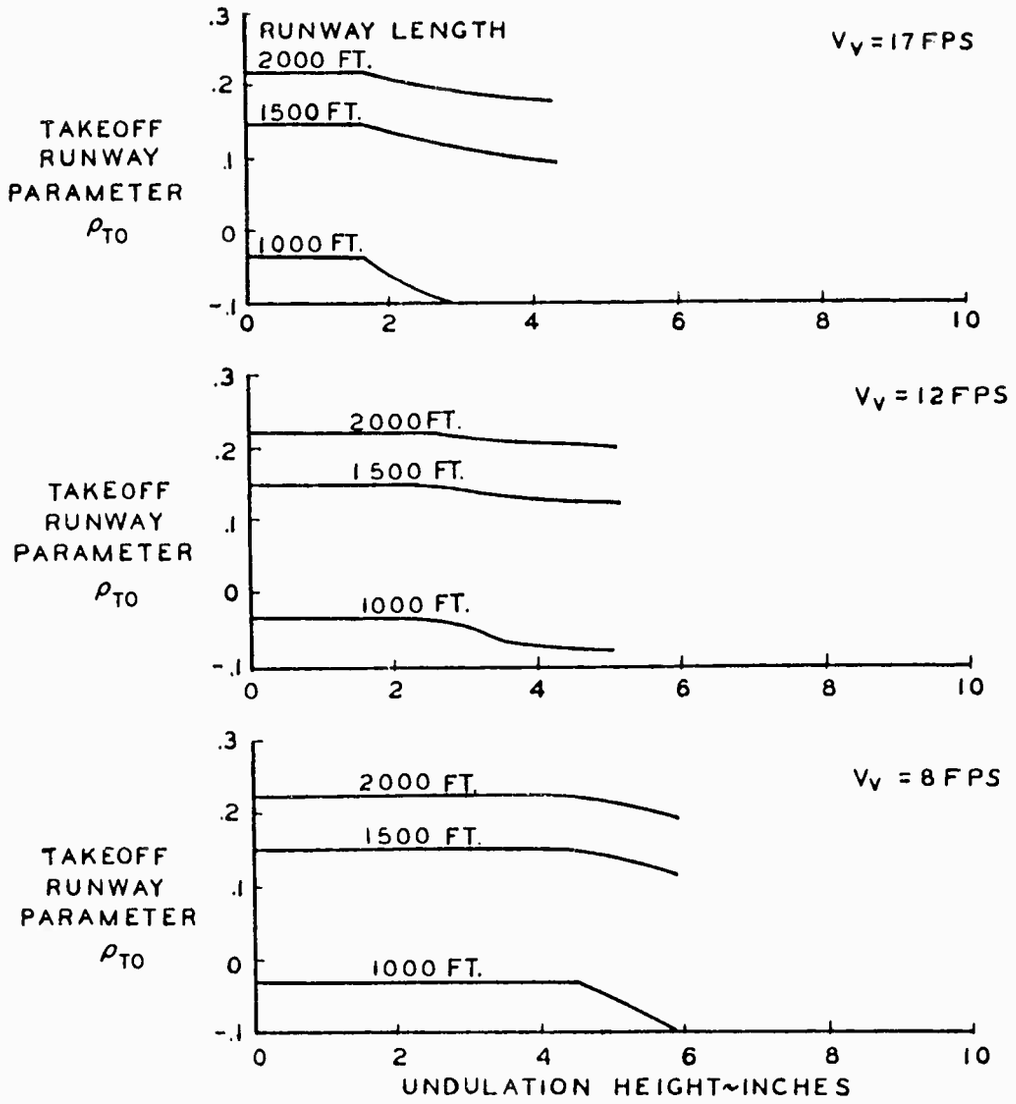

Figure 62. Take-Off Runway Parameter Versus Undulation Height and Runway Length Required for Equal VTOL/OV-1 Performance. Undulation Length = 27.4 Inches.

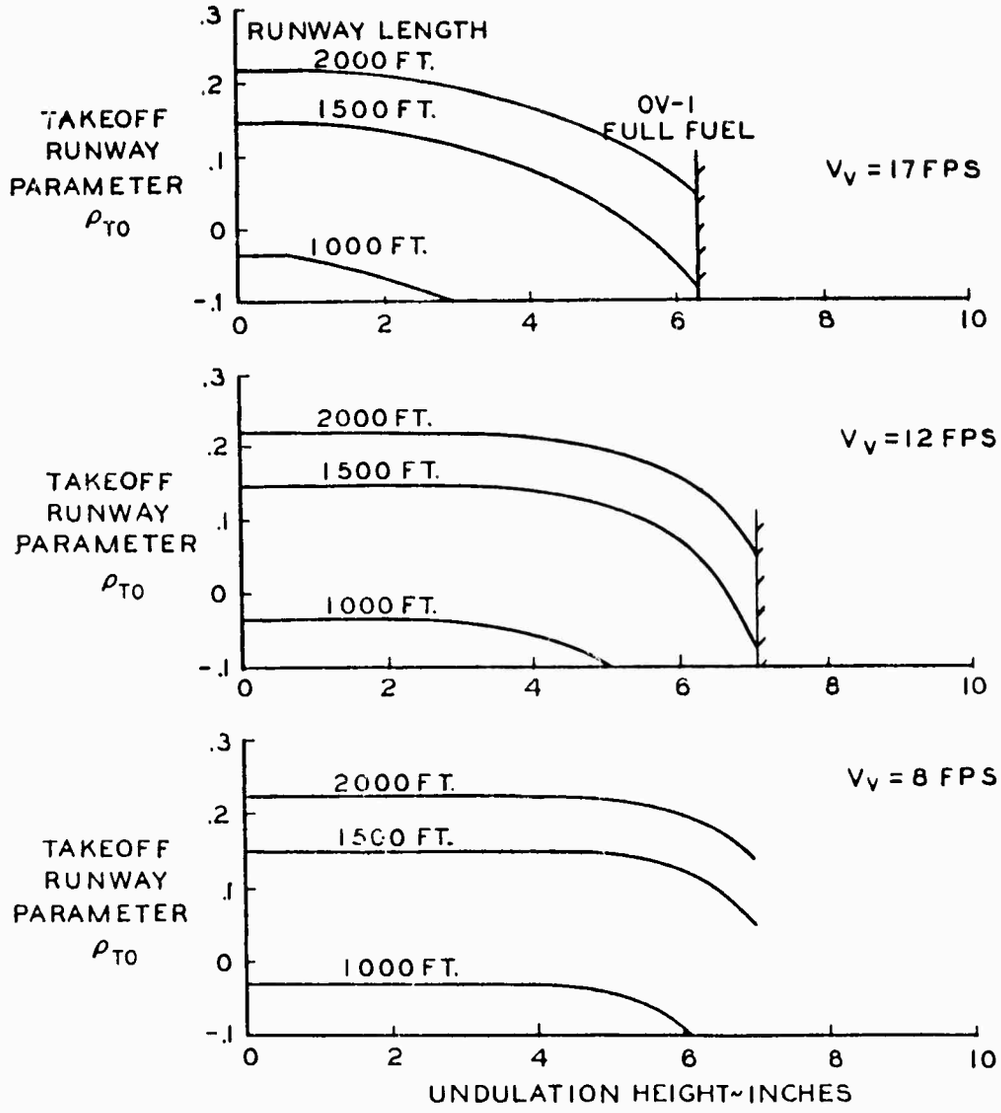

Figure 63. Take-Off Runway Parameter Versus Undulation Height, OV-1 Runway Length Required for Equal VTOL/OV-1 Performance. Undulation Length = 45.67 Inches.

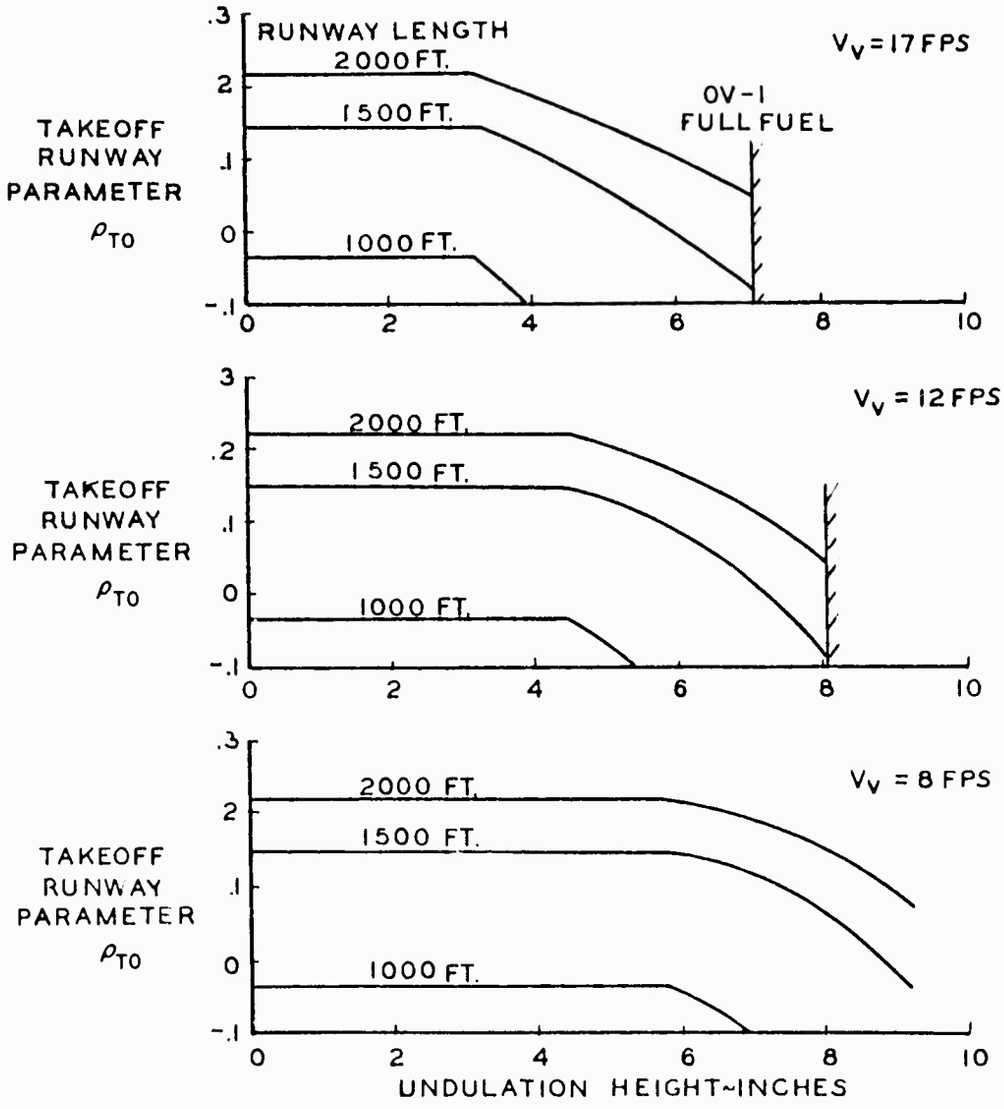

Figure 64. Take-Off Runway Parameter Versus Undulation Height and OV-1 Runway Length Required for Equal VTOL/OV-1 Performance. Undulation Length = 137 Inches.

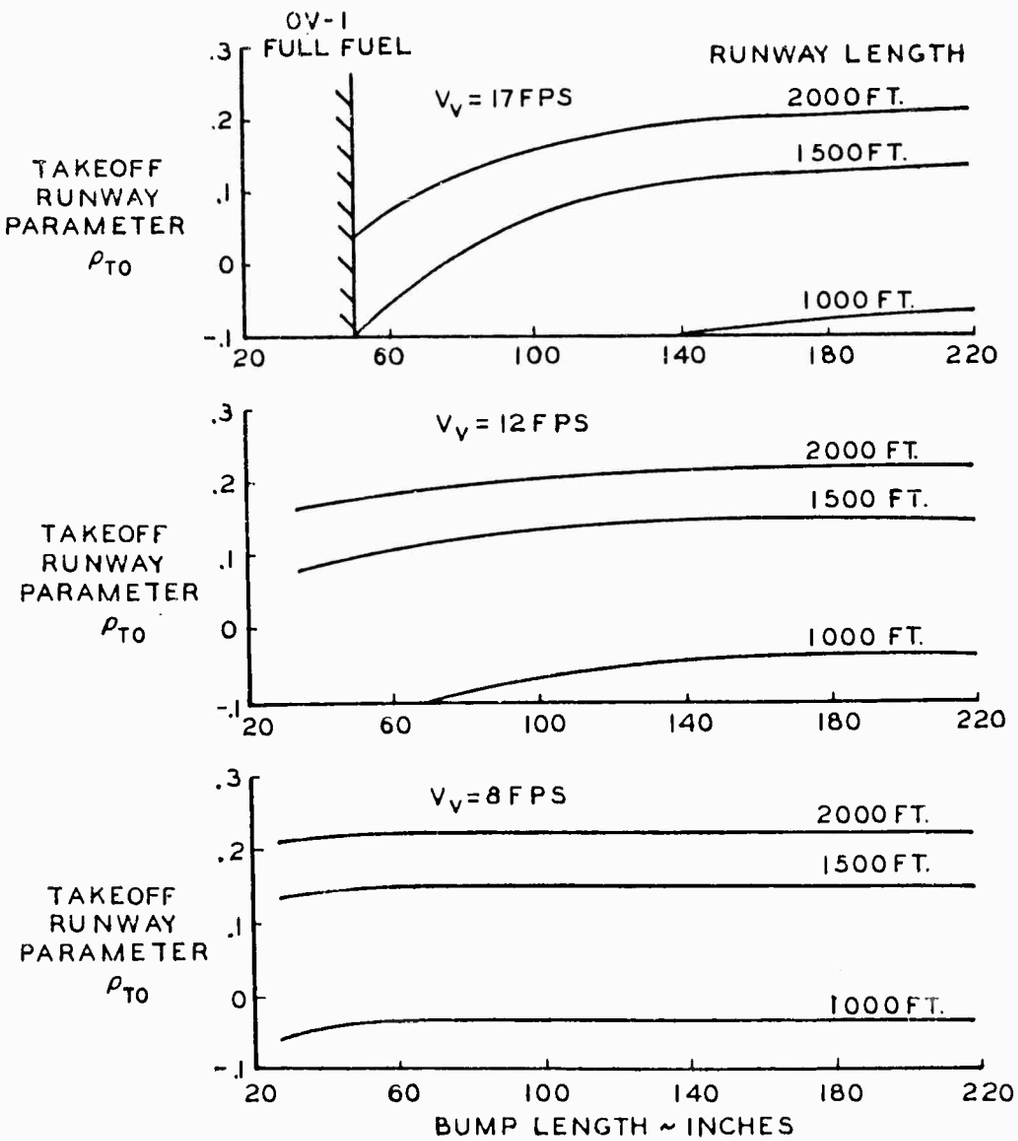

Figure 65. Take-Off Runway Parameter Versus Bump Length and OV-1 Runway Length Required for Equal VTOL/OV-1 Performance. Bump Height = 3 Inches.

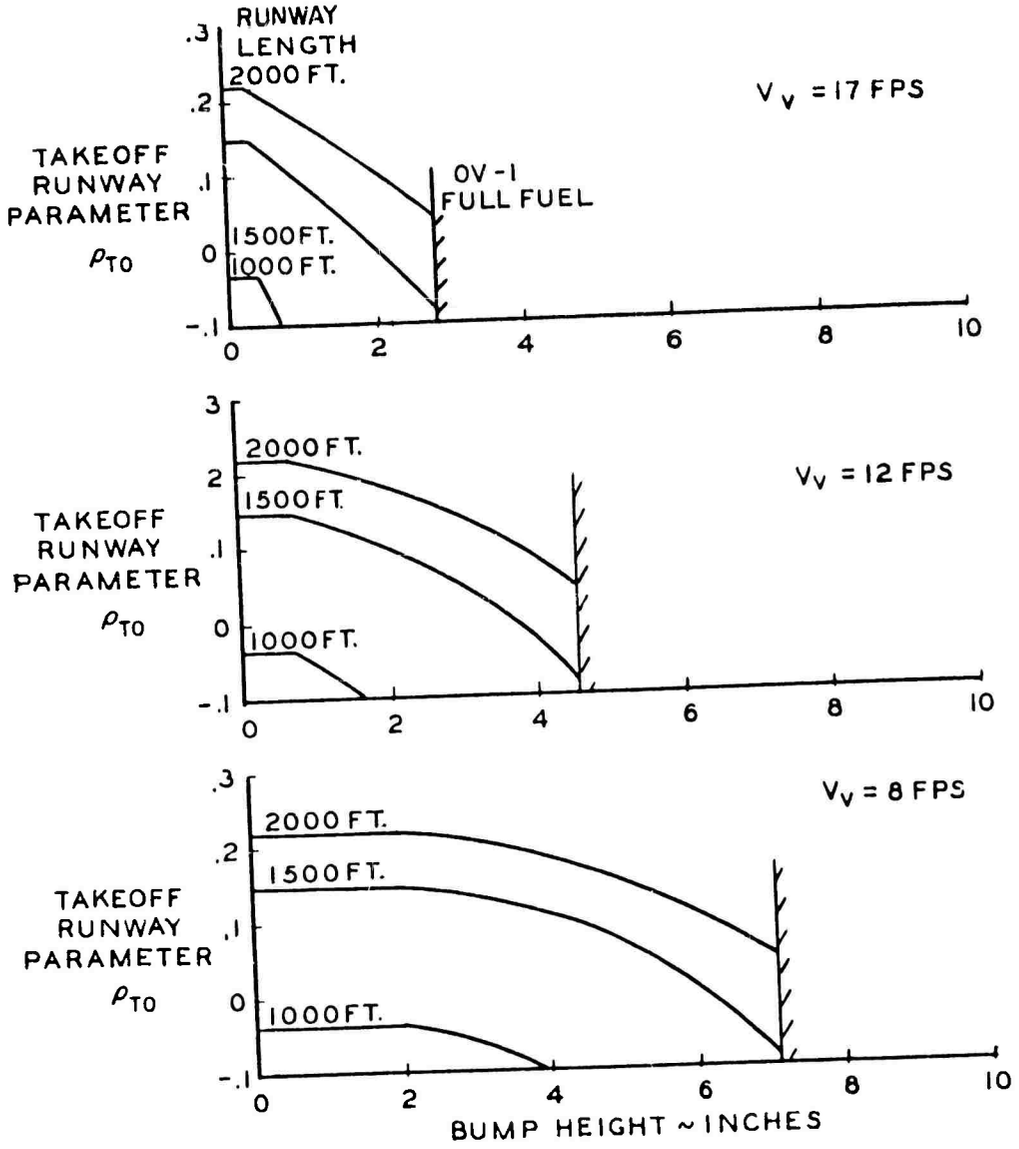

Figure 66. Take-Off Runway Parameter Versus Bump Height and OV-1 Runway Length Required for Equal VTOL/OV-1 Performance. Bump Length = 9.12 x Bump Height.

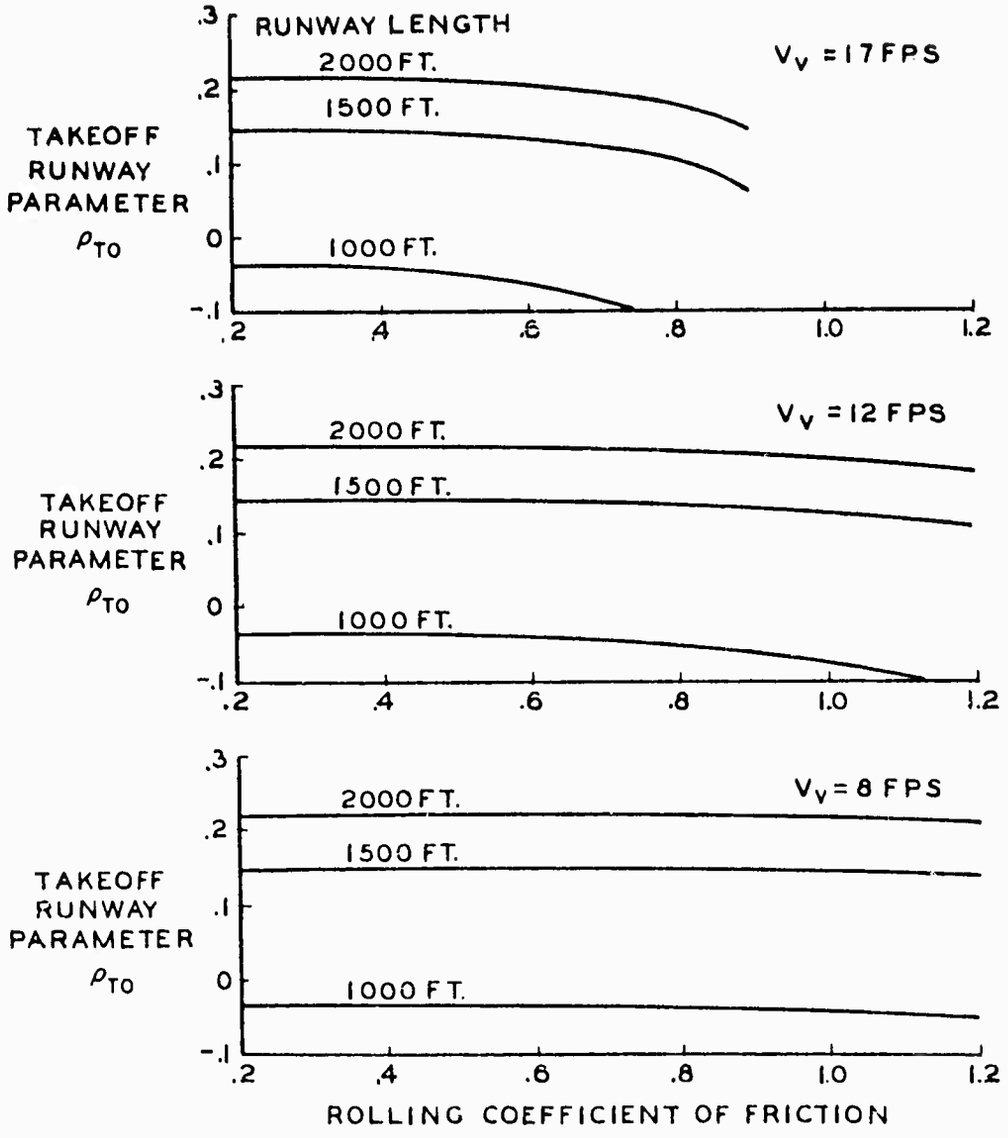

Figure 67. Take-Off Runway Parameter Versus Rolling Coefficient of Friction and Runway Length Required for Equal VTOL/OV-1 Performance.

Direction of Positive Displacements and Forces

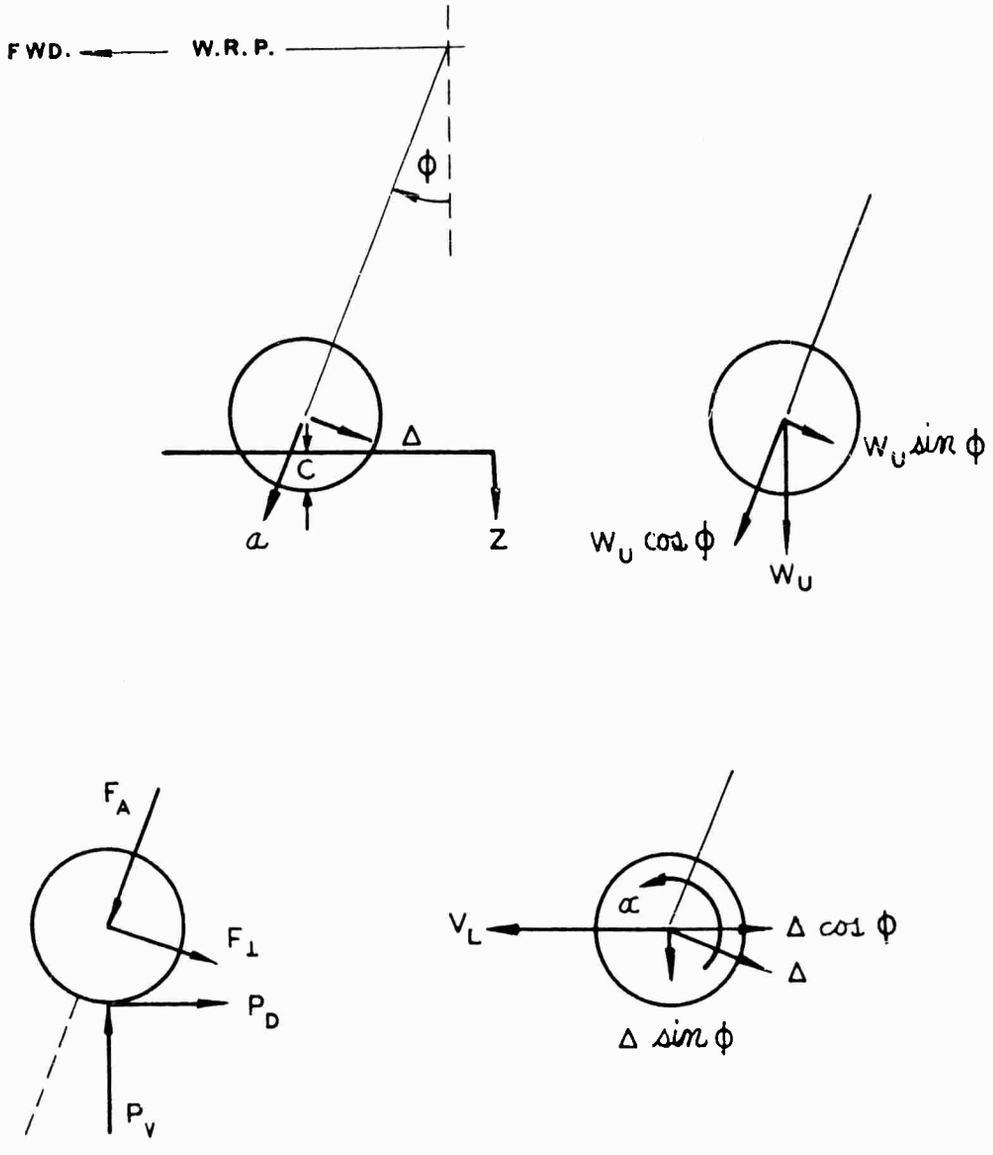

Figure 68. Sign Conventions.

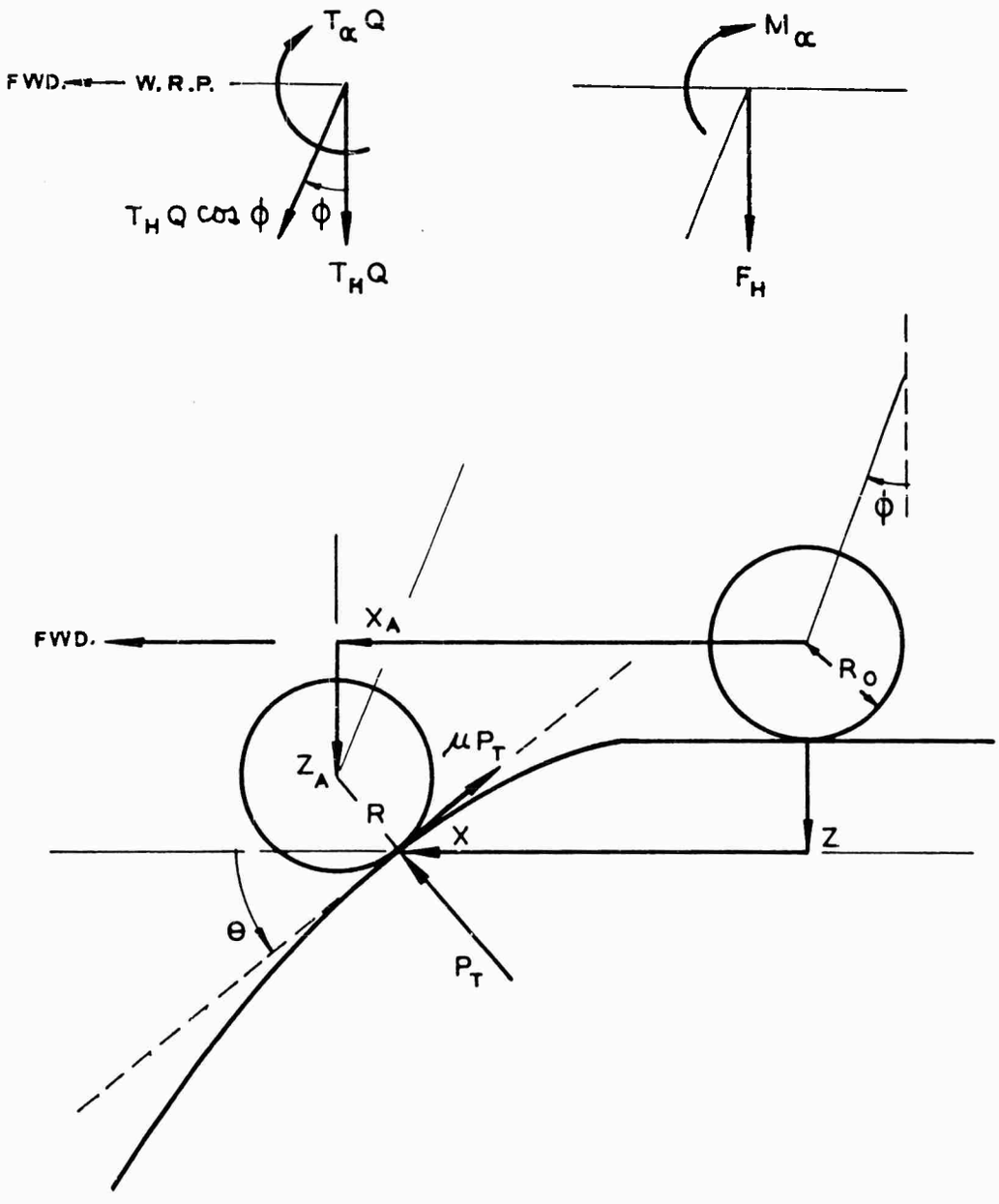

Figure 68. Sign Conventions (Cont'd).

VA	Vertical accelerations - Positive upward (resulting in downward inertia forces)
PA	Pitching accelerations - Positive leading edge up
SH	Shear - Positive shear produces positive bending moment
BM	Bending moment - Positive moment produces compression in upper elements of wing and fuselage
TQ	Torque - Positive torque produces nose up twist of wing
AA	Airplane angle - Positive nose up
AV	Airplane pitching velocity - Positive nose up
APA	Airplane pitching acceleration - Positive nose up
VP	Vertical position of airplane C.G. - Positive up
VV	Vertical velocity of airplane C.G. - Positive up
AVA	Vertical acceleration of airplane C.G. - Positive up
HA	Horizontal acceleration of C.G. - Positive forward

Figure 68. Sign Conventions (Cont'd).

DISTRIBUTION

U. S. Army Test and Evaluation Command	2
Second U. S. Army	2
U. S. Army Command and General Staff College	1
Army War College	1
U. S. Army Aviation Test Board	5
U. S. Army Aviation Test Activity	1
Deputy Chief of Staff for Logistics, D/A	2
The Research Analysis Corporation	1
Army Research Office, Durham	2
Office of Chief of R&D, D/A	1
Naval Air Test Center	2
Army Research Office, OCRD	1
Chief of R&D, D/A	1
U. S. Army Combat Developments Command Aviation Agency	1
Deputy Chief of Staff for Military Operations, D/A	1
U. S. Army Human Engineering Laboratories	1
Chief of Transportation	1
U. S. Army Combat Developments Command Transportation Agency	1
U. S. Army Transportation Board	1
U. S. Army Aviation and Surface Materiel Command	7
U. S. Army Transportation Center and Fort Eustis	4
U. S. Army Transportation Research Command	37
U. S. Army Transportation School	3
U. S. Army Airborne, Electronics and Special Warfare Board	1
Office of the United States Army Attache´	1
U. S. Army Research and Development Group (Europe)	2
U. S. Army Engineer Waterways Experiment Station	1
U. S. Army Aviation School	1
Allied Land Forces, Southeastern Europe	2
U. S. Army, Communication Zone Europe	3
U. S. Army Caribbean	4
Air University Library, Maxwell AFB	1
Air Force Systems Command, Wright-Patterson AFB	3
Bureau of Naval Weapons	2
David Taylor Model Basin	1
U. S. Army Standardization Group, Canada	1
Canadian Army Liaison Officer, U. S. Army Transportation School	3

British Army Staff, British Embassy	4
U. S. Army Standardization Group, U. K.	1
NASA-LRC, Langley Station	2
Ames Research Center, NASA	2
Scientific and Technical Information Facility	1
U. S. Government Printing Office	1
Defense Documentation Center	10
U. S. Army Mobility Command	2
U. S. Army Materiel Command	3
Air Proving Ground Center, Eglin AFB	1

Douglas Aircraft Co., Long Beach, Calif., A STUDY OF ROUGH-TERRAIN-INDUCED STRUCTURAL LANDING LOADS, F. C. Allen, D. M. Rehder, and L. B. Mosby, TRECOM Technical Report 63-68, December 1963, 162 pp. (Contract DA44-177-TC-735) USATRECOM Task 1D121401A14602.

The general purpose of this investigation was to develop rough-terrain landing design criteria by an analysis of the effect of rough-terrain landings on the loads, weights and performance of an Army STOL Observation airplane. A dynamic loads analysis was made for landings on fields of varying degrees

1. Landing Loads
2. Rough Terrain
3. Dynamic Loads
4. Landing Design Criteria
5. OV-1 Airplane
6. Contract DA44-177-TC-735

Douglas Aircraft Co., Long Beach, Calif., A STUDY OF ROUGH-TERRAIN-INDUCED STRUCTURAL LANDING LOADS, F. C. Allen, D. M. Rehder, and L. B. Mosby, TRECOM Technical Report 63-68, December 1963, 162 pp. (Contract DA44-TC-735) USATRECOM Task 1D121401A14602.

The general purpose of this investigation was to develop rough-terrain landing design criteria by an analysis of the effect of rough-terrain landings on the loads, weights and performance of an Army STOL Observation airplane. A dynamic loads analysis was made for landings on fields of varying degrees

1. Landing Loads
2. Rough Terrain
3. Dynamic Loads
4. Landing Design Criteria
5. OV-1 Airplane
6. Contract DA44-177-TC-735

Douglas Aircraft Co., Long Beach, Calif., A STUDY OF ROUGH-TERRAIN-INDUCED STRUCTURAL LANDING LOADS, F. C. Allen, D. M. Rehder, and L. B. Mosby, TRECOM Technical Report 63-68, December 1963, 162 pp. (Contract DA44-177-TC-735) USATRECOM Task 1D121401A14602.

The general purpose of this investigation was to develop rough-terrain landing design criteria by an analysis of the effect of rough-terrain landings on the loads, weights and performance of an Army STOL Observation airplane. A dynamic loads analysis was made for landings on fields of varying degrees

1. Landing Loads
2. Rough Terrain
3. Dynamic Loads
4. Landing Design Criteria
5. OV-1 Airplane
6. Contract DA44-177-TC-735

Douglas Aircraft Co., Long Beach, Calif., A STUDY OF ROUGH-TERRAIN-INDUCED STRUCTURAL LANDING LOADS, F. C. Allen, D. M. Rehder, and L. B. Mosby, TRECOM Technical Report 63-68, December 1963, 162 pp. (Contract DA44-177-TC-735) USATRECOM Task 1D121401A14602.

The general purpose of this investigation was to develop rough-terrain landing design criteria by an analysis of the effect of rough-terrain landings on the loads, weights and performance of an Army STOL Observation airplane. A dynamic loads analysis was made for landings on fields of varying degrees

1. Landing Loads
2. Rough Terrain
3. Dynamic Loads
4. Landing Design Criteria
5. OV-1 Airplane
6. Contract DA44-177-TC-735

of roughness, weight increments necessary to prevent failure were computed, and the effect of these weights on aircraft range was determined. As a final step, the degree of terrain roughness at which the range of the STOL aircraft was reduced to that of a VTOL aircraft of equal size was computed. Rough-terrain landing criteria were formulated on the assumption that the STOL aircraft should not be required to land on fields whose roughness made it less efficient than a comparable VTOL aircraft.

This work was concerned primarily with maximum loads and corresponding weight and performance penalties, however, calculations were made for the roll-out phase of the landing and for taxiing in order that observations could be made on the importance of the repeated loads encountered in rough-terrain operations.

of roughness, weight increments necessary to prevent failure were computed, and the effect of these weights on aircraft range was determined. As a final step, the degree of terrain roughness at which the range of the STOL aircraft was reduced to that of a VTOL aircraft of equal size was computed. Rough-terrain landing criteria were formulated on the assumption that the STOL aircraft should not be required to land on fields whose roughness made it less efficient than a comparable VTOL aircraft.

This work was concerned primarily with maximum loads and corresponding weight and performance penalties, however, calculations were made for the roll-out phase of the landing and for taxiing in order that observations could be made on the importance of the repeated loads encountered in rough-terrain operations.

of roughness, weight increments necessary to prevent failure were computed, and the effect of these weights on aircraft range was determined. As a final step, the degree of terrain roughness at which the range of the STOL aircraft was reduced to that of a VTOL aircraft of equal size was computed. Rough-terrain landing criteria were formulated on the assumption that the STOL aircraft should not be required to land on fields whose roughness made it less efficient than a comparable VTOL aircraft.

This work was concerned primarily with maximum loads and corresponding weight and performance penalties, however, calculations were made for the roll-out phase of the landing and for taxiing in order that observations could be made on the importance of the repeated loads encountered in rough-terrain operations.

of roughness, weight increments necessary to prevent failure were computed, and the effect of these weights on aircraft range was determined. As a final step, the degree of terrain roughness at which the range of the STOL aircraft was reduced to that of a VTOL aircraft of equal size was computed. Rough-terrain landing criteria were formulated on the assumption that the STOL aircraft should not be required to land on fields whose roughness made it less efficient than a comparable VTOL aircraft.

This work was concerned primarily with maximum loads and corresponding weight and performance penalties, however, calculations were made for the roll-out phase of the landing and for taxiing in order that observations could be made on the importance of the repeated loads encountered in rough-terrain operations.

Douglas Aircraft Co., Long Beach, Calif., A STUDY OF ROUGH-TERRAIN-INDUCED STRUCTURAL LANDING LOADS, F. C. Allen, D. M. Rehder, and L. B. Mosby, TRECOM Technical Report 63-68, December 1963, 162 pp. (Contract DA44-177-TC-735) USATRECOM Task 1D121401A14602.

The general purpose of this investigation was to develop rough-terrain landing design criteria by an analysis of the effect of rough-terrain landings on the loads, weights and performance of an Army STOL Observation airplane. A dynamic loads analysis was made for landings on fields of varying degrees

1. Landing Loads
2. Rough Terrain
3. Dynamic Loads
4. Landing Design Criteria
5. OV-1 Airplane
6. Contract DA44-177-TC-735

Douglas Aircraft Co., Long Beach, Calif., A STUDY OF ROUGH-TERRAIN-INDUCED STRUCTURAL LANDING LOADS, F. C. Allen, D. M. Rehder, and L. B. Mosby, TRECOM Technical Report 63-68, December 1963, 162 pp. (Contract DA44-177-TC-735) USATRECOM Task 1D121401A14602.

The general purpose of this investigation was to develop rough-terrain landing design criteria by an analysis of the effect of rough-terrain landings on the loads, weights and performance of an Army STOL Observation airplane. A dynamic loads analysis was made for landings on fields of varying degrees

1. Landing Loads
2. Rough Terrain
3. Dynamic Loads
4. Landing Design Criteria
5. OV-1 Airplane
6. Contract DA44-177-TC-735

Douglas Aircraft Co., Long Beach, Calif., A STUDY OF ROUGH-TERRAIN-INDUCED STRUCTURAL LANDING LOADS, F. C. Allen, D. M. Rehder, and L. B. Mosby, TRECOM Technical Report 63-68, December 1963, 162 pp. (Contract DA44-177-TC-735) USATRECOM Task 1D121401A14602.

The general purpose of this investigation was to develop rough-terrain landing design criteria by an analysis of the effect of rough-terrain landings on the loads, weights and performance of an Army STOL Observation airplane. A dynamic loads analysis was made for landings on fields of varying degrees

1. Landing Loads
2. Rough Terrain
3. Dynamic Loads
4. Landing Design Criteria
5. OV-1 Airplane
6. Contract DA44-177-TC-735

of roughness, weight increments necessary to prevent failure were computed, and the effect of these weights on aircraft range was determined. As a final step, the degree of terrain roughness at which the range of the STOL aircraft was reduced to that of a VTOL aircraft of equal size was computed. Rough-terrain landing criteria were formulated on the assumption that the STOL aircraft should not be required to land on fields whose roughness made it less efficient than a comparable VTOL aircraft.

This work was concerned primarily with maximum loads and corresponding weight and performance penalties, however, calculations were made for the roll-out phase of the landing and for taxiing in order that observations could be made on the importance of the repeated loads encountered in rough-terrain operations.

of roughness, weight increments necessary to prevent failure were computed, and the effect of these weights on aircraft range was determined. As a final step, the degree of terrain roughness at which the range of the STOL aircraft was reduced to that of a VTOL aircraft of equal size was computed. Rough-terrain landing criteria were formulated on the assumption that the STOL aircraft should not be required to land on fields whose roughness made it less efficient than a comparable VTOL aircraft.

This work was concerned primarily with maximum loads and corresponding weight and performance penalties, however, calculations were made for the roll-out phase of the landing and for taxiing in order that observations could be made on the importance of the repeated loads encountered in rough-terrain operations.

of roughness, weight increments necessary to prevent failure were computed, and the effect of these weights on aircraft range was determined. As a final step, the degree of terrain roughness at which the range of the STOL aircraft was reduced to that of a VTOL aircraft of equal size was computed. Rough-terrain landing criteria were formulated on the assumption that the STOL aircraft should not be required to land on fields whose roughness made it less efficient than a comparable VTOL aircraft.

This work was concerned primarily with maximum loads and corresponding weight and performance penalties, however, calculations were made for the roll-out phase of the landing and for taxiing in order that observations could be made on the importance of the repeated loads encountered in rough-terrain operations.

of roughness, weight increments necessary to prevent failure were computed, and the effect of these weights on aircraft range was determined. As a final step, the degree of terrain roughness at which the range of the STOL aircraft was reduced to that of a VTOL aircraft of equal size was computed. Rough-terrain landing criteria were formulated on the assumption that the STOL aircraft should not be required to land on fields whose roughness made it less efficient than a comparable VTOL aircraft.

This work was concerned primarily with maximum loads and corresponding weight and performance penalties, however, calculations were made for the roll-out phase of the landing and for taxiing in order that observations could be made on the importance of the repeated loads encountered in rough-terrain operations.